Hybrid Materials Based on a Terpyridine Carboxylate Ligand: A Method for Introducing Light Harvesting and Auxiliary Metal Centers into Metal-Organic Frameworks

by

George K. Norton

B.S., University at Buffalo, 2006

Submitted to the Graduate Faculty of

Arts and Sciences in partial fulfillment

of the requirements for the degree of

Master of Science in Chemistry

University of Pittsburgh

2008

UNIVERSITY OF PITTSBURGH

ARTS AND SCIENCES

This thesis was presented

by

George K. Norton

It was defended on

December 10, 2008

and approved by

Dr. Toby M. Chapman, Associate Professor, Department of Chemistry

Dr. David H. Waldeck, Professor, Department of Chemistry

Thesis Director: Dr. Nathaniel L. Rosi, Assistant Professor, Department of Chemistry

Hybrid Materials Based on a Terpyridine Carboxylate Ligand: A Method for Introducing Light Harvesting and Auxiliary Metal Centers into Metal-Organic Frameworks

George K. Norton, M.S.

University of Pittsburgh, 2008

Metal-organic frameworks (MOFs) are attractive canditates for hydrogen storage and photovoltaic applications owing to their extremely high surface area (often exceeding 1,000 m^2/g), and tunable chemical functionality.[1-3] Although the hydrogen storage capacity of MOFs has been extensively explored, the design of MOFs for photovoltaic applications is still in its infancy. In this work, a method for introducing light-harvesting and auxiliary metal centers (for hydrogen storage) into metal-organic frameworks is proposed. Toward this goal, nine metal-organic materials based on 4'-(4-carboxyphenyl)-2,2':6',2"-terpyridine[4] (H**L**) were synthesized and structurally characterized by single crystal X-ray diffraction. Two of these materials which exhibit channels greater than one nanometer in diameter were fully characterized by TGA, EA, and PXRD. Additionally, a number of discrete $[M(\mathbf{L})_2]$ complexes were synthesized and the photoactive ruthenium complex, $[Ru(H\mathbf{L})_2][PF_6]_2$, was reacted with metal salts under solvothermal conditions. Evidence is presented which indicates the air-sensitive crystals produced by reaction of this complex with zinc(II) ions in *N*,*N*-dimethylformamide have the same topology as the large-pore metal-organic framework, MOF-5.[5] Further studies to reveal the potential of this type of material in photocells are proposed.

TABLE OF CONTENTS

LIST OF TABLES

LIST OF FIGURES

PREFACE

I thank my advisor for helping me prepare for independent scientific research, and Steven Geib for patiently teaching me how to solve crystal structures.

I acknowledge Chris Fennig, an undergraduate researcher in the Rosi lab, for his synthesis of compound **7** and a number of the [M(**L**)$_2$] complexes presented in this work. I also acknowledge Chunlong Chen, a post-doctoral fellow in the Rosi group, for his original syntheses of compound **1** and his solution of the crystal structure of compound **8**. In addition, I appreciate Nat Rosi's and Chunlong Chen's assistance solving the crystal structure of **6**.

1.0 INTRODUCTION

1.1 HYDROGEN STORAGE IN METAL-ORGANIC FRAMEWORKS (MOFS)

1.1.1 STATEMENT OF THE PROBLEM

The lack of safe and economic hydrogen storage technology is an outstanding barrier to the use of molecular hydrogen as a transportation fuel.[6] The 2010 U.S. Department of Energy target for mobile applications requires a hydrogen storage system with a gravimetric storage density of 6 weight % hydrogen, a volumetric capacity of 0.045 kg H_2 L^{-1} and should be able to reversibly adsorb/desorb H_2 in the temperature range of -30 to 50 ºC at a maximum pressure of 100 atm.[7] Despite an outpouring of research effort, no materials or systems meet these criteria.[8]

Chemisorption and physisorption are two means of storing hydrogen, and both of these processes allow the storage of hydrogen under much more ambient conditions than simple pressurization in an empty tank.[6] Chemisorption materials (*e.g.* metal hydrides) provide a high uptake capacity for hydrogen; however, hydrogen release requires high energy conditions.[9, 10] Physisorption in nanoporous materials allows for easy release of adsorbed gas molecules, but at present time the weakness of the H_2-adsorbate interaction limits the practical application of these technologies.[8,11]

Metal-organic frameworks (MOFs) are promising candidates for hydrogen storage applications owing to their very large surface area and the tailorablity of their chemical composition, including pore size, shape and functionality.[1, 12, 13] Moreover, as a result of their high periodicity, the nature of the interaction between hydrogen and the framework can be determined at the atomic scale.[14-16] **Figure 1** illustrates a successful design strategy employed for MOFs in which predesigned molecular building blocks are assembled into extended networks.[2, 17-21]

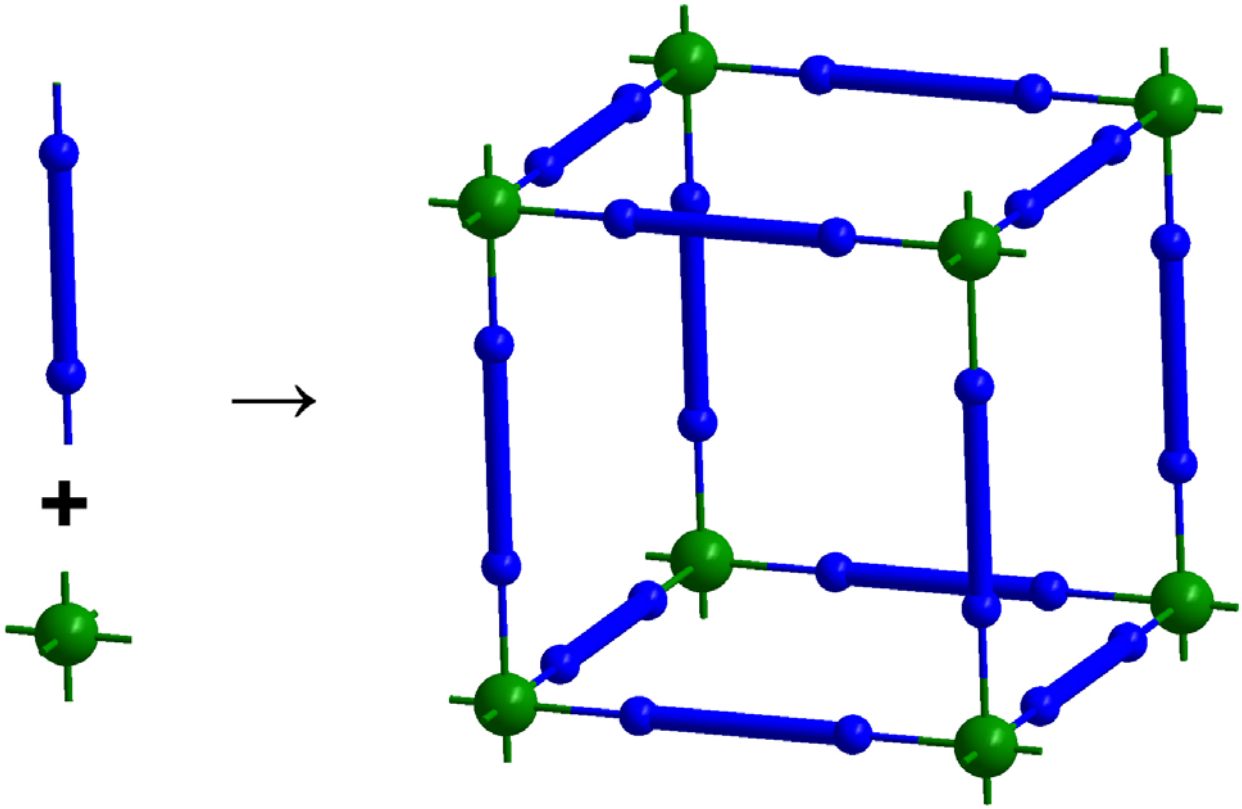

Figure 1. Scheme illustrating modular design of MOFs

The hydrogen uptake capacities of metal-organic frameworks show great promise. For example, MOF-177, a MOF with exceptionally high surface area, exhibits a saturation uptake of H_2 at 7.5 wt%, among the highest reported for any material.[22, 23] However, as a result of the weakness of the interaction between hydrogen and the pore surface, these values are necessarily obtained at high pressures and low temperatures. To increase this interaction strength, much effort has been made to determine the mechanism of hydrogen storage in MOFs.[24-44] Experiment[26, 27, 29] and simulation[35-38, 43] show that in the case of MOF-5 (**Figure 2**), binding sites closer to the zinc carboxylate cluster are stronger (α, β, 7-8 kJ mol^{-1}) than the binding sites around the organic linker (δ, ε; 4-5 kJ mol^{-1}). This is a consequence of the stronger hydrogen-metal ion electrostatic interactions taking precedent over the hydrogen-linker dispersion interactions.[44]

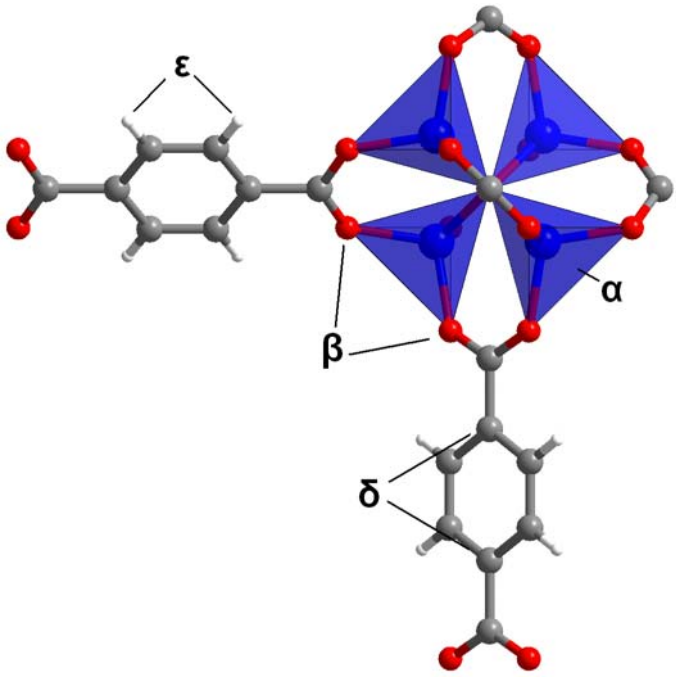

Figure 2. Hydrogen binding sites in MOF-5[27]

1.1.2 APPROACH AND GOALS

Three of the most common strategies to improve hydrogen storage in MOFs are to: a) optimize the pore size/shape to promote framework-H_2 interaction,[45, 46] b) optimize the organic linker[37, 47] and c) introduce exposed/auxiliary metal sites.[24, 48] One method for introducing auxiliary metal centers into MOFs is to use an organic linker that can chelate metal ions and consequently incorporate these ions into the framework.[49-51] With this type of approach in mind, we have chosen the rigid aromatic linker 4'-(4-carboxyphenyl)-2,2':6',2"-terpyridine (H**L**, **Figure 3**)[4] for the formation of robust open frameworks.

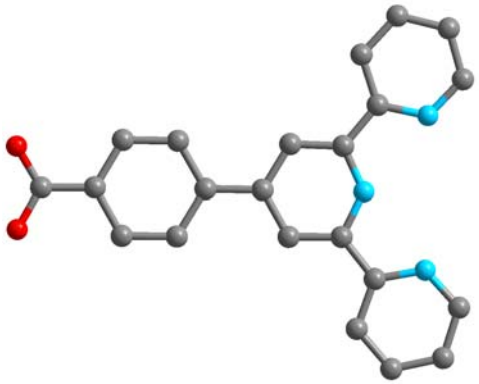

Figure 3. 4'-(4-carboxyphenyl)-2,2':6',2"-terpyridine (H**L**)

Bis-2,2':6',2"-terpyridine complexes of the type [M(**L**)$_2$] can function as supramolecular analogs of linear dicarboxylate linkers,[52] which provides access to a large number of open MOFs based on the dicarboxylate motif (see section **1.3** for targeted frameworks). **Figure 4** shows positions on the ligand where hydrogen may "stick" due to both electrostatic and dispersion interactions. Since, to my knowledge, no porous materials constructed from ligands with the 2,2':6',2"-terpyridine (also referred to simply as *terpyridine*) functionality have been reported in the literature,[53-60] some exploratory research was necessary to determine the nature of the accessible building blocks from which to construct microporous MOFs.

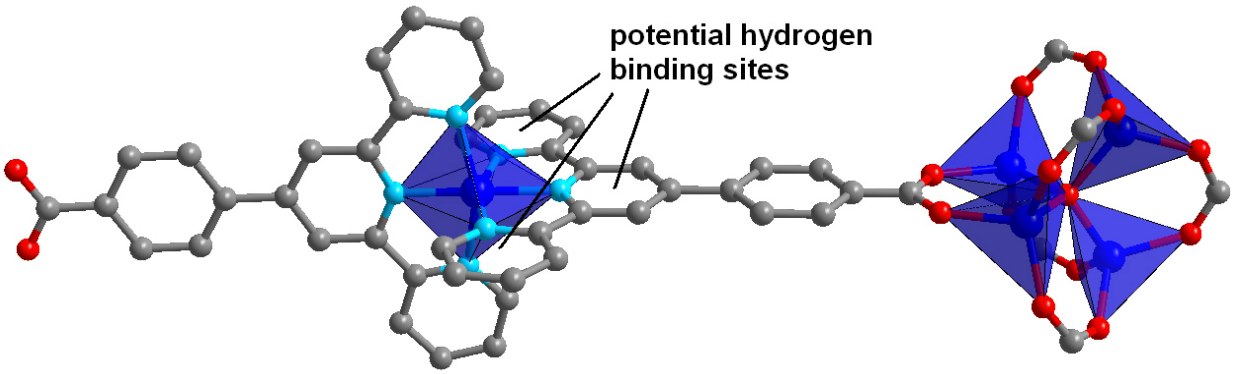

Figure 4. Potential H_2 binding sites on [M(**L**)$_2$], a supramolecular analog of a dicarboxylate linker

The goal of this research is to construct porous materials based on a terpyridine carboxylate ligand (H**L**) and investigate their hydrogen storage properties. These materials can then be probed to determine the location of the hydrogen binding sites and the strength of these interactions. Ultimately, these studies may help in the effort to develop materials able to store hydrogen under the conditions targeted by the DOE (especially at higher temperatures).

1.2 MOF-BASED SOLAR CELLS

1.2.1 STATEMENT OF THE PROBLEM

The fabrication of light-harvesting devices based on organic molecules is a prominent research area. Excitonic solar cells[61] (*i.e.*, Gratzel's dye-sensitized solar cells (DSSCs)[62, 63] and bulk heterojunction solar cells (HJSCs)[64, 65]) are experiencing tremendous growth due to the lower processing costs and molecular tunability when compared with purely inorganic solar cells. Particularly, DSSCs are very stable,[66] and have reached light conversion efficiencies of over 10%.[67]

In the DSSC, a photon is absorbed by a light-harvesting dye anchored onto a wide bandgap nanostructured semiconductor surface (typically TiO_2). The dye injects an electron into the conductance band of the semiconductor where it can travel to the contact, and the dye is reduced back to its original state by a liquid electrolyte or solid p-type semiconductor. One of the reasons for the very high efficiencies of these cells compared with bulk heterojunction cells is the very slow interfacial recombination rate between the metal oxide (electron conductor) and the hole conductor/electrolyte (the self exchange rate for the reduction of I_2 is 10^2 M^{-1} s^{-1} on TiO_2). For these reasons, the active layer can have a high thickness (~10 μm) and surface area (~1000 times the geometrical surface area of the film) without electron collection being favored over exciton recombination.[61]

The efficiency of the DSSC is limited by the number of incoming photons that lead to exciton formation and dissociation on the light harvesting dye. The synthesis of dyes that absorb light better at longer wavelengths[68, 69] has so far met with limited success. Another way to increase the efficiency of these solar cells is to create a highly ordered molecular environment to

decrease the number of electron traps in the active layer.[70, 71] A higher electron mobility allows for an increase in the thickness of the active layer and the absorption of more photons. For example, Law, *et al*. constructed a photocell with highly oriented ZnO nanowires in place of randomly ordered ZnO nanoparticles.[72] Better electron transport properties were observed in the nanowire over the particle photoanode. However, the much smaller surface area and subsequent lower dye loading in the nanowire photocells resulted in lower efficiencies (1.5 %) compared to classic TiO_2 DSSCs.

1.2.2 APPROACH AND GOALS

Assembly of the proper rigid organic and inorganic building blocks, as in metal-organic frameworks, could allow the crystallization of one or two photoactive components into a porous matrix.[73-75] Host-guest chemistry can then be used to introduce the other components (an electron and hole acceptor). The resulting material would have a very ordered structure for high electron transport rates in addition to a large surface area. As a consequence, the active layer of the photocell could be thickened while maintaining high dye loading.

With the correct metal ion (Ru^{2+}, Os^{2+} or Ir^{3+}), *bis*-2,2':6'2"-terpyridine complexes of the type depicted in **Figure 4** are known to eject an electron, which in turn can be accepted by an electron acceptor, such as a fullerene or TiO_2.[76-79] This brought us to the hypothesis that a MOF constructed from this ligand could be used as an active component in a photovoltaic cell if the proper components are incorporated into the matrix (**Figure 5**). With regard to the synthesis of the proper networks, many topologies of MOFs based on linear dicarboxylate linkers have been established, and this topic is discussed in section **1.3**.

The goal of this research is to synthesize porous MOFs incorporating the $[M^{n+}(\mathbf{L})_2]$ motif (where $M^{n+} = Ru^{2+}$, Os^{2+}, or Ir^{3+}) and to introduce guests that are able to accept electrons from the framework. The technical obstacles associated with fabricating a photocell from this MOF material will then be addressed.

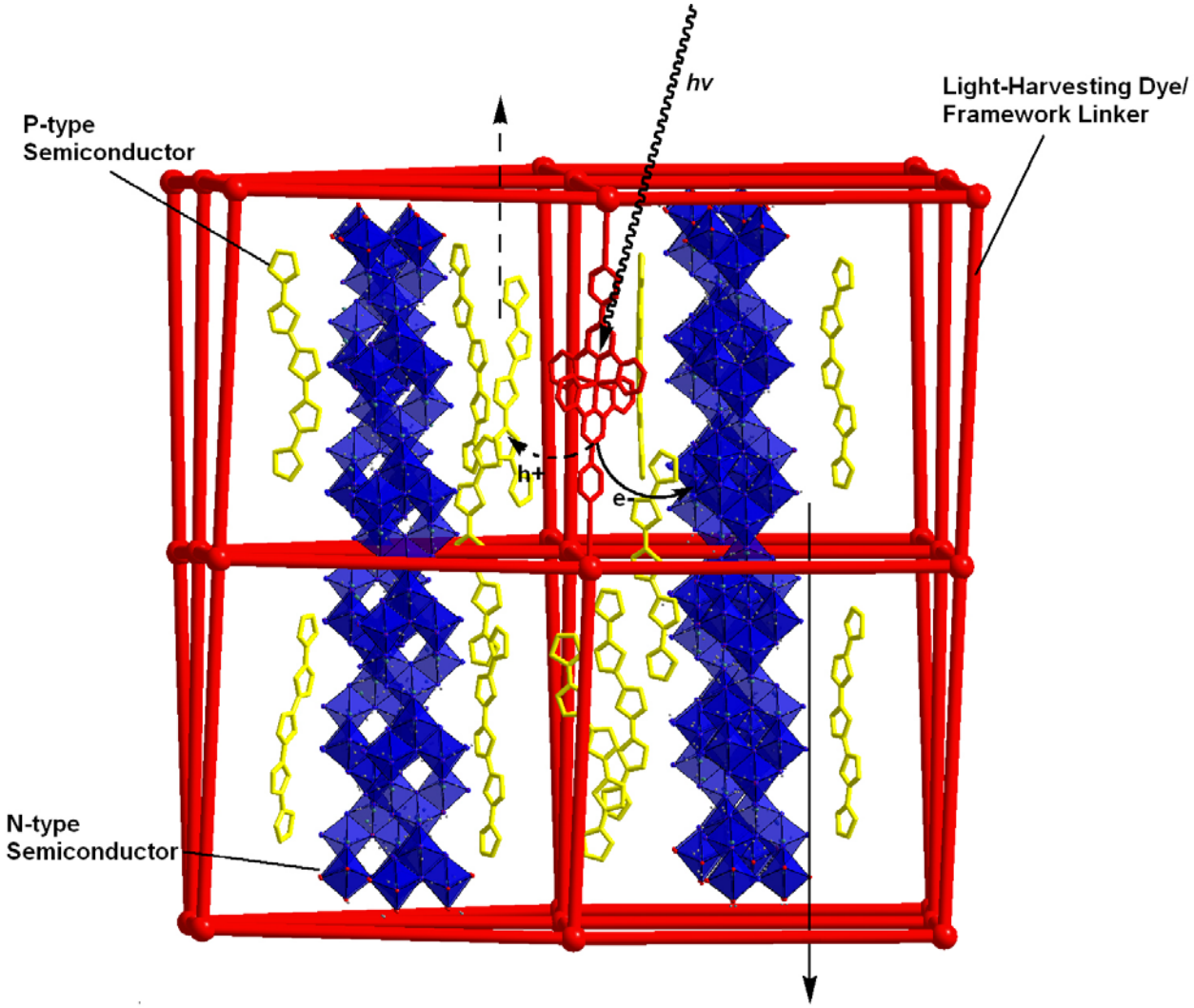

Figure 5. Hypothetical MOF photocell. Top to bottom length is 5.5 nanometers

1.3 MOF DESIGN

Upon reacting ligand H**L** with transition metal salts under MOF-forming conditions, the *in situ* formation of the *bis* complex [M(**L**)$_2$] may be anticipated,[80-83] and some of the topologies of linear dicarboxylate linkers, such as terephthalic acid (1,4-bdc), can be targeted. A strong chelate effect is expected to be a significant driving force for the *bis* complex to form and remain intact during the reaction. It should be noted, however, [M(**L**)$_2$] and 1,4-bdc differ with respect to the twist of the carboxylates relative to one another. While the unsubstituted 1,4-bdc has coplanar carboxyl groups at room temperature, in the case of [M(**L**)$_2$] the carboxylates are twisted 90º with respect to one another (see **Figure 4**). Based on this observation, [M(**L**)$_2$], when combined with specific inorganic building units, can be used to target particular topologies, including the B net in CaB_6,[5] the NbO net,[84] quartz,[85] and diamond (**Figure 6**).[86, 87]

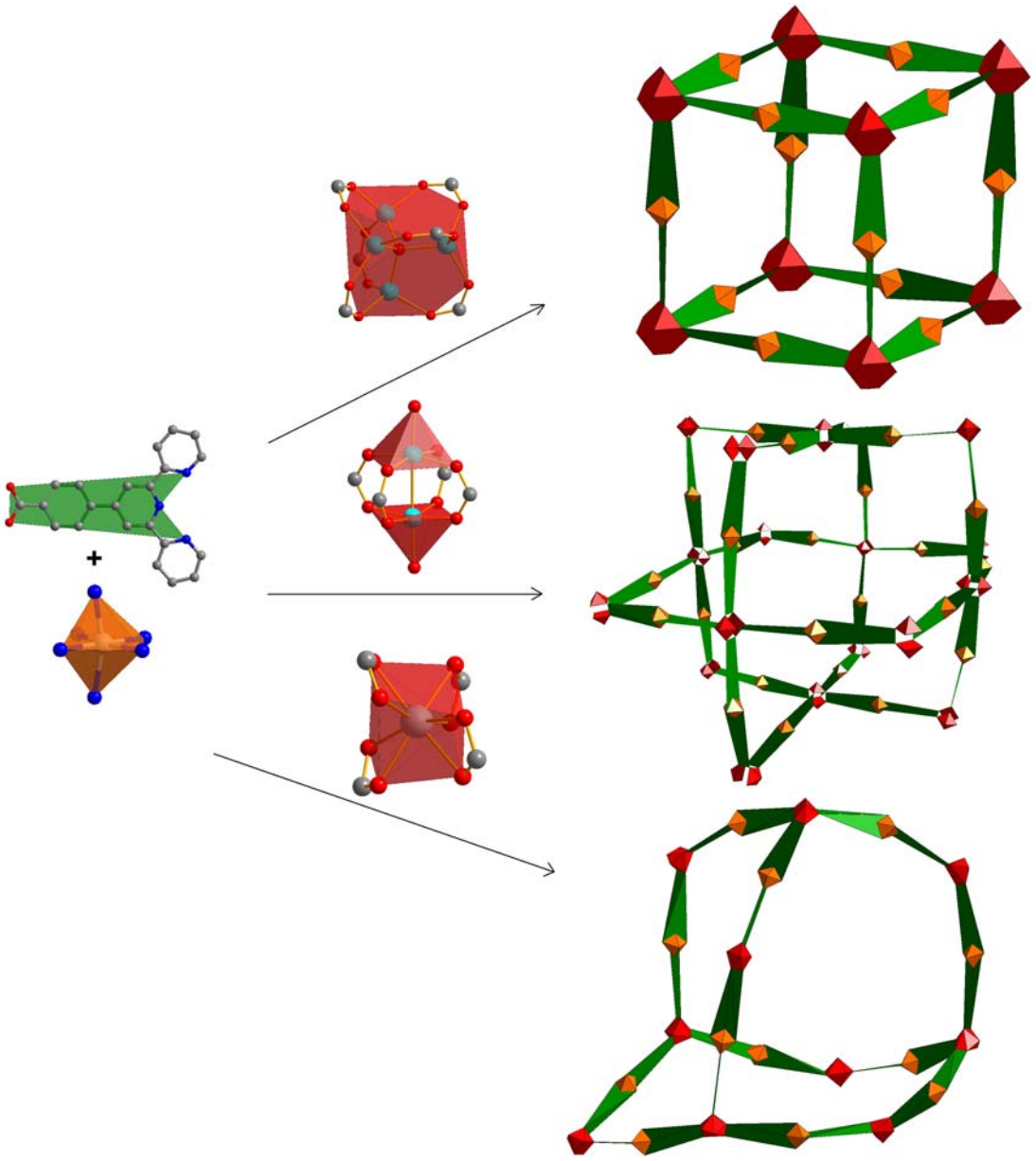

Figure 6. Potential topologies from building units used in this work. Upper: B in CaB_6,[5] Middle: NbO,[84] Lower: diamond

2.0 RESULTS

2.1 $Zn(L)(CF_3COO)\cdot 0.3(H_2O)1.8(DMF)$ (1)

Heating a mixture of H**L** and $Zn(CF_3COO)_2$ in DMF/water at 85 ºC produced yellow hexagonal crystals of hexamer **1**. Single crystal X-ray diffraction revealed one crystallographically independent zinc atom in distorted square pyramidal geometry. Three nitrogens from a chelating terpyridine molecule and one carbonyl oxygen from a different **L** occupy the equatorial positions (**Figure 7**). The apical position on Zn1 is occupied by a carbonyl oxygen from a monodentate trifluoroacetate molecule. The bond lengths around the zinc center range from 1.96 Å (Zn-O) – 2.19 Å (Zn-N) (**Table 2**) and the phenylene and central pyridine ring of **L** are twisted slightly out of conjugation (C9-C8-C16-C21 torsion angle of 23º).

Six of these basic building units combine to form a macrocycle, and these macrocycles pack along the crystallographic *c* axis to form 1-D channels (**Figure 10**). The hexamers have a chair-like packing motif, and are additionally supported by π-stacking interactions (distance between the least square planes of two terpyridine units is 3.4 Å). Analysis with the computer program PLATON[88] reveals the largest sphere that can be made inside the empty channels (guest water molecules excluded) without making contact to the van der Waals surface of the cavities is 11.4 Å. The accessible void volume is estimated to be 37% of the total crystal volume.

Compound **1** was obtained as a pure-phase material as evidenced by powder X-ray diffraction (PXRD) (see **Figures 50** and **51**) and elemental analysis (EA). From the TGA results shown in **Figure 11**, the first weight loss between 20°C and 200°C corresponds to the loss of 0.3 water molecules and 1.8 DMF molecules (calculated 20.5%, found 20.1%). The second weight loss between 200°C and 300°C corresponds to the loss of trifluoroacetate ligands (calculated 16.5%, found 11.35%). The weight loss between 300°C and 400°C results from the loss of **L** ligands (calculated 51.8%, found 48.4%). The TGA data for **1** exchanged with acetonitrile, benzene and chloroform are shown in **Figures 12 – 14**.

Preliminary gas sorption measurements revealed a surface area of 70.6 m^2/g and a hydrogen uptake of 1.5 mg/g (0.15 weight %) at 77 K and 1 atm.

Table 1. Crystallographic data for compounds **1-3**

Identification code	$Zn(\mathbf{L})(CF_3COO)\cdot(H_2O)_{0.3}(DMF)_{1.9}$ (**1**)	$Zn(HCOO)(\mathbf{L})$ (**2**)	$Zn_2(H\mathbf{L})(\mathbf{L})_2(BF_4)_2$ (**4**)
Empirical formula	$C_{432}H_{252}F_{54}N_{54}O_{126}Zn_{18}$	$C_{184}H_{112}N_{24}O_{40}Zn_8$	$C_{264}H_{168}B_8F_{32}N_{36}O_{24}Zn_8$
Formula weight	10417.9	3822.1	5637.94
Temperature	173(2) K	173(2) K	173(2) K
Crystal system	Hexagonal	Monoclinic	Monoclinic
Space group	R-3 (#148)	P2(1)/c (#14)	P2(1)/c (#14)
Unit cell dimensions	a = 39.349(4) Å	a = 12.0730(8) Å	a = 16.126(4) Å
	b = 39.349(4) Å	b = 25.7653(18) Å	b = 16.174(4) Å
	c = 10.5898(14) Å	c = 13.9304(8) Å	c = 27.975(5) Å
	α= 90°	α= 90°	α= 90°
	β= 90°	β= 116.520(4)°	β= 120.307(10)°
	γ = 120°	γ = 90°	γ = 90°
Volume	14200(3) $Å^3$	3877.3(4) $Å^3$	6299(2) $Å^3$
Z	1	1	1
Density (calculated)	1.218 Mg/m^3	1.637 Mg/m^3	1.486 mg/m^3
Goodness-of-fit on F2	1.316	0.694	1.463
Final R indices [I>2sigma(I)]	R1 = 0.0864, wR2 = 0.2597	R1 = 0.0501, wR2 = 0.1219	R1 = 0.1366, wR2 = 0.3360
R indices (all data)	R1 = 0.1693, wR2 = 0.2866	R1 = 0.0941, wR2 = 0.1461	R1 = 0.2363, wR2 = 0.3686
Largest diff. peak and hole	0.676 and -0.534 $e.Å^{-3}$	0.653 and -0.519 $e.Å^{-3}$	2.622 and -0.800 $e.Å^{-3}$

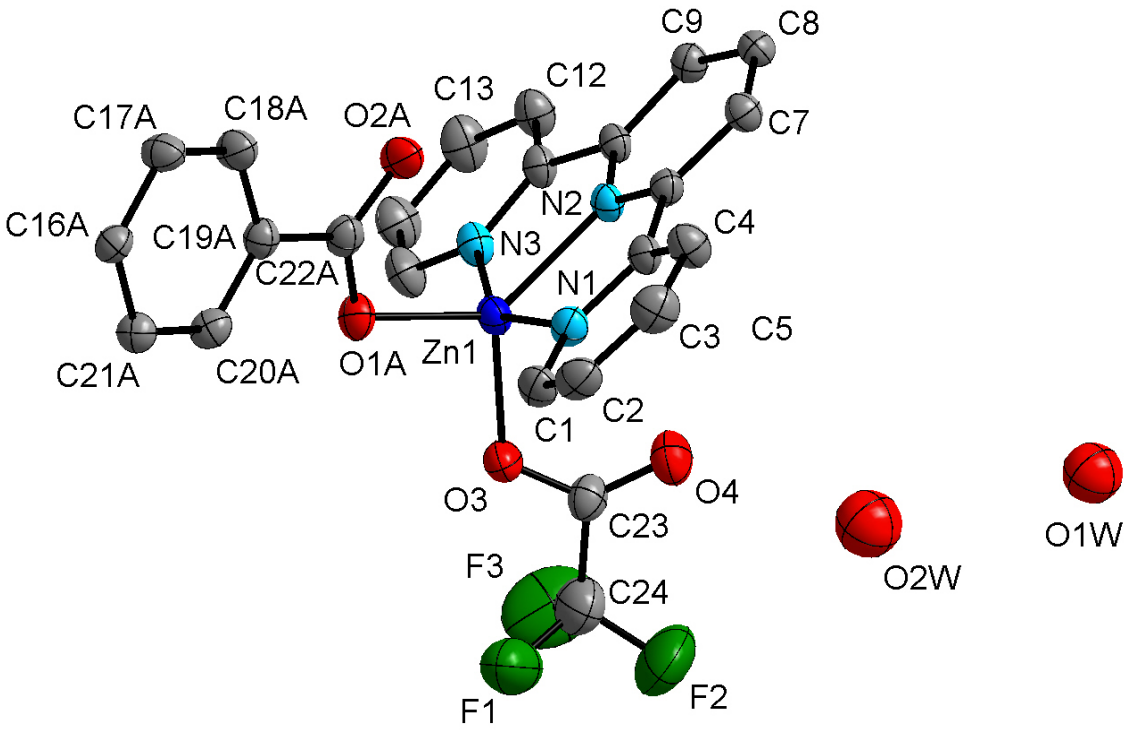

Figure 7. ORTEP view of **1** at 30% probability

Table 2. Selected bond lengths (Å) and angles (°) for compound **1**

Zn1-O1A	1.959(4)	O1-C22	1.273(7)
Zn1-O3	1.991(4)	O2-C22	1.251(7)
Zn1-N2	2.065(4)	O3-C23	1.242(7)
Zn1-N3	2.160(5)	O4-C23	1.200(7)
Zn1-N1	2.188(5)		
O1A-Zn1-N3	105.98(17)	N2-Zn1-N3	75.96(17)
O3-Zn1-N3	96.49(18)	O1A-Zn1-N1	91.74(16)
O1A-Zn1-O3	100.39(17)	O3-Zn1-N1	101.75(18)
O1A-Zn1-N2	131.50(17)	N2-Zn1-N1	75.87(16)
O3-Zn1-N2	127.90(17)	N3-Zn1-N1	151.80(17)

Symmetry transformations used to generate equivalent atoms:
A. y+1/3,-x+y+2/3,-z+2/3

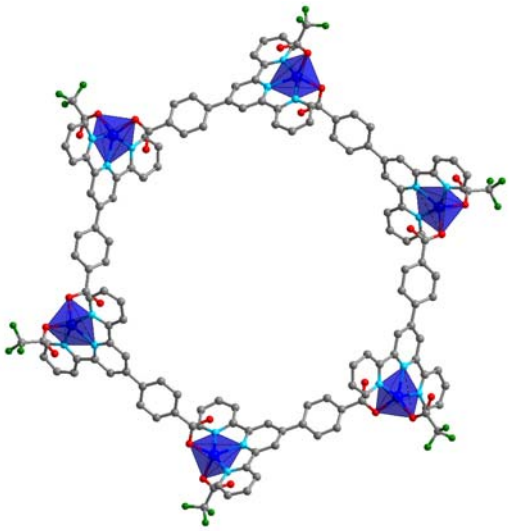

Figure 8. One macrocyclic unit of **1**
Hydrogen atoms are omitted for clarity.
Color key: Zn (dark blue), N (light blue), O (red), C (dark gray), F (green)

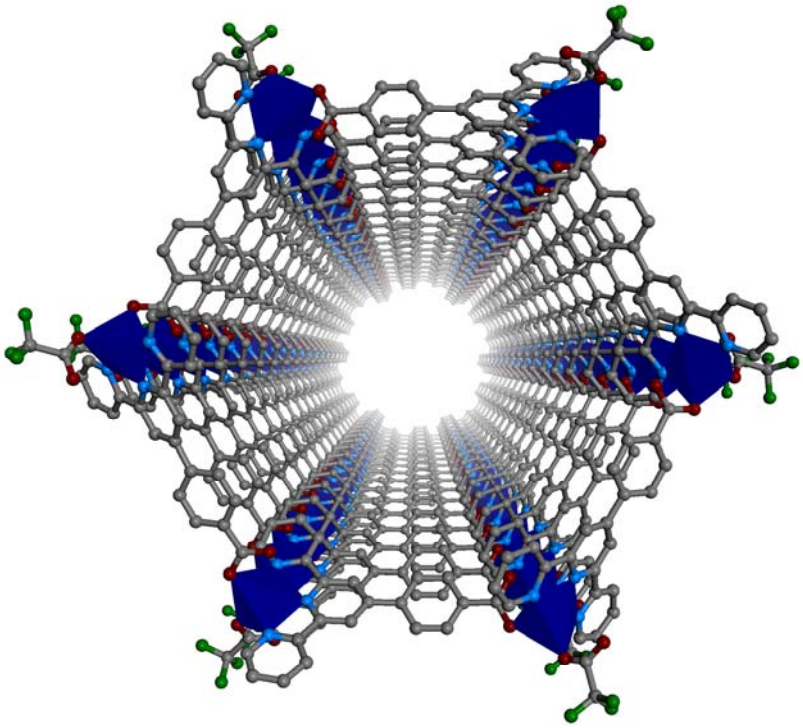

Figure 9. One channel of the supramolecular structure of **1**, viewed down the *c* axis
Hydrogen atoms are omitted for clarity.
Color key: Zn (dark blue), N (light blue), O (red), C (dark gray), F (green)

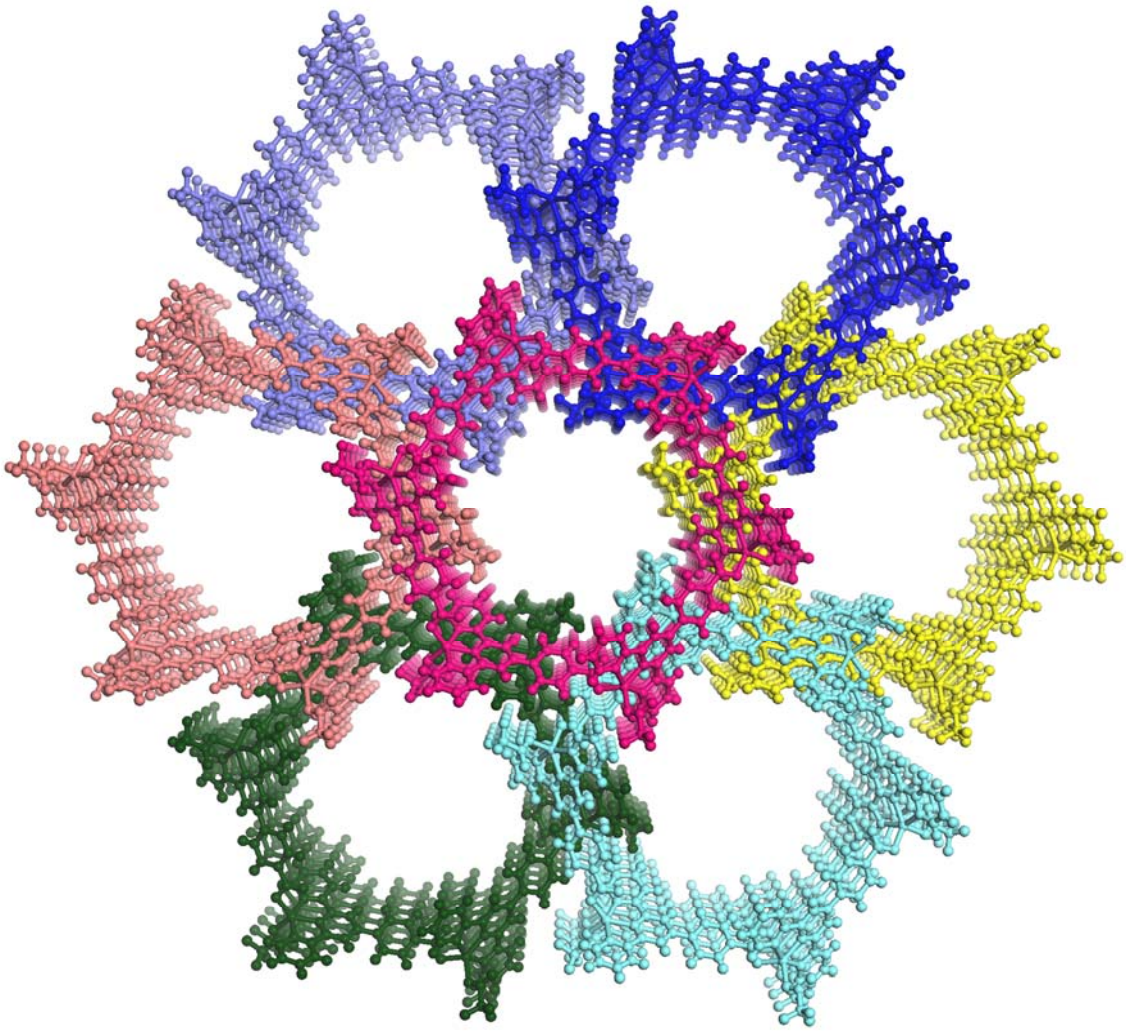

Figure 10. Packing diagram of **1**, viewed down the *c* axis
Hydrogen atoms are omitted for clarity.

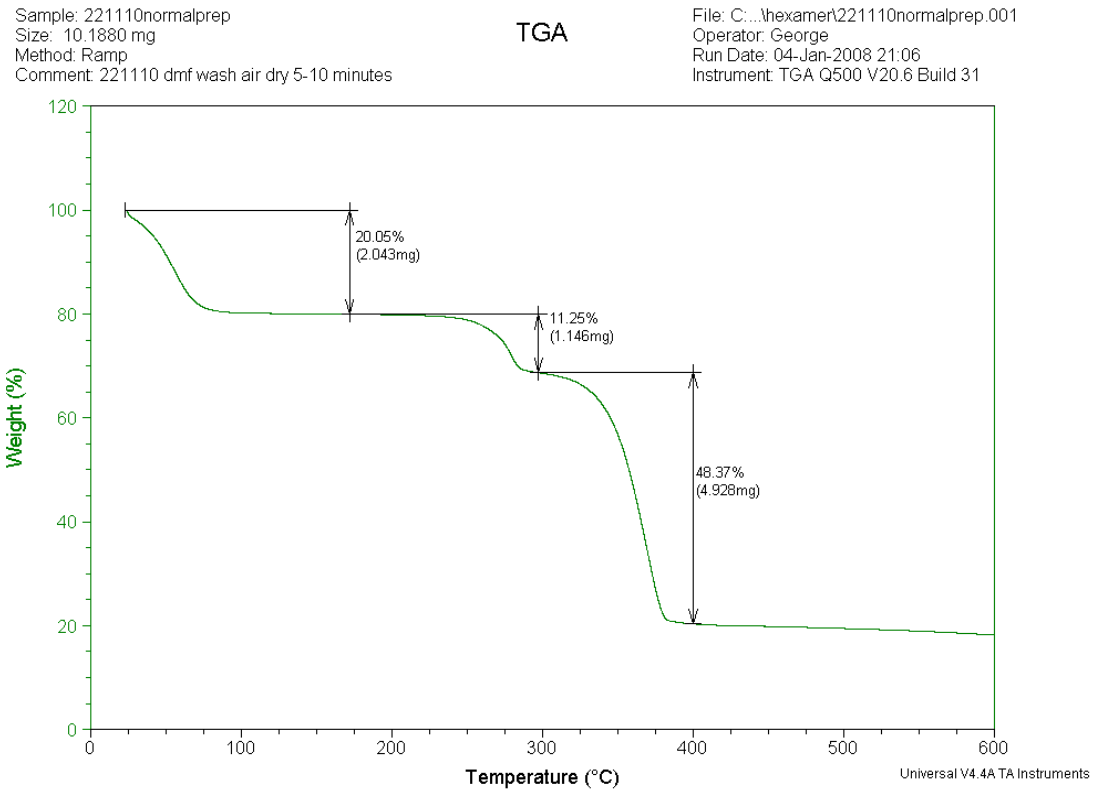

Figure 11. As synthesized thermal gravimetric analysis for **1**

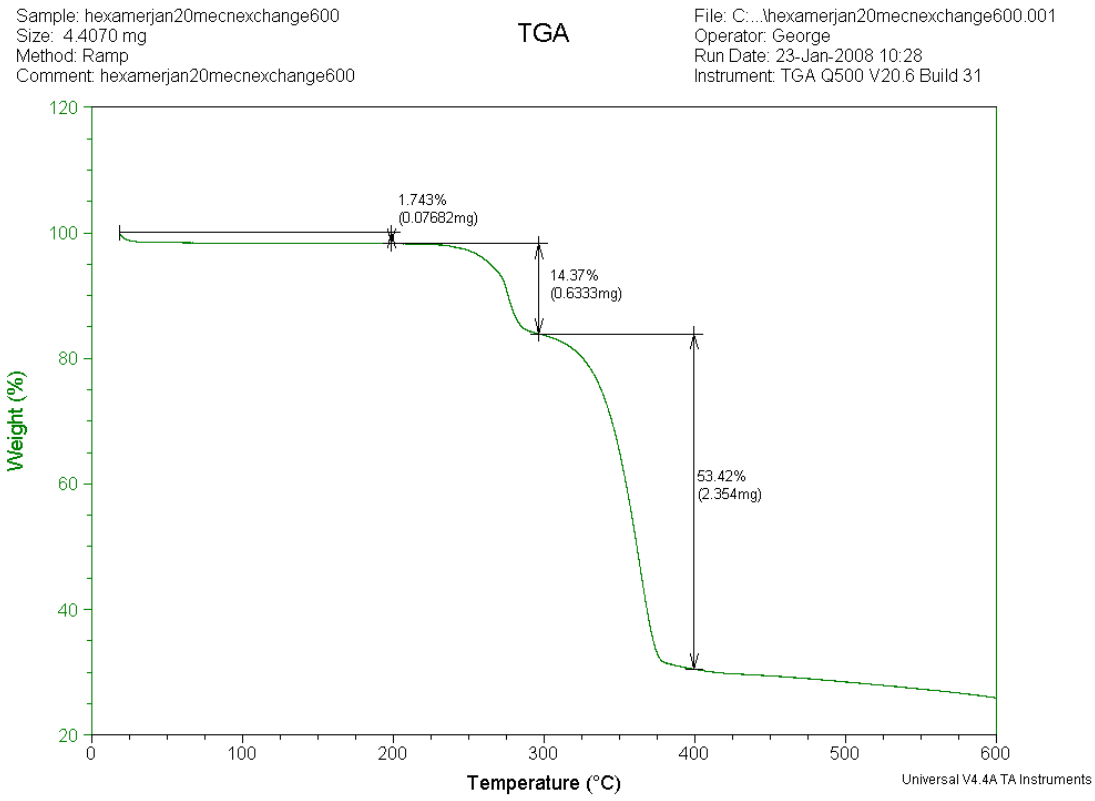

Figure 12. Thermal gravimetric analysis for acetonitrile exchanged **1**

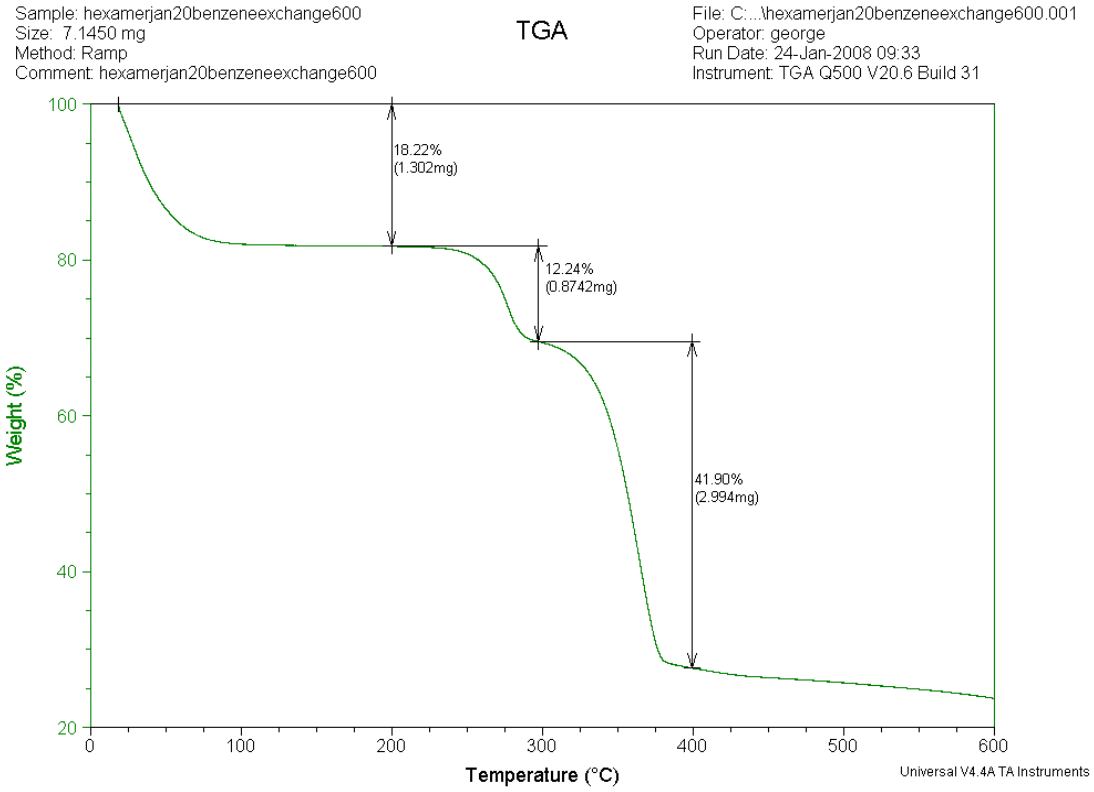

Figure 13. Thermal gravimetric analysis for benzene exchanged **1**

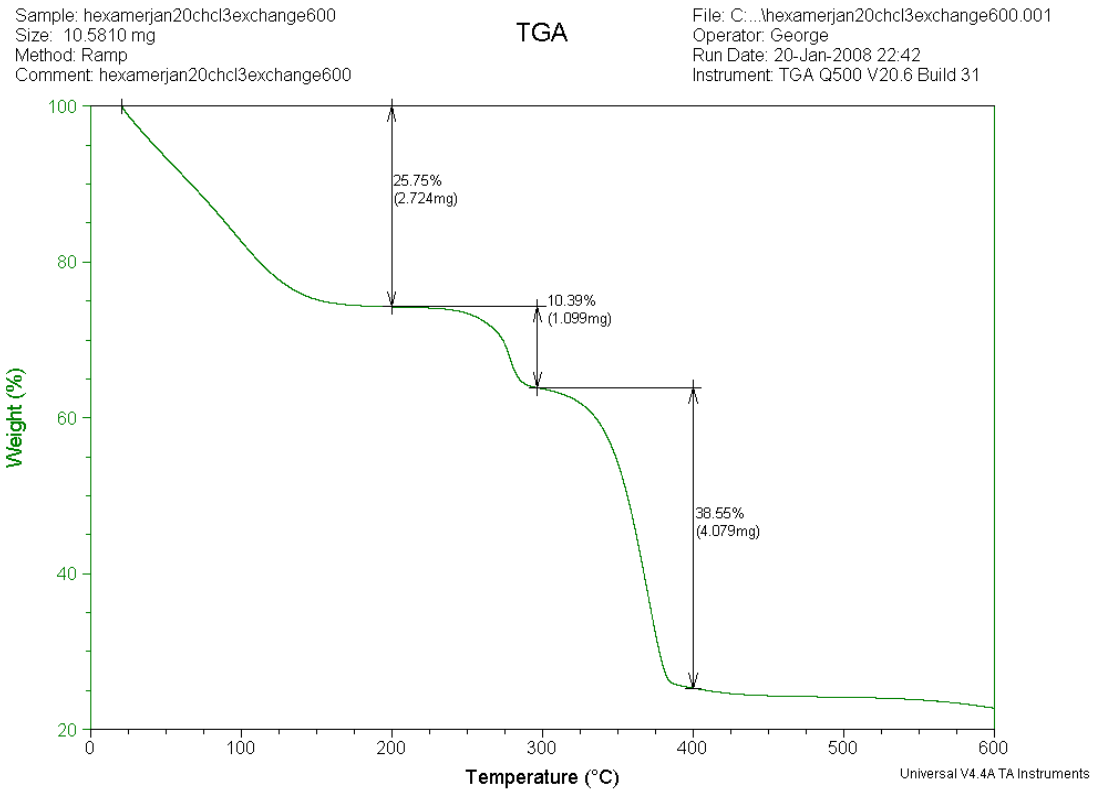

Figure 14. Thermal gravimetric analysis for chloroform exchanged **1**

2.2 Zn(HCOO)(L) (2)

Reaction of zinc tetrafluoroborate and H**L** in 25% aqueous DMF at 130 ºC led to the formation of charge-neutral 1-D chains of alternating $\mathbf{L}^-$ and zinc(II) ions. The asymmetric unit of **2** contains two ligands, two formate anions (from the hydrolysis of DMF), and two crystallographically independent zinc atoms in distorted square pyramidal geometry (**Figure 15**).

The apical sites on Zn1 and Zn2 are occupied by monodentate formate oxygens, and the remaining four sites on each zinc ion contain a tridentate terpyridine and a monodentate carbonyl from a different ligand. Selected bond lengths are given in **Table 3**. Briefly, the Zn-N distances range from 2.07 – 2.24 Å and the Zn-O distances from 1.96 -1.99 Å. Both of the zinc ions play the same role as chain-linkers in the structure (**Figure 16**), and the chains interact through weak π-stacking, with a centroid-centroid distance of 3.93 Å.

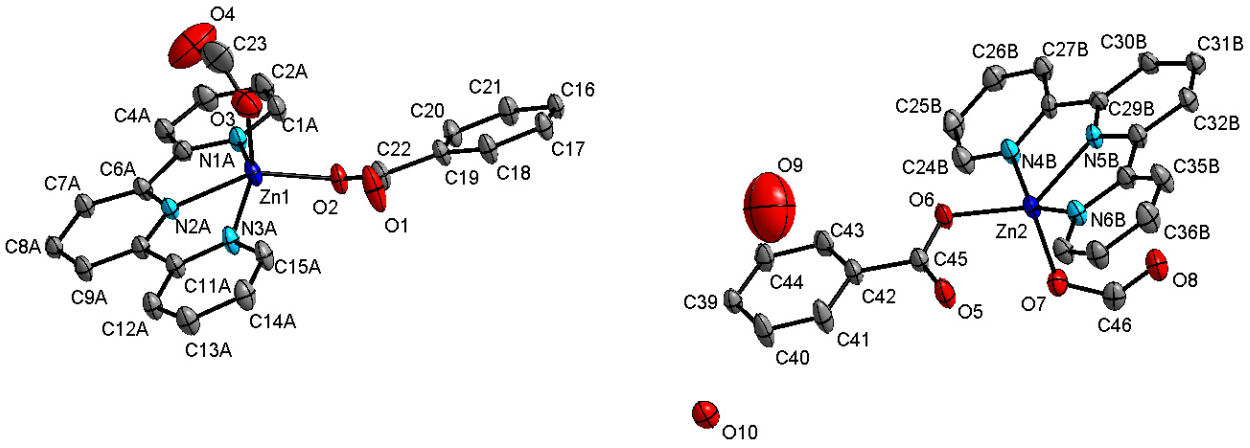

Figure 15. ORTEP plot of **2** at 30% probability

Table 3. Selected bond lengths (Å) and angles (°) for compound **2**

Zn1-O3	1.957(3)	Zn2-N4B	2.243(4)
Zn1-O2	1.979(3)	O1-C22	1.221(5)
Zn1-N2A	2.086(3)	O2-C22	1.289(5)
Zn1-N3A	2.211(3)	O3-C23	1.247(7)
Zn1-N1A	2.215(4)	O4-C23	1.218(8)
Zn2-O6	1.956(3)	O5-C45	1.229(5)
Zn2-O7	1.991(3)	O6-C45	1.277(5)
Zn2-N5B	2.086(3)	O7-C46	1.284(5)
Zn2-N6B	2.168(3)	O8-C46	1.221(5)
O3-Zn1-O2	107.34(13)	O6-Zn2-O7	103.78(11)
O3-Zn1-N2A	114.13(14)	O6-Zn2-N5B	137.37(12)
O2-Zn1-N2A	137.67(12)	O7-Zn2-N5B	115.44(12)
O3-Zn1-N3A	93.92(14)	O6-Zn2-N6B	112.20(13)
O2-Zn1-N3A	110.83(12)	O7-Zn2-N6B	102.92(12)
N2A-Zn1-N3A	75.12(12)	N5B-Zn2-N6B	75.65(12)
O3-Zn1-N1A	108.46(15)	O6-Zn2-N4B	85.13(12)
O2-Zn1-N1A	85.18(12)	O7-Zn2-N4B	98.32(13)
N2A-Zn1-N1A	74.33(12)	N5B-Zn2-N4B	73.71(12)
N3A-Zn1-N1A	147.50(12)	N6B-Zn2-N4B	148.01(12)

Symmetry transformations used to generate equivalent atoms:
A. -x+1,y+1/2,-z+3/2 B. -x,y-1/2,-z+1/2

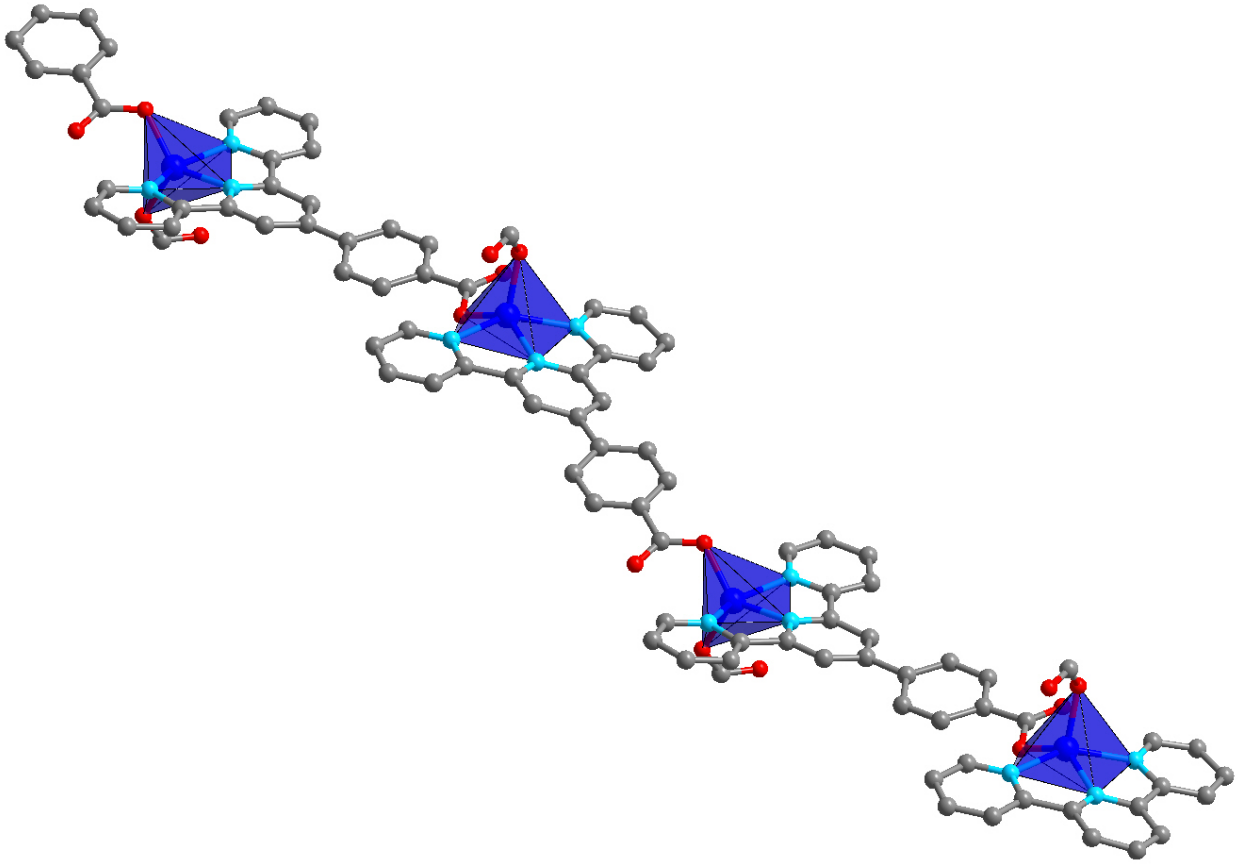

Figure 16. Crystal structure of **2**
Hydrogen atoms are omitted for clarity.
Color key: Zn (dark blue), N (light blue), O (red), C (dark gray)

2.3 $Zn_2(HL)(L)_2(BF_4)_2$ (3)

Heating a mixture of H**L** and zinc(II) tetrafluoroborate in water at 180 ºC produced yellow crystals of 1-D polymer **3**. X-ray diffraction revealed two crystallographically independent zinc atoms in the asymmetric unit (**Figure 17**). Zn1 adopts a distorted square pyramidal geometry and is coordinated by one carboxylate oxygen from each of two ligands and a terpyridine from another ligand. The bond lengths around Zn1 are typical, ranging from 1.96 – 2.18 Å, and the angles span from 76.5 – 151.0 Å. Zn2 adopts a pseudo octahedral geometry, being chelated by two terpyridine moieties (bond lengths: 2.08 – 2.19 Å). The extended structure of **3** is a 1-D chain built up of $[Zn(\mathbf{L})_2]$ complexes bound together at the carboxylate ends by zinc ions (**Figure 18**).

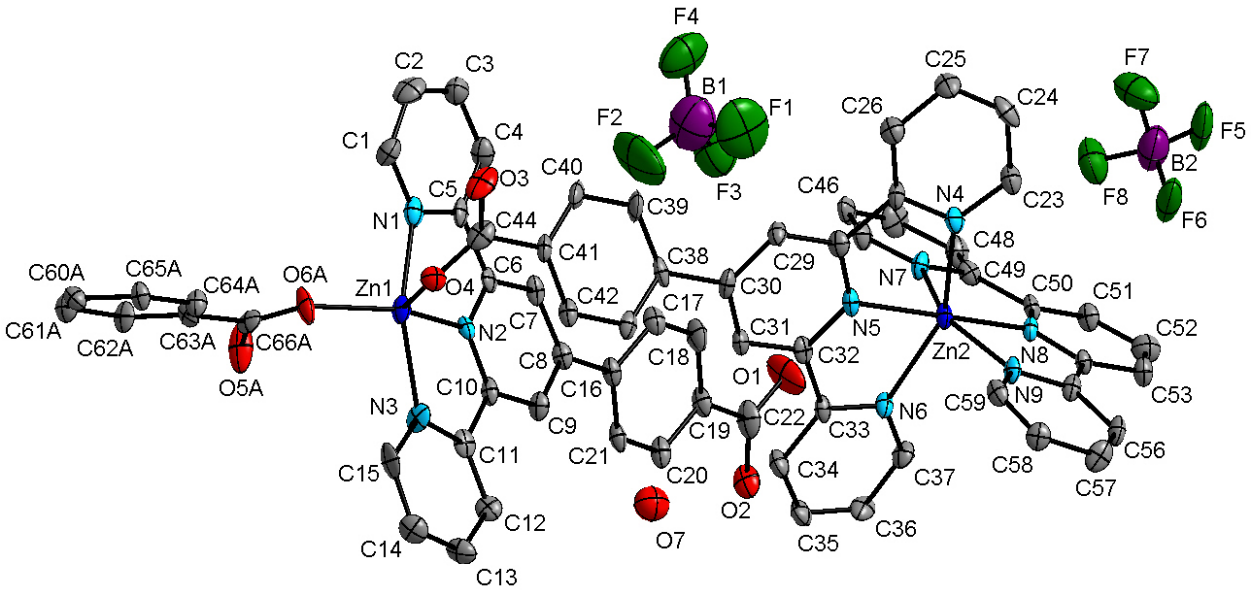

Figure 17. ORTEP plot of **3** at 30% probability

Table 4. Selected bond lengths (Å) and angles (°) for compound **3**

Zn1-O4	1.962(7)	Zn2-N6	2.190(7)
Zn1-O6A	1.964(6)	Zn2-N7	2.193(7)
Zn1-N2	2.060(7)	O1-C22	1.265(13)
Zn1-N3	2.162(8)	O2-C22	1.283(13)
Zn1-N1	2.179(9)	O3-C44	1.251(12)
Zn2-N8	2.075(6)	O4-C44	1.276(12)
Zn2-N5	2.083(7)	O5-C66	1.235(11)
Zn2-N9	2.149(7)	O6-C66	1.231(11)
Zn2-N4	2.171(8)		
O4-Zn1-O6A	93.1(3)	N8-Zn2-N4	107.6(3)
O4-Zn1-N2	122.6(3)	N5-Zn2-N4	75.4(3)
O6A-Zn1-N2	144.2(3)	N9-Zn2-N4	94.5(3)
O4-Zn1-N3	102.1(3)	N8-Zn2-N6	101.2(3)
O6A-Zn1-N3	100.0(3)	N5-Zn2-N6	75.5(3)
N2-Zn1-N3	76.5(3)	N9-Zn2-N6	95.7(3)
O4-Zn1-N1	95.8(3)	N4-Zn2-N6	151.0(3)
O6A-Zn1-N1	101.6(3)	N8-Zn2-N7	75.3(3)
N3-Zn1-N1	151.0(3)	N5-Zn2-N7	98.3(3)
N8-Zn2-N5	172.8(3)	N9-Zn2-N7	151.7(3)
N8-Zn2-N9	76.5(3)	N4-Zn2-N7	92.5(3)
N5-Zn2-N9	110.0(3)	N6-Zn2-N7	91.2(3)

Symmetry transformations used to generate equivalent atoms:
A. x+1,y,z+1

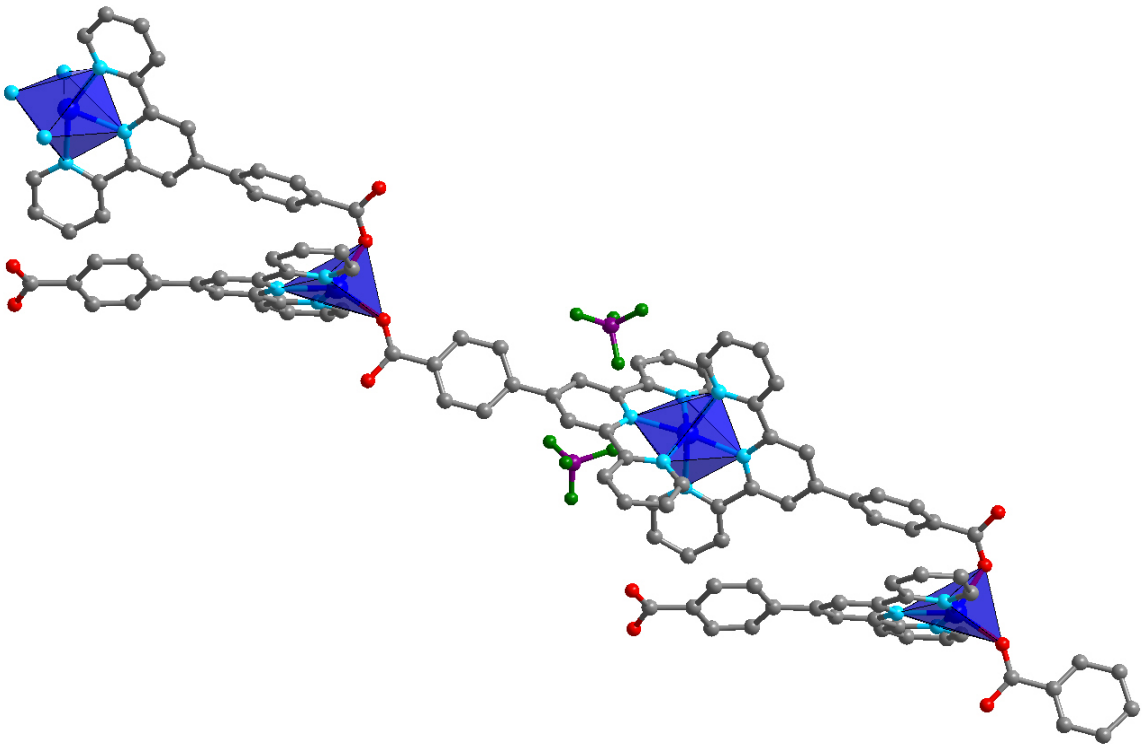

Figure 18. Supramolecular structure of **3**
Hydrogen atoms are omitted for clarity.
Color key: Zn (dark blue), N (light blue), O (red), C (dark gray), F (green), B (purple)

2.4 $Zn_4(\mu\text{-}OH)(L)_4(HCOO)(BF_4)$ (4)

Reaction of H**L** and zinc (II) tetrafluoroborate in 75 % aqueous DMF at 130 ºC led to the formation of two-dimensional compound **4**. Single crystal X-ray diffraction revealed two crystallographically independent Zn^{2+} metal centers in the asymmetric unit. Although the coordination environment around Zn2 is clearly distorted square pyramidal, the crystal data did not allow for accurate determination of the coordination environment around Zn1. The lack of accurate atomic coordinates extended to O3, O4, and C38-C44, although the remainder of the framework structure was clearly visible.

Zn1 is surrounded by one carbonyl oxygen and one tridentate terpyridine from two ligands (**Figure 19**). One coordination site on Zn1 is occupied by a hydroxide ion bridging it to a crystallographically identical Zn^{2+} ion (Zn-O 1.90 Å, Zn-O-Zn 136º). These atoms make up a dinuclear building unit, Zn_2[μ-OH], which acts as a three-connected node in the structure. Zn2 adopts a distorted square pyramidal geometry with a monodentate formate in the apical position. The bond lengths to Zn2 are typical, spanning from 1.93 – 2.05 Å, and the angles range from 57.5 – 152.1.º

The **L**-Zn2-**L** groups act as bent linkers bridging together each Zn1 ion, forming a two-dimensional structure (**Figure 20**). If each coplanar Zn1 ion is connected by a line, the structure can be simplified to a grid (**Figure 21**). These grids are interwoven as depicted in **Figure 22**. Charge balancing BF_4^- ions (not located by crystallography) excluded, the supramolecular structure of **4** is a matrix of very small connected cavities (~4.5 Å, **Figures 23** – **25**). Analysis of the structure with PLATON[88] reveals 21% of the crystal structure volume is accessible to solvent (after subtraction of 7% for the presence of charge compensating BF_4^- ions). Sorption experiments are required to determine if these cavities are accessible to gas molecules.

Table 5. Crystallographic data for compounds **4**-**6**

Identification code	$Zn_4(\mu\text{-}OH)(\mathbf{L})_4(HCOO)(BF_4)_2$ (**4**)	$Zn_2(\mu\text{-}OH)(\mathbf{L})_2(BF_4)$ (**5**)	$Pb(\mathbf{L})(NO_3)\cdot 1.3(H_2O)1.3(DMF)$ (**6**)
Empirical formula	$C_{360}N_{48}O_{52}Zn_{16}$	$C_{352}H_{192}N_{48}O_{152}Zn_{16}$	$C_{352}H_{272}N_{64}O_{104}Pb_{16}$
Formula weight	7354.32	8571.78	10377.38
Temperature	173(2) K	173(2) K	173(2) K
Crystal system	Tetragonal	Tetragonal	Tetragonal
Space group	I-4 (#82)	I-42d (#122)	P4/ncc (#130)
Unit cell dimensions	a = 14.9993(15) Å	a = 14.549(4) Å	a = 25.7511(18) Å
	b = 14.9993(15) Å	b = 14.549(4) Å	b = 25.7511(18) Å
	c = 41.776(8) Å	c = 47.06(2) Å	c = 17.0110(17) Å
	α= 90°	α= 90°	α= 90°
	β= 90°	β= 90°	β= 90°
	γ = 90°	γ = 90°	γ = 90°
Volume	9399(2) $Å^3$	9961(6) $Å^3$	11280.3(16) $Å^3$
Z	1	1	1
Density (calculated)	1.299 Mg/m^3	1.429 mg/m^3	1.528 mg/m^3
Goodness-of-fit on F2	1.342	0.974	1.031
Final R indices [I>2sigma(I)]	R1 = 0.1386, wR2 = 0.2939	R1 = 0.1183, wR2 = 0.2735	R1 = 0.0653, wR2 = 0.1769
R indices (all data)	R1 = 0.3066, wR2 = 0.3445	R1 = 0.2944, wR2 = 0.3443	R1 = 0.1466, wR2 = 0.2172
Largest diff. peak and hole	1.194 and -0.713 $e.Å^{-3}$	0.929 and -0.546 $e.Å^{-3}$	1.816 and -0.702 $e.Å^{-3}$

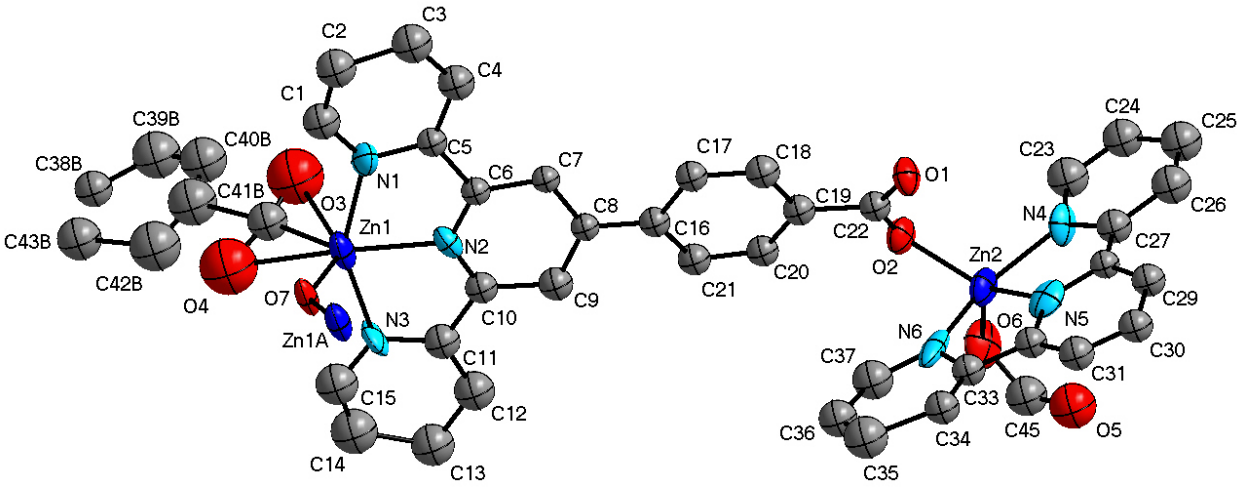

Figure 19. ORTEP plot of **4** at 30% probability

Table 6. Selected bond lengths (Å) and angles (°) for compound **4**

Zn1-O7	1.903(4)	Zn2-N4	2.053(12)
Zn1-C44	2.06(2)	Zn2-N5	2.120(12)
Zn1-N2	2.110(10)	O1-C22	1.217(15)
Zn1-N1	2.173(12)	O2-C22	1.249(16)
Zn1-N3	2.210(12)	O3-C44	1.14(2)
Zn1-O4	2.46(2)	O4-C44	1.24(3)
Zn1-O3	2.47(2)	O5-C45	1.25(2)
Zn2-O6	1.930(12)	O6-C45	1.35(2)
Zn2-O2	1.960(9)	O7-Zn1A	1.903(4)
Zn2-N6	2.009(19)		
O7-Zn1-C44	111.4(7)	C44-Zn1-O3	27.4(7)
O7-Zn1-N2	117.0(4)	N2-Zn1-O3	106.8(6)
C44-Zn1-N2	131.5(7)	N1-Zn1-O3	86.8(6)
O7-Zn1-N1	94.1(3)	N3-Zn1-O3	101.4(6)
C44-Zn1-N1	103.5(7)	O4-Zn1-O3	57.5(7)
N2-Zn1-N1	76.0(4)	O6-Zn2-O2	99.3(5)
O7-Zn1-N3	99.0(3)	O6-Zn2-N6	98.3(5)
C44-Zn1-N3	95.5(7)	O2-Zn2-N6	90.6(4)
N2-Zn1-N3	75.0(4)	O6-Zn2-N4	100.2(5)
N1-Zn1-N3	151.0(4)	O2-Zn2-N4	106.7(5)
O7-Zn1-O4	83.9(7)	N6-Zn2-N4	152.1(5)
C44-Zn1-O4	30.2(7)	O6-Zn2-N5	125.8(5)
N2-Zn1-O4	154.4(6)	O2-Zn2-N5	133.6(4)
N1-Zn1-O4	119.2(6)	N6-Zn2-N5	74.1(5)
N3-Zn1-O4	88.0(6)	N4-Zn2-N5	78.1(5)
O7-Zn1-O3	135.1(6)		

Symmetry transformations used to generate equivalent atoms:
A. -x-1,-y,z B. x-1/2,y+1/2,z+1/2

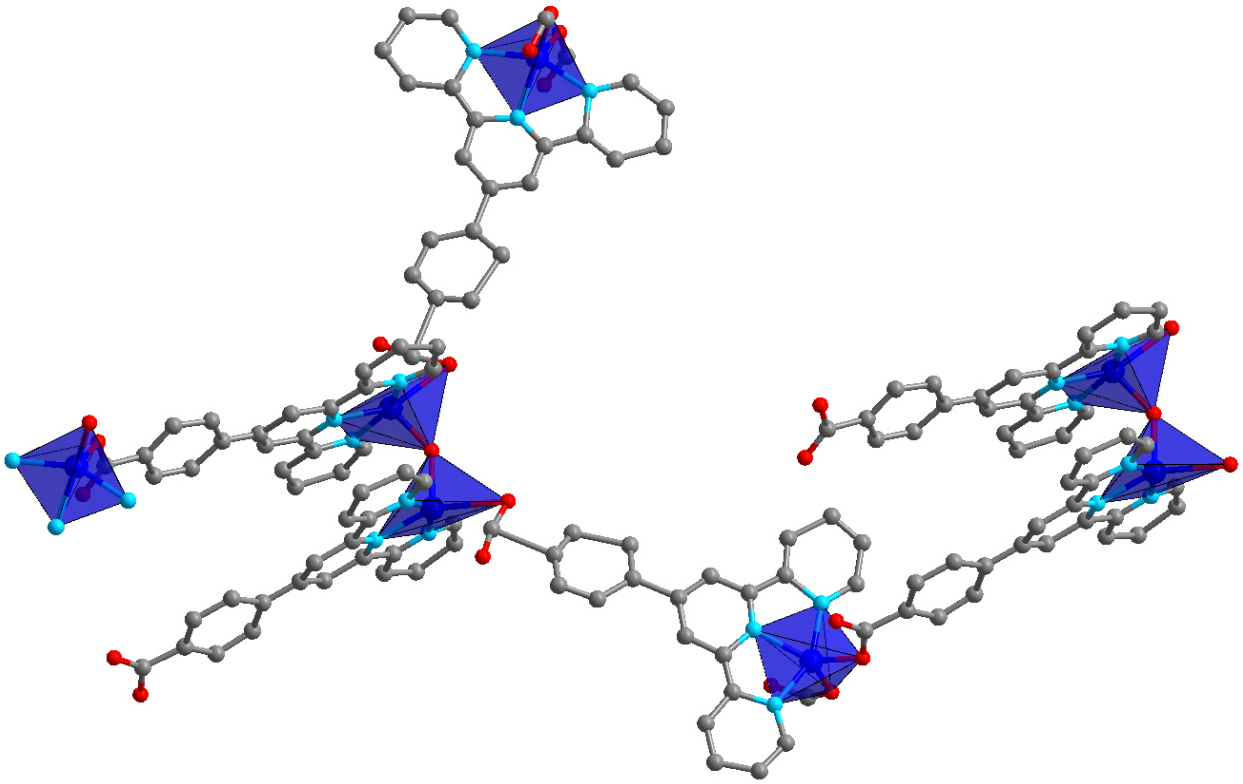

Figure 20. Connectivity of the building units in **4**
Hydrogen atoms are omitted for clarity.
Color key: Zn (dark blue), N (light blue), O (red), C (dark gray)

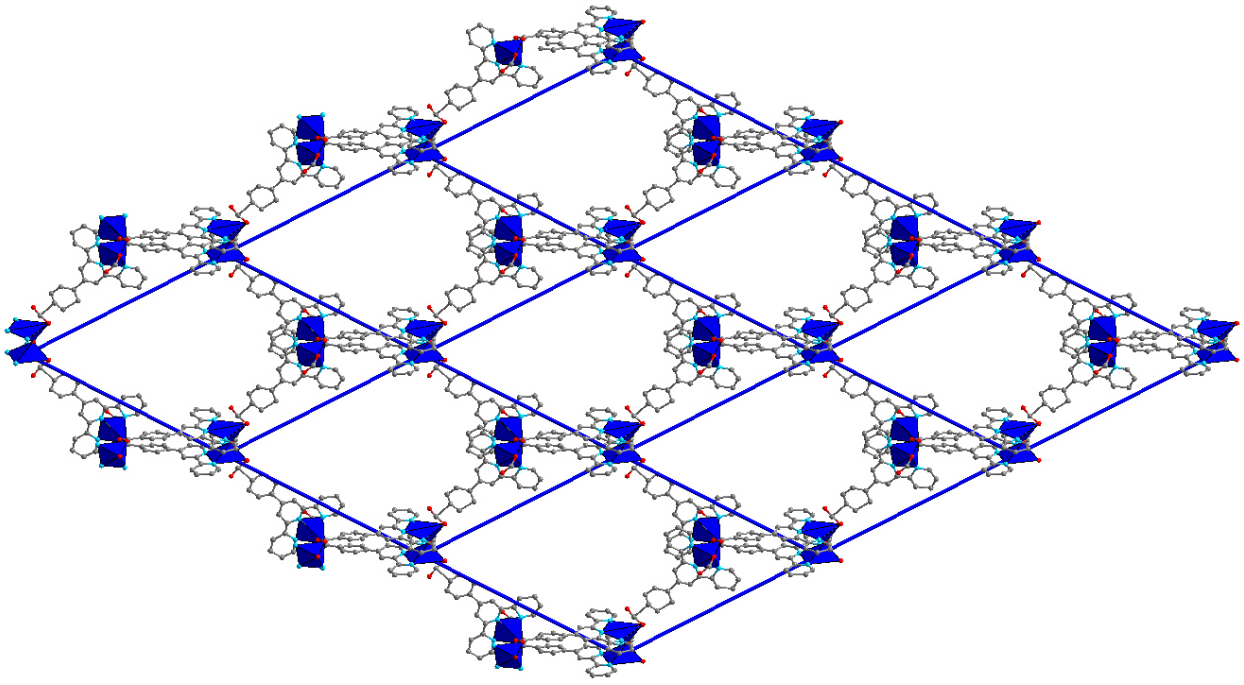

Figure 21. The grid-like structure of one independent net in **4**
Hydrogen atoms are omitted for clarity.
Color key: Zn (dark blue), N (light blue), O (red), C (dark gray)

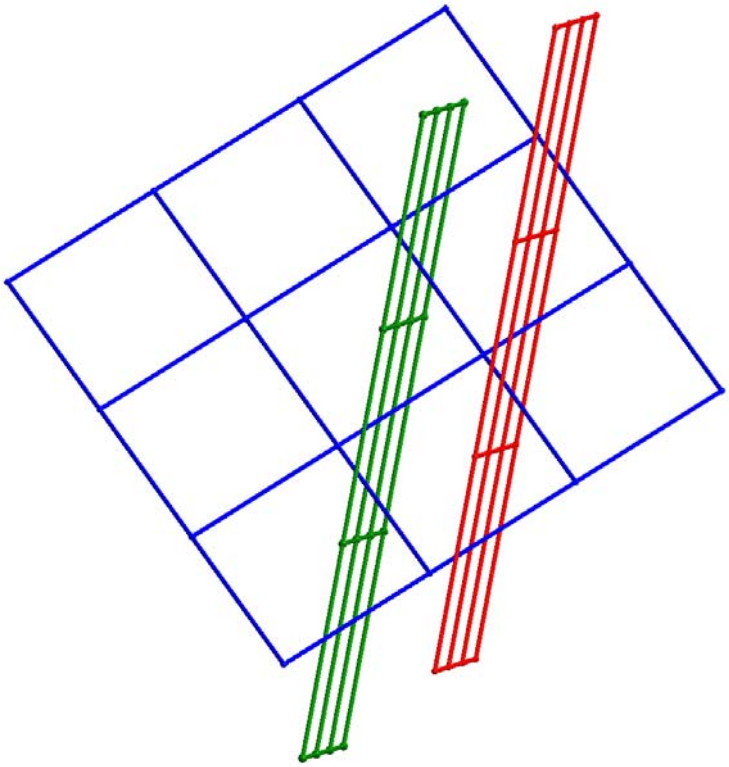

Figure 22. Scheme depicting the interweaving of **4**

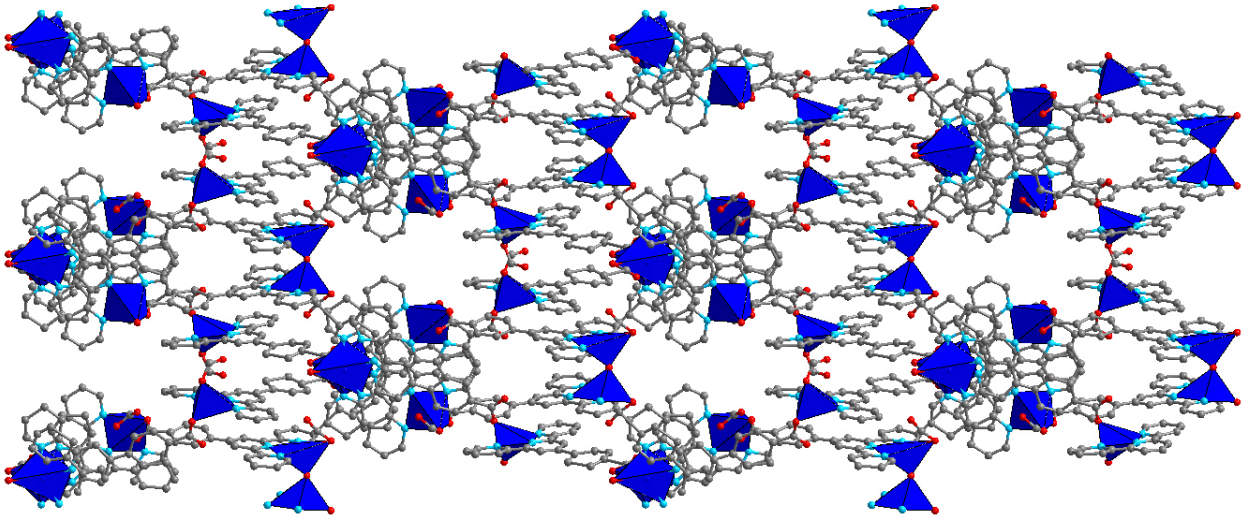

Figure 23. Supramolecular structure of **4**
Hydrogen atoms are omitted for clarity.
Color key: Zn (dark blue), N (light blue), O (red), C (dark gray)

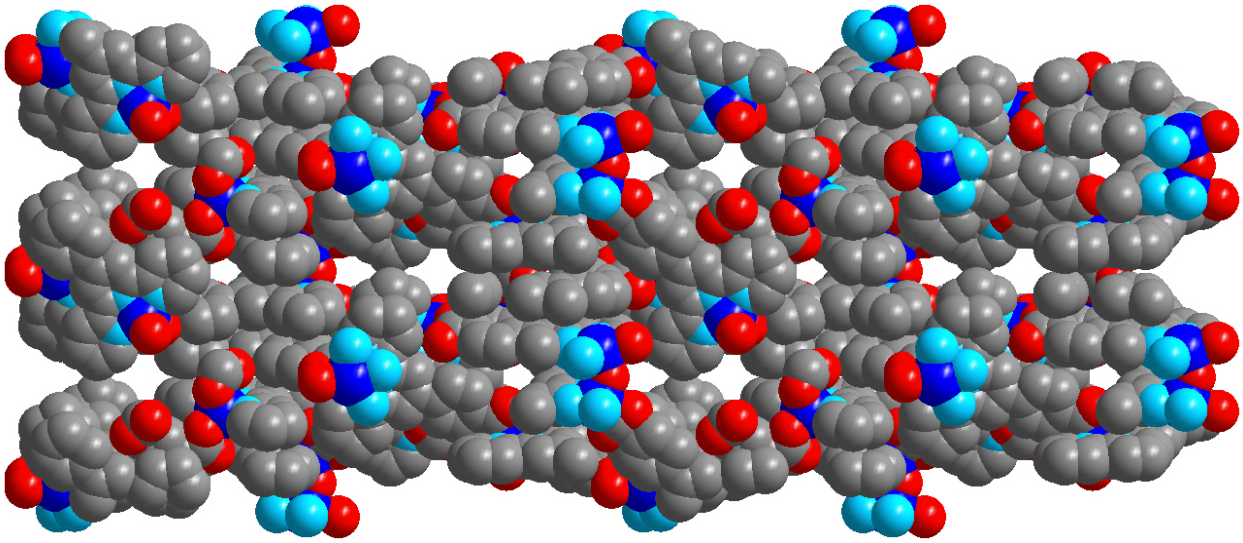

Figure 24. Space-fill representation of **4**
Hydrogen atoms are omitted for clarity.
Color key: Zn (dark blue), N (light blue), O (red), C (dark gray)

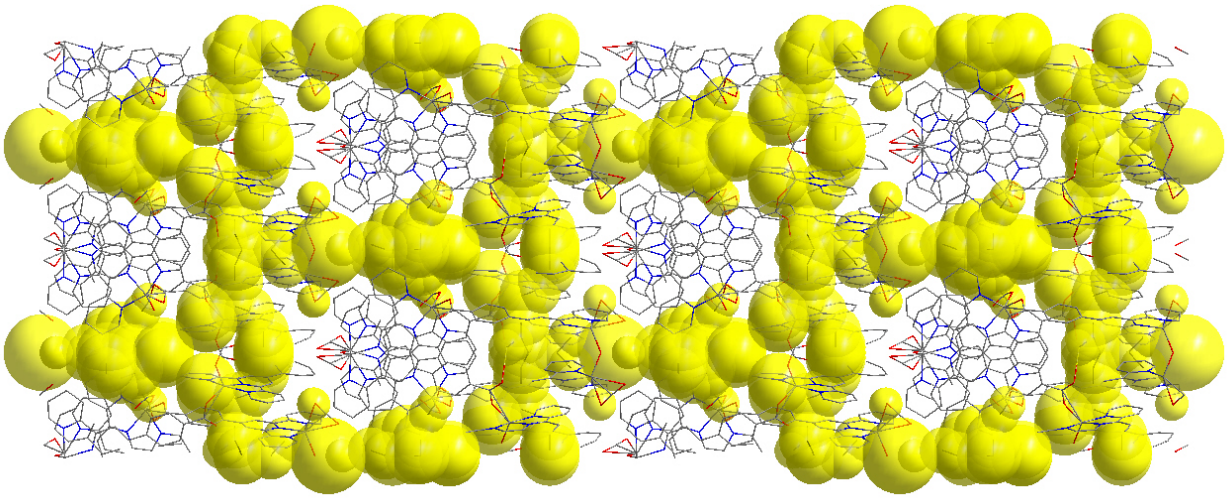

Figure 25. Line representation of **4** with the pore space represented by yellow spheres
Hydrogen atoms are omitted for clarity.
Color key: Zn (dark blue), N (light blue), O (red), C (dark gray)

2.5 $Zn_2(\mu\text{-}OH)(L)_2(BF_4)$ (5)

Reaction of H**L** and zinc(II) tetrafluoroborate in the presence of HBF_4, KOH, and Na_2SiO_3 with water as solvent at 180 ºC led to a three-dimensional net (**5**). The building unit, a hydroxyl bridged dinuclear zinc center (Zn_2[μ-OH]), is similar to that found in structure **4** (**Figure 19**). The crystallographically distinct zinc ion adopts a distorted square pyramidal geometry, with the bridging hydroxyl in the apical position (**Figure 26**). The dinuclear zinc(II) center observed in **4** and **5** has been observed in discrete molecular complexes,[89] and the bond lengths and angles are consistent with a bridging hydroxyl group (Zn-O 1.92 Å, Zn-O-Zn 156º). The equatorial positions on Zn1 are occupied by a chelating terpyridine (Zn-N 2.10 – 2.17 Å) and a carboxylate oxygen (Zn-O 1.93 Å) from a different ligand.

Structure **5** has the topology of Si in the $ThSi_2$[18] and is 2-fold interpenetrated (**Figures 27 – 29**). Analysis with PLATON[88] revealed the largest sphere that can be made inside the framework without contacting the van der walls surface of the structure is 5.4 Å in diameter (neglecting the charge-balancing BF_4^- ions). The solvent accessible space within the framework is 30% (including 7% subtracted for tetrafluoroborate ions) of the crystal volume.

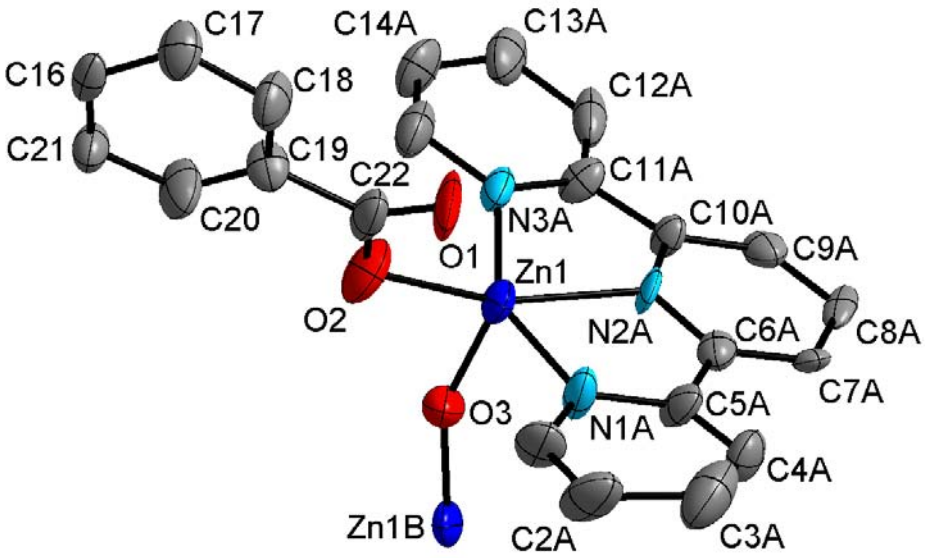

Figure 26. ORTEP plot of **5** at 30% probability

Table 7. Selected bond lengths (Å) and angles (°) for compound **5**

Zn1-O3	1.918(3)	O3-Zn1B	1.918(3)
Zn1-O2	1.933(10)	Zn1-N3A	2.171(12)
Zn1-N2A	2.095(8)	O1-C22	1.239(18)
Zn1-N1A	2.124(10)	O2-C22	1.292(19)
O3-Zn1-O2A	92.0(5)	N2A-Zn1-N1A	77.2(4)
O3-Zn1-N2A	102.5(4)	O3-Zn1-N3A	94.5(2)
O2-Zn1-N2A	163.5(5)	O2-Zn1-N3A	97.7(4)
O3-Zn1-N1A	98.2(4)	N2A-Zn1-N3A	73.5(4)
O2-Zn1-N1A	108.9(4)	N1A-Zn1-N3A	150.0(3)

Symmetry transformations used to generate equivalent atoms:
A. -y-1/2,-x-1,z-1/4 B. -x,-y-1,z

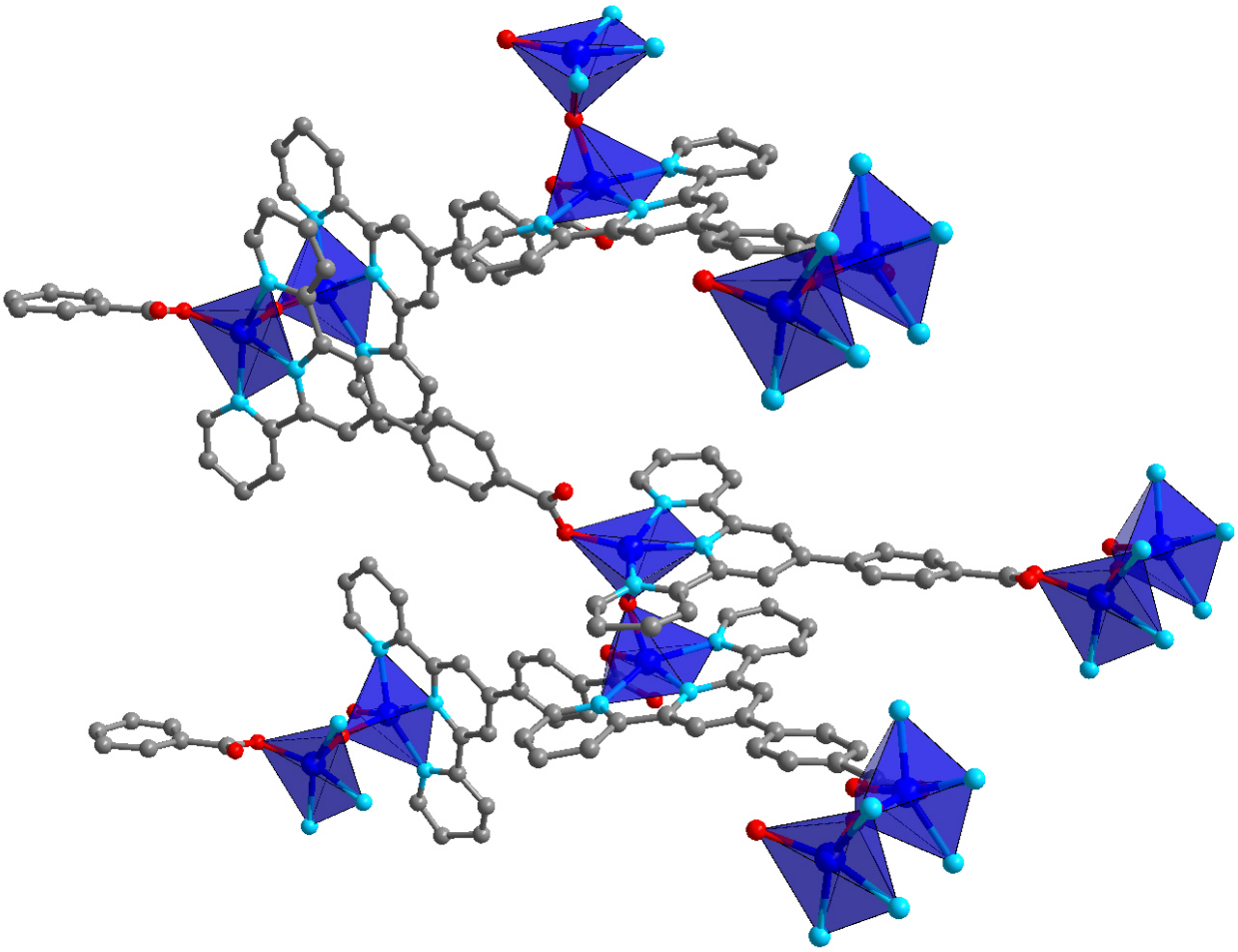

Figure 27. Basic connectivity of the building units in **5**
Hydrogen atoms are omitted for clarity.
Color key: Zn (dark blue), N (light blue), O (red), C (dark gray)

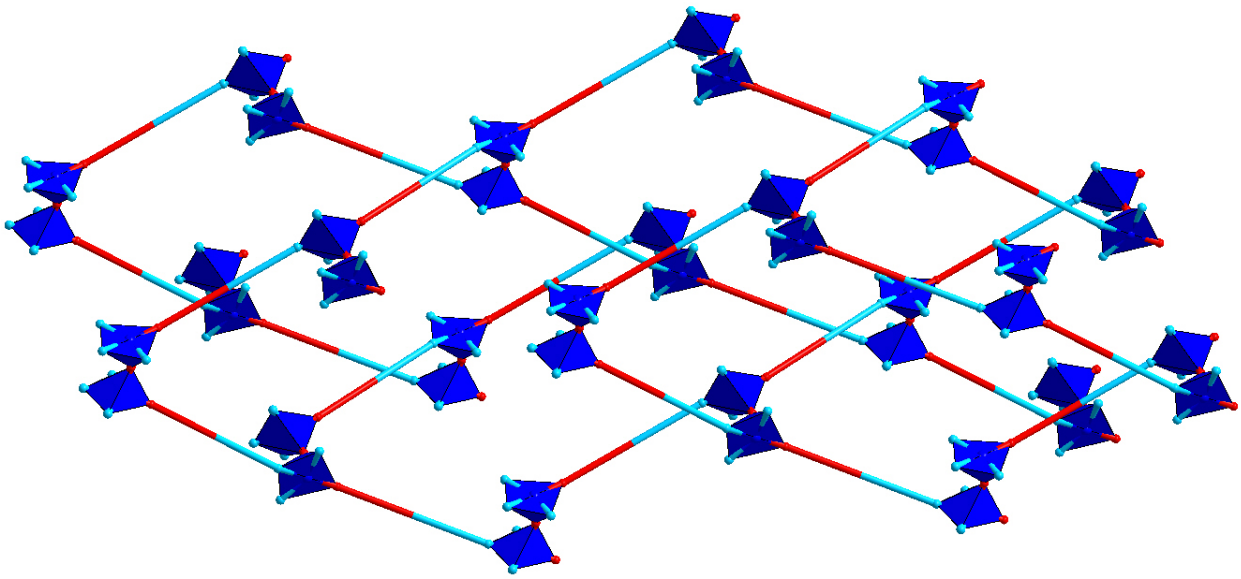

Figure 28. A segment of the $ThSi_2$ net in **5**. Terpyridine ends of **L** ligands are represented as blue lines, carboxylate ends as red lines

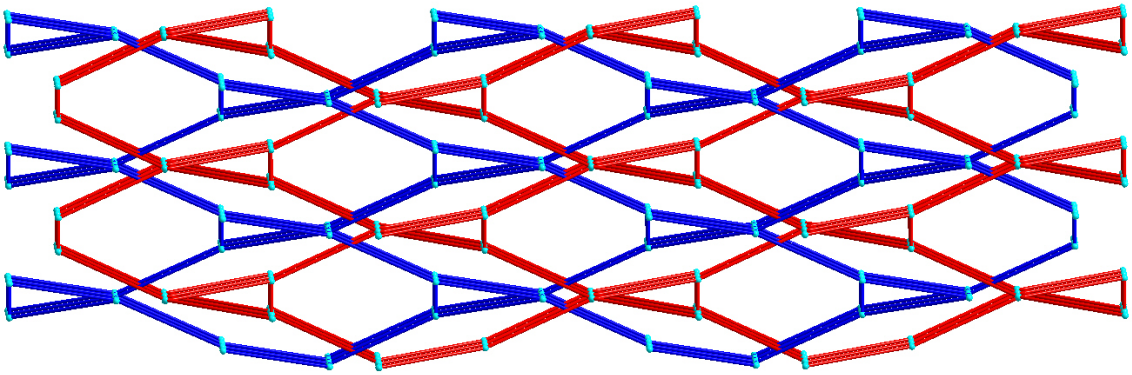

Figure 29. Line representation of the net of **5**. Red and blue represent the two independent interpenetrated $ThSi_2$ nets

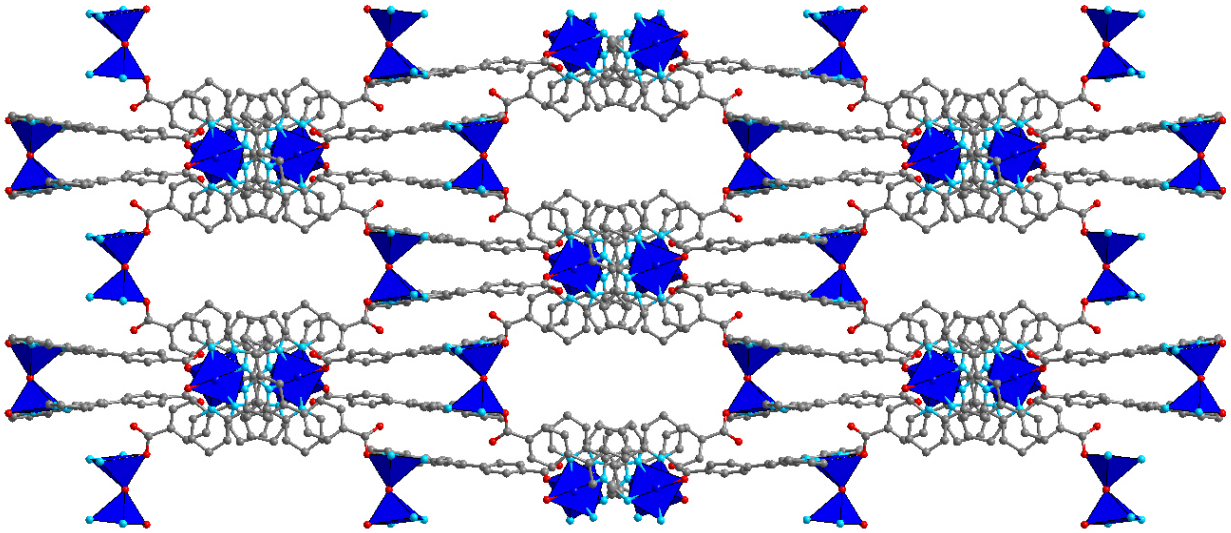

Figure 30. Supramolecular structure of **5**, viewed down the *a* or *b* axis. Anions are omitted Hydrogen atoms are omitted for clarity.
Color key: Zn (dark blue), N (light blue), O (red), C (dark gray)

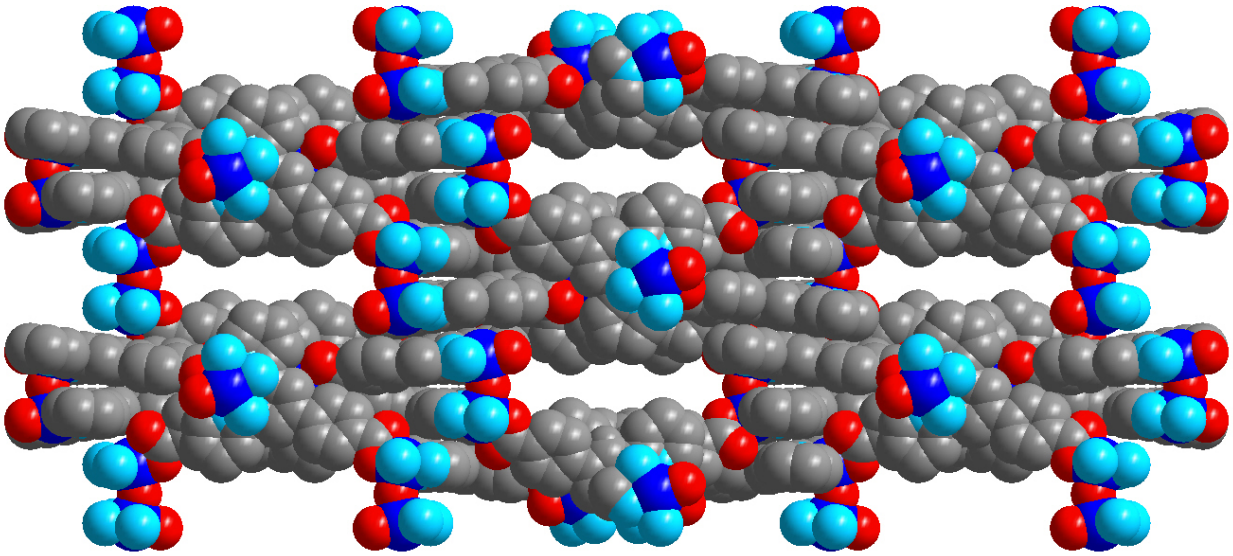

Figure 31. Space-fill representation of **5**, viewed down the *a* or *b* axis
Hydrogen atoms are omitted for clarity.
Color key: Zn (dark blue), N (light blue), O (red), C (dark gray)

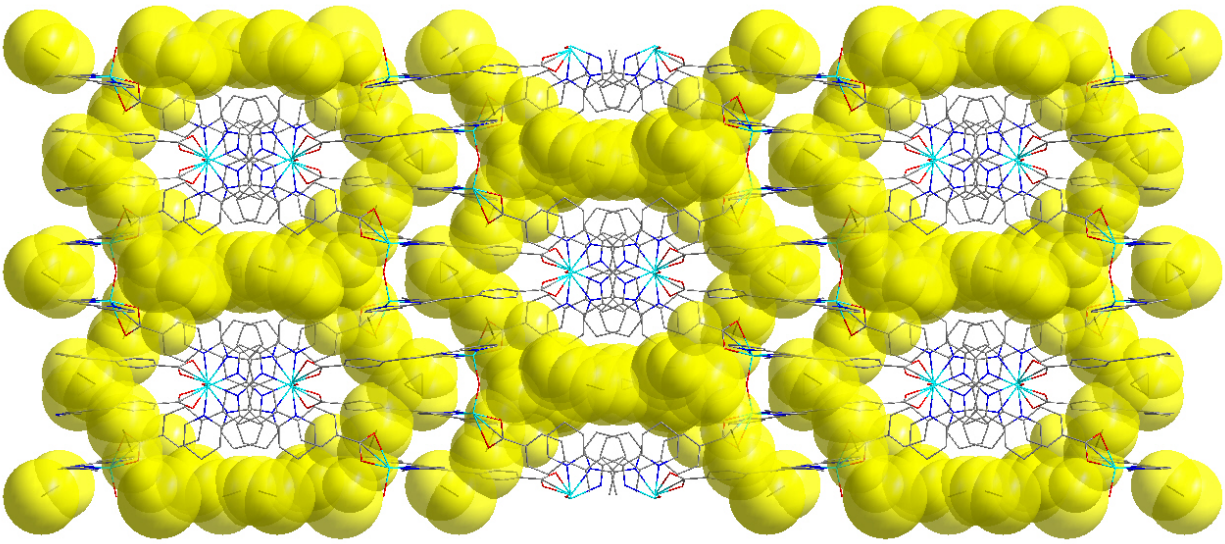

Figure 32. Line representation of **5**, with the pore space represented by yellow spheres Hydrogen atoms are omitted for clarity.
Color key: Zn (light blue), N (dark blue), O (red), C (dark gray)

2.6 $Pb(L)(NO_3)\cdot 1.3(H_2O)1.3(DMF)$ (6)

Colorless blocks of **6** were produced by heating a solution of lead(II) nitrate and H**L** in DMF in a sealed vial for one day. Single crystal X-ray diffraction revealed one independent lead(II) cation, one $\mathbf{L}^-$ anion, and one disordered nitrate anion in the asymmetric unit. If a minimum bond threshold of 3 Å is used for heteroatom-Pb^{2+} distances, the metal center is eight coordinated (**Figure 33**). The bond lengths to the coordinated carboxylate oxygens, coordinated nitrogens and coordinated water oxygens are 2.36 – 2.88 Å, 2.54 – 2.56 Å and 2.56 – 2.97 Å, respectively.

The secondary building unit (SBU) in **6** is a lead-oxide circle, with carboxylate oxygens from four ligands bridging together four lead ions (**Figure 34**). The center of the circle is occupied by two disordered crystallographically distinct water molecules. This SBU is surrounded by eight ligands to form a square grid structure, where each pair of ligands is bound through pi-stacking interactions (difference between least square planes fitted to two ligands is ~ 3.4 Å. **Figures 35** and **36**). The largest sphere able to be made in the framework without contacting the van der Waals surface is 10.5 Å (this value does not include the nitrate ions, which are disordered throughout the pores), and the solvent accessible void volume is on the order of 30%.[88]

EA and PXRD studies on compound **6** indicate it was obtained as a pure phase (**Figures 59** and **60**). A combination of EA, TGA , and PXRD studies confirms the compound is stable up to 280 °C in the absence of solvent. The 17.4 % weight loss between 20 and 200 °C for the as synthesized sample (**Figure 37**) corresponds reasonably well to the theoretical value of 13.6 % determined by EA. The 3.8 % discrepancy may result from the absorption of atmospheric moisture between heating and elemental analysis.

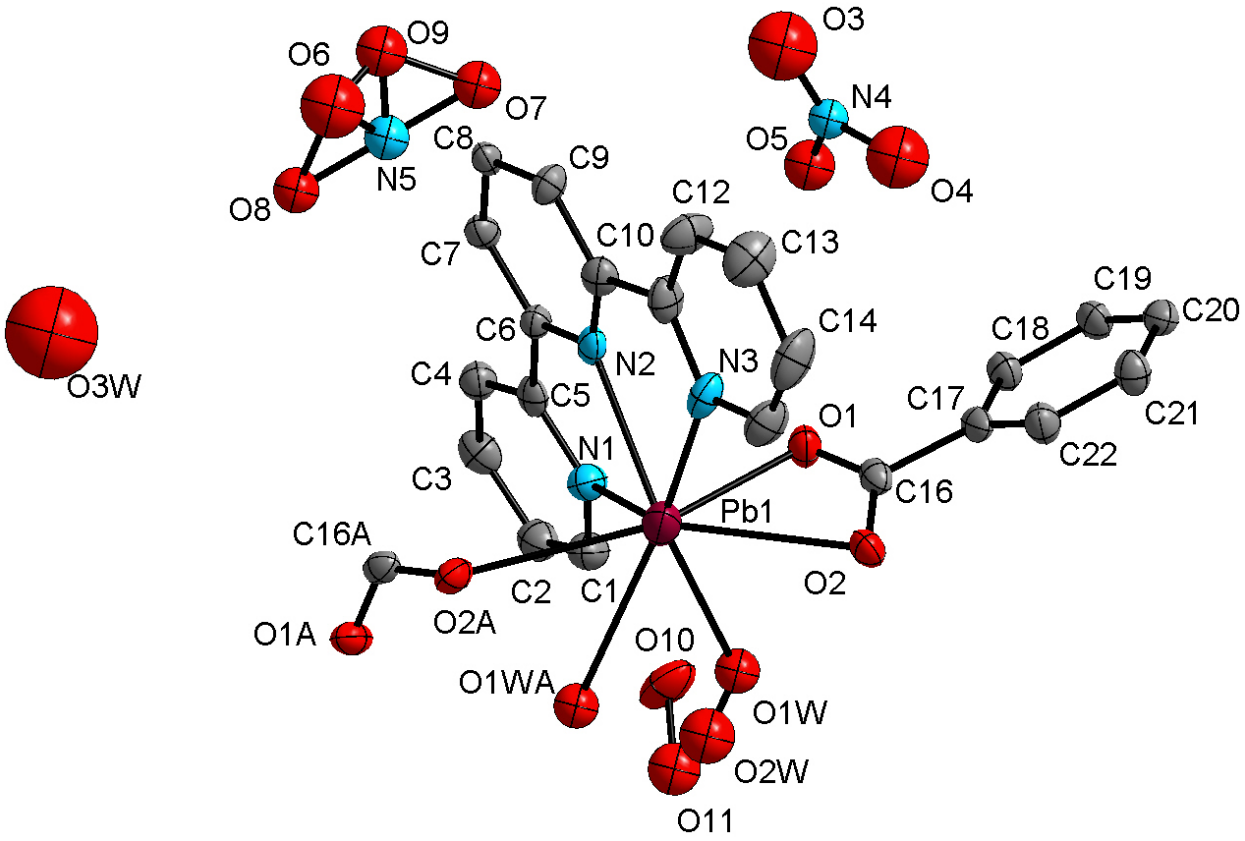

Figure 33. ORTEP plot of **6** at 30% probability

Table 8. Selected bond lengths (Å) and angles (°) for compound **6**

Pb1-O1	2.364(8)	Pb1-O2A	2.88(1)
Pb1-N2	2.542(10)	Pb1-O1WA	2.97(1)
Pb1-N1	2.551(11)	Pb1-O2	2.78(1)
Pb1-N3	2.556(12)	O1-C16	1.264(14)
Pb1-O1W	2.56(2)	O2-C16)	1.241(15)
N1-Pb1-N3	126.2(3)	O1-Pb1-O1W	78.3(5)
O1-Pb1-N1	80.5(3)	N2-Pb1-O1W	142.1(5)
N2-Pb1-N1	64.2(3)	N1-Pb1-O1W	81.1(5)
O1-Pb1-N3	80.8(3)	N3-Pb1-O1W	141.8(5)
N2-Pb1-N3	63.2(3)		

Symmetry transformations used to generate equivalent atoms:
A. -y+1/2,x,z B. y,-x+1/2,z C. -x+1/2,-y+1/2,z

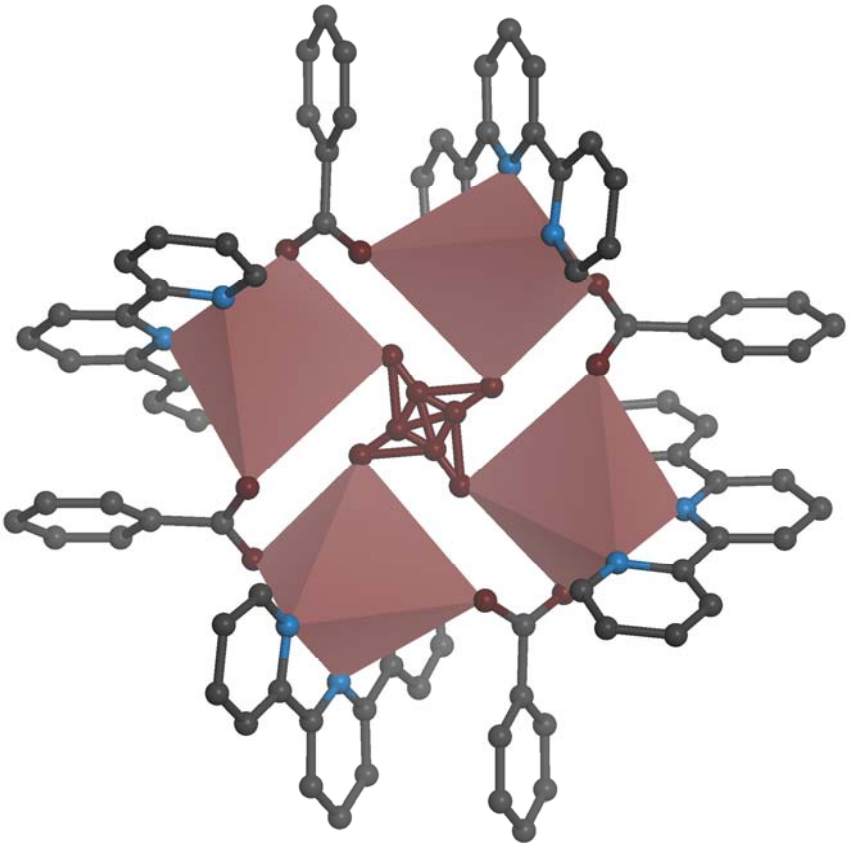

Figure 34. The basic building unit of **6** viewed down the *c* axis
Hydrogen atoms are omitted for clarity.
Color key: Pb (maroon), N (dark blue), O (red), C (dark gray)

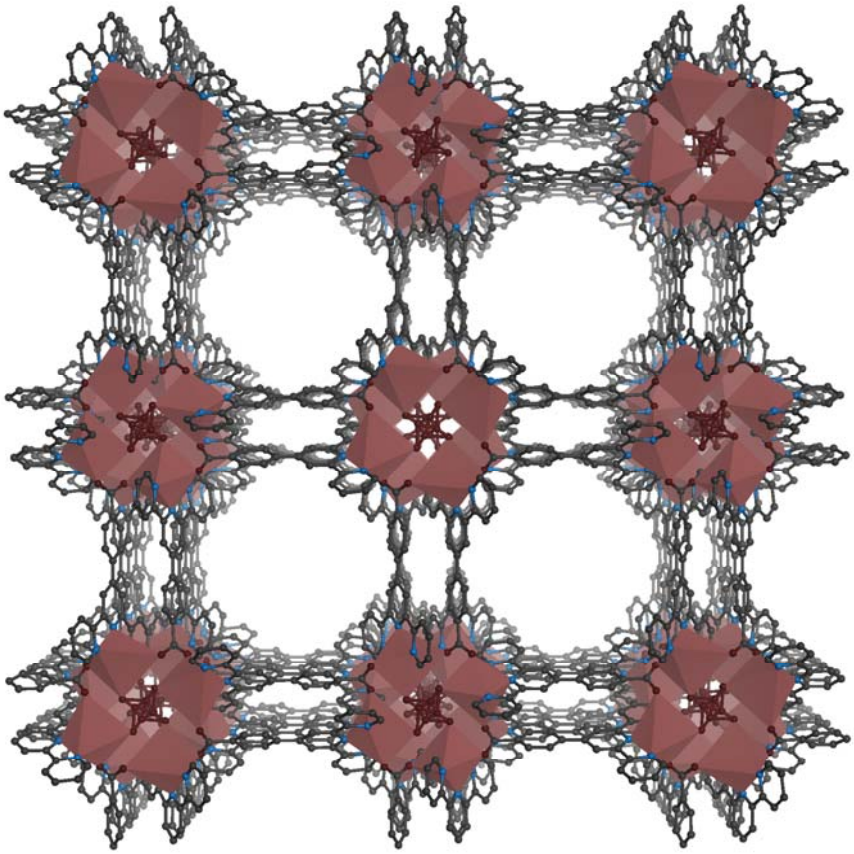

Figure 35. The grid structure of **6** viewed down the *c* axis
Hydrogen atoms are omitted for clarity.
Color key: Pb (maroon), N (dark blue), O (red), C (dark gray)

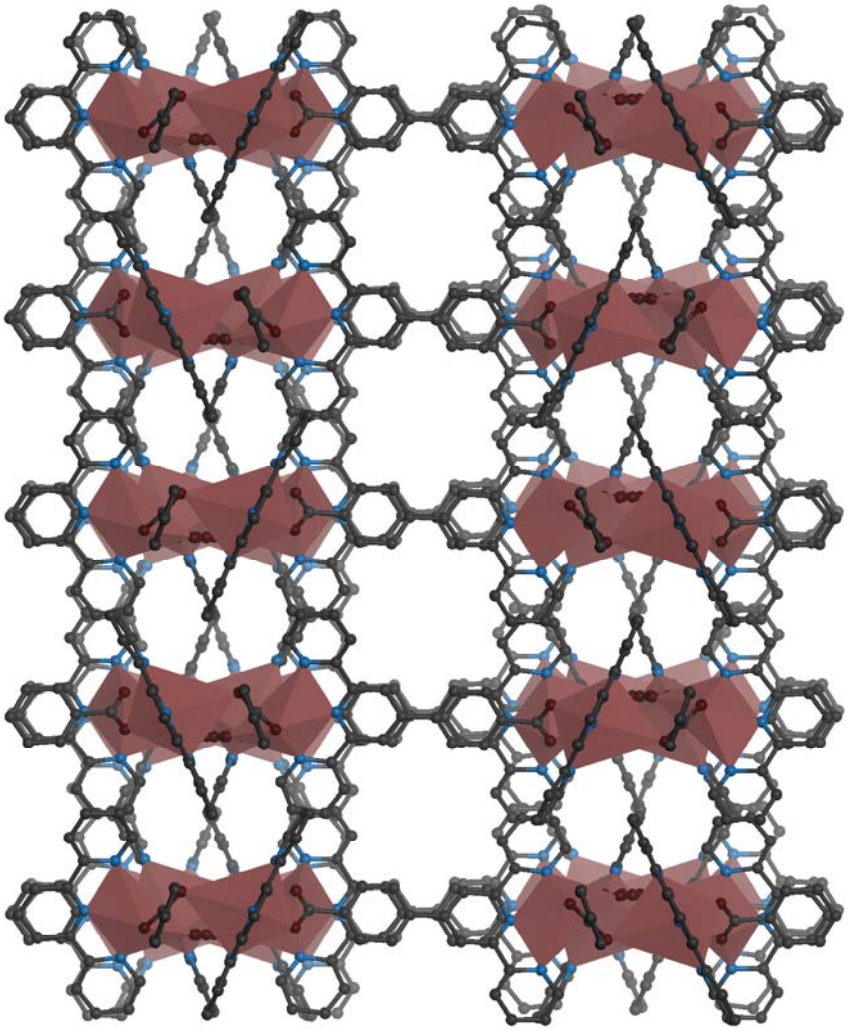

Figure 36. The supramolecular structure of **6** viewed down the *a* or *b* axis
Hydrogen atoms are omitted for clarity.
Color key: Pb (maroon), N (dark blue), O (red), C (dark gray)

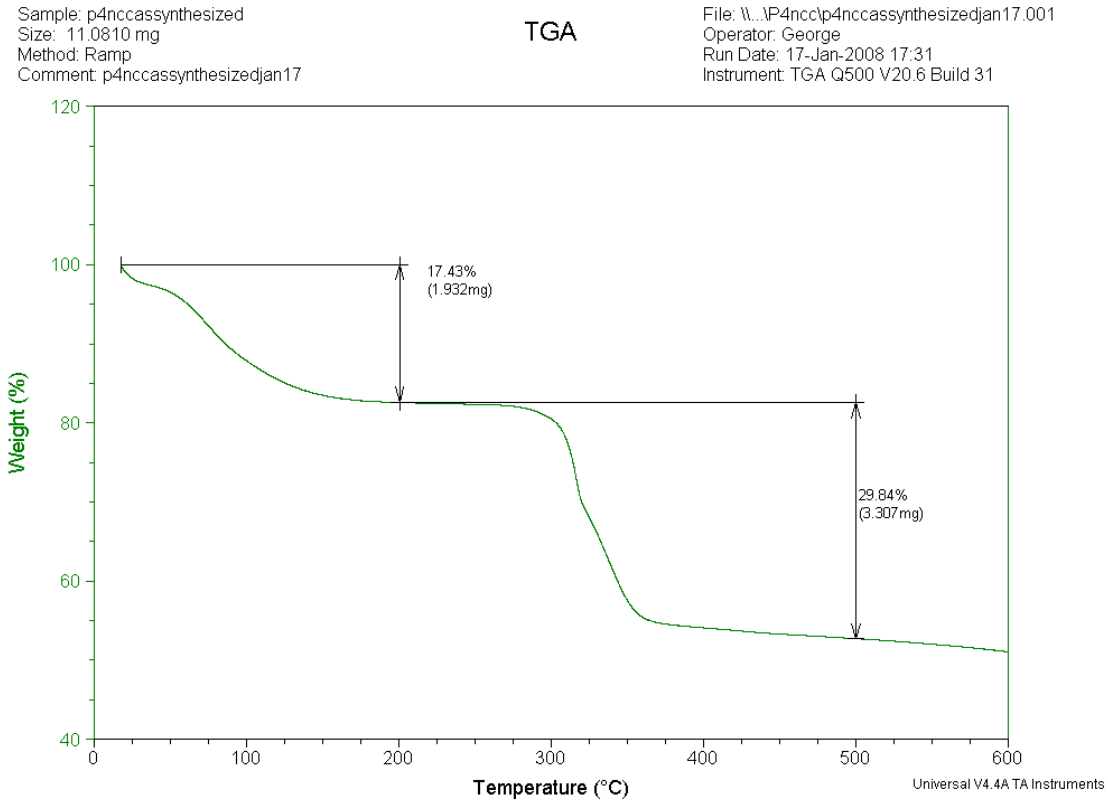

Figure 37. As synthesized TGA for **6**

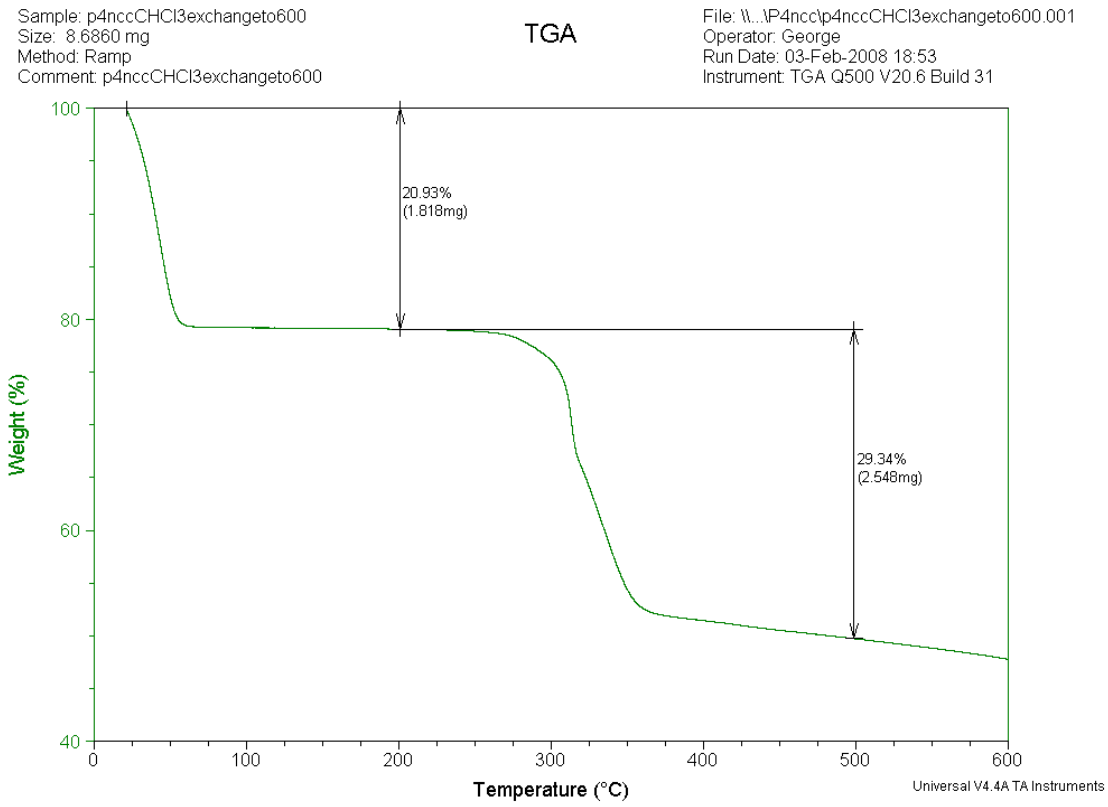

Figure 38. $CHCl_3$ exchanged TGA for **6**

2.7 Pb(L)(BF_4) (7)

Compound **7**, produced by reaction of H**L** and $Pb(BF_4)_2$, is remarkably similar to **6**. However, **7** contains different charge-balancing anions (BF_4^- rather than NO_3^-) in the cavities and differs subtly in the arrangement of the ligands with respect to one another. The change in counter anion results in slightly different bond lengths (longer, on average) and angles (**Table 10**). The bond lengths to the coordinated carboxylate oxygens, coordinated nitrogens and coordinated water oxygens are 2.35 – 3.14 Å, 2.53 – 2.56 Å and 2.85 – 2.95 Å, respectively. Additionally, the structure crystallizes in a lower symmetry tetragonal space group (P4/ncc for **6** and P4/n for **7**).

Table 9. Crystallographic data for compounds **7**-**9**

Identification code	Pb(**L**)(BF_4) (**7**)	Pb_2(**L**)$_2$(NO_3)Cl (**8**)	Gd(**L**)$_3$ (**9**)
Empirical formula	$C_{17.60}H_{10.40}N_{2.40}O_{7.20}Pb_{0.80}$	$C_{14.67}C_{l0.33}N_{2.33}O_{5.33}Pb_{0.67}$	$C_{264}H_{168}Gd_4N_{36}O_{24}$
Formula weight	536.44	444.11	4857.34
Temperature	446(2) K	173(2) K	446(2) K
Wavelength	0.71073 Å	0.71073 Å	0.71073 Å
Crystal system	Tetragonal	Tetragonal	Monoclinic
Space group	P4/n (#85)	P-4 (#81)	C2/c (#15)
Unit cell dimensions	a = 25.7765(18) Å	a = 17.9555(5) Å	a = 33.619(5) Å
	b = 25.7765(18) Å	b = 17.9555(5) Å	b = 13.8463(17) Å
	c = 8.3638(8) Å	c = 9.0390(5) Å	c = 12.1501(15) Å
	α= 90°	α= 90°	α= 90°
	β= 90°	β= 90°	β= 108.827(5)°
	γ = 90°	γ = 90°	γ = 90°
Volume	5557.1(8) $Å^3$	2914.2(2) $Å^3$	5353.3(12) $Å^3$
Z	10	6	1
Density (calculated)	1.603 Mg/m^3	1.518 Mg/m^3	1.507 Mg/m^3
Final R indices [I>2sigma(I)]	R1 = 0.0574, wR2 = 0.1406	R1 = 0.1217, wR2 = 0.3605	R1 = 0.0562, wR2 = 0.1338
R indices (all data)	R1 = 0.1186, wR2 = 0.1624	R1 = 0.1293, wR2 = 0.3653	R1 = 0.0782, wR2 = 0.1498
Largest diff. peak and hole	1.719 and -1.038 e.$Å^{-3}$	10.298 and -8.311 e.$Å^{-3}$	2.554 and -0.537 e.$Å^{-3}$

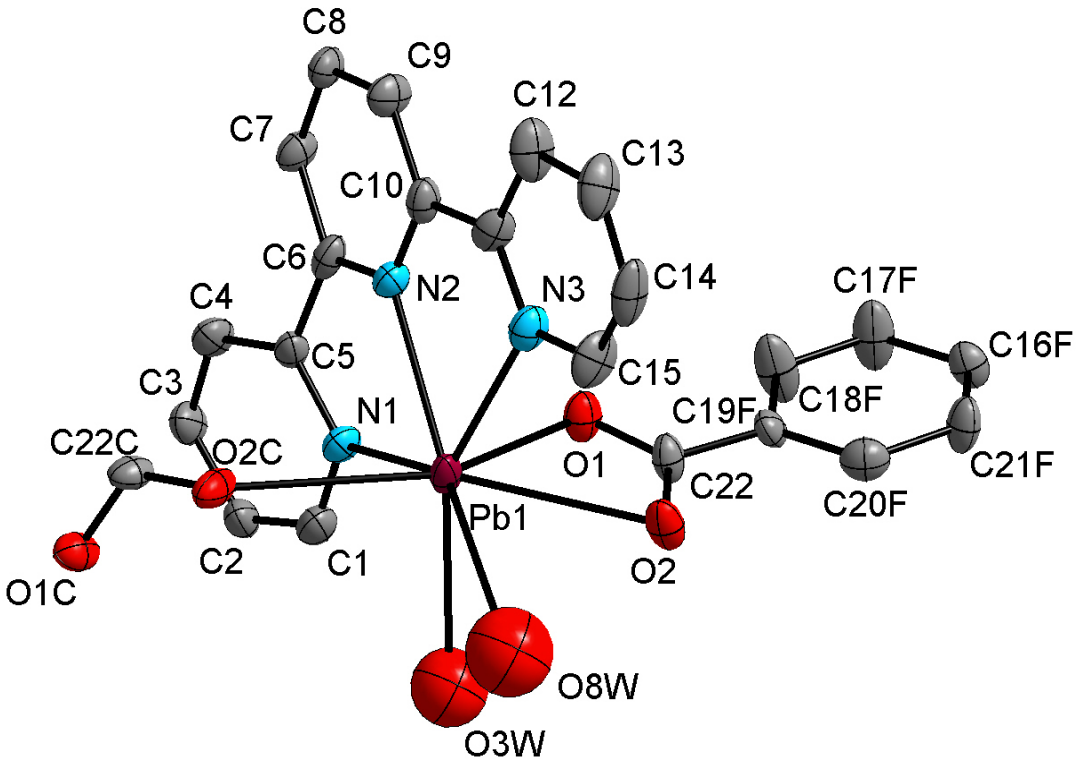

Figure 39. ORTEP plot of **7** at 30% probability

Table 10. Selected bond lengths (Å) and angles (°) for compound **7**

Pb1-O1	2.353(7)	Pb1-O8W	2.95(1)
Pb1-O3W	2.849(18)	Pb1-O2C	3.14(1)
Pb1-N2	2.534(8)	Pb1-O2	2.81(1)
Pb1-N1	2.532(8)	Pb1-N3	2.581(10)
O1-C22	1.286(12)	O2-C22	1.244(12)
O1-Pb1-O3W	92.5(4)	N2-Pb1-N1	65.8(3)
O1-Pb1-N2	79.1(3)	O1-Pb1-N3	82.3(3)
O3W-Pb1-N2	146.1(4)	O3W-Pb1-N3	149.5(4)
O1-Pb1-N1	78.9(3)	N2-Pb1-N3	62.5(3)
O3W-Pb1-N1	80.4(4)	N1-Pb1-N3	127.3(3)

Symmetry transformations used to generate equivalent atoms:
A. -x+1,-y+1,-z-1 B. y,-x+1/2,z C. -y+1/2,x,z

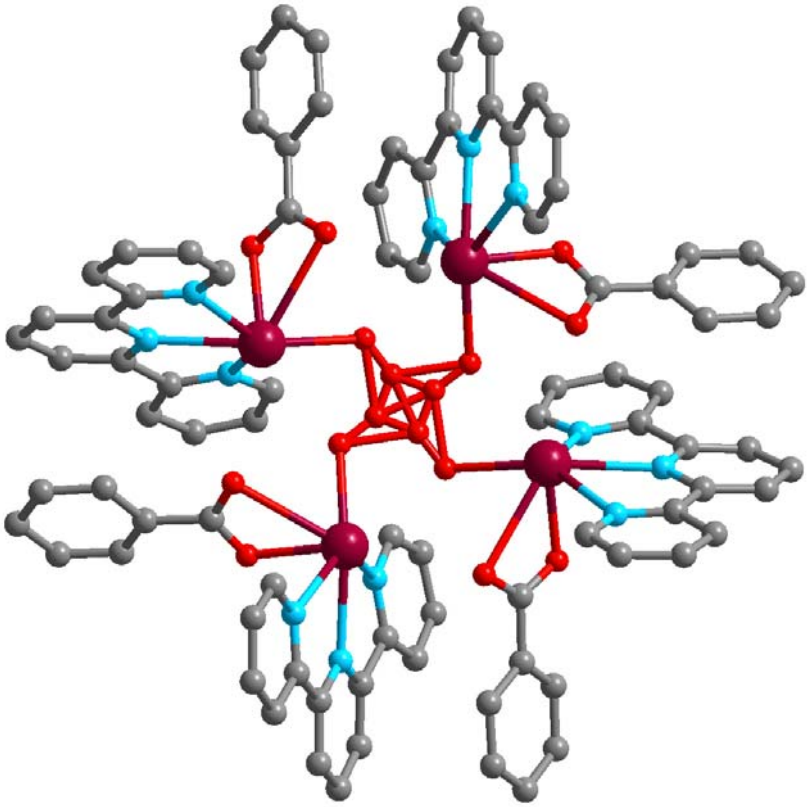

Figure 40. The basic building unit of **7** viewed down the *c* axis
Hydrogen atoms are omitted for clarity.
Color key: Pb (maroon), N (blue), O (red), C (dark gray)

2.8 $Pb_2(L)_2(NO_3)Cl$ (8)

Reaction of $Pb(NO)_2$ and H**L** in the presence of HCl produced colorless blocks of **8**. Like **6** and **7**, compound **8** is a square grid framework of the type $[Pb\mathbf{L}]^{+}$. Compound **8** differs from **6** and **7** in the orientation of the ligands with respect to one another and crystallizes in the tetragonal space group P-4. It displays a mixed Cl^- and NO_3^- anionic system to balance the charge on the cationic framework. Powder X-ray diffraction shows the compound was obtained as a pure phase (**Figure 63**). The Pb-atom bond lengths for **8** are the shortest of the $[Pb\mathbf{L}]^{+}$ compounds (**6**, **7** and **8**) and are 2.50 – 2.77 Å, 2.47 – 2.55 Å and 2.04 – 2.80 Å to the coordinated carboxylate oxygens, coordinated nitrogens and coordinated water oxygens, respectively.

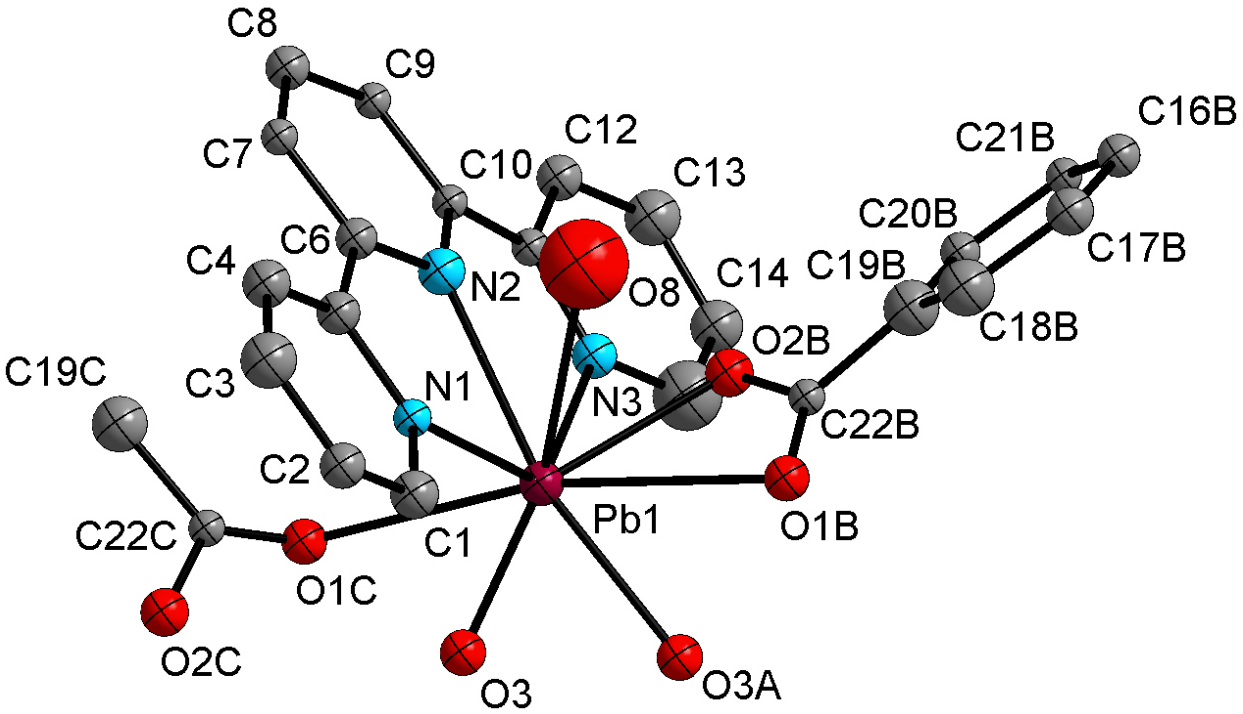

Figure 41. ORTEP plot of **8** at 30% probability

Table 11. Selected bond lengths (Å) and angles (°) for compound **8**

Pb1-O3	2.044(18)	Pb1-N2	2.534(10)
Pb1-O3A	2.397(19)	Pb1-N3	2.547(13)
Pb1-N1	2.474(11)	Pb1-O8	2.80(5)
Pb1-O2B	2.50(2)	Pb1-O1C	2.755(18)
Pb1-O1B	2.77(1)		
O3-Pb1-O3A	63.5(10)	N2-Pb1-N3	64.3(5)
O3-Pb1-N1	83.7(6)	O3-Pb1-O8	137.4(12)
O3A-Pb1-N1	124.1(5)	O3A-Pb1-O8	123.6(12)
O3-Pb1-O2B	145.2(7)	N1-Pb1-O8	56.9(12)
O3A-Pb1-O2B	83.0(6)	O2B-Pb1-O8	68.7(13)
N1-Pb1-O2B	125.5(6)	N2-Pb1-O8	48.0(12)
O3-Pb1-N2	129.9(6)	N3-Pb1-O8	85.4(13)
O3A-Pb1-N2	166.7(6)	O3-Pb1-O1C	57.4(6)
N1-Pb1-N2	62.7(5)	O3A-Pb1-O1C	113.7(6)
O2B-Pb1-N2	83.9(6)	N1-Pb1-O1C	76.9(5)
O3-Pb1-N3	135.5(6)	O2B-Pb1-O1C	139.5(6)
O3A-Pb1-N3	107.4(6)	N2-Pb1-O1C	78.3(5)
N1-Pb1-N3	126.9(5)	N3-Pb1-O1C	95.2(5)
O2B-Pb1-N3	44.4(6)	O8-Pb1-O1C	119.6(12)

Symmetry transformations used to generate equivalent atoms:
A. -y+1,x,-z+4 B. y-1,-x+1,-z+4 C. -x+1,-y+2,z

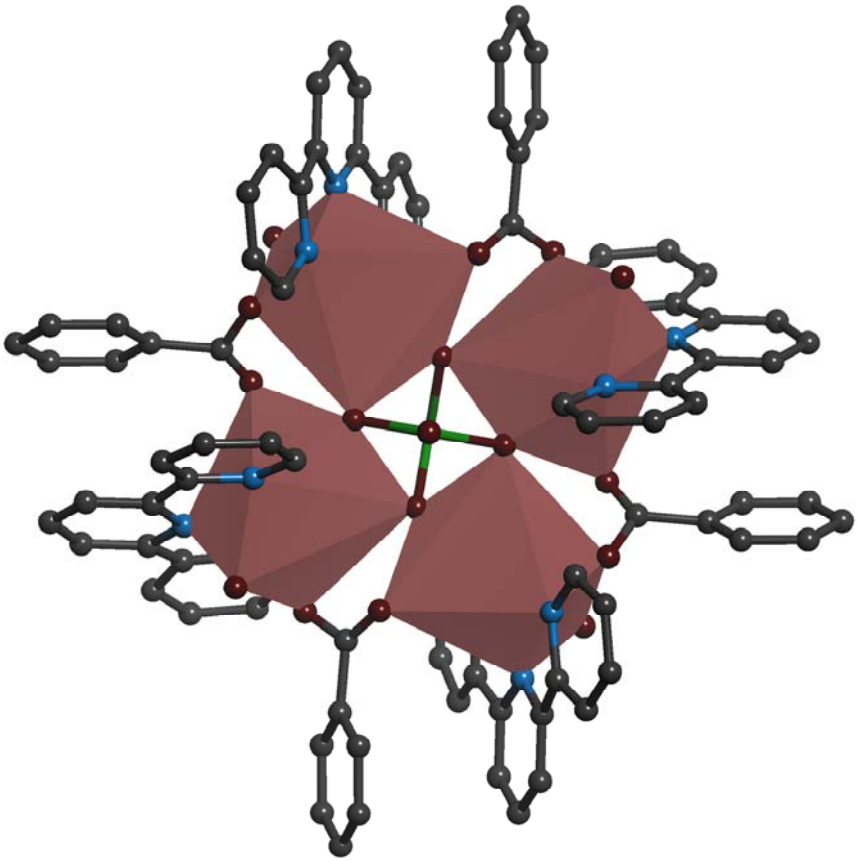

Figure 42. The basic building unit of **8** viewed down the *c* axis
Hydrogen atoms are omitted for clarity.
Color key: Pb (maroon), N (blue), O (red), C (dark gray), Cl (green)

2.9 $Gd(L)_3$ (9)

Reaction of $Gd(NO_3)_3$ and H**L** in DMF/water at 85º C resulted in the formation of 1-D chain structure **9**. The crystallographically independent Gd^{3+} ion is surrounded by bidentate carboxylates of three ligands and the tridentate terpyridine of a different ligand (**Figure 43**). The Gd-oxygen bond lengths are 2.4 – 2.5 Å, and the Gd-N bond lengths are approximately 2.5 Å (**Table 12**). The structure consists of 1-D chains (**Figure 44**) held together by weak aromatic stacking interactions (minimum distance between the rings is ~ 3.9 Å).

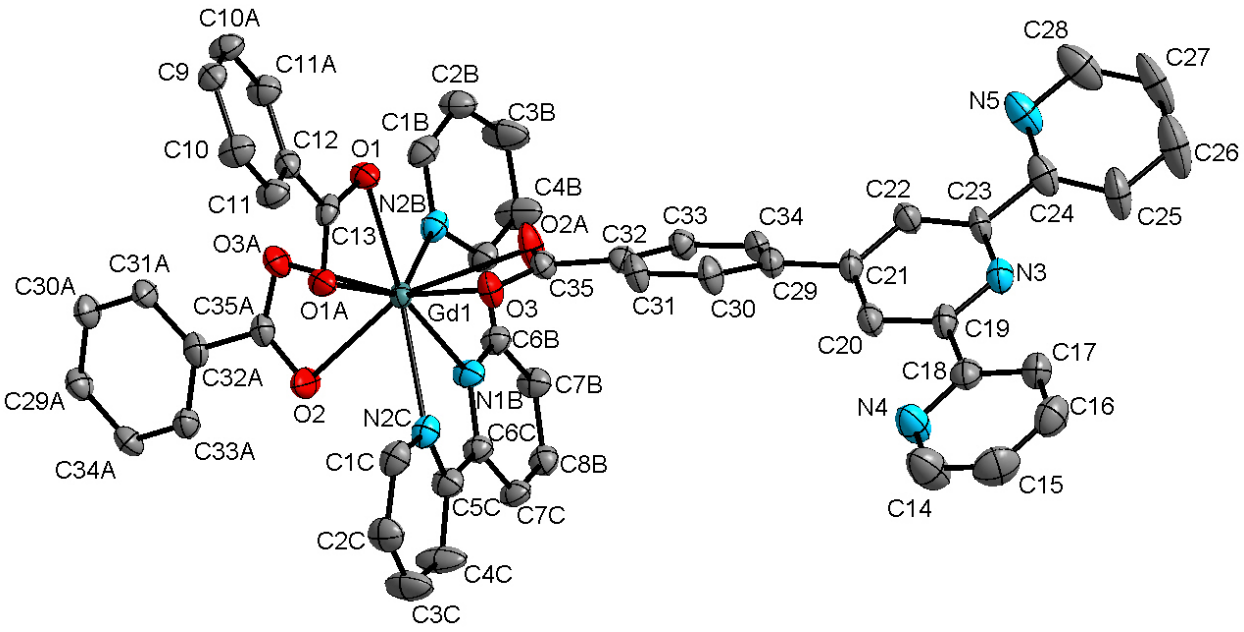

Figure 43. ORTEP plot of **9** at 30% probability

Table 12. Selected bond lengths (Å) and angles (°) for compound **9**

Gd1-O1A	2.405(3)	Gd1-N2B	2.513(4)
Gd1-O1	2.405(3)	Gd1-N2C	2.513(4)
Gd1-O2	2.446(3)	Gd1-N1B	2.534(5)
Gd1-O2A	2.446(3)	O1-C13	1.272(4)
Gd1-O3A	2.480(4)	O2-C35A	1.260(6)
Gd1-O3	2.480(4)	O3-C35	1.263(6)
O1A-Gd1-O1	55.41(15)	O2A-Gd1-N2B	66.64(13)
O1A-Gd1-O2	87.54(14)	O3A-Gd1-N2B	75.05(13)
O1-Gd1-O2	121.22(12)	O3-Gd1-N2B	118.73(13)
O1A-Gd1-O2A	121.22(12)	O1A-Gd1-N2C	89.52(12)
O1-Gd1-O2A	87.54(14)	O1-Gd1-N2C	141.13(12)
O2-Gd1-O2A	148.9(2)	O2-Gd1-N2C	66.64(13)
O1A-Gd1-O3A	79.25(12)	O2A-Gd1-N2C	99.38(14)
O1-Gd1-O3A	74.53(11)	O3A-Gd1-N2C	118.73(13)
O2-Gd1-O3A	52.98(12)	O3-Gd1-N2C	75.05(13)
O2A-Gd1-O3A	137.69(13)	N2B-Gd1-N2C	128.44(18)
O1A-Gd1-O3	74.53(11)	O1A-Gd1-N1B	152.29(8)
O1-Gd1-O3	79.25(12)	O1-Gd1-N1B	152.29(8)
O2-Gd1-O3	137.69(13)	O2-Gd1-N1B	74.43(10)
O2A-Gd1-O3	52.98(12)	O2A-Gd1-N1B	74.43(10)
O3A-Gd1-O3	150.34(17)	O3A-Gd1-N1B	104.83(9)
O1A-Gd1-N2B	141.13(12)	O3-Gd1-N1B	104.83(9)
O1-Gd1-N2B	89.52(12)	N2B-Gd1-N1B	64.22(9)
O2-Gd1-N2B	99.38(14)	N2C-Gd1-N1B	64.22(9)

Symmetry transformations used to generate equivalent atoms:
A. y+1/3,-x+y+2/3,-z+2/3 B. x-y+1/3,x-1/3,-z+2/3 C. -x,y-1,-z-1/2

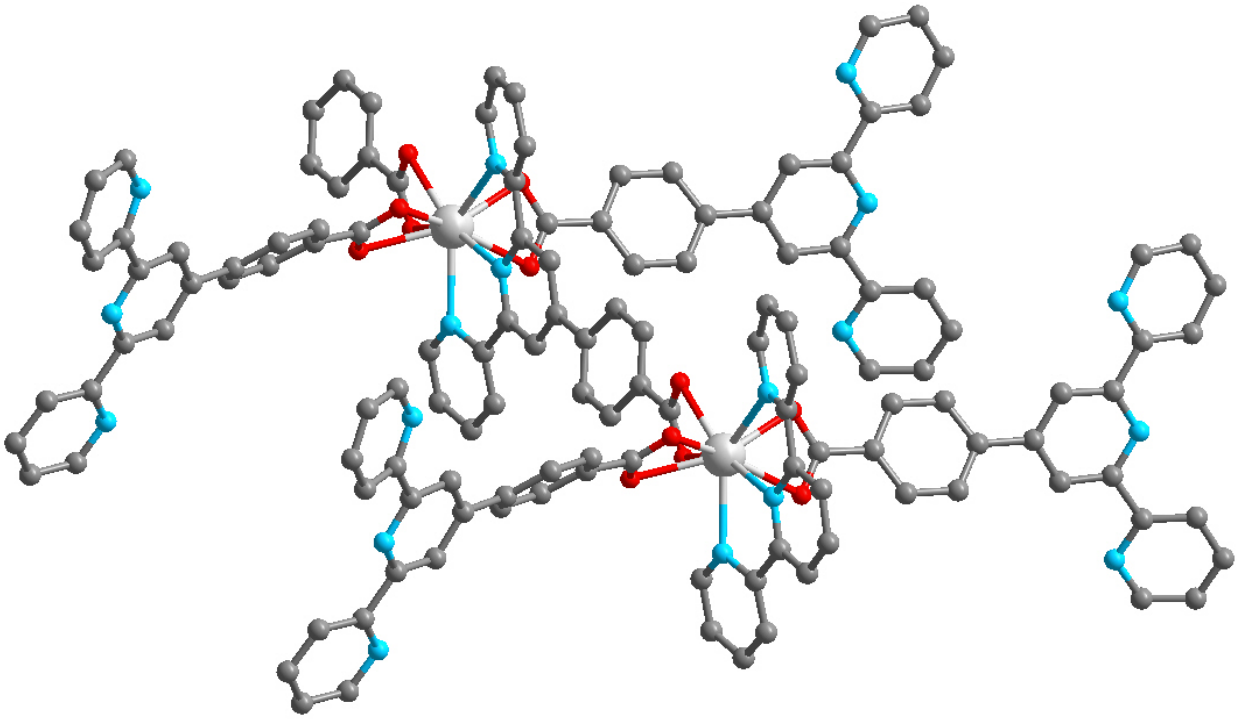

Figure 44. Supramolecular 1-D chain structure of **9**
Hydrogen atoms are omitted for clarity.
Color key: Gd (white), N (blue), O (red), C (dark gray)

2.10 DISCRETE $[M(L)_2]$ COMPLEXES AND OTHER L-CONTAINING CRYSTALS

Many reactions of H**L** with transition metals formed discrete $[M(\mathbf{L})_2]$ complexes (**Figure 45**). A notable observation to be made from analysis of these crystal structures is the general trend in M-N bond lengths (bond lengths: $Zn^{2+} > Cu^{2+} \approx Ni^{2+} \approx Ru^{2+} > Co^{2+}$) and maximum N-M-N angles on the same **L** (bond angles: $Co^{2+} > Ru^{2+} > Ni^{2+} \approx Cu^{2+} > Zn^{2+}$, **Tables 13-16**). This may indicate increasing strength of the M-N bond as the *d* electron count approaches 6.

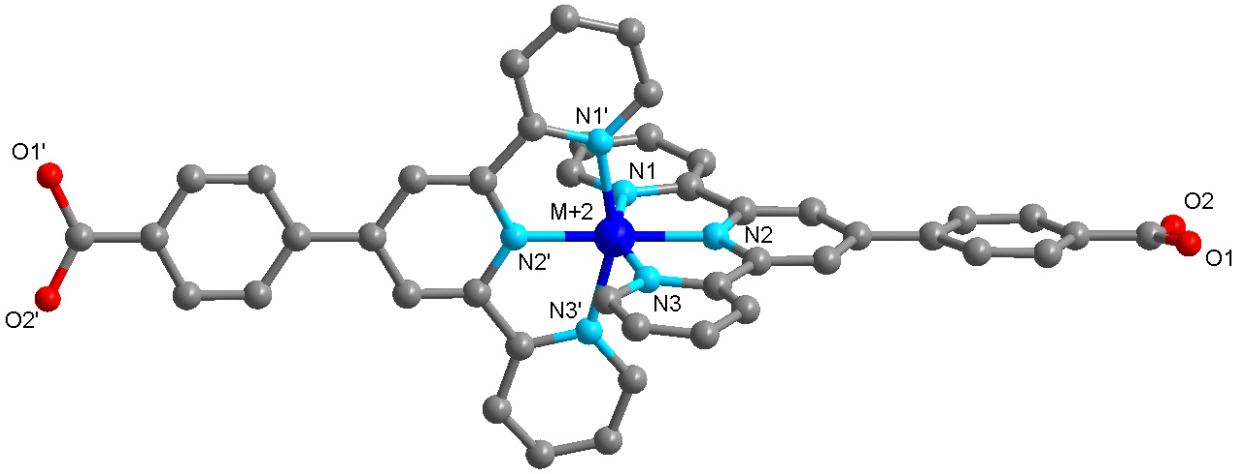

Figure 45. Basic structure of the [M(**L**)$_2$] complex

After synthesis of the structures described above, the focus was shifted to the construction of large pore MOFs using the [Ru(**L**)$_2$] complex as a starting material. Second and third row d^6 *bis*-terpyridine metal complexes are highly photoresponsive and exhibit predictable supramolecular chemistry.[78] Consequently the synthetic chemistry of these complexes has reached a sophisticated level, and it was not difficult to find conditions that could be adapted for the synthesis of [Ru(**L**)$_2$].[4] By heating a mixture of $RuCl_3$ and H**L** in ethanol in an autoclave for 15 h at 150 °C, [Ru(**L**)$_2$] was obtained as an impure purple solid. The purification of this very polar complex required column chromatography with a 50% aqueous acetonitrile solvent. After optimization of the purification procedure, the complex was obtained in 70 % yield.

Table 13. Crystallographic data for compounds **10a-10c**

Compound	**10a**	**10b**	**10c**
M+2	Ru	Ru	Ru
Empirical formula	$C_{176}H_{112}N_{24}O_{44}Ru_4$	$C_{88}H_{56}Cl_2N_{12}O_{16}Ru_2$	$C_{88}H_{56}B_2F_8N_{12}O_{20}Ru_2$
Formula weight	2469.96	1834.49	1766.76
Temperature	173(2) K	173(2) K	173(2) K
Crystal system	Tetragonal	Triclinic	Triclinic
Space group	I41/a (#88)	P-1 (#2)	P-1 (#2)
Unit cell dimensions	a = 11.599(7) Å	a = 9.1016(17) Å	a = 9.2185(15) Å
	b = 11.599(7) Å	b = 12.833(2) Å	b = 12.3601(19) Å
	c = 35.55(3) Å	c = 17.219(3) Å	c = 19.556(3) Å
	α= 90°	α= 79.833(4)°	α= 94.112(5)°
	β= 90°	β= 76.731(4)°	β= 103.496(4)°
	γ = 90°	γ = 89.251(4)°	γ = 91.565(4)°
Volume	4783(6) $Å^3$	1926.0(6) $Å^3$	2158.9(6) $Å^3$
Z	1	1	1
Density (calculated)	0.858 Mg/m^3	1.582 Mg/m^3	1.359 Mg/m^3
Goodness-of-fit on F2	2.221	1.371	1.430
Final R indices [I>2sigma(I)]	R1 = 0.1401, wR2 = 0.3619	R1 = 0.1262, wR2 = 0.3283	R1 = 0.1163, wR2 = 0.2904
R indices (all data)	R1 = 0.1778, wR2 = 0.3741	R1 = 0.1695, wR2 = 0.3471	R1 = 0.1884, wR2 = 0.3264
Largest diff. peak and hole	2.230 and -0.819 $e.Å^{-3}$	2.442 and -1.635 $e.Å^{-3}$	3.562 and -0.863 $e.Å^{-3}$
Minimum N-M+2 distance	1.963 Å	1.978 Å	1.961 Å
Maximum N-M+2 distance	2.059 Å	2.077 Å	2.085 Å
Minimum N1-M+2-N3 angle	157.49°	157.49°	157.91°
Maximum N1-M+2-N3 angle	157.49°	157.86°	157.98°

Table 14. Crystallographic data for compounds **10d-10f**

Compound	**10d**	**10e**	**10f**
M+2	Zn	Zn	Zn
Empirical formula	$C_{184}H_{112}F_{12}N_{28}O_{28}Zn_4$	$C_{88}H_{56}B_2F_8N_{12}O_{18}Zn_2$	$C_{176}H_{112}N_{28}O_{38}Zn_4$
Formula weight	3579.92	1873.81	3015.52
Temperature	173(2)(2) K	173(2) K	173(2) K
Crystal system	Monoclinic	Triclinic	Monoclinic
Space group	P2(1)/c (#14)	P-1 (#2)	P2(1)/c (#14)
Unit cell dimensions	a = 9.1159(12) Å	a = 9.9290(16) Å	a = 9.3793(11) Å
	b = 34.491(4) Å	b = 14.019(2) Å	b = 24.811(3) Å
	c = 13.0231(16) Å	c = 15.599(2) Å	c = 20.0078(18) Å
	α= 90°	α= 97.995(4)°	α= 90°
	β= 91.125(3)°	β= 95.846(5)°	β= 104.119(4)°
	γ = 90°	γ = 99.879(4)°	γ = 90°
Volume	4093.9(9) $Å^3$	2100.6(5) $Å^3$	4515.4(9) $Å^3$
Z	1	1	1
Density (calculated)	1.452 Mg/m^3	1.481 Mg/m^3	1.109 Mg/m^3
Goodness-of-fit on F2	1.555	1.002	1.793
Final R indices [I>2sigma(I)]	R1 = 0.0964, wR2 = 0.2610	R1 = 0.0934, wR2 = 0.2270	R1 = 0.1877, wR2 = 0.4978
R indices (all data)	R1 = 0.1380, wR2 = 0.2813	R1 = 0.1768, wR2 = 0.2800	R1 = 0.2667, wR2 = 0.5364
Largest diff. peak and hole	2.602 and -0.938 $e.Å^{-3}$	1.270 and -0.647 $e.Å^{-3}$	3.340 and -0.866 $e.Å^{-3}$
Minimum N-M+2 distance	2.065 Å	2.068 Å	2.075 Å
Maximum N-M+2 distance	2.190 Å	2.197 Å	2.176 Å
Minimum N1-M+2-N3 angle	151.15°	151.29°	151.41°
Maximum N1-M+2-N3 angle	151.84°	151.66°	152.19°

Table 15. Crystallographic data for compounds **10g-10i**

Compound	**10g**	**10h**	**10i**
M+2	Cu	Ni	Co
Empirical formula	$C_{88}H_{56}B_4Cu_2F_{14}N_{12}O_{16}$	$C_{100}H_{74}B_2F_8N_{16}Ni_2O_{12}$	$C1_{76}H_{112}Co_4N_{24}O_{24}$
Formula weight	1993.34	1908.16	4315.72
Temperature	173(2) K	173(2) K	173(2) K
Crystal system	Triclinic	Triclinic	Monoclinic
Space group	P-1 (#2)	P-1 (#2)	P(2)1/c (#14)
Unit cell dimensions	a = 9.2138(15) Å	a = 12.6958(18) Å	a = 10.1113(12) Å
	b = 12.468(2) Å	b = 14.232(3) Å	b = 16.911(2) Å
	c = 19.522(3) Å	c = 14.725(2) Å	c = 22.415(3) Å
	α= 85.817(4)°	α= 106.558(3)°	α= 90°
	β= 77.438(4)°	β= 95.188(4)°	β= 90.521(3)°
	γ= 89.579(4)°	γ = 111.117(4)°	γ = 90°
Volume	2183.0(6) $Å^3$	2322.9(7) $Å^3$	3832.6(8) $Å^3$
Z	1	1	1
Density (calculated)	1.516 Mg/m^3	1.364 Mg/m^3	1.870 Mg/m^3
Goodness-of-fit on F2	1.108	2.937	1.874
Final R indices [I>2sigma(I)]	R1 = 0.1014, wR2 = 0.2894	R1 = 0.1954, wR2 = 0.4613	R1 = 0.1478, wR2 = 0.4003
R indices (all data)	R1 = 0.1480, wR2 = 0.3361	R1 = 0.2198, wR2 = 0.4722	R1 = 0.2539, wR2 = 0.4302
Largest diff. peak and hole	1.449 and -0.612 $e.Å^{-3}$	3.747 and -2.410 $e.Å^{-3}$	2.046 and -0.519 $e.Å^{-3}$
Minimum N-M+2 distance	1.957 Å	1.964 Å	1.867 Å
Maximum N-M+2 distance	2.195 Å	2.155 Å	2.083 Å
Minimum N1-M+2-N3 angle	155.32°	156.43°	158.90°
Maximum N1-M+2-N3 angle	156.00°	156.46°	161.02°

Table 16. Crystallographic data for compounds **10j-12**

Compound	**10j**	**L** (**11**)	Cd(**L**)$(NO_3)_2$(DMF) (**12**)
M+2	Co	-	-
Empirical formula	$C_{88}H_{56}B_2Co_2F_6N_{12}O_{16}$	$C_{22}H_{15}N_3O_2$	$C_{100}H_{80}Cd_4N_{24}O_{40}$
Formula weight	1630.50	352.36	2210.76
Temperature	173(2) K	173(2) K	173(2) K
Crystal system	Triclinic	Monoclinic	Monoclinic
Space group	P-1 (#2)	P2(1)/c (#14)	C2/c (#15)
Unit cell dimensions	a = 9.3828(10) Å	a = 10.1886(16) Å	a = 13.695(3) Å
	b = 10.3152(11) Å	b = 7.1724(11) Å	b = 21.447(6) Å
	c = 22.452(2) Å	c = 22.360(4) Å	c = 11.161(2) Å
	α= 87.433(2)°.	α= 90°.	α= 90°.
	β= 78.798(2)°.	β= 90.611(3)°.	β= 126.733(5)°.
	γ = 77.754(2)°.	γ = 90°.	γ = 90°.
Volume	2083.1(4) $Å^3$	1633.9(4) $Å^3$	2627.2(10) $Å^3$
Z	1	4	1
Density (calculated)	1.300 Mg/m^3	1.432 Mg/m^3	1.397 Mg/m^3
Goodness-of-fit on F2	2.035	1.089	1.200
Final R indices [I>2sigma(I)]	R1 = 0.1615, wR2 = 0.4136	R1 = 0.0521, wR2 = 0.1245	R1 = 0.0701, wR2 = 0.1852
R indices (all data)	R1 = 0.2471, wR2 = 0.4439	R1 = 0.0786, wR2 = 0.1401	R1 = 0.1004, wR2 = 0.2044
Largest diff. peak and hole	2.193 and -0.540 $e.Å^{-3}$	0.344 and -0.232 $e.Å^{-3}$	2.241 and -0.988 $e.Å^{-3}$
Minimum N-M+2 distance	1.857 Å	-	2.288 Å
Maximum N-M+2 distance	1.949 Å	-	2.332 Å
Minimum N1-M+2-N3 angle	164.12°	-	141.2°
Maximum N1-M+2-N3 angle	165.35°	-	-

2.11 IRMOF BASED ON THE [Ru(L)$_2$] MOTIF (13)?

Heating a mixture of [Ru(H**L**)$_2$] with excess Zn(BF$_4$)$_2$ in DMF produced highly transparent red crystals. These crystals were very fragile and fragmented quickly upon exposure to air. After numerous attempts to obtain useful crystal data, an adequate number of reflections to observe some features of the crystal structure was collected (see **Table 17** for crystallographic data). The data was good enough to determine the coordinates of the zinc, ruthenium and some coordinated oxygen atoms (**Figure 46**, atomic coordinates and iso/anisotropic displacement parameters are given in **Table 72** and **73**).

The conditions used for the synthesis of this structure were similar to those employed by Yaghi, *et al*.[90] to obtain single crystals of the prototypical large-pore metal-organic framework, MOF-5. The atom-atom distances and bond angles (**Table 18**) are very similar to what would be expected if these crystals were isostructural to MOF-5.[91] The theoretical atom-atom distances and bond angles were determined by analysis of the single crystal data for [Ru(**L**)$_2$] (**10a**) and MOF-5. **Figure 47** shows the probable structure of **13**. It is topologically equivalent to IRMOF-1 (MOF-5), or more specifically, the terphenyl dicarboxylate IRMOF-16,[91] in which the zinc clusters are twisted 90º with respect to one another.

Table 17. Crystallographic data for compound **13**

Identification code	**13**
Empirical formula	$C_{0.52}O_{0.40}Ru_{0.14}Zn_{0.10}$
Formula weight	33.43
Temperature	273(2) K
Crystal system	Cubic
Space group	P23
Unit cell dimensions	a = 27.969(6) Å α= 90°.
	b = 27.969(6) Å β= 90°.
	c = 27.969(6) Å γ = 90°.
Volume	21879(8) $Å^3$
Z	42
Density (calculated)	0.107 Mg/m^3
Absorption coefficient	0.211 mm^{-1}
F(000)	652
Theta range for data collection	3.09 to 28.50°.
Index ranges	-37<=h<=36, -37<=k<=37, -37<=l<=37
Reflections collected	201363
Independent reflections	18443 [R(int) = 1.7889]
Completeness to theta = 28.50°	99.4 %
Refinement method	Full-matrix least-squares on F^2
Data / restraints / parameters	18443 / 0 / 38
Goodness-of-fit on F^2	1.385
Final R indices [I>2sigma(I)]	R1 = 0.3713, wR2 = 0.4921
R indices (all data)	R1 = 0.6938, wR2 = 0.5865
Largest diff. peak and hole	0.734 and -0.450 e. $Å^{-3}$

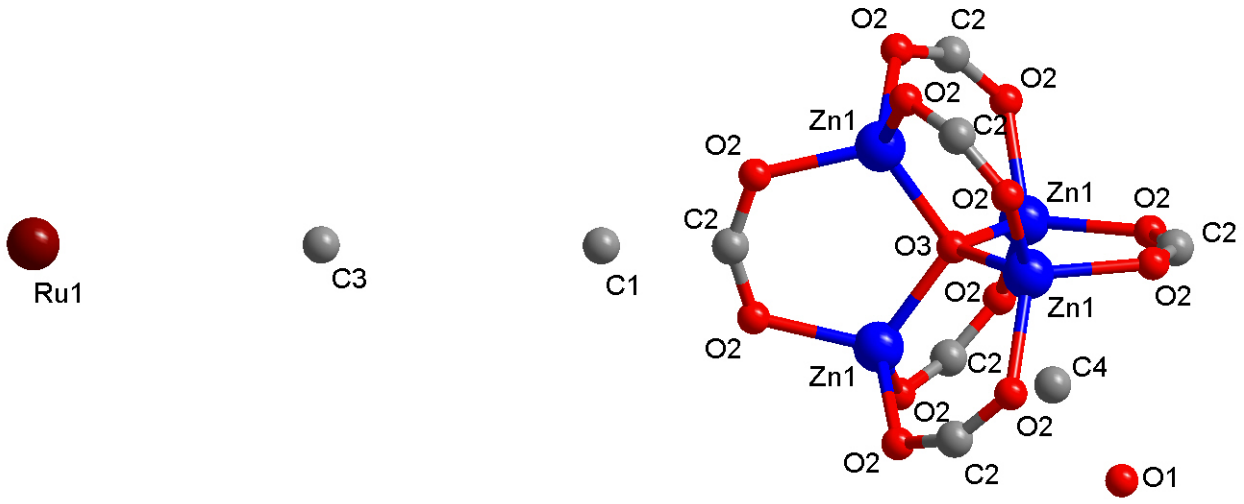

Figure 46. Atom types and positions for **13**, determined by single crystal X-ray diffraction

Table 18. Selected atom-atom lengths (Å) and bond angles (°) for compound **13** (see text)

	experimental	theoretical
RU1-O3	13.99(1)	14.04(1)
ZN1-O2	1.95(1)	1.92(1)
ZN1-O3	1.94(1)	1.94(1)
O2-O2	2.28(1)	2.20(1)
ZN1-O3-ZN1	109.5	109.5
O2-ZN1-O2	109.5	109.5

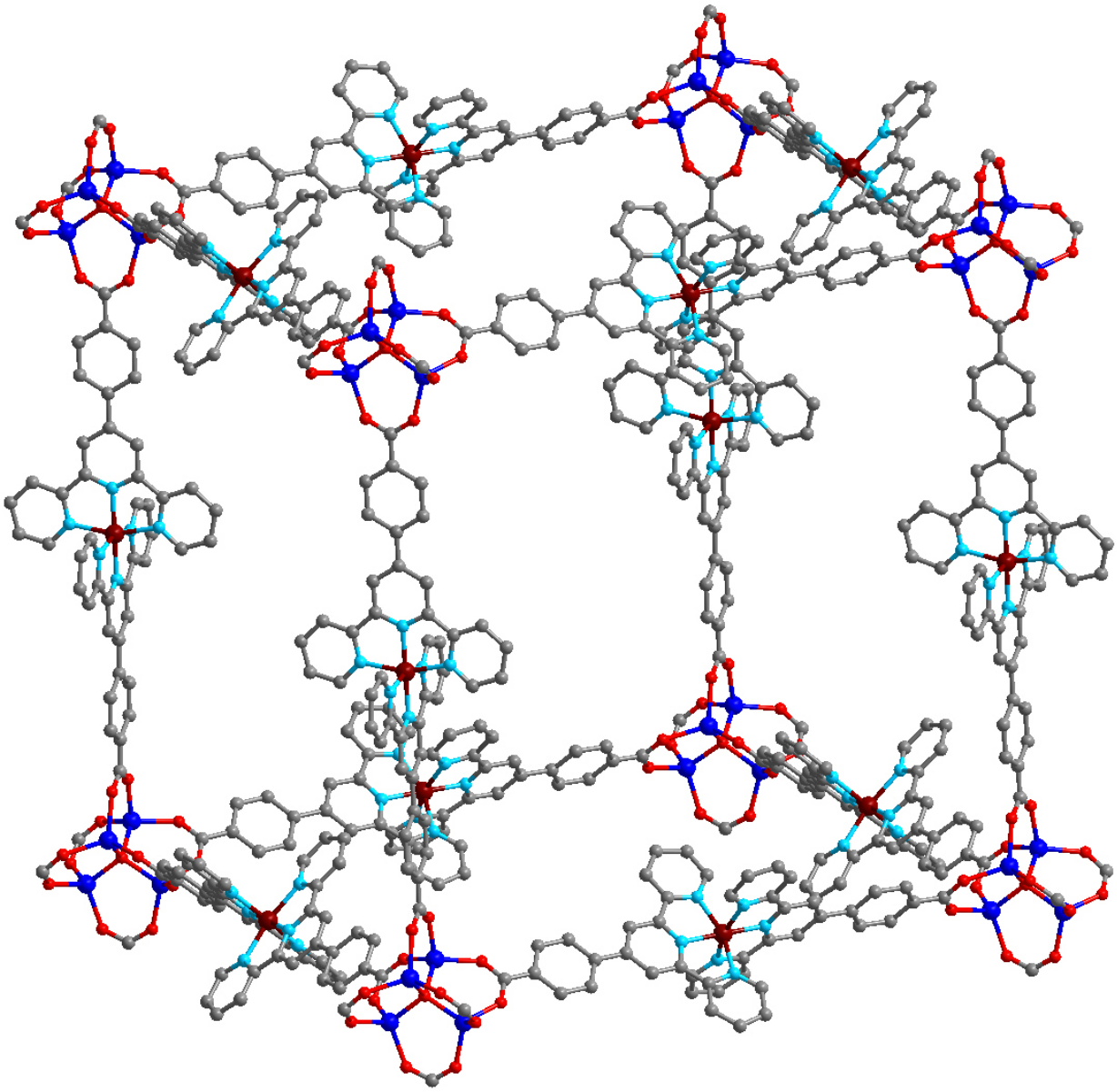

Figure 47. Probable structure of **13**
Oxygen, zinc and ruthenium coordinates were determined by single crystal X-ray diffraction. **L** was fitted to the model by molecular mechanics (mm2) calculations.
Hydrogen atoms are omitted for clarity.
Color key: Zn (dark blue), N (light blue), O (red), C (dark gray), Ru (maroon)

3.0 DISCUSSION

3.1 DEVELOPMENT OF REACTION CONDITIONS TO FAVOR THE FORMATION OF HIGH-DIMENSIONAL POROUS MOFS FROM HL AS STARTING MATERIAL

With the goal of constructing microporous materials showing significant uptake of hydrogen gas, H**L**, prepared according to a modified literature procedure,[4] was reacted with a variety of metal cations under solvo- and hydro-thermal conditions. Metal salt, pH, reaction vessel, temperature, solvent, and amount of exposure to air were varied in an effort to construct rigid, open frameworks.

Compounds **1** and **2** are each based on square planar single metal ion building blocks (**Figure 48**). The arrangement of the ligands with respect to one another determines if the structure is an array of discrete macrocycles (**1**) or infinite 1-D chains (**2**). Both structures are supported by π- π interactions, particularly **1**, which has continuous aromatic stacking down the *c* axis. In addition to these interactions, the macrocycle **1** displays a noteworthy chair-like stacking motif, which may contribute to the rigidity of the structure in the absence of guest molecules.

The TGA results for hexamer **1** reveal a remarkable trend. Chloroform, which boils at 61 ºC, remains in the pores at temperatures up to 150 ºC (**Figure 14**), whereas more polar molecules such as water, DMF (**Figure 11**) and acetonitrile (**Figure 12**) are released prior to the

temperature reaching 100 ºC. These results indicate the CF_3-coated channel walls of **1** possess high hydrophobicity, pointing toward the possibility of carrying out separations on the basis of polarity.[92-97] Moreover, substitution of the CF_3COO^- anions with carboxylate ions of different size or hydrophobicity (*e.g.* $HCOO^-$, CH_3COO^-, or $CF_3CF_2COO^-$) can provide opportunities for the fine tuning of the channel environment for highly selective separations.

To synthesize **1** with a specific carboxylate, the proper zinc(II) carboxylate salt and H**L** can be reacted under similar conditions to those used for **1**. Alternatively, if the zinc(II) carboxylate salt is inaccessible, a zinc(II) salt (*e.g.* $Zn(BF_4)_2$) combined with the analogous carboxylic acid can be substituted. A library of compounds could be identified by comparison of the simulated and experimental powder X-ray diffraction patterns using **1** as the structural model.[91] This would obviate the need to grow crystals suitable for single crystal X-ray diffraction for each structure.

These theoretical compounds' selectivities toward different components of mixtures can be determined as a function of channel diameter and hydrophobicity. One relatively simple experiment is the separation of oil from water. The protocol used for a CF_3 functionalized silica aerogel[98] involves the suspension of the material in an oil/water mixture and subsequent determination of the oil content in the dried solid.[99] Vapor[100] or gas[92] adsorption can also be used to determine guest selectivity.

Compound **3** contains the anticipated $[Zn(\mathbf{L})_2]$ complex as a building unit (refer to section **1.3**), and represents the first example of a coordination polymer based on the expanded 1,4-benzenedicarboxylate ligand.[53] Like **1** and **2**, this structure is low-dimensional (1-D), being based on small single metal ion vertices. To synthesize materials showing a high hydrogen uptake capacity, it was preferable to synthesize higher-dimensional structures. An analysis of

compounds **1** – **3** showed that an increase in the connectivity of the vertices would allow access to two- and three-dimensional structures (the vertices in compound **1** – **3** are all two-connected). Three ways to increase the connectivity of the vertices are: a) use conditions to favor the formation of frameworks based on polynuclear metal clusters, b) employ larger metal ions with more available coordination sites, and c) use inert [M(**L**)$_2$] complexes as starting materials to access chemistry based on dicarboxylate ligands and to ensure the terpyridine is not involved as a point-of-extension in the framework.

By using conditions that produced a dinuclear building block, Zn_2[μ-OH], it was possible to access the two-dimensional structure **4**. Compound **4** arises from the combination of Zn_2[μ-OH] with the square-pyramidal building unit observed in **2**. The absence of formate ions in the reaction mixture resulted in a further increase in dimensionality, producing a 3-D framework (compound **5**) based solely on the three-connected Zn_2[μ-OH] vertex. Higher nuclearity secondary building units (> 2 zinc ions) proved inaccessible under the conditions attempted, this being a result of the geometrical constraints imposed by the tridentate terpyridine moiety, which inhibit the formation of large zinc oxide clusters[5, 17, 101-103] commonly seen in MOF chemistry. The structures and building units of compounds **1** – **5** are depicted schematically in **Figure 48**.

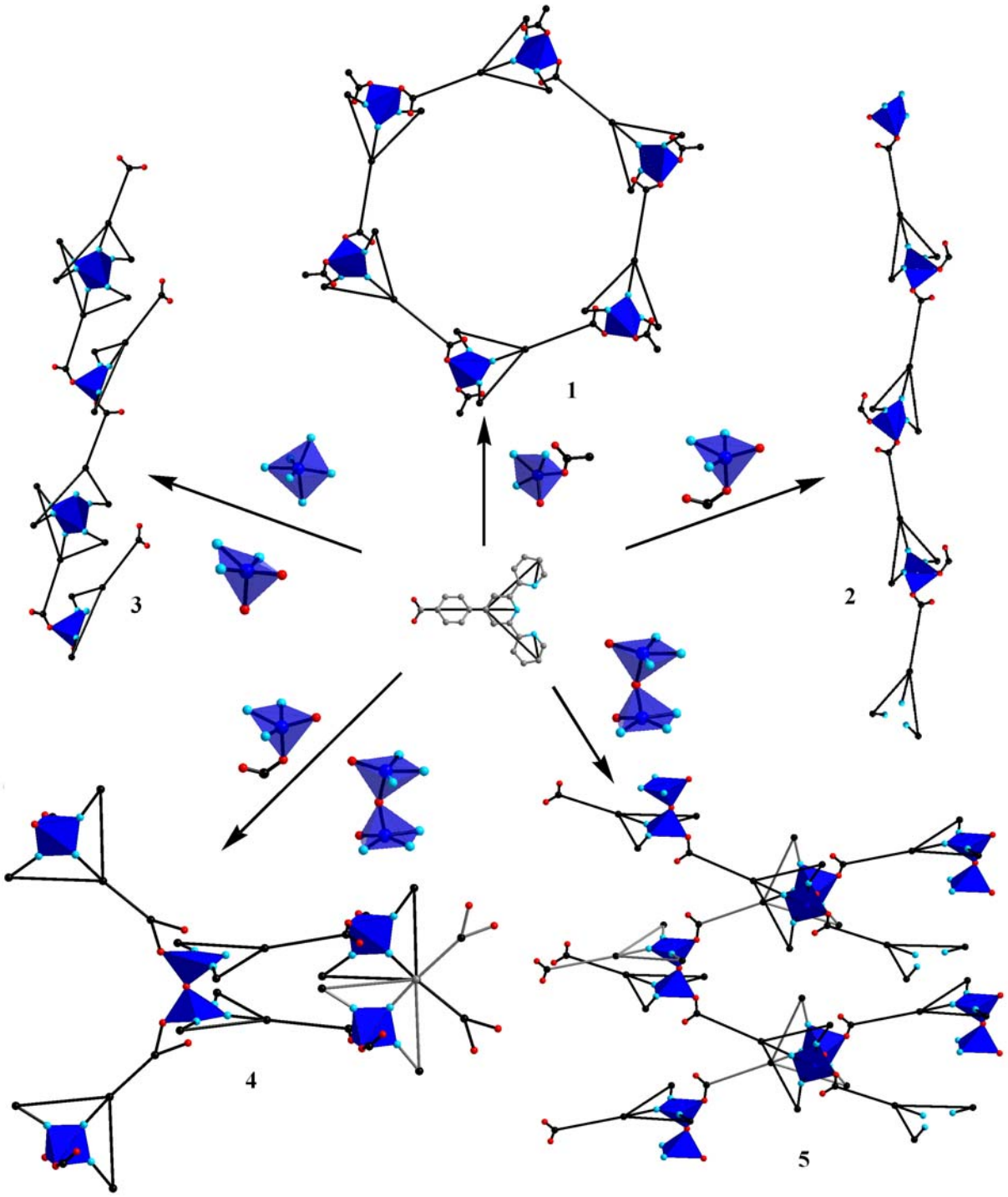

Figure 48. Scheme showing the building units and structures obtained with **L** and zinc (compounds **1** – **5**)

The strategy of increasing the connectivity and dimensionality of **L**-based frameworks by employing a larger metal ion produced positive results. Solvothermal reaction of H**L** with $Pb(NO_3)_2$ in DMF produced colorless crystals of **6** as a pure phase (**Figure 49**). The crystallographically independent Pb^{2+} ion in this structure is eight coordinated and displays significantly longer (~0.3 – 0.4 Å) bond lengths compared to the zinc ions in structures **1** – **5**. Similarly to **1**, compound **6** consists of $M_x\mathbf{L}_x$ macrocycles (for **1**: x=6, M=Zn; for **6**: x=4, M=Pb), which interact through π-stacking. Unlike **1**, however, the larger Pb^{2+} ions in **6** have additional coordination sites, which enable the macrocycles to share corners through carboxylate oxygens and coordinated water molecules.

. The $Pb_4\mathbf{L}_4$ corner-sharing results in less efficient packing of the macrocycles along the *c* axis compared to structure **1**, and consequently the channel walls in compounds **6** – **8** are less dense, which may allow channel to channel guest diffusion (see **Figure 36**). This "scaffold" like structural aspect is believed to allow gas molecules easier access to the cavity space.[16]

Frameworks **6** – **8** are cationic, making anion exchange a possibility for tuning the gas storage or separation properties of the materials.[104-106] More specifically, the incorporation of chiral anions into the pores will provide opportunities for chiral separations.[107-109] The ease in which the pore environment can be tuned by ion exchange makes this an attractive way to carry out systematic studies on these processes.

Examples of chiral anions with the potential to be incorporated into these frameworks include tartrate, 10-camphorsulphonate, and *bis*-catecholato borate anions.[110, 111] Anion exchange in metal-organic frameworks is accomplished by introduction of the anion salt solution over an extended period.[105] After ion exchange, the enantioselectivity of the resulting materials can be determined by introduction of the racemic guests *via* solution or vapor phase and subsequent extraction with solvent. The enantiomeric excess can be determined by chiral GC or HPLC analysis of the extracts.[109]

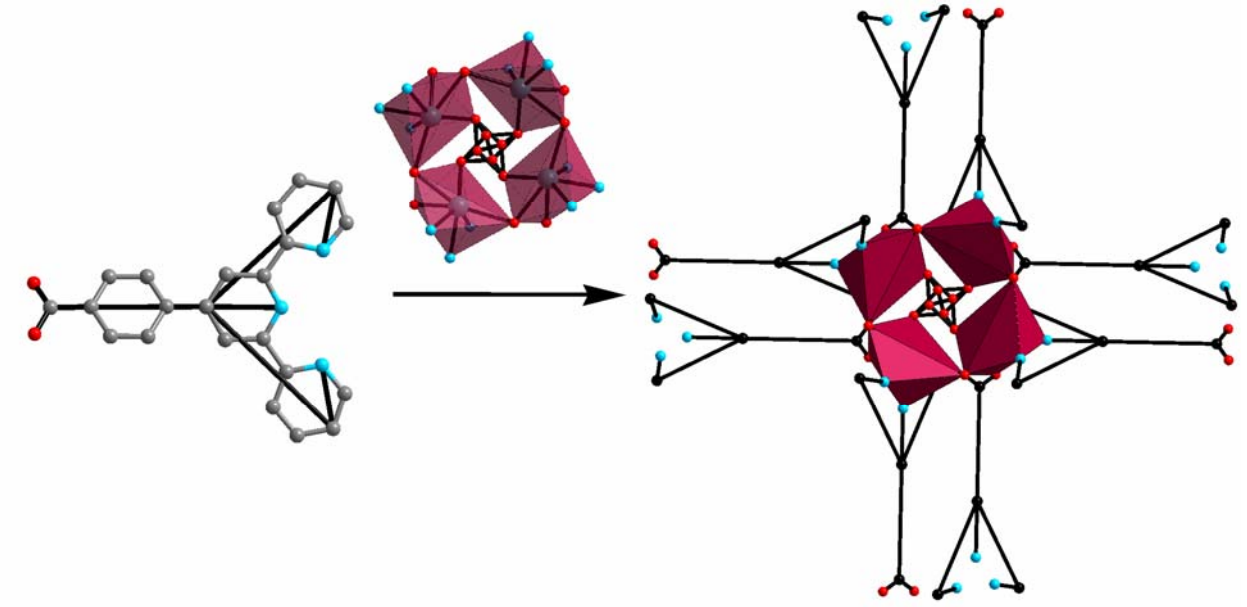

Figure 49. Scheme showing the building unit and structure obtained with lead and **L** (compound **6**)

Crystals of one-dimensional structure **9** were obtained from reactions of **L** with gadolinium(III) cations under various conditions. Use of the $CF_3SO_3^-$ and NO_3^- salts at different temperatures (85 – 180 ºC) with different solvent mixtures (water, DMF, methanol, and others) lead to the same product. In compound **9**, two **L** molecules act as terminal ligands and preclude the formation of high-dimensional structures. The oxophilic nature of lanthanide cations may be responsible for this product preference.

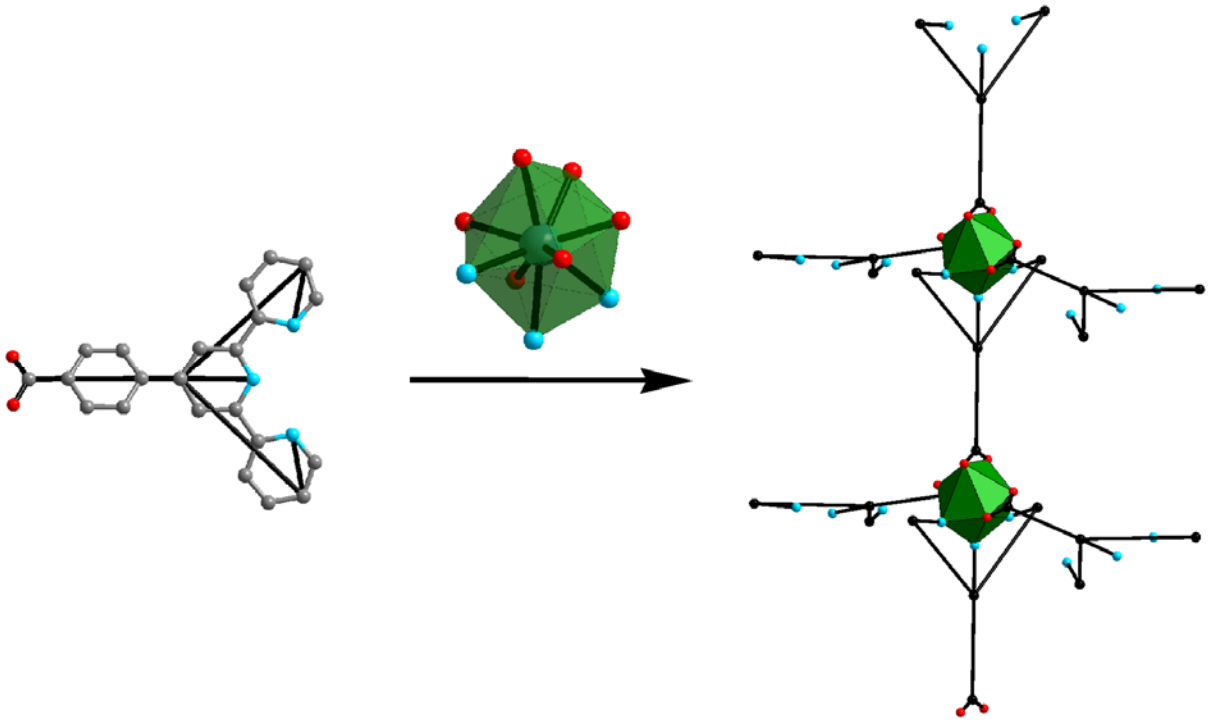

Figure 50. Scheme showing the building unit and structure obtained with gadolinium and **L** (compound **9**)

3.2 [RU(L)$_2$] AS STARTING MATERIAL FOR THE SYNTHESIS OF LARGE PORE MOFS

It became clear that the use of H**L** as a starting material was not a reliable method for producing frameworks based on the *bis*-terpyridine motif, and the third strategy for increasing the dimensionality of the frameworks, the use of an inert [M(**L**)$_2$] complex as the starting material, was employed. The synthesis of the ligand [Ru(**L**)$_2$] was not entirely straightforward. Despite significant alterations in the literature procedure,[4] thin-layer chromatography revealed an impurity after the work-up. To remove the impurities and create the possibly more DMF-soluble diacid, [Ru(H**L**)$_2$][PF$_6$]$_2$ (DMF is a common solvent for MOF synthesis), the product was purified by column chromatography (**Figure 51**) and the pure fraction was treated with excess NH_4PF_6.

After optimization of the purification protocol, [Ru(H**L**)$_2$][PF$_6$]$_2$ was obtained in 70 % yield. The compound dissolved completely at a 0.01 M concentration in DMF. To synthesize porous MOFs, this photoactive complex was reacted with Co^{2+}, Cu^{2+}, and Zn^{2+} under solvothermal conditions. Upon heating [Ru(H**L**)$_2$][PF$_6$]$_2$ with excess $Zn(BF_4)_2$ in DMF, transparent red crystals were obtained (compound **13**). These crystals were very air sensitive and were loaded into a capillary under nitrogen to determine the unit cell and metal locations by X-ray diffraction. In the results section, I presented evidence these crystals possess the same topology as MOF-5, in which case the voids are large enough to allow diffusion of large guests (up to 1.8 nm) into the framework.

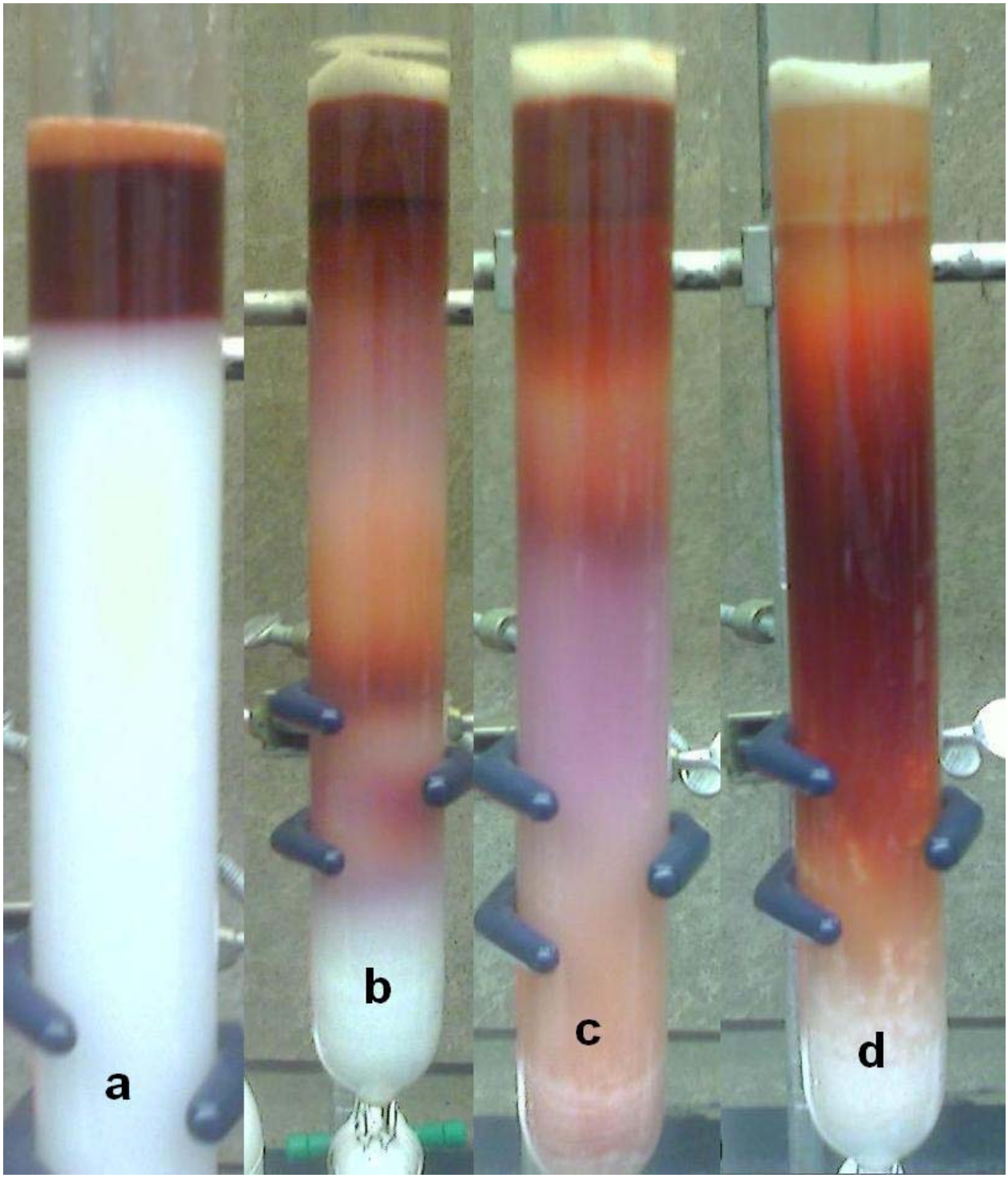

Figure 51. Column chromatography on Ru(**L**)$_2$ complex, arranged left to right by elution time **a**: immediately after loading column **b**: some colored impurities come out quickly with 7:3 MeCN:H_2O/12:3:1 MeCN:H_2O:KNO_3(sat. aq.) **c**: after fast moving impurities are eluted, solvent is switched to 1:1 MeCN:H_2O/6:3:1 MeCN:H_2O:KNO_3(sat. aq.) **d**: product is the last band (broad red), eluting with 1:1 MeCN:H_2O

4.0 CONCLUSIONS AND OUTLOOK

Having quickly obtained a promising structure, **13**, with the preformed $[Ru(H\mathbf{L})_2][PF_6]_2$ complex, I suspect the best approach for synthesizing high-dimensional porous frameworks based on **L** is to use the *bis*-terpyridine complex as a starting material. The d^6 iron(II) complex, $[Fe(\mathbf{L})_2]$ which is expected to be more easily formed than the Ru(II) complex,[53, 54] and $[Co(\mathbf{L})_2]$ (compound **10i**), in which the bond lengths are comparatively short, are also good potential starting materials.

Although the MOFs synthesized thus far with H**L** still need to be investigated for their hydrogen storage capabilities, the goal of attaining frameworks with suitable pore size for hydrogen storage (> 5 Å) was achieved. Experiments need to be done on compounds **1** and **6** – **8** to prove their potential in hydrophobic or enantioselective separations.

It was shown that under the conditions used for this study, combination of single zinc(II) ions with **L** resulted in the formation of low-dimensional structures (compounds **1** – **3**). This limitation was overcome by employing a metal cluster (Zn_2[μ-OH], as in **4** and **5**) or a larger metal ion (Pb^{2+}, as in **6** – **8**) to favor the formation of higher dimensional structures. Reaction of H**L** with other metals used in this study (copper(II), nickel(II), cobalt(II), and ruthenium(II)) resulted in the crystallization of discrete $[M(\mathbf{L})_2]$ complexes (**10a** – **10j**).

Perhaps the most exciting result in this thesis is the acquisition of compound **13**. Strong evidence was presented showing these crystals are isostructural to MOF-5. Such a MOF

incorporating a light-responsive organic linker has great potential as an advanced material, and could provide fundamental insight into the nature of hybrid photocatalysis and photovoltaics.

After characterization and synthesis of the targeted MOFs from the [Ru(**L**)$_2$] complex, a method for proving the existence of photoinduced charge transfer to a guest molecule in the pores can be formulated. Flash photolysis may provide insight into the nature of transient species within the framework.[73] Furthermore, a method for growing electrically conductive nanoparticles or wires in these materials will provide opportunities for photoinduced electron transfer experiments. Although some advances have been made with regard to the growth of nanoparticles in MOFs,[112-114] the broad applicability of these results has yet to be determined.

Methods for growing films of oriented MOF crystals on electrodes will be indispensible in the fabrication of the MOF-based solar cells proposed in this study. Similarly to the preparation of nanoparticles in MOFs, this research is still at an early stage.[115] Despite these technical challenges, studies on large-pore metal-organic frameworks constructed from light-harvesting dyes are expected to enhance our understanding of photoinduced electron transfer and transport in the solid state.

5.0 EXPERIMENTAL SECTION

5.1 MATERIALS AND METHODS

All starting chemicals were purchased from commercial sources and used as received. The elemental microanalysis was performed by the University of Illinois, Department of Chemistry Microanalytical Laboratory using an Exeter Analytical CE440. Thermogravimetric analysis (TGA) was performed using a TA Q500 thermal analysis system. All TGA experiments were run under a N_2 atmosphere from 25–600 °C at a rate of 1 °C/min. Data were analyzed using the TA Universal Analysis software package. Fourier transform infrared (FT–IR) spectra were measured using KBr pellet samples. Absorptions are described as follows: very strong (vs), strong (s), medium (m), and weak (w). X–ray powder diffraction patterns were taken using a Philips X'Pert powder diffractometer at 40 kV, 30 mA for Cu Kα, (λ = 1.5406 Å) with a scan speed of 0.5 sec/step and a step size of 0.02°. The data were analyzed using the Philips X'Pert Software package. The simulated powder patterns were calculated using Mercury 1.4.2.

Solvent exchange of the DMF and H_2O guest molecules in **1** and **6** was performed using anhydrous solvents as follows: 5 min soak in exchange solvent (ES) followed by solvent removal; 30 min soak in ES—solvent removal; 3 h soak in ES—solvent removal; overnight soak in ES—solvent removal; addition of fresh solvent. The sorption experiment for **1** was done on an Quantachrome Autosorb-1 machine.

5.2 LIGAND SYNTHESES

5.2.1 4'-(4-carboxyphenyl)-2,2':6',2"-terpyridine (HL)

H**L** was prepared according to a modified literature procedure.[4] 30% NH_4OH solution (6 mL) and NaOH (2.92 g) dissolved in a minimum amount of water were added to a solution of 4-methoxycarbonylbenzaldehyde (6.0 g, 36.6 mmol) and 2- acetylpyridine (8.2 mL, 73 mmol) in ethanol (150 mL). After the addition of the NaOH, the solution turned yellow and after about 1 h red. The solution was stirred vigorously at room temperature in a flask open to air for 17 h, after which a yellow suspension was obtained. Water (300 mL) was added and the red solution was slowly acidified with HNO_3 (2 M), with stirring, to pH ~ 4. The greenish solid was filtered by suction and dried overnight in air and refluxed in ethanol (300 mL) until the color turned from green to white. The chalky white solid was dried and refluxed in water (300 mL) until the color was a pale yellow. The product was obtained as a pale yellow solid (4.97 g, 38.4 %). The proton NMR was in agreement with the literature spectra.[4] ;δ_H/ppm (300 MHz, DMSO-d_6): 13.18 (br s, 1H), 8.79-8.77 (m, 4H), 8.70 (d, 2H, J = 8.1 Hz), 8.15 (d, 2H, J = 8.4 Hz), 8.09 (m, 4H), 7.55 (ddd, 2H, J = 0.9, 4.8, 7.5). See appendix for spectra.

5.2.2 Ru(L)$_2$

The dicarboxylate zwitterionic complex, Ru(**L**)$_2$, was prepare using the procedure reported by Constable, et al.[4] H**L** (342 mg, 0.97 mmol), $RuCl_3 \cdot 3H_2O$ (126.5 mg, 0.48 mmol) and NEt_3 (0.3 mL, 2.2 mmol) were suspended in ethanol (3 mL). The mixture was sealed in a Teflon-lined

stainless steel autoclave (23 mL), heated at 150 °C for 18 h, and allowed to cool to room temperature.

The precipitate formed was filtered over Celite and washed with ethanol (5 mL), water containing 10 drops of 2 M NaOH (10 mL) and water (10 mL). The product was extracted with boiling methanol (350 mL). After evaporation of the solvent, a purple-red powder was obtained. A purple spot (R_f = .63, SiO_2, MeOH), in addition to the presumed orange product (R_f < 0.10, SiO_2, MeOH) was observed by TLC. The ^{1}H NMR was in close agreement with the literature spectra. δ_H/ppm (300 MHz, DMSO-d_6): 9.53 (s, 4H), 9.15 (d, 4H, *J* = 8.4 Hz), 8.45 (d, 4H, *J* = 7.8 Hz) , 8.21 (d, 4H, *J* = 7.8 Hz) , 8.07 (t, 4H, *J* = 7.5 Hz) , 7.56 (d, 4H, *J* = 5.1 Hz) , 7.28 (t, 4H, *J* = 6.3 Hz). See appendix for spectra

5.2.3 $[Ru(HL)_2][PF_6]_2$

The dicarboxylic acid complex ion, $[Ru(H\mathbf{L})_2][PF_6]_2$, was prepare using a modified procedure reported by Constable, et al.[4] for the zwitterionic complex ($Ru(\mathbf{L})_2$, see above). H**L** (342 mg, 0.97 mmol), $RuCl_3 \cdot 3H_2O$ (126.5 mg, 0.48 mmol) and NEt_3 (0.3 mL, 2.2 mmol) were suspended in ethanol (3 mL). The mixture was sealed in a Teflon-lined stainless steel autoclave (23 mL), heated at 150 °C for 18 h, and allowed to cool to room temperature.

The ethanol was removed under vacuum and the product was dissolved in 1:1 MeCN:H_2O (250 mL) by boiling and ultrasonication. Silica Gel (43-60 mesh, 20 mL) was added to the solution and the solvent was removed until most of the orange color had come out of the solution. The suspension was filtered to remove the water and the solid was dried overnight in an oven (60 – 85 °C). The residue was purified by silica gel column chromatography (3.5 cm x 20 cm) packed with 12:3:1 MeCN:H_2O:saturated aqueous KNO_3. The column conditions were

developed by TLC (R_f(product) = 0.18 with SiO_2 and 7:3 MeCN: H_2O; R_f = 0.36 with SiO_2 and 1:1 MeCN:H_2O). The silica gel/product mixture was dry loaded onto the column and eluted with 7:3 MeCN:H_2O, and occasionally 12:3:1 MeCN:H_2O:Saturated KNO_3 (when the product began sticking to the silica gel) until the majority of colored impurities were eluted. The last red/orange fraction was collected with 1:1 MeCN:H_2O, and occasionally 6:3:1 MeCN:H_2O: sat. aq. KNO_3. The column is shown in **Figure 51**. NH_4PF_6 (40 mL, 0.4 M, 16 mmol) and HNO_3 (3.5 mL, 1.0 M, 3.5 mmol) were added to the product fraction to yield a red precipitate.

The suspension was allowed to stand overnight and vacuum filtered over Whatman Grade 50 filter paper. The filtration was repeated over the same filter paper until the filtrate was free of red particles. The solid was washed with copious amounts of water and dried in an oven at 85 °C for 24 h. 370 mg (0.34 mmol, 70 %) of red solid product was obtained. This compound (the diacid, $[Ru(H\mathbf{L})_2][PF_6]$) is much more soluble in DMF (up to 0.01 M) and DMSO than the zwitterionic complex, $Ru(\mathbf{L})_2$, and the author recommends the protonated acid for MOF-forming reactions that require these solvents. δ_H/ppm (300 MHz, DMSO-d_6): 13.37 (s, 2H), 9.56 (s, 4H), 9.14 (d, 4H, J = 8.1 Hz), 8.57 (d, 4H, J = 8.7 Hz) , 8.30 (d, 4H, J = 8.4 Hz) , 8.09 (dt, 4H, J = 1.2, 7.8 Hz) , 7.57 (d, 4H, J = 5.1 Hz) , 7.29 (t, 4H, J = 6.9 Hz); m/z 953 ($[M - PF6]^+$, 404 $[(M - 2PF6)/2]^+$). See appendix for spectra

5.3 MATERIALS SYNTHESES

5.3.1 Zn(L)(CF_3COO)·0.3(H_2O)1.8(DMF) (1)

$Zn(CF_3COO)_2·5H_2O$ (152.6 mg, 0.4 mmol), H**L** (141.3 mg, 0.4 mmol), and CF_3COOH (1 M (H_2O), 0.3 mL) were dissolved in DMF (8 mL) in a vial (20 mL). Water (3.2 mL) was added and the vial was tightly capped and heated at 85 °C for 24 h. The yellow hexagonal crystals obtained were washed three times with a DMF:H_2O mixture (8:3.2, 5 mL) and the product was stored in this solution (260.0 mg, 0.38 mmol, 97 %). Anal Calcd. (%) for Zn(**L**)(tfa)•$(H_2O)_{0.3}(DMF)_{1.8}$: C, 52.88; H, 4.11; N, 10.07. Found: C, 53.03; H, 4.55; N, 10.14. Anal Calcd. (%) for material heated to 150° C Zn(**L**)(tfa): C, 54.81; H, 2.60; N, 7.97. Found: C, 54.31; H, 2.66; N, 7.92. Anal Calcd. (%) for $CHCl_3$ exchanged material Zn(**L**)(tfa)•$(DMF)_1(CHCl_3)_{1.4}$: C, 43.95; H, 3.62; N, 6.45. Found: C, 43.88; H, 2.45; N, 6.42. FT-IR (KBr): 3436 (w), 3070 (w), 1670 (s), 1613.34 (s), 1563 (m), 1477 (m), 1430 (m), 1384 (s), 1251 (w), 1200 (m), 1137 (w), 1015 (w), 817 (m), 800 (m), 785 (m). The purity and homogeneity of the bulk products were determined by comparison of the simulated and experimental X–ray powder diffraction patterns.

5.3.2 Zn(HCOO)(L) (2)

$Zn(BF_4)_2·6H_2O$ (50 mg, 0.15 mmol) and H**L** (35.3 mg, 0.1 mmol) were suspended in a mixture of DMF (3 mL) and H_2O (1 mL) in a Teflon-capped glass pressure vial (15 mL). The vial was capped and heated at 130 ºC for 24 h and allowed to cool naturally to room temperature. Yellow rods were collected and characterized by single crystal X-ray crystallography. See notebook #2, page 160, reaction #1

5.3.3 $Zn_2(HL)(L)_2(BF_4)_2$ (3)

$Zn(BF_4)_2 \cdot 6H_2O$ (51.7 mg, 0.15 mmol) and H**L** (72.6 mg, 0.2 mmol) were suspended in water (10 mL) in a Teflon-lined stainless steel autoclave (23 mL). The autoclave was sealed and heated at 5 ºC/min to 180 ºC, held at that temperature 72 h, and cooled at a rate 0.1 ºC/min to ambient temperature. Yellow rods suitable for single crystal XRD were obtained. See notebook #2, page 142, reaction #2

5.3.4 $Zn_4(\mu\text{-}OH)(L)_4(HCOO)(BF_4)_2$ (4)

$Zn(BF_4)_2 \cdot 6H_2O$ (69.4 mg, 0.2 mmol) and H**L** (35.3 mg, 0.1 mmol) were suspended in a mixture of DMF (1 mL) and H_2O (3 mL) in a Teflon-capped glass pressure vial (15 mL). The vial was capped and heated at 130 ºC for 32 hours and cooled at a rate of 0.2 ºC/min to ambient temperature. Yellow prismatic crystals were obtained and characterized by single crystal XRD. PXRD indicated the product was not a pure phase. Performing the reaction under more dilute conditions or a higher metal:ligand ratio may result in a more complete reaction. See notebook #2, page 167, reaction #3

5.3.5 $Zn_2(\mu\text{-}OH)(L)_2(BF_4)$ (5)

H**L** (176.7 mg), Na_2SiO_3 (56.8 mg, 0.2 mmol), $Zn(BF_4)_2 \cdot 6H_2O$) (173.5 mg, 0.5 mmol), and KOH (0.75 mL, 1 mol/L) were suspended in H_2O (10 mL). The pH was adjusted to ~ 5 by addition of aqueous HBF_4 and the suspension was placed in a teflon-lined stainless steel autoclave (23 mL). The autoclave was sealed and heated at a rate of 3° C/min to 180° C, held at that temperature for

100 h, and cooled at a rate of 0.1° C/min to ambient temperature. Yellow prisms suitable for single crystal X-ray analysis were formed. Performing the reaction under more dilute conditions or a higher metal:ligand ratio may result in a more complete reaction. See notebook #2, page 197, reaction #2

5.3.6 Pb(L)(NO_3)·1.3(H_2O)1.3(DMF) (6)

$Pb(NO_3)_2$ (132.5 mg, 0.4 mmol), H**L** (70.7 mg, 0.2 mmol), and HNO_3 (1 M (H_2O), 0.3 mL) were dissolved in DMF (10 mL) in a vial (20 mL). The vial was capped and heated at 85° C for 24 h. The resulting colorless block crystals were washed three times with DMF (5 mL) and were stored in this solvent (110.4 mg, 0.15 mmol, 75 %). Anal Calcd. (%) for Pb(**L**)(NO_3)•(H_2O)$_{1.3}$(DMF)$_{1.3}$: C, 42.04; H, 3.50; N, 10.03. Found: C, 41.98; H, 3.43; N, 10.08. Anal Calcd. (%) for product after heating to 200° C Pb(**L**)(NO_3)•(H_2O): C, 41.31; H, 2.52; N, 8.76. Found: C, 41.41; H, 2.19; N, 8.62. FT-IR (KBr): 3434 (w), 3074 (w), 2925 (w, DMF), 1667 (s, DMF), 1609 (m), 1594 (m), 1547 (m), 1481 (m), 1385 (s), 1243 (m), 1096 (m), 1007 (m), 818 (m), 783 (s). The purity and homogeneity of the bulk products were determined by comparison of the simulated and experimental X–ray powder diffraction patterns. See notebook #2, page 141, reaction #5.

5.3.7 Pb(L)(BF_4) (7)

Single crystals of this compound were synthesized in a similar way to 5.3.2 with $Pb(BF_4)_2$ (50% aqueous) in place of $Pb(NO_3)_2$, and HBF_4 in place of HNO_3. Block crystals were

obtained along with a white microcrystalline phase. See Chris Fennig's notebook, page 98, reaction #8.

5.3.8 $Pb_2(L)_2(NO_3)Cl$ (8)

Single crystals of this compound were synthesized in a similar way to 5.3.2, with HCl in place of HNO_3. The purity and homogeneity of the bulk products were determined by comparison of the simulated and experimental X–ray powder diffraction patterns.

5.3.9 $Gd(L)_3$ (9)

$Gd(NO_3)_3 \cdot 6H_2O$ (4.5 mg, 0.01 mmol) and H**L** (3.5 mg, 0.01 mmol) were suspended in a mixture of DMF (0.55 mL) and H_2O (0.55 mL) in a vial (4 mL). The vial was capped and heated at 85 ºC for 24 hours to yield colorless football-shaped single crystals of 5.3.5. This compound was also obtained at higher temperature (up to 180 ºC) with water as the solvent. See notebook #2, page 127, reaction #2

5.3.10 $[M(L)_2]$ complexes and Other L-containing Crystals

5.3.10.1 $Ru(L)_2$ (10a) $Ru(\mathbf{L})_2$ (0.002 mmol), $Sm(NO_3)_3$ (0.002 mmol), and HBF_4 (0.2 M, 0.01 mL) were suspended in DMF (0.65 mL) and H_2O (0.45 mL) in a vial (20 mL). The vial was heated at 85 ºC for 24 h and allowed to stand at room temperature for three weeks. Very dark red prismatic crystals were formed.

5.3.10.2 Ru(L)$_2$ (10b) Ru(**L**)$_2$ (0.002 mmol), $HClO_4$ (1 M, 0.025 mL), and $Pb(ClO_4)_2 \cdot 3H_2O$ (0.008 mmol) in DMF (0.5 mL) and H_2O (0.2 mL) were frozen in liquid nitrogen and flame sealed in a thick-walled Pyrex tube under vacuum. The tube was placed in an oven set to 85 ºC for 24 h and allowed to cool naturally to room temperature.

5.3.10.3 Ru(L)$_2$ (10c) $Zn(BF_4)_2 \cdot 5H_2O$ (0.1 mmol, 23.8 mg), $RuCl_3 \cdot 3H_2O$ (0.2 mmol, 52.3 mg), and H**L** (0.133 mmol, 47.1 mg) were suspended in water (10 mL). The suspension was placed in a teflon lined stainless steel autoclave (23 mL), heated at 180 ºC for 3 days, and cooled at a rate of 0.1 ºC/min to ambient temperature.

5.3.10.4 Zn(L)$_2$ (10d) $Zn(BF_4)_2 \cdot 5H_2O$ (0.01 mmol), $Mg(NO_3)_2$ (0.02 mmol), and H**L** (0.02 mmol), suspended in a biphasic mixture of H_2O (0.4 mL) and 1-butanol (0.5 mL) were frozen in liquid nitrogen and flame sealed in a thick-walled Pyrex tube under vacuum. The tube was heated at 100 ºC in an oven for two days.

5.3.10.5 Zn(L)$_2$ (10e) $Zn(BF_4)_2 \cdot 5H_2O$ (0.01 mmol) and H**L** (0.02 mmol), suspended in a biphasic mixture of hexanes (0.5 mL) and water (0.5 mL) were frozen in liquid nitrogen and flame sealed in a thick-walled Pyrex tube under vacuum. The tube was heated at 100 ºC in an oven for two days.

5.3.10.6 Zn(L)$_2$ (10f) $Zn(BF_4)_2 \cdot 5H_2O$ (0.4 mmol, 95.5 mg), $Emu(SO_3CF_3)_3 \cdot 6H_2O$ (0.4 mmol, 239.8 mg), and H**L** (0.133 mmol, 47.1 mg) were suspended in water (10 mL). The suspension was placed in a teflon lined stainless steel autoclave (23 mL), heated at 180 ºC for 3 days, and cooled at a rate of 0.1 ºC/min to ambient temperature.

5.3.10.7 $Cu(L)_2$ (10g) $Cu(BF_4)_2 \cdot 6H_2O$ (0.2 mmol, 47.0 mg) and H**L** (0.2 mmol, 70.6 mg) were suspended in water (10 mL). The suspension was placed in a teflon lined stainless steel autoclave (23 mL), heated at 180 ºC for 3 days and cooled at a rate of 0.1 ºC/min to ambient temperature.

5.3.10.8 $Ni(L)_2$ (10h) H**L** (0.02 mmol) and $Ni(BF_4)_2 \cdot 6H_2O$ (0.01 mmol) in DMF (0.6 mL) were frozen in liquid nitrogen and flame sealed in a thick-walled Pyrex tube under vacuum. The tube was placed in an oven set to 85 ºC for 24 h and allowed to cool naturally to room temperature.

5.3.10.9 $Co(L)_2$ (10i) H**L** (0.01 mmol) and $Co(BF_4)_2 \cdot 6H_2O$ (0.02 mmol) in DMF (0.4 mL) and H_2O (0.4 mL) were frozen in liquid nitrogen and flame sealed in a thick-walled Pyrex tube under vacuum. The tube was placed in an oven set to 85 ºC for 24 h and allowed to cool naturally to room temperature.

5.3.10.10 $Co(L)_2$ (10j) $Co(BF_4)_2 \cdot 6H_2O$ (0.2 mmol, 68.3 mg) and H**L** (0.2 mmol, 70.6 mg) were suspended in water (10 mL). The suspension was placed in a teflon lined stainless steel autoclave (23 mL), heated at 180 ºC for 3 days and cooled at a rate of 0.1 ºC/min to ambient temperature. Red blocks were formed which were insoluble in DMF and soluble in DMSO.

5.3.10.11 HL (11) $Eu(CF_3SO_3)_3 \cdot 6H_2O$ (0.2 mmol, 112.5 mg) and H**L** (0.2 mmol, 72.1 mg) were suspended in water (10 mL). The suspension was placed in a teflon lined stainless steel autoclave (23 mL), heated at 180 ºC for 3 days and cooled at a rate of 0.1 ºC/min to ambient temperature.

5.3.10.12 $Cd(HL)(NO_3)_2$ (12) HL (0.05 mmol), $Cd(NO_3)_2$ (0.05 mmol) and HNO_3 (1 M, 0.15 mL) were dissolved in DMF (0.5 mL) and isopropanol (0.6 mL) in a vial (20 mL). Large colorless needles formed after the vial was stood at room temperature for 5 days.

5.4 X-RAY CRYSTALLOGRAPHY

Crystals were coated in an inert hydrocarbon–based oil and mounted on a Bruker SMART APEX II CCD diffractometer equipped with a normal focus Mo–target X–ray tube (λ = 0.71073 Å) operated at 1575 W power (45 kV, 35 mA). The X–ray intensities were measured at 173(2) K; the detector was placed at a distance of 5.001 cm from the crystal. The frames were integrated with the SAINT software package with a narrow frame algorithm. The structures were solved by direct methods and the subsequent difference Fourier syntheses and refined with the SHELXTL[116] (version 6.14) software package. Compound **1** was solved in space group R3, and higher symmetry found and transformed by PLATON[88] to centrosymmetric space group R-3. Hydrogen atoms were placed in calculated positions and refined isotropically. Isolated oxygen atoms (to model high electron density in the pores) were refined isotropically. All other atoms in **1** were refined anisotropically. For compounds **2**, **4**, **5**, **6**, **7**, and **9**, hydrogen atoms were placed in calculated positions and refined isotropically. All other atoms were refined anisotropically. For structure **4**, all heavy skeleton atoms (C, N, O, Zn) could be located, although one benzoate ring and its attached carbonyl was very distorted. All heteroatoms, excluding the ones assigned to unresolved solvent electron density and O3, O4, and O5, were refined anisotropically. All carbon atoms were refined isotropically. Hydrogen atoms for **4** were placed in calculated positions and refined isotropically. All atoms in compound **8** were refined isotropically.

For compound **13**, the data were integrated by SAINT unconstrained, after first attempting to integrate while constrained to a cubic Laue class. The constraints resulted in a very poor quality structural model. The space group recommended by XPREP, P23 (#195, the lowest symmetry cubic space group), was chosen to solve the structure. After enough refinement cycles to lower the R value to 37%, an attempt was made to find higher symmetry with the PLATON program. The space group found by PLATON resulted in a very poor quality structure model (R value > 47%). All atoms found in the structure were refined anisotropically.

APPENDIX

SPECTRA AND CRYSTAL DATA

Table 19. Crystal data and structure refinement for **1**

Identification code	$Zn(L)(tfa)\cdot(H_2O)_{0.3}(DMF)_{1.9}$	
Empirical formula	$C_{432}H_{252}F_{54}N_{54}O_{126}Zn_{18}$	
Formula weight	10417.90	
Temperature	173(2) K	
Wavelength	0.71073 Å	
Crystal system	Hexagonal	
Space group	R-3 (#148)	
Unit cell dimensions	a = 39.349(4) Å	α= 90°.
	b = 39.349(4) Å	β= 90°.
	c = 10.5898(14) Å	γ = 120°.
Volume	14200(3) $Å^3$	
Z	1	
Density (calculated)	1.218 Mg/m^3	
Absorption coefficient	0.835 mm^{-1}	
F(000)	5255	
Crystal size	0.3 x 0.2 x 0.15 mm^3	
Theta range for data collection	3.59 to 28.37°.	
Index ranges	-51<=h<=51, -52<=k<=52, -14<=l<=13	
Reflections collected	39580	
Independent reflections	7446 [R(int) = 0.1611]	
Completeness to theta = 28.37°	94.2 %	
Absorption correction	SADABS	
Refinement method	Full-matrix least-squares on F^2	
Data / restraints / parameters	7446 / 0 / 326	
Goodness-of-fit on F^2	1.316	
Final R indices [I>2sigma(I)]	R1 = 0.0864, wR2 = 0.2597	
R indices (all data)	R1 = 0.1693, wR2 = 0.2866	

Largest diff. peak and hole 0.676 and -0.534 e.Å^{-3}

Table 20. Atomic coordinates[a] and equivalent isotropic displacement parameters[b] for **1**

	x	y	z	U(eq)[c]
Zn(1)	2959(1)	2185(1)	4141(1)	44(1)
F(1)	1956(2)	2173(2)	6521(5)	133(2)
F(2)	1836(2)	1673(2)	7452(7)	166(3)
F(3)	1633(2)	1670(3)	5574(7)	182(3)
O(1)	3799(1)	-150(1)	3199(4)	51(1)
O(2)	4385(1)	327(1)	3815(4)	60(1)
O(3)	2496(1)	2137(1)	5061(4)	58(1)
O(4)	2388(1)	1618(1)	6166(5)	74(1)
O(1W)	2181(2)	424(2)	9296(8)	108(2)
O(2W)	1924(5)	901(5)	7652(15)	134(5)
N(1)	3399(1)	2383(1)	5642(4)	47(1)
N(2)	3156(1)	1788(1)	4094(4)	39(1)
N(3)	2634(1)	1795(1)	2605(5)	49(1)
C(1)	3531(2)	2715(2)	6312(6)	52(1)
C(2)	3844(2)	2850(2)	7104(6)	58(2)
C(3)	4028(2)	2638(2)	7233(6)	63(2)
C(4)	3893(2)	2289(2)	6540(6)	55(2)
C(5)	3589(2)	2174(2)	5754(5)	42(1)
C(6)	3437(2)	1831(1)	4883(5)	40(1)
C(7)	3575(2)	1568(2)	4878(5)	44(1)
C(8)	3431(2)	1263(2)	3996(5)	41(1)
C(9)	3150(2)	1237(2)	3131(5)	43(1)
C(10)	3016(1)	1510(1)	3225(5)	38(1)
C(11)	2719(2)	1512(2)	2369(5)	43(1)
C(12)	2534(2)	1245(2)	1397(6)	55(2)
C(13)	2256(2)	1269(2)	693(7)	68(2)
C(14)	2173(2)	1558(2)	927(7)	67(2)
C(15)	2362(2)	1815(2)	1890(7)	61(2)
C(16)	3569(2)	978(2)	3955(5)	43(1)
C(17)	3934(2)	1078(2)	4432(6)	53(2)
C(18)	4077(2)	817(2)	4343(6)	55(2)
C(19)	3859(2)	462(2)	3767(5)	43(1)
C(20)	3496(2)	360(2)	3314(5)	45(1)
C(21)	3344(2)	611(2)	3410(5)	44(1)
C(22)	4027(2)	195(2)	3606(5)	49(1)
C(23)	2318(2)	1868(2)	5835(6)	55(2)
C(24)	1935(3)	1837(3)	6329(10)	100(3)

[a] x 10^4
[b] $Å^2$ x 10^3
[c] U(eq) is defined as one third of the trace of the orthogonalized U^{ij} tensor.

Table 21. Bond lengths (Å) and angles (°) for **1**

Zn(1)-O(1)#1	1.959(4)	C(13)-C(14)	1.354(9)
Zn(1)-O(3)	1.991(4)	C(13)-H(13)	0.9300
Zn(1)-N(2)	2.065(4)	C(14)-C(15)	1.365(9)
Zn(1)-N(3)	2.160(5)	C(14)-H(14)	0.9300
Zn(1)-N(1)	2.188(5)	C(15)-H(15)	0.9300
F(1)-C(24)	1.298(10)	C(16)-C(17)	1.378(8)
F(2)-C(24)	1.316(11)	C(16)-C(21)	1.386(7)
F(3)-C(24)	1.304(11)	C(17)-C(18)	1.399(8)
O(1)-C(22)	1.273(7)	C(17)-H(17)	0.9300
O(1)-Zn(1)#2	1.959(4)	C(18)-C(19)	1.365(8)
O(2)-C(22)	1.251(7)	C(18)-H(18)	0.9300
O(3)-C(23)	1.242(7)	C(19)-C(20)	1.366(7)
O(4)-C(23)	1.200(7)	C(19)-C(22)	1.503(7)
N(1)-C(1)	1.344(7)	C(20)-C(21)	1.387(7)
N(1)-C(5)	1.362(7)	C(20)-H(20)	0.9300
N(2)-C(10)	1.320(6)	C(21)-H(21)	0.9300
N(2)-C(6)	1.326(7)	C(23)-C(24)	1.541(11)
N(3)-C(11)	1.336(7)		
N(3)-C(15)	1.344(7)	O(1)#1-Zn(1)-O(3)	100.39(17)
C(1)-C(2)	1.359(9)	O(1)#1-Zn(1)-N(2)	131.50(17)
C(1)-H(1)	0.9300	O(3)-Zn(1)-N(2)	127.90(17)
C(2)-C(3)	1.356(9)	O(1)#1-Zn(1)-N(3)	105.98(17)
C(2)-H(2)	0.9300	O(3)-Zn(1)-N(3)	96.49(18)
C(3)-C(4)	1.409(8)	N(2)-Zn(1)-N(3)	75.96(17)
C(3)-H(3)	0.9300	O(1)#1-Zn(1)-N(1)	91.74(16)
C(4)-C(5)	1.336(8)	O(3)-Zn(1)-N(1)	101.75(18)
C(4)-H(4)	0.9300	N(2)-Zn(1)-N(1)	75.87(16)
C(5)-C(6)	1.490(7)	N(3)-Zn(1)-N(1)	151.80(17)
C(6)-C(7)	1.391(7)	C(22)-O(1)-Zn(1)#2	109.8(3)
C(7)-C(8)	1.397(7)	C(23)-O(3)-Zn(1)	120.1(4)
C(7)-H(7)	0.9300	C(1)-N(1)-C(5)	118.6(5)
C(8)-C(9)	1.401(7)	C(1)-N(1)-Zn(1)	125.6(4)
C(8)-C(16)	1.473(7)	C(5)-N(1)-Zn(1)	115.1(3)
C(9)-C(10)	1.415(7)	C(10)-N(2)-C(6)	121.5(4)
C(9)-H(9)	0.9300	C(10)-N(2)-Zn(1)	119.0(3)
C(10)-C(11)	1.484(7)	C(6)-N(2)-Zn(1)	119.4(3)
C(11)-C(12)	1.390(8)	C(11)-N(3)-C(15)	118.6(5)
C(12)-C(13)	1.368(8)	C(11)-N(3)-Zn(1)	115.3(4)
C(12)-H(12)	0.9300	C(15)-N(3)-Zn(1)	126.1(4)

N(1)-C(1)-C(2)	122.8(6)	C(12)-C(13)-H(13)	120.1
N(1)-C(1)-H(1)	118.6	C(13)-C(14)-C(15)	119.1(6)
C(2)-C(1)-H(1)	118.6	C(13)-C(14)-H(14)	120.4
C(3)-C(2)-C(1)	118.6(6)	C(15)-C(14)-H(14)	120.4
C(3)-C(2)-H(2)	120.7	N(3)-C(15)-C(14)	122.3(6)
C(1)-C(2)-H(2)	120.7	N(3)-C(15)-H(15)	118.8
C(2)-C(3)-C(4)	119.4(6)	C(14)-C(15)-H(15)	118.8
C(2)-C(3)-H(3)	120.3	C(17)-C(16)-C(21)	118.8(5)
C(4)-C(3)-H(3)	120.3	C(17)-C(16)-C(8)	119.9(5)
C(5)-C(4)-C(3)	119.4(6)	C(21)-C(16)-C(8)	121.3(5)
C(5)-C(4)-H(4)	120.3	C(16)-C(17)-C(18)	120.6(5)
C(3)-C(4)-H(4)	120.3	C(16)-C(17)-H(17)	119.7
C(4)-C(5)-N(1)	121.2(5)	C(18)-C(17)-H(17)	119.7
C(4)-C(5)-C(6)	125.3(5)	C(19)-C(18)-C(17)	120.2(5)
N(1)-C(5)-C(6)	113.5(5)	C(19)-C(18)-H(18)	119.9
N(2)-C(6)-C(7)	120.7(5)	C(17)-C(18)-H(18)	119.9
N(2)-C(6)-C(5)	116.1(4)	C(18)-C(19)-C(20)	119.1(5)
C(7)-C(6)-C(5)	123.2(5)	C(18)-C(19)-C(22)	119.7(5)
C(6)-C(7)-C(8)	120.1(5)	C(20)-C(19)-C(22)	121.2(5)
C(6)-C(7)-H(7)	119.9	C(19)-C(20)-C(21)	121.7(5)
C(8)-C(7)-H(7)	119.9	C(19)-C(20)-H(20)	119.1
C(7)-C(8)-C(9)	117.7(5)	C(21)-C(20)-H(20)	119.1
C(7)-C(8)-C(16)	122.0(5)	C(16)-C(21)-C(20)	119.5(5)
C(9)-C(8)-C(16)	120.3(5)	C(16)-C(21)-H(21)	120.2
C(8)-C(9)-C(10)	118.6(5)	C(20)-C(21)-H(21)	120.2
C(8)-C(9)-H(9)	120.7	O(2)-C(22)-O(1)	123.4(5)
C(10)-C(9)-H(9)	120.7	O(2)-C(22)-C(19)	119.0(5)
N(2)-C(10)-C(9)	121.2(5)	O(1)-C(22)-C(19)	117.4(5)
N(2)-C(10)-C(11)	115.1(4)	O(4)-C(23)-O(3)	129.0(6)
C(9)-C(10)-C(11)	123.7(5)	O(4)-C(23)-C(24)	117.0(6)
N(3)-C(11)-C(12)	121.1(5)	O(3)-C(23)-C(24)	113.7(6)
N(3)-C(11)-C(10)	114.7(5)	F(1)-C(24)-F(3)	100.9(9)
C(12)-C(11)-C(10)	124.2(5)	F(1)-C(24)-F(2)	102.3(9)
C(13)-C(12)-C(11)	118.9(6)	F(3)-C(24)-F(2)	109.5(9)
C(13)-C(12)-H(12)	120.5	F(1)-C(24)-C(23)	114.2(8)
C(11)-C(12)-H(12)	120.5	F(3)-C(24)-C(23)	116.0(9)
C(14)-C(13)-C(12)	119.8(6)	F(2)-C(24)-C(23)	112.5(8)
C(14)-C(13)-H(13)	120.1		

Symmetry transformations used to generate equivalent atoms:
#1 y+1/3,-x+y+2/3,-z+2/3 #2 x-y+1/3,x-1/3,-z+2/3

Table 22. Anisotropic displacement parameters for **1**[d]

U^{11}	U^{22}	U^{33}	U^{23}	U^{13}	U^{12}

Zn(1)	49(1)	35(1)	51(1)	3(1)	2(1)	23(1)
F(1)	162(6)	178(6)	105(4)	13(4)	17(4)	121(5)
F(2)	175(6)	190(7)	135(5)	80(5)	64(5)	92(6)
F(3)	71(4)	240(8)	171(7)	-34(6)	-40(4)	29(5)
O(1)	57(2)	49(2)	60(2)	0(2)	7(2)	36(2)
O(2)	63(3)	73(3)	65(3)	-14(2)	-16(2)	49(2)
O(3)	61(3)	62(3)	60(3)	13(2)	8(2)	38(2)
O(4)	73(3)	71(3)	84(3)	16(3)	-4(3)	40(3)
N(1)	57(3)	39(2)	41(3)	-2(2)	0(2)	22(2)
N(2)	44(2)	29(2)	43(2)	0(2)	-1(2)	18(2)
N(3)	48(3)	41(3)	59(3)	5(2)	-3(2)	21(2)
C(1)	69(4)	41(3)	50(3)	-4(3)	0(3)	29(3)
C(2)	69(4)	44(3)	52(4)	-10(3)	4(3)	21(3)
C(3)	63(4)	61(4)	57(4)	-11(3)	-12(3)	24(3)
C(4)	60(4)	49(3)	56(4)	-10(3)	-12(3)	28(3)
C(5)	46(3)	33(3)	45(3)	4(2)	3(2)	19(2)
C(6)	45(3)	34(3)	39(3)	3(2)	2(2)	19(2)
C(7)	44(3)	42(3)	46(3)	-2(2)	-4(2)	22(3)
C(8)	41(3)	39(3)	45(3)	-1(2)	-1(2)	21(2)
C(9)	47(3)	39(3)	41(3)	-1(2)	-3(2)	19(2)
C(10)	39(3)	29(2)	45(3)	3(2)	-1(2)	16(2)
C(11)	43(3)	36(3)	48(3)	2(2)	-5(2)	18(2)
C(12)	60(4)	44(3)	60(4)	-6(3)	-12(3)	24(3)
C(13)	69(4)	61(4)	70(4)	-12(3)	-28(4)	29(4)
C(14)	59(4)	71(4)	75(5)	-3(4)	-19(4)	36(4)
C(15)	59(4)	57(4)	76(4)	1(3)	-13(3)	35(3)
C(16)	51(3)	41(3)	40(3)	-2(2)	0(2)	25(3)
C(17)	53(3)	48(3)	63(4)	-13(3)	-14(3)	29(3)
C(18)	56(4)	62(4)	60(4)	-10(3)	-11(3)	39(3)
C(19)	47(3)	45(3)	42(3)	2(2)	3(2)	27(3)
C(20)	56(3)	37(3)	46(3)	0(2)	-3(3)	26(3)
C(21)	48(3)	40(3)	48(3)	1(2)	-2(3)	24(3)
C(22)	56(4)	61(4)	40(3)	0(3)	0(3)	37(3)
C(23)	52(4)	61(4)	51(4)	7(3)	-6(3)	26(3)
C(24)	102(7)	88(6)	106(7)	25(6)	21(6)	45(6)

[d] in $Å^2$ x $10.^3$ The anisotropic displacement factor exponent takes the form: $-2\pi^2[h^2 a^{*2}U^{11} + ... + 2 h k a^* b^* U^{12}]$

Table 23. Hydrogen coordinates[a] and isotropic displacement parameters[b] for **1**

	x	y	z	U(eq)[c]
H(1)	3403	2858	6231	63
H(2)	3931	3083	7547	70

H(3)	4241	2723	7775	76
H(4)	4014	2139	6628	65
H(7)	3763	1594	5463	52
H(9)	3053	1045	2508	52
H(12)	2599	1052	1227	66
H(13)	2124	1088	55	82
H(14)	1989	1581	439	80
H(15)	2301	2010	2058	74
H(17)	4085	1320	4817	64
H(18)	4322	887	4677	66
H(20)	3346	117	2931	54
H(21)	3094	534	3110	53

[a] x 10^4
[b] Å^2 x 10^3

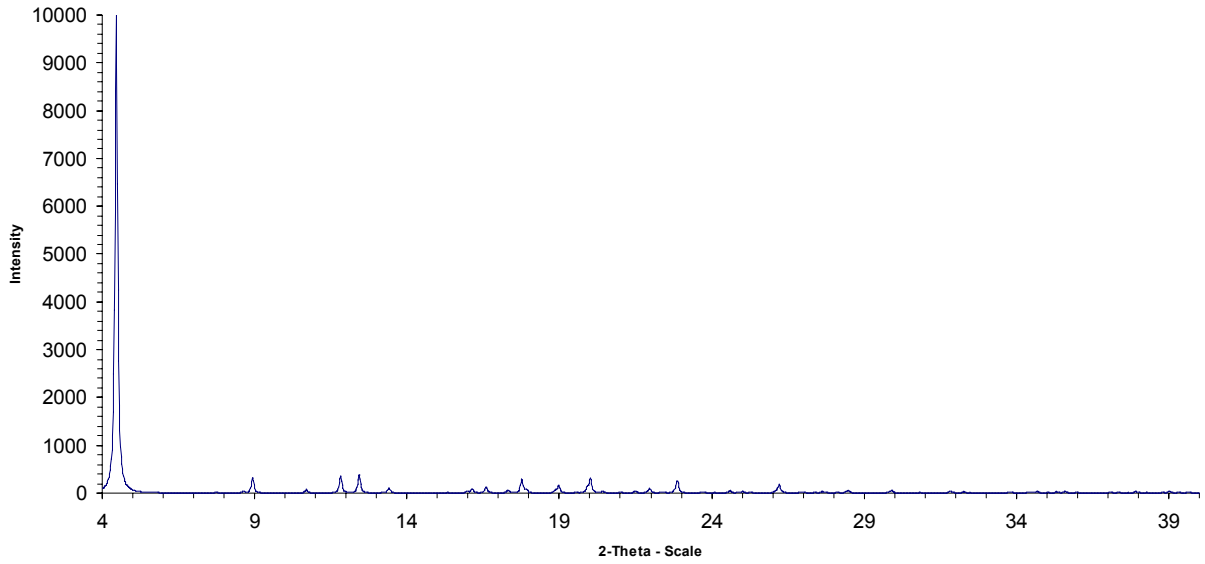

Figure 52. Calculated PXRD pattern of **1**

The structure was solved using data collected at 173 K. The below PXRD pattern was simulated by substituting the unit cell parameters (hexagonal, a=39.5700, c=10.7300) obtained from single crystal X-ray diffraction measured at room temperature in place of the original unit cell parameters obtained at 173 K.

Table 24. Calculated PXRD peaks of **1**

Angle (2θ)°	d Spacing (Å)	Intensity (%)	*hkl*	Angle (2θ)°	d Spacing (Å)	Intensity (%)	*hkl*
4.463	19.78500	100.00	110	20.021	4.43147	2.71	32-2
8.932	9.89250	3.32	220			0.10	232
10.698	8.26293	0.71	211	21.960	4.04423	0.01	152
		0.06	12-1			0.97	51-2
11.825	7.47803	2.90	140	22.871	3.88516	0.48	342
		0.64	410			1.93	43-2
12.431	7.11466	1.74	31-1	26.217	3.39644	1.55	54-2
		1.98	131			0.14	452
13.415	6.59500	1.11	330	27.624	3.22660	0.01	413
16.139	5.48737	0.67	520			0.03	41-3
		0.21	250			0.14	143
16.591	5.33886	0.06	15-1			0.09	14-3
		1.12	511	28.486	3.13090	0.04	372
17.768	4.98800	0.06	34-1			0.45	73-2
		2.66	431	29.910	2.98497	0.01	912
18.980	4.67205	1.12	312			0.04	562
		0.37	13-2			0.39	65-2
						0.12	19-2

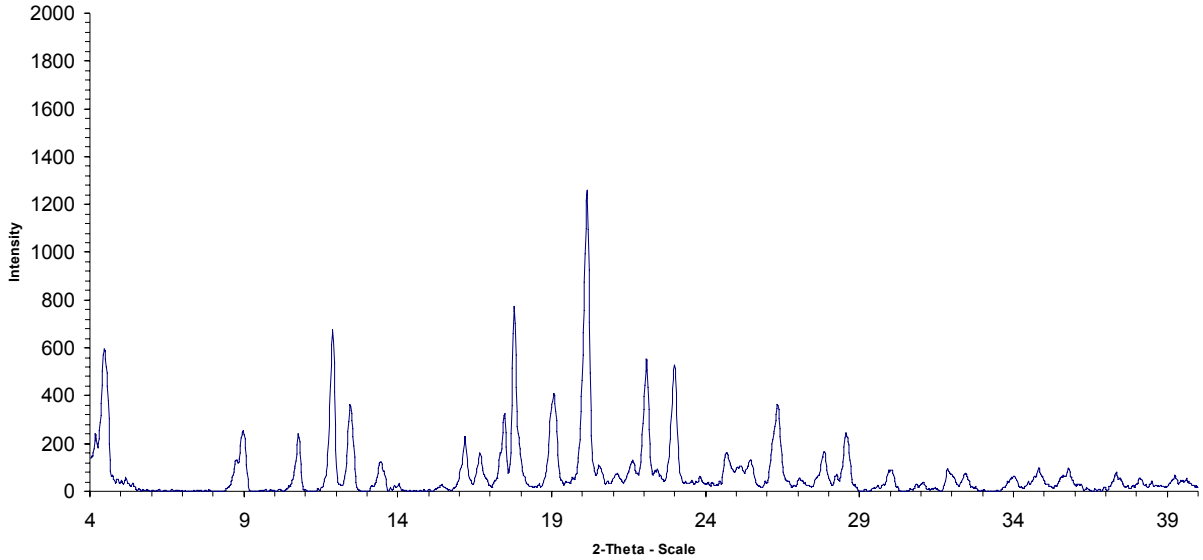

Figure 53. As synthesized PXRD pattern for **1**

Table 25. As synthesized PXRD peaks of **1**

Angle (2θ)°	d Spacing (Å)	Intensity (%)	*hkl*	Angle (2θ)°	d Spacing (Å)	Intensity (%)	*hkl*
4.47	19.752	47.30	110	20.15	4.403	100.00	32-2
8.97	9.851	19.98	220				232
10.77	8.208	19.20	211	22.07	4.024	43.87	152
			12-1				51-2
11.89	7.437	53.52	140	22.99	3.865	41.75	342
			410				43-2
12.45	7.104	28.93	31-1	26.33	3.382	28.96	54-2
			131				452
13.43	6.588	9.86	330	27.85	3.201	13.14	413
16.19	5.470	18.21	520				41-3
			250				143
16.67	5.314	12.69	15-1				14-3
			511	28.57	3.122	19.29	372
17.79	4.982	61.25	34-1				73-2
			431	30.01	2.975	7.20	912
19.07	4.650	32.56	312				562
			13-2				65-2
							19-2

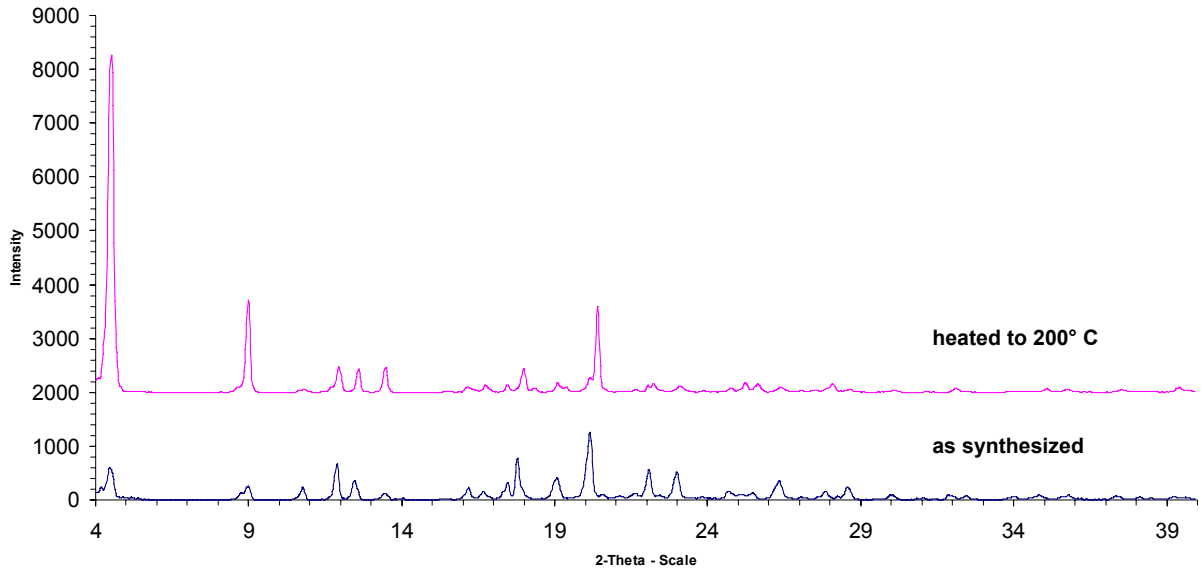

Figure 54. PXRD pattern of **1** after heating to 200° C

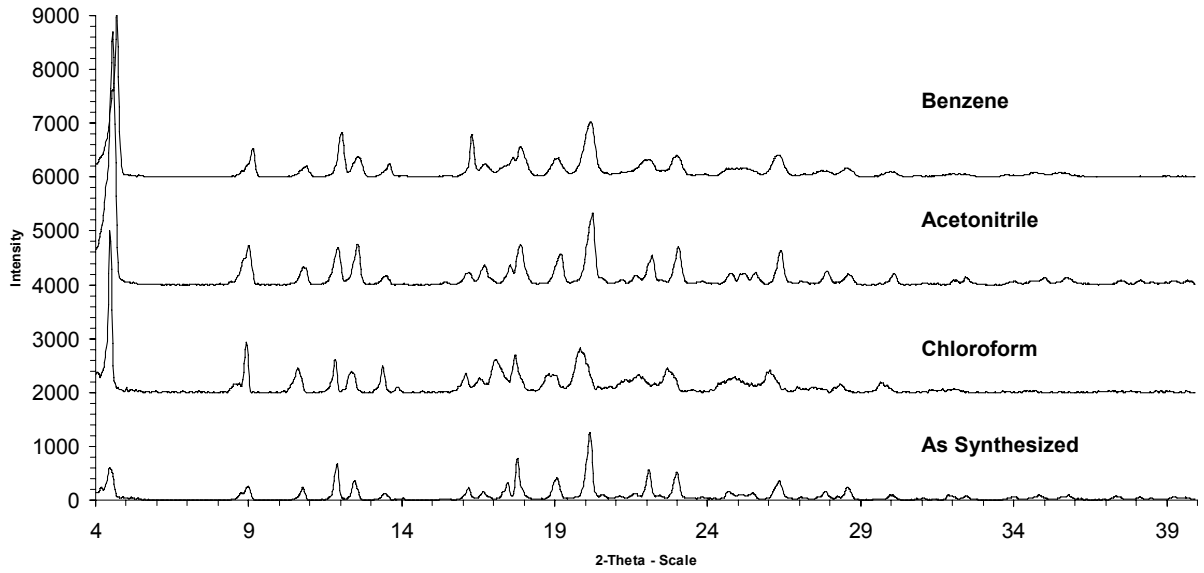

Figure 55. PXRD pattern of **1** after solvent exchange for 48 hours

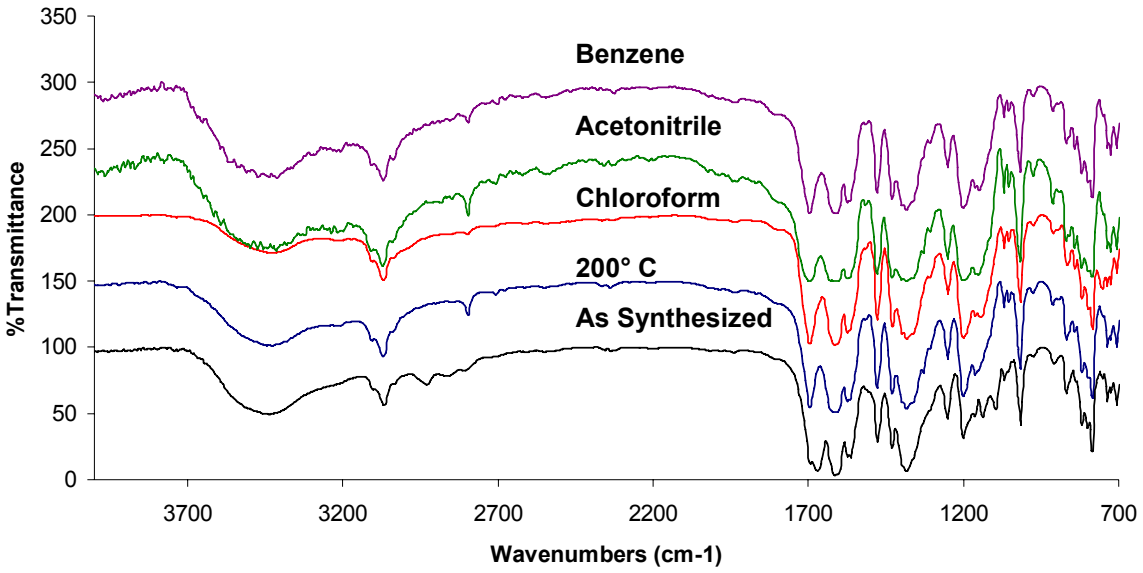

Figure 56. FT-IR spectra for as synthesized, heated, and solvent exchanged samples of **1**

For as synthesized sample: FT-IR (KBr): 3436 (w), 3070 (w), 1670 (s), 1613.34 (s), 1563 (m), 1477 (m), 1430 (m), 1384 (s), 1251 (w), 1200 (m), 1137 (w), 1015 (w), 817 (m), 800 (m), 785 (m).

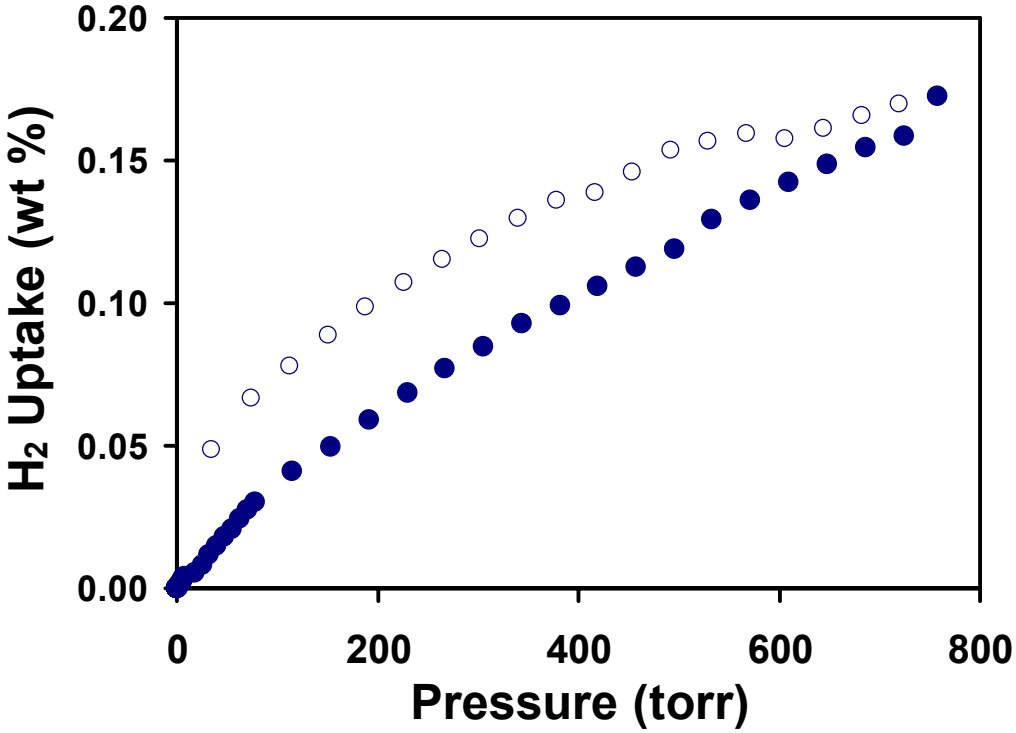

Figure 57. H_2 isotherm for **1**

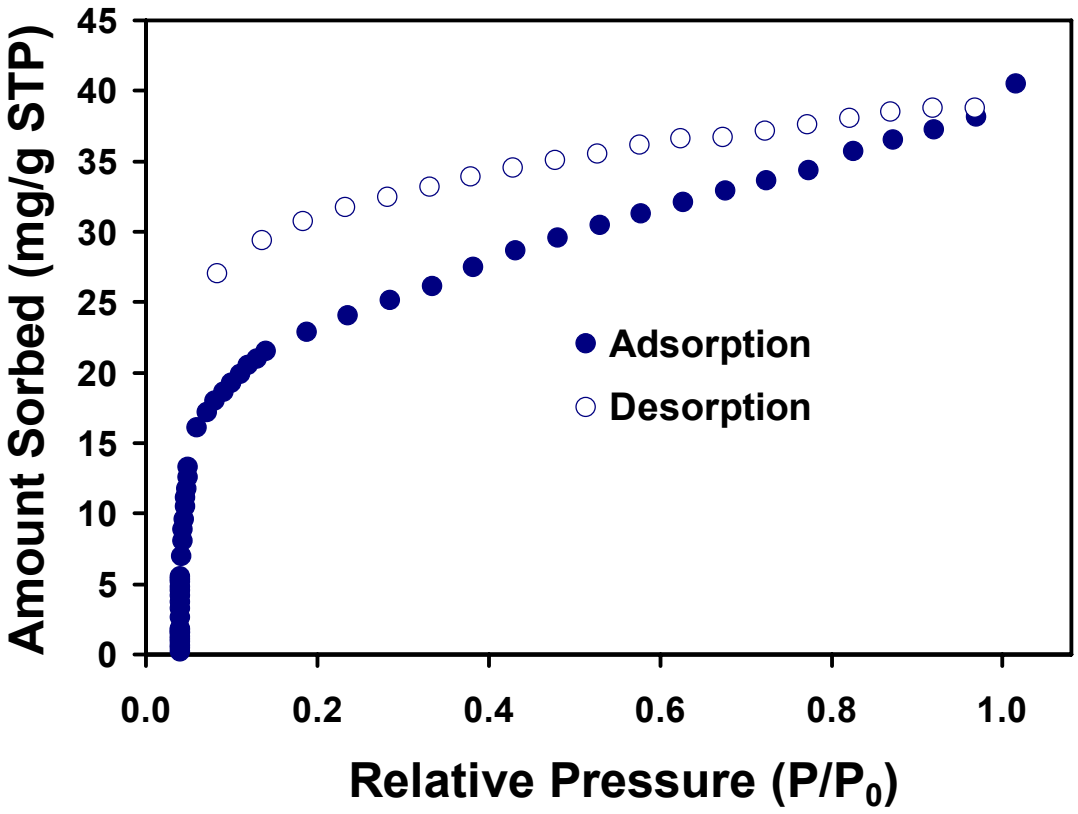

Figure 58. N_2 isotherm for **1**

Table 26. Crystal data and structure refinement for **2**

Identification code	Zn(HCOO)(**L**)	
Empirical formula	$C_{184}H_{112}N_{24}O_{40}Zn_8$	
Formula weight	3822.10	
Temperature	173(2) K	
Wavelength	0.71073 Å	
Crystal system	Monoclinic	
Space group	P21/c	
Unit cell dimensions	a = 12.0730(8) Å	α= 90°.
	b = 25.7653(18) Å	β= 116.520(4)°.
	c = 13.9304(8) Å	γ = 90°.
Volume	3877.3(4) $Å^3$	
Z	1	
Density (calculated)	1.637 Mg/m^3	
Absorption coefficient	1.311 mm^{-1}	
F(000)	1944	
Theta range for data collection	1.58 to 28.36°.	
Index ranges	-16<=h<=16, -33<=k<=34, -18<=l<=18	
Reflections collected	29558	
Independent reflections	8573 [R(int) = 0.0877]	
Completeness to theta = 28.36°	88.4 %	
Refinement method	Full-matrix least-squares on F^2	
Data / restraints / parameters	8573 / 0 / 577	
Goodness-of-fit on F^2	0.694	
Final R indices [I>2sigma(I)]	R1 = 0.0501, wR2 = 0.1219	
R indices (all data)	R1 = 0.0941, wR2 = 0.1461	
Largest diff. peak and hole	0.653 and -0.519 $e.Å^{-3}$	

Table 27. Atomic coordinates[a] and equivalent isotropic displacement parameters[b] for **2**

	x	y	z	U(eq)[c]
Zn(1)	5450(1)	1748(1)	8536(1)	24(1)
Zn(2)	-1110(1)	-4338(1)	2334(1)	22(1)
O(1)	4221(4)	839(1)	9161(3)	53(1)
O(2)	4675(3)	1085(1)	7846(2)	28(1)
O(3)	6801(3)	1581(1)	9943(3)	48(1)
O(4)	8321(5)	1829(2)	9587(5)	103(2)
O(5)	-2092(3)	-3374(1)	3101(3)	40(1)
O(6)	-617(2)	-3611(1)	2640(2)	29(1)
O(7)	-2744(3)	-4305(1)	1045(2)	30(1)
O(8)	-3158(3)	-5150(1)	1069(3)	44(1)
O(9)	869(9)	-2250(3)	5334(8)	181(4)

O(10)	-2581(3)	-1082(1)	4174(2)	36(1)
N(1)	3799(3)	-3235(1)	7653(3)	27(1)
N(2)	4603(3)	-2475(1)	6906(3)	23(1)
N(5)	244(3)	-61(1)	2352(3)	22(1)
N(3)	5671(3)	-2859(1)	5786(3)	26(1)
N(6)	1564(3)	321(1)	1464(3)	24(1)
N(4)	-102(3)	655(1)	3505(3)	29(1)
C(1)	3498(4)	-3645(2)	8073(4)	31(1)
C(2)	2995(4)	-3599(2)	8792(4)	33(1)
C(3)	2773(4)	-3109(2)	9066(4)	33(1)
C(4)	3084(4)	-2681(2)	8641(4)	30(1)
C(5)	3597(3)	-2758(2)	7935(3)	25(1)
C(6)	4027(3)	-2324(1)	7477(3)	23(1)
C(7)	3904(4)	-1802(1)	7672(3)	25(1)
C(8)	4458(3)	-1428(1)	7307(3)	23(1)
C(9)	5090(4)	-1596(2)	6741(3)	25(1)
C(10)	5122(3)	-2120(1)	6532(3)	22(1)
C(11)	5732(3)	-2334(1)	5898(3)	23(1)
C(12)	6321(4)	-2028(2)	5458(3)	29(1)
C(13)	6870(4)	-2260(2)	4882(3)	31(1)
C(14)	6811(4)	-2796(2)	4765(3)	31(1)
C(15)	6207(4)	-3077(2)	5229(3)	30(1)
C(16)	4416(3)	-871(1)	7556(3)	24(1)
C(17)	4129(4)	-715(1)	8374(3)	27(1)
C(18)	4121(4)	-197(1)	8613(3)	28(1)
C(19)	4398(3)	185(1)	8060(3)	24(1)
C(20)	4685(4)	36(2)	7238(3)	27(1)
C(21)	4684(4)	-481(2)	6977(3)	28(1)
C(22)	4428(4)	743(2)	8398(3)	28(1)
C(23)	7912(6)	1663(2)	10184(6)	60(2)
C(24)	-306(4)	1057(2)	4021(4)	34(1)
C(25)	-1048(4)	1020(2)	4529(4)	33(1)
C(26)	-1620(4)	548(2)	4511(4)	32(1)
C(27)	-1432(3)	133(2)	3970(3)	26(1)
C(28)	-675(3)	200(1)	3468(3)	22(1)
C(29)	-406(3)	-211(1)	2869(3)	23(1)
C(30)	-740(4)	-727(1)	2866(3)	27(1)
C(31)	-382(3)	-1101(1)	2332(3)	23(1)
C(32)	261(3)	-928(1)	1771(3)	26(1)
C(33)	563(3)	-408(1)	1804(3)	25(1)
C(34)	1264(3)	-186(1)	1264(3)	25(1)
C(35)	1557(4)	-470(2)	569(4)	35(1)
C(36)	2192(4)	-232(2)	72(4)	38(1)
C(37)	2516(4)	289(2)	282(3)	30(1)
C(38)	2188(4)	548(2)	980(3)	27(1)
C(39)	-632(4)	-1661(1)	2412(3)	24(1)

C(40)	-1421(5)	-1814(2)	2830(5)	42(1)
C(41)	-1602(5)	-2330(2)	2978(4)	40(1)
C(42)	-992(4)	-2716(1)	2707(3)	26(1)
C(43)	-222(4)	-2566(2)	2265(4)	31(1)
C(44)	-44(4)	-2050(2)	2111(4)	30(1)
C(45)	-1265(4)	-3276(1)	2842(3)	26(1)
C(46)	-3428(4)	-4711(2)	706(3)	28(1)

[a] x 10^4
[b] $Å^2$ x 10^3
[c] U(eq) is defined as one third of the trace of the orthogonalized U^{ij} tensor.

Table 28. Bond lengths (Å) and angles (°) for **2**

Zn(1)-O(3)	1.957(3)	N(6)-Zn(2)#4	2.168(3)
Zn(1)-O(2)	1.979(3)	N(4)-C(24)	1.344(5)
Zn(1)-N(2)#1	2.086(3)	N(4)-C(28)	1.351(5)
Zn(1)-N(3)#1	2.211(3)	N(4)-Zn(2)#4	2.243(4)
Zn(1)-N(1)#1	2.215(4)	C(1)-C(2)	1.390(6)
Zn(2)-O(6)	1.956(3)	C(1)-H(1B)	0.9300
Zn(2)-O(7)	1.991(3)	C(2)-C(3)	1.379(6)
Zn(2)-N(5)#2	2.086(3)	C(2)-H(2B)	0.9300
Zn(2)-N(6)#2	2.168(3)	C(3)-C(4)	1.381(6)
Zn(2)-N(4)#2	2.243(4)	C(3)-H(3B)	0.9300
O(1)-C(22)	1.221(5)	C(4)-C(5)	1.391(6)
O(2)-C(22)	1.289(5)	C(4)-H(4B)	0.9300
O(3)-C(23)	1.247(7)	C(5)-C(6)	1.489(5)
O(4)-C(23)	1.218(8)	C(6)-C(7)	1.393(5)
O(5)-C(45)	1.229(5)	C(7)-C(8)	1.393(5)
O(6)-C(45)	1.277(5)	C(7)-H(7A)	0.9300
O(7)-C(46)	1.284(5)	C(8)-C(9)	1.387(6)
O(8)-C(46)	1.221(5)	C(8)-C(16)	1.483(5)
N(1)-C(1)	1.333(5)	C(9)-C(10)	1.387(5)
N(1)-C(5)	1.345(5)	C(9)-H(9A)	0.9300
N(1)-Zn(1)#3	2.215(4)	C(10)-C(11)	1.486(5)
N(2)-C(6)	1.328(5)	C(11)-C(12)	1.375(6)
N(2)-C(10)	1.339(5)	C(12)-C(13)	1.383(6)
N(2)-Zn(1)#3	2.086(3)	C(12)-H(12A)	0.9300
N(5)-C(29)	1.337(5)	C(13)-C(14)	1.390(6)
N(5)-C(33)	1.338(5)	C(13)-H(13A)	0.9300
N(5)-Zn(2)#4	2.086(3)	C(14)-C(15)	1.376(6)
N(3)-C(15)	1.336(5)	C(14)-H(14A)	0.9300
N(3)-C(11)	1.359(5)	C(15)-H(15A)	0.9300
N(3)-Zn(1)#3	2.211(3)	C(16)-C(17)	1.390(6)
N(6)-C(34)	1.350(5)	C(16)-C(21)	1.413(6)
N(6)-C(38)	1.347(5)	C(17)-C(18)	1.377(5)

C(17)-H(17A)	0.9300
C(18)-C(19)	1.380(6)
C(18)-H(18A)	0.9300
C(19)-C(20)	1.390(6)
C(19)-C(22)	1.507(5)
C(20)-C(21)	1.381(5)
C(20)-H(20A)	0.9300
C(21)-H(21A)	0.9300
C(24)-C(25)	1.371(6)
C(24)-H(24A)	0.9300
C(25)-C(26)	1.391(6)
C(25)-H(25A)	0.9300
C(26)-C(27)	1.385(6)
C(26)-H(26A)	0.9300
C(27)-C(28)	1.386(5)
C(27)-H(27A)	0.9300
C(28)-C(29)	1.471(5)
C(29)-C(30)	1.388(5)
C(30)-C(31)	1.400(6)
C(30)-H(30A)	0.9300
C(31)-C(32)	1.398(6)
C(31)-C(39)	1.487(5)
C(32)-C(33)	1.385(5)
C(32)-H(32A)	0.9300
C(33)-C(34)	1.474(6)
C(34)-C(35)	1.381(6)
C(35)-C(36)	1.383(6)
C(35)-H(35A)	0.9300
C(36)-C(37)	1.393(6)
C(36)-H(36A)	0.9300
C(37)-C(38)	1.375(6)
C(37)-H(37A)	0.9300
C(38)-H(38A)	0.9300
C(39)-C(40)	1.377(6)
C(39)-C(44)	1.397(6)
C(40)-C(41)	1.377(6)
C(40)-H(40A)	0.9300
C(41)-C(42)	1.386(6)
C(41)-H(41A)	0.9300
C(42)-C(43)	1.381(6)
C(42)-C(45)	1.511(5)
C(43)-C(44)	1.377(6)
C(43)-H(43A)	0.9300
C(44)-H(44A)	0.9300
O(3)-Zn(1)-O(2)	107.34(13)
O(3)-Zn(1)-N(2)#1	114.13(14)
O(2)-Zn(1)-N(2)#1	137.67(12)
O(3)-Zn(1)-N(3)#1	93.92(14)
O(2)-Zn(1)-N(3)#1	110.83(12)
N(2)#1-Zn(1)-N(3)#1	75.12(12)
O(3)-Zn(1)-N(1)#1	108.46(15)
O(2)-Zn(1)-N(1)#1	85.18(12)
N(2)#1-Zn(1)-N(1)#1	74.33(12)
N(3)#1-Zn(1)-N(1)#1	147.50(12)
O(6)-Zn(2)-O(7)	103.78(11)
O(6)-Zn(2)-N(5)#2	137.37(12)
O(7)-Zn(2)-N(5)#2	115.44(12)
O(6)-Zn(2)-N(6)#2	112.20(13)
O(7)-Zn(2)-N(6)#2	102.92(12)
N(5)#2-Zn(2)-N(6)#2	75.65(12)
O(6)-Zn(2)-N(4)#2	85.13(12)
O(7)-Zn(2)-N(4)#2	98.32(13)
N(5)#2-Zn(2)-N(4)#2	73.71(12)
N(6)#2-Zn(2)-N(4)#2	148.01(12)
C(22)-O(2)-Zn(1)	119.1(3)
C(23)-O(3)-Zn(1)	123.2(4)
C(45)-O(6)-Zn(2)	122.5(2)
C(46)-O(7)-Zn(2)	120.8(3)
C(1)-N(1)-C(5)	118.3(4)
C(1)-N(1)-Zn(1)#3	126.6(3)
C(5)-N(1)-Zn(1)#3	115.1(3)
C(6)-N(2)-C(10)	119.7(3)
C(6)-N(2)-Zn(1)#3	120.1(2)
C(10)-N(2)-Zn(1)#3	119.9(3)
C(29)-N(5)-C(33)	120.2(3)
C(29)-N(5)-Zn(2)#4	120.3(2)
C(33)-N(5)-Zn(2)#4	118.0(3)
C(15)-N(3)-C(11)	117.9(4)
C(15)-N(3)-Zn(1)#3	127.1(3)
C(11)-N(3)-Zn(1)#3	114.8(3)
C(34)-N(6)-C(38)	118.4(3)
C(34)-N(6)-Zn(2)#4	114.4(3)
C(38)-N(6)-Zn(2)#4	127.0(3)
C(24)-N(4)-C(28)	118.4(4)
C(24)-N(4)-Zn(2)#4	126.2(3)
C(28)-N(4)-Zn(2)#4	115.4(3)
N(1)-C(1)-C(2)	122.9(4)
N(1)-C(1)-H(1B)	118.6
C(2)-C(1)-H(1B)	118.6
C(1)-C(2)-C(3)	118.5(4)
C(1)-C(2)-H(2B)	120.7

C(3)-C(2)-H(2B)	120.7	C(19)-C(18)-C(17)	121.8(4)
C(4)-C(3)-C(2)	119.2(4)	C(19)-C(18)-H(18A)	119.1
C(4)-C(3)-H(3B)	120.4	C(17)-C(18)-H(18A)	119.1
C(2)-C(3)-H(3B)	120.4	C(18)-C(19)-C(20)	118.3(3)
C(3)-C(4)-C(5)	118.9(4)	C(18)-C(19)-C(22)	118.9(4)
C(3)-C(4)-H(4B)	120.6	C(20)-C(19)-C(22)	122.7(4)
C(5)-C(4)-H(4B)	120.6	C(21)-C(20)-C(19)	120.9(4)
N(1)-C(5)-C(4)	122.1(4)	C(21)-C(20)-H(20A)	119.6
N(1)-C(5)-C(6)	114.7(4)	C(19)-C(20)-H(20A)	119.6
C(4)-C(5)-C(6)	123.1(3)	C(20)-C(21)-C(16)	120.5(4)
N(2)-C(6)-C(7)	121.9(4)	C(20)-C(21)-H(21A)	119.7
N(2)-C(6)-C(5)	114.4(3)	C(16)-C(21)-H(21A)	119.7
C(7)-C(6)-C(5)	123.6(4)	O(1)-C(22)-O(2)	124.9(4)
C(8)-C(7)-C(6)	119.2(4)	O(1)-C(22)-C(19)	118.6(4)
C(8)-C(7)-H(7A)	120.4	O(2)-C(22)-C(19)	116.5(4)
C(6)-C(7)-H(7A)	120.4	O(4)-C(23)-O(3)	126.2(6)
C(7)-C(8)-C(9)	117.8(3)	N(4)-C(24)-C(25)	122.7(4)
C(7)-C(8)-C(16)	120.8(4)	N(4)-C(24)-H(24A)	118.6
C(9)-C(8)-C(16)	121.3(3)	C(25)-C(24)-H(24A)	118.6
C(10)-C(9)-C(8)	119.9(4)	C(24)-C(25)-C(26)	119.0(4)
C(10)-C(9)-H(9A)	120.1	C(24)-C(25)-H(25A)	120.5
C(8)-C(9)-H(9A)	120.1	C(26)-C(25)-H(25A)	120.5
N(2)-C(10)-C(9)	121.4(4)	C(27)-C(26)-C(25)	118.9(4)
N(2)-C(10)-C(11)	114.9(3)	C(27)-C(26)-H(26A)	120.5
C(9)-C(10)-C(11)	123.7(3)	C(25)-C(26)-H(26A)	120.5
N(3)-C(11)-C(12)	122.2(4)	C(28)-C(27)-C(26)	118.9(4)
N(3)-C(11)-C(10)	114.9(3)	C(28)-C(27)-H(27A)	120.5
C(12)-C(11)-C(10)	122.9(3)	C(26)-C(27)-H(27A)	120.5
C(11)-C(12)-C(13)	119.2(4)	N(4)-C(28)-C(27)	122.0(4)
C(11)-C(12)-H(12A)	120.4	N(4)-C(28)-C(29)	114.0(3)
C(13)-C(12)-H(12A)	120.4	C(27)-C(28)-C(29)	124.0(3)
C(12)-C(13)-C(14)	119.0(4)	N(5)-C(29)-C(30)	120.9(4)
C(12)-C(13)-H(13A)	120.5	N(5)-C(29)-C(28)	115.4(3)
C(14)-C(13)-H(13A)	120.5	C(30)-C(29)-C(28)	123.6(4)
C(15)-C(14)-C(13)	118.5(4)	C(29)-C(30)-C(31)	120.2(4)
C(15)-C(14)-H(14A)	120.8	C(29)-C(30)-H(30A)	119.9
C(13)-C(14)-H(14A)	120.8	C(31)-C(30)-H(30A)	119.9
N(3)-C(15)-C(14)	123.2(4)	C(32)-C(31)-C(30)	117.2(3)
N(3)-C(15)-H(15A)	118.4	C(32)-C(31)-C(39)	122.3(3)
C(14)-C(15)-H(15A)	118.4	C(30)-C(31)-C(39)	120.4(4)
C(17)-C(16)-C(21)	117.9(3)	C(33)-C(32)-C(31)	119.6(4)
C(17)-C(16)-C(8)	121.3(4)	C(33)-C(32)-H(32A)	120.2
C(21)-C(16)-C(8)	120.9(4)	C(31)-C(32)-H(32A)	120.2
C(16)-C(17)-C(18)	120.7(4)	N(5)-C(33)-C(32)	121.7(4)
C(16)-C(17)-H(17A)	119.7	N(5)-C(33)-C(34)	114.2(3)
C(18)-C(17)-H(17A)	119.7	C(32)-C(33)-C(34)	124.1(4)

N(6)-C(34)-C(35)	121.9(4)	C(39)-C(40)-H(40A)	119.1
N(6)-C(34)-C(33)	115.6(3)	C(41)-C(40)-H(40A)	119.1
C(35)-C(34)-C(33)	122.5(3)	C(42)-C(41)-C(40)	120.8(4)
C(36)-C(35)-C(34)	119.2(4)	C(42)-C(41)-H(41A)	119.6
C(36)-C(35)-H(35A)	120.4	C(40)-C(41)-H(41A)	119.6
C(34)-C(35)-H(35A)	120.4	C(41)-C(42)-C(43)	117.8(4)
C(35)-C(36)-C(37)	119.3(4)	C(41)-C(42)-C(45)	118.7(4)
C(35)-C(36)-H(36A)	120.4	C(43)-C(42)-C(45)	123.4(4)
C(37)-C(36)-H(36A)	120.4	C(42)-C(43)-C(44)	121.5(4)
C(38)-C(37)-C(36)	118.2(4)	C(42)-C(43)-H(43A)	119.3
C(38)-C(37)-H(37A)	120.9	C(44)-C(43)-H(43A)	119.3
C(36)-C(37)-H(37A)	120.9	C(43)-C(44)-C(39)	120.7(4)
N(6)-C(38)-C(37)	123.0(4)	C(43)-C(44)-H(44A)	119.6
N(6)-C(38)-H(38A)	118.5	C(39)-C(44)-H(44A)	119.6
C(37)-C(38)-H(38A)	118.5	O(5)-C(45)-O(6)	125.8(4)
C(40)-C(39)-C(44)	117.4(4)	O(5)-C(45)-C(42)	118.8(3)
C(40)-C(39)-C(31)	120.9(4)	O(6)-C(45)-C(42)	115.3(4)
C(44)-C(39)-C(31)	121.7(4)	O(8)-C(46)-O(7)	126.3(4)
C(39)-C(40)-C(41)	121.8(4)		

Symmetry transformations used to generate equivalent atoms:
#1 -x+1,y+1/2,-z+3/2 #2 -x,y-1/2,-z+1/2 #3 -x+1,y-1/2,-z+3/2
#4 -x,y+1/2,-z+1/2

Table 29. Anisotropic displacement parameters for **2**[d]

	U^{11}	U^{22}	U^{33}	U^{23}	U^{13}	U^{12}
Zn(1)	37(1)	12(1)	28(1)	0(1)	18(1)	0(1)
Zn(2)	32(1)	12(1)	29(1)	1(1)	18(1)	1(1)
O(1)	115(3)	19(2)	52(2)	-3(2)	61(2)	-3(2)
O(2)	45(2)	14(1)	31(2)	-3(1)	23(1)	-4(1)
O(3)	52(2)	40(2)	44(2)	-5(2)	14(2)	9(2)
O(4)	68(3)	152(6)	82(4)	-13(4)	27(3)	-35(3)
O(5)	52(2)	18(2)	66(2)	1(1)	42(2)	-1(1)
O(6)	37(1)	14(1)	44(2)	-3(1)	25(1)	0(1)
O(7)	36(2)	24(2)	31(2)	2(1)	16(1)	-3(1)
O(8)	51(2)	22(2)	57(2)	-1(2)	23(2)	-4(1)
O(9)	241(10)	153(7)	159(7)	-29(6)	98(7)	-34(7)
O(10)	44(2)	32(2)	40(2)	2(1)	27(2)	2(1)
N(1)	36(2)	15(2)	35(2)	3(1)	20(2)	1(1)
N(2)	29(2)	13(2)	30(2)	-1(1)	17(1)	-2(1)
N(5)	31(2)	13(2)	26(2)	0(1)	18(1)	2(1)
N(3)	41(2)	15(2)	30(2)	-2(1)	23(2)	3(1)
N(6)	34(2)	18(2)	27(2)	0(1)	18(1)	-2(1)
N(4)	39(2)	15(2)	39(2)	-1(1)	25(2)	-1(1)

C(1)	41(2)	15(2)	43(2)	1(2)	25(2)	0(2)
C(2)	43(2)	24(2)	41(2)	5(2)	27(2)	-5(2)
C(3)	42(2)	28(2)	39(2)	0(2)	28(2)	-4(2)
C(4)	39(2)	18(2)	43(2)	-1(2)	27(2)	-3(2)
C(5)	27(2)	19(2)	34(2)	0(2)	18(2)	-2(1)
C(6)	31(2)	15(2)	29(2)	-3(2)	21(2)	-2(1)
C(7)	34(2)	17(2)	34(2)	-1(2)	23(2)	-1(2)
C(8)	28(2)	15(2)	31(2)	2(2)	17(2)	0(1)
C(9)	36(2)	15(2)	31(2)	2(2)	21(2)	-2(2)
C(10)	28(2)	16(2)	25(2)	0(2)	15(2)	0(1)
C(11)	32(2)	15(2)	27(2)	-1(2)	18(2)	-1(1)
C(12)	41(2)	18(2)	34(2)	-1(2)	23(2)	2(2)
C(13)	46(2)	22(2)	37(2)	-1(2)	30(2)	-1(2)
C(14)	48(2)	24(2)	32(2)	-3(2)	27(2)	2(2)
C(15)	47(2)	16(2)	34(2)	-3(2)	24(2)	2(2)
C(16)	33(2)	12(2)	31(2)	-3(2)	19(2)	0(1)
C(17)	41(2)	16(2)	37(2)	1(2)	28(2)	-3(2)
C(18)	48(2)	14(2)	35(2)	-1(2)	29(2)	-1(2)
C(19)	36(2)	12(2)	30(2)	2(2)	20(2)	1(1)
C(20)	40(2)	16(2)	31(2)	3(2)	20(2)	-1(2)
C(21)	43(2)	18(2)	35(2)	-2(2)	29(2)	-3(2)
C(22)	44(2)	18(2)	29(2)	-1(2)	22(2)	1(2)
C(23)	64(4)	48(3)	75(4)	-20(3)	38(3)	8(3)
C(24)	48(2)	19(2)	43(3)	-5(2)	27(2)	-2(2)
C(25)	45(2)	25(2)	38(2)	-7(2)	26(2)	3(2)
C(26)	35(2)	32(2)	37(2)	-2(2)	24(2)	1(2)
C(27)	32(2)	21(2)	33(2)	0(2)	21(2)	1(2)
C(28)	30(2)	13(2)	28(2)	3(2)	18(2)	5(1)
C(29)	23(2)	17(2)	30(2)	-1(2)	14(2)	-2(1)
C(30)	30(2)	19(2)	37(2)	-1(2)	21(2)	-5(2)
C(31)	28(2)	17(2)	29(2)	-2(2)	17(2)	-1(1)
C(32)	36(2)	16(2)	32(2)	-4(2)	20(2)	-1(2)
C(33)	32(2)	17(2)	31(2)	1(2)	19(2)	-1(1)
C(34)	30(2)	19(2)	33(2)	0(2)	20(2)	-1(1)
C(35)	53(3)	17(2)	49(3)	-7(2)	36(2)	-6(2)
C(36)	53(3)	29(2)	50(3)	-6(2)	40(2)	0(2)
C(37)	43(2)	24(2)	35(2)	3(2)	28(2)	0(2)
C(38)	38(2)	21(2)	28(2)	0(2)	19(2)	-3(2)
C(39)	32(2)	17(2)	32(2)	0(2)	21(2)	-2(1)
C(40)	65(3)	16(2)	72(4)	-1(2)	55(3)	1(2)
C(41)	62(3)	18(2)	66(3)	0(2)	51(3)	-3(2)
C(42)	36(2)	14(2)	32(2)	-1(2)	19(2)	0(2)
C(43)	39(2)	18(2)	46(3)	-5(2)	29(2)	0(2)
C(44)	41(2)	20(2)	43(2)	-6(2)	30(2)	-4(2)
C(45)	32(2)	16(2)	31(2)	-1(2)	17(2)	0(2)
C(46)	38(2)	26(2)	29(2)	-5(2)	25(2)	-4(2)

[d] in $Å^2$ x 10.[3] The anisotropic displacement factor exponent takes the form: $-2\pi^2[h^2 a^{*2}U^{11} + ... + 2 h k a^* b^* U^{12}]$

Table 30. Crystal data and structure refinement for **3**

Identification code	$Zn_2(H\mathbf{L})(\mathbf{L})_2(BF_4)_2$	
Empirical formula	C264 H168 B8 F32 N36 O36 Zn8	
Formula weight	5637.94	
Temperature	173(2) K	
Wavelength	0.71073 Å	
Crystal system	Monoclinic	
Space group	P21/c	
Unit cell dimensions	a = 16.126(4) Å	α= 90°.
	b = 16.174(4) Å	β= 120.307(10)°.
	c = 27.975(5) Å	γ = 90°.
Volume	6299(2) $Å^3$	
Z	1	
Density (calculated)	1.486 Mg/m^3	
Absorption coefficient	0.851 mm^{-1}	
F(000)	2859	
Theta range for data collection	1.46 to 28.48°.	
Index ranges	-21<=h<=21, -21<=k<=21, -37<=l<=37	
Reflections collected	63766	
Independent reflections	15847 [R(int) = 0.1798]	
Completeness to theta = 28.48°	99.3 %	
Refinement method	Full-matrix least-squares on F^2	
Data / restraints / parameters	15847 / 0 / 845	
Goodness-of-fit on F^2	1.463	
Final R indices [I>2sigma(I)]	R1 = 0.1366, wR2 = 0.3360	
R indices (all data)	R1 = 0.2363, wR2 = 0.3686	
Largest diff. peak and hole	2.622 and -0.800 e.$Å^{-3}$	

Table 31. Atomic coordinates[a] and equivalent isotropic displacement parameters[b] for **3**

	x	y	z	U(eq)[c]
Zn(1)	4633(1)	5368(1)	6788(1)	36(1)
Zn(2)	742(1)	5375(1)	2157(1)	31(1)
F(1)	2363(9)	7692(8)	3784(5)	180(6)
F(2)	2150(11)	7584(10)	4491(5)	227(8)
F(3)	867(8)	7917(7)	3693(4)	143(4)

F(4)	2119(8)	8821(7)	4103(5)	145(4)
F(5)	-561(7)	7674(5)	-69(3)	111(3)
F(6)	293(8)	6532(5)	385(3)	126(4)
F(7)	890(6)	7799(6)	657(4)	119(3)
F(8)	-224(6)	7351(6)	797(3)	109(3)
O(1)	-2375(6)	5944(7)	2705(3)	101(4)
O(2)	-2645(5)	4742(5)	3010(3)	54(2)
O(3)	6640(5)	6179(5)	6520(3)	64(2)
O(4)	5839(5)	5315(4)	6776(3)	43(2)
O(5)	-5733(5)	5331(7)	-2116(3)	82(3)
O(6)	-4702(5)	5407(5)	-2400(2)	58(2)
O(7)	2000(7)	3191(6)	4622(4)	84(3)
O(8)	-6569(8)	4489(6)	-1519(4)	102(3)
O(9)	-4319(10)	6282(8)	490(5)	146(5)
N(1)	4365(6)	6675(5)	6576(3)	41(2)
N(2)	3308(5)	5413(5)	6076(3)	28(2)
N(3)	4173(5)	4092(5)	6650(3)	38(2)
N(4)	1833(5)	6235(5)	2231(3)	35(2)
N(5)	1715(5)	5442(5)	3004(3)	31(2)
N(6)	147(5)	4549(5)	2529(3)	33(2)
N(7)	-222(5)	6376(5)	2099(3)	34(2)
N(8)	-352(5)	5371(5)	1335(3)	29(2)
N(9)	1157(5)	4410(5)	1792(3)	31(2)
C(1)	4981(8)	7301(7)	6834(4)	45(3)
C(2)	4851(8)	8081(8)	6615(5)	59(3)
C(3)	4002(9)	8246(7)	6113(4)	55(3)
C(4)	3352(8)	7611(7)	5842(4)	46(3)
C(5)	-884(6)	4739(6)	3948(3)	37(2)
C(6)	2936(6)	6098(6)	5806(3)	30(2)
C(7)	2085(6)	6134(6)	5316(3)	29(2)
C(8)	1588(6)	5399(6)	5070(3)	30(2)
C(9)	1981(6)	4680(6)	5350(3)	33(2)
C(10)	2844(6)	4700(6)	5861(3)	31(2)
C(11)	3332(6)	3932(6)	6175(3)	31(2)
C(12)	3028(6)	3147(6)	5988(4)	37(2)
C(13)	3556(7)	2493(6)	6316(4)	48(3)
C(14)	4389(7)	2614(7)	6806(4)	46(3)
C(15)	4664(8)	3447(8)	6977(4)	54(3)
C(16)	647(6)	5387(6)	4543(3)	30(2)
C(17)	389(6)	6032(6)	4153(4)	39(2)
C(18)	-490(7)	6032(7)	3687(4)	51(3)
C(19)	-1143(6)	5380(6)	3569(3)	37(2)
C(20)	3549(6)	6828(6)	6081(3)	34(2)
C(21)	5(6)	4744(6)	4420(3)	34(2)
C(22)	-2116(7)	5363(8)	3055(4)	55(3)
C(23)	1829(7)	6643(7)	1800(4)	42(2)

C(24)	2450(7)	7321(7)	1904(4)	49(3)
C(25)	3058(7)	7583(7)	2428(4)	46(3)
C(26)	3083(6)	7116(6)	2858(4)	39(2)
C(27)	2497(6)	6464(6)	2758(3)	32(2)
C(28)	2460(6)	5977(6)	3195(4)	33(2)
C(29)	3088(6)	6037(6)	3752(3)	33(2)
C(30)	2972(6)	5541(6)	4121(3)	35(2)
C(31)	2195(7)	5012(6)	3912(3)	33(2)
C(32)	1566(6)	4976(6)	3349(3)	29(2)
C(33)	674(6)	4463(6)	3072(3)	31(2)
C(34)	392(7)	3942(6)	3367(4)	40(2)
C(35)	-462(7)	3534(6)	3078(4)	41(2)
C(36)	-1008(7)	3638(6)	2528(4)	44(3)
C(37)	-684(6)	4137(6)	2264(4)	38(2)
C(38)	3692(6)	5604(6)	4724(3)	33(2)
C(39)	4129(8)	6359(7)	4947(4)	50(3)
C(40)	4833(8)	6407(7)	5499(4)	49(3)
C(41)	5149(6)	5690(6)	5827(3)	30(2)
C(42)	4682(6)	4962(6)	5610(3)	32(2)
C(43)	3957(6)	4908(6)	5050(3)	33(2)
C(44)	5930(6)	5743(7)	6422(4)	44(3)
C(45)	-126(7)	6849(6)	2510(4)	39(2)
C(46)	-795(8)	7414(6)	2470(4)	45(3)
C(47)	-1643(9)	7460(7)	1968(5)	60(3)
C(48)	-1752(7)	6957(7)	1527(4)	47(3)
C(49)	-1036(6)	6434(6)	1595(4)	32(2)
C(50)	-1086(6)	5880(6)	1166(3)	28(2)
C(51)	-1809(6)	5862(6)	625(3)	35(2)
C(52)	-1792(6)	5335(6)	244(3)	33(2)
C(53)	-1016(6)	4800(6)	431(3)	36(2)
C(54)	-309(6)	4827(5)	989(3)	27(2)
C(55)	533(6)	4256(6)	1259(3)	30(2)
C(56)	643(7)	3576(6)	990(4)	39(2)
C(57)	1420(6)	3047(6)	1288(4)	42(3)
C(58)	2065(6)	3221(6)	1833(4)	34(2)
C(59)	1924(6)	3909(6)	2065(3)	35(2)
C(60)	-2591(6)	5320(6)	-351(3)	34(2)
C(61)	-3532(6)	5515(6)	-470(4)	41(2)
C(62)	-4264(6)	5505(6)	-1019(3)	37(2)
C(63)	-4086(6)	5345(6)	-1438(3)	32(2)
C(64)	-3163(6)	5181(6)	-1322(4)	36(2)
C(65)	-2419(6)	5156(6)	-783(3)	31(2)
C(66)	-4906(6)	5386(6)	-2032(4)	36(2)
B(1)	1918(16)	8002(15)	4045(9)	101(6)
B(2)	69(13)	7298(11)	416(6)	68(4)

[a] x 10^4
[b] $Å^2$ x 10^3
[c] U(eq) is defined as one third of the trace of the orthogonalized U^{ij} tensor.

Table 32. Bond lengths (Å) and angles (°) for **3**

Zn(1)-O(4)	1.962(7)	N(7)-C(49)	1.362(10)
Zn(1)-O(6)#1	1.964(6)	N(8)-C(50)	1.318(10)
Zn(1)-N(2)	2.060(7)	N(8)-C(54)	1.336(10)
Zn(1)-N(3)	2.162(8)	N(9)-C(55)	1.335(10)
Zn(1)-N(1)	2.179(9)	N(9)-C(59)	1.347(11)
Zn(2)-N(8)	2.075(6)	C(1)-C(2)	1.372(15)
Zn(2)-N(5)	2.083(7)	C(1)-H(1A)	0.9300
Zn(2)-N(9)	2.149(7)	C(2)-C(3)	1.406(15)
Zn(2)-N(4)	2.171(8)	C(2)-H(2A)	0.9300
Zn(2)-N(6)	2.190(7)	C(3)-C(4)	1.387(15)
Zn(2)-N(7)	2.193(7)	C(3)-H(3A)	0.9300
F(1)-B(1)	1.35(2)	C(4)-C(20)	1.391(13)
F(2)-B(1)	1.30(2)	C(4)-H(4A)	0.9300
F(3)-B(1)	1.48(2)	C(5)-C(21)	1.374(11)
F(4)-B(1)	1.35(2)	C(5)-C(19)	1.388(12)
F(5)-B(2)	1.359(16)	C(5)-H(5A)	0.9300
F(6)-B(2)	1.306(16)	C(6)-C(7)	1.367(11)
F(7)-B(2)	1.401(18)	C(6)-C(20)	1.482(13)
F(8)-B(2)	1.369(16)	C(7)-C(8)	1.404(12)
O(1)-C(22)	1.265(13)	C(7)-H(7A)	0.9300
O(2)-C(22)	1.283(13)	C(8)-C(9)	1.367(12)
O(3)-C(44)	1.251(12)	C(8)-C(16)	1.490(11)
O(4)-C(44)	1.276(12)	C(9)-C(10)	1.405(11)
O(5)-C(66)	1.235(11)	C(9)-H(9A)	0.9300
O(6)-C(66)	1.231(11)	C(10)-C(11)	1.496(12)
O(6)-Zn(1)#2	1.964(6)	C(11)-C(12)	1.366(13)
N(1)-C(1)	1.343(12)	C(12)-C(13)	1.377(13)
N(1)-C(20)	1.368(11)	C(12)-H(12A)	0.9300
N(2)-C(6)	1.305(11)	C(13)-C(14)	1.365(13)
N(2)-C(10)	1.340(11)	C(13)-H(13A)	0.9300
N(3)-C(15)	1.349(12)	C(14)-C(15)	1.424(15)
N(3)-C(11)	1.361(10)	C(14)-H(14A)	0.9300
N(4)-C(27)	1.365(10)	C(15)-H(15A)	0.9300
N(4)-C(23)	1.371(11)	C(16)-C(21)	1.383(12)
N(5)-C(32)	1.339(11)	C(16)-C(17)	1.413(12)
N(5)-C(28)	1.353(11)	C(17)-C(18)	1.358(12)
N(6)-C(33)	1.320(10)	C(17)-H(17A)	0.9300
N(6)-C(37)	1.337(11)	C(18)-C(19)	1.408(14)
N(7)-C(45)	1.323(11)	C(18)-H(18A)	0.9300

C(19)-C(22)	1.501(13)	C(49)-C(50)	1.468(12)
C(21)-H(21A)	0.9300	C(50)-C(51)	1.366(11)
C(23)-C(24)	1.413(14)	C(51)-C(52)	1.377(12)
C(23)-H(23A)	0.9300	C(51)-H(51A)	0.9300
C(24)-C(25)	1.357(13)	C(52)-C(53)	1.389(12)
C(24)-H(24A)	0.9300	C(52)-C(60)	1.504(11)
C(25)-C(26)	1.403(13)	C(53)-C(54)	1.393(11)
C(25)-H(25A)	0.9300	C(53)-H(53A)	0.9300
C(26)-C(27)	1.349(12)	C(54)-C(55)	1.494(12)
C(26)-H(26A)	0.9300	C(55)-C(56)	1.394(12)
C(27)-C(28)	1.482(12)	C(56)-C(57)	1.394(13)
C(28)-C(29)	1.368(11)	C(56)-H(56A)	0.9300
C(29)-C(30)	1.391(12)	C(57)-C(58)	1.373(12)
C(29)-H(29A)	0.9300	C(57)-H(57A)	0.9300
C(30)-C(31)	1.380(13)	C(58)-C(59)	1.363(12)
C(30)-C(38)	1.491(12)	C(58)-H(58A)	0.9300
C(31)-C(32)	1.378(11)	C(59)-H(59A)	0.9300
C(31)-H(31A)	0.9300	C(60)-C(65)	1.395(12)
C(32)-C(33)	1.495(12)	C(60)-C(61)	1.414(12)
C(33)-C(34)	1.407(12)	C(61)-C(62)	1.386(11)
C(34)-C(35)	1.364(13)	C(61)-H(61A)	0.9300
C(34)-H(34A)	0.9300	C(62)-C(63)	1.366(12)
C(35)-C(36)	1.342(13)	C(62)-H(62A)	0.9300
C(35)-H(35A)	0.9300	C(63)-C(64)	1.380(12)
C(36)-C(37)	1.363(12)	C(63)-C(66)	1.515(11)
C(36)-H(36A)	0.9300	C(64)-C(65)	1.376(11)
C(37)-H(37A)	0.9300	C(64)-H(64A)	0.9300
C(38)-C(43)	1.375(12)	C(65)-H(65A)	0.9300
C(38)-C(39)	1.391(13)		
C(39)-C(40)	1.382(13)	O(4)-Zn(1)-O(6)#1	93.1(3)
C(39)-H(39A)	0.9300	O(4)-Zn(1)-N(2)	122.6(3)
C(40)-C(41)	1.404(13)	O(6)#1-Zn(1)-N(2)	144.2(3)
C(40)-H(40A)	0.9300	O(4)-Zn(1)-N(3)	102.1(3)
C(41)-C(42)	1.364(13)	O(6)#1-Zn(1)-N(3)	100.0(3)
C(41)-C(44)	1.501(12)	N(2)-Zn(1)-N(3)	76.5(3)
C(42)-C(43)	1.408(11)	O(4)-Zn(1)-N(1)	95.8(3)
C(42)-H(42A)	0.9300	O(6)#1-Zn(1)-N(1)	101.6(3)
C(43)-H(43A)	0.9300	N(2)-Zn(1)-N(1)	74.7(3)
C(45)-C(46)	1.375(13)	N(3)-Zn(1)-N(1)	151.0(3)
C(45)-H(45A)	0.9300	N(8)-Zn(2)-N(5)	172.8(3)
C(46)-C(47)	1.381(14)	N(8)-Zn(2)-N(9)	76.5(3)
C(46)-H(46A)	0.9300	N(5)-Zn(2)-N(9)	110.0(3)
C(47)-C(48)	1.415(14)	N(8)-Zn(2)-N(4)	107.6(3)
C(47)-H(47A)	0.9300	N(5)-Zn(2)-N(4)	75.4(3)
C(48)-C(49)	1.364(13)	N(9)-Zn(2)-N(4)	94.5(3)
C(48)-H(48A)	0.9300	N(8)-Zn(2)-N(6)	101.2(3)

N(5)-Zn(2)-N(6)	75.5(3)	C(3)-C(4)-C(20)	119.0(10)
N(9)-Zn(2)-N(6)	95.7(3)	C(3)-C(4)-H(4A)	120.5
N(4)-Zn(2)-N(6)	151.0(3)	C(20)-C(4)-H(4A)	120.5
N(8)-Zn(2)-N(7)	75.3(3)	C(21)-C(5)-C(19)	119.8(9)
N(5)-Zn(2)-N(7)	98.3(3)	C(21)-C(5)-H(5A)	120.1
N(9)-Zn(2)-N(7)	151.7(3)	C(19)-C(5)-H(5A)	120.1
N(4)-Zn(2)-N(7)	92.5(3)	N(2)-C(6)-C(7)	123.5(9)
N(6)-Zn(2)-N(7)	91.2(3)	N(2)-C(6)-C(20)	112.7(8)
C(44)-O(4)-Zn(1)	119.5(6)	C(7)-C(6)-C(20)	123.8(9)
C(66)-O(6)-Zn(1)#2	138.4(6)	C(6)-C(7)-C(8)	119.4(8)
C(1)-N(1)-C(20)	118.7(9)	C(6)-C(7)-H(7A)	120.3
C(1)-N(1)-Zn(1)	126.4(7)	C(8)-C(7)-H(7A)	120.3
C(20)-N(1)-Zn(1)	114.1(6)	C(9)-C(8)-C(7)	117.0(8)
C(6)-N(2)-C(10)	118.9(7)	C(9)-C(8)-C(16)	120.1(8)
C(6)-N(2)-Zn(1)	122.6(6)	C(7)-C(8)-C(16)	122.8(8)
C(10)-N(2)-Zn(1)	118.4(6)	C(8)-C(9)-C(10)	119.9(9)
C(15)-N(3)-C(11)	118.1(9)	C(8)-C(9)-H(9A)	120.0
C(15)-N(3)-Zn(1)	125.8(7)	C(10)-C(9)-H(9A)	120.0
C(11)-N(3)-Zn(1)	116.0(6)	N(2)-C(10)-C(9)	121.2(8)
C(27)-N(4)-C(23)	118.2(8)	N(2)-C(10)-C(11)	116.3(7)
C(27)-N(4)-Zn(2)	115.6(5)	C(9)-C(10)-C(11)	122.4(9)
C(23)-N(4)-Zn(2)	125.5(6)	N(3)-C(11)-C(12)	122.6(8)
C(32)-N(5)-C(28)	121.4(7)	N(3)-C(11)-C(10)	112.7(8)
C(32)-N(5)-Zn(2)	119.0(6)	C(12)-C(11)-C(10)	124.5(8)
C(28)-N(5)-Zn(2)	119.5(6)	C(11)-C(12)-C(13)	118.4(9)
C(33)-N(6)-C(37)	117.9(8)	C(11)-C(12)-H(12A)	120.8
C(33)-N(6)-Zn(2)	115.4(6)	C(13)-C(12)-H(12A)	120.8
C(37)-N(6)-Zn(2)	126.7(6)	C(14)-C(13)-C(12)	121.6(10)
C(45)-N(7)-C(49)	119.2(8)	C(14)-C(13)-H(13A)	119.2
C(45)-N(7)-Zn(2)	126.6(6)	C(12)-C(13)-H(13A)	119.2
C(49)-N(7)-Zn(2)	113.9(5)	C(13)-C(14)-C(15)	117.1(9)
C(50)-N(8)-C(54)	121.1(7)	C(13)-C(14)-H(14A)	121.5
C(50)-N(8)-Zn(2)	120.2(5)	C(15)-C(14)-H(14A)	121.5
C(54)-N(8)-Zn(2)	118.6(6)	N(3)-C(15)-C(14)	121.7(9)
C(55)-N(9)-C(59)	118.7(8)	N(3)-C(15)-H(15A)	119.1
C(55)-N(9)-Zn(2)	115.2(6)	C(14)-C(15)-H(15A)	119.1
C(59)-N(9)-Zn(2)	125.8(6)	C(21)-C(16)-C(17)	118.2(8)
N(1)-C(1)-C(2)	123.3(10)	C(21)-C(16)-C(8)	121.2(8)
N(1)-C(1)-H(1A)	118.4	C(17)-C(16)-C(8)	120.7(8)
C(2)-C(1)-H(1A)	118.4	C(18)-C(17)-C(16)	120.0(9)
C(1)-C(2)-C(3)	118.1(10)	C(18)-C(17)-H(17A)	120.0
C(1)-C(2)-H(2A)	121.0	C(16)-C(17)-H(17A)	120.0
C(3)-C(2)-H(2A)	121.0	C(17)-C(18)-C(19)	121.3(10)
C(4)-C(3)-C(2)	119.5(10)	C(17)-C(18)-H(18A)	119.4
C(4)-C(3)-H(3A)	120.2	C(19)-C(18)-H(18A)	119.4
C(2)-C(3)-H(3A)	120.2	C(5)-C(19)-C(18)	118.7(8)

C(5)-C(19)-C(22)	119.1(9)	C(33)-C(34)-H(34A)	121.0
C(18)-C(19)-C(22)	122.3(9)	C(36)-C(35)-C(34)	120.1(9)
N(1)-C(20)-C(4)	121.4(9)	C(36)-C(35)-H(35A)	119.9
N(1)-C(20)-C(6)	115.5(9)	C(34)-C(35)-H(35A)	119.9
C(4)-C(20)-C(6)	123.0(8)	C(35)-C(36)-C(37)	119.0(9)
C(5)-C(21)-C(16)	122.0(8)	C(35)-C(36)-H(36A)	120.5
C(5)-C(21)-H(21A)	119.0	C(37)-C(36)-H(36A)	120.5
C(16)-C(21)-H(21A)	119.0	N(6)-C(37)-C(36)	123.1(9)
O(1)-C(22)-O(2)	124.2(10)	N(6)-C(37)-H(37A)	118.5
O(1)-C(22)-C(19)	120.4(11)	C(36)-C(37)-H(37A)	118.5
O(2)-C(22)-C(19)	115.4(9)	C(43)-C(38)-C(39)	120.3(8)
N(4)-C(23)-C(24)	120.2(9)	C(43)-C(38)-C(30)	119.9(9)
N(4)-C(23)-H(23A)	119.9	C(39)-C(38)-C(30)	119.8(8)
C(24)-C(23)-H(23A)	119.9	C(40)-C(39)-C(38)	119.6(10)
C(25)-C(24)-C(23)	121.2(9)	C(40)-C(39)-H(39A)	120.2
C(25)-C(24)-H(24A)	119.4	C(38)-C(39)-H(39A)	120.2
C(23)-C(24)-H(24A)	119.4	C(39)-C(40)-C(41)	120.5(9)
C(24)-C(25)-C(26)	116.7(9)	C(39)-C(40)-H(40A)	119.8
C(24)-C(25)-H(25A)	121.6	C(41)-C(40)-H(40A)	119.8
C(26)-C(25)-H(25A)	121.6	C(42)-C(41)-C(40)	119.0(8)
C(27)-C(26)-C(25)	121.9(9)	C(42)-C(41)-C(44)	120.5(9)
C(27)-C(26)-H(26A)	119.0	C(40)-C(41)-C(44)	120.3(9)
C(25)-C(26)-H(26A)	119.0	C(41)-C(42)-C(43)	120.7(9)
C(26)-C(27)-N(4)	121.5(8)	C(41)-C(42)-H(42A)	119.6
C(26)-C(27)-C(28)	124.1(8)	C(43)-C(42)-H(42A)	119.6
N(4)-C(27)-C(28)	114.3(8)	C(38)-C(43)-C(42)	119.5(9)
N(5)-C(28)-C(29)	119.7(8)	C(38)-C(43)-H(43A)	120.2
N(5)-C(28)-C(27)	114.3(7)	C(42)-C(43)-H(43A)	120.2
C(29)-C(28)-C(27)	126.0(8)	O(3)-C(44)-O(4)	125.9(9)
C(28)-C(29)-C(30)	120.3(8)	O(3)-C(44)-C(41)	115.9(10)
C(28)-C(29)-H(29A)	119.9	O(4)-C(44)-C(41)	118.1(8)
C(30)-C(29)-H(29A)	119.9	N(7)-C(45)-C(46)	124.9(9)
C(31)-C(30)-C(29)	118.5(8)	N(7)-C(45)-H(45A)	117.5
C(31)-C(30)-C(38)	122.9(8)	C(46)-C(45)-H(45A)	117.5
C(29)-C(30)-C(38)	118.6(8)	C(45)-C(46)-C(47)	116.8(9)
C(32)-C(31)-C(30)	119.8(8)	C(45)-C(46)-H(46A)	121.6
C(32)-C(31)-H(31A)	120.1	C(47)-C(46)-H(46A)	121.6
C(30)-C(31)-H(31A)	120.1	C(46)-C(47)-C(48)	118.7(10)
N(5)-C(32)-C(31)	120.3(8)	C(46)-C(47)-H(47A)	120.7
N(5)-C(32)-C(33)	114.4(7)	C(48)-C(47)-H(47A)	120.7
C(31)-C(32)-C(33)	125.3(8)	C(49)-C(48)-C(47)	120.7(10)
N(6)-C(33)-C(34)	121.8(8)	C(49)-C(48)-H(48A)	119.6
N(6)-C(33)-C(32)	115.6(7)	C(47)-C(48)-H(48A)	119.6
C(34)-C(33)-C(32)	122.6(8)	N(7)-C(49)-C(48)	119.6(8)
C(35)-C(34)-C(33)	118.0(8)	N(7)-C(49)-C(50)	115.5(7)
C(35)-C(34)-H(34A)	121.0	C(48)-C(49)-C(50)	124.8(9)

N(8)-C(50)-C(51)	119.6(8)	C(61)-C(60)-C(52)	118.4(8)
N(8)-C(50)-C(49)	114.8(7)	C(62)-C(61)-C(60)	118.2(9)
C(51)-C(50)-C(49)	125.6(8)	C(62)-C(61)-H(61A)	120.9
C(50)-C(51)-C(52)	122.1(8)	C(60)-C(61)-H(61A)	120.9
C(50)-C(51)-H(51A)	119.0	C(63)-C(62)-C(61)	121.5(8)
C(52)-C(51)-H(51A)	119.0	C(63)-C(62)-H(62A)	119.3
C(51)-C(52)-C(53)	117.4(8)	C(61)-C(62)-H(62A)	119.3
C(51)-C(52)-C(60)	121.7(8)	C(62)-C(63)-C(64)	120.3(8)
C(53)-C(52)-C(60)	120.9(8)	C(62)-C(63)-C(66)	119.2(8)
C(52)-C(53)-C(54)	118.3(8)	C(64)-C(63)-C(66)	120.5(8)
C(52)-C(53)-H(53A)	120.8	C(65)-C(64)-C(63)	120.2(8)
C(54)-C(53)-H(53A)	120.8	C(65)-C(64)-H(64A)	119.9
N(8)-C(54)-C(53)	121.4(8)	C(63)-C(64)-H(64A)	119.9
N(8)-C(54)-C(55)	114.0(7)	C(64)-C(65)-C(60)	120.0(8)
C(53)-C(54)-C(55)	124.6(8)	C(64)-C(65)-H(65A)	120.0
N(9)-C(55)-C(56)	121.4(8)	C(60)-C(65)-H(65A)	120.0
N(9)-C(55)-C(54)	115.5(7)	O(6)-C(66)-O(5)	124.1(8)
C(56)-C(55)-C(54)	123.1(8)	O(6)-C(66)-C(63)	117.7(8)
C(57)-C(56)-C(55)	118.8(8)	O(5)-C(66)-C(63)	117.9(9)
C(57)-C(56)-H(56A)	120.6	F(2)-B(1)-F(1)	110.6(19)
C(55)-C(56)-H(56A)	120.6	F(2)-B(1)-F(4)	117.4(19)
C(58)-C(57)-C(56)	119.1(9)	F(1)-B(1)-F(4)	105(2)
C(58)-C(57)-H(57A)	120.5	F(2)-B(1)-F(3)	106(2)
C(56)-C(57)-H(57A)	120.5	F(1)-B(1)-F(3)	110.4(17)
C(59)-C(58)-C(57)	118.8(8)	F(4)-B(1)-F(3)	107.2(16)
C(59)-C(58)-H(58A)	120.6	F(6)-B(2)-F(5)	116.8(12)
C(57)-C(58)-H(58A)	120.6	F(6)-B(2)-F(8)	109.0(14)
N(9)-C(59)-C(58)	123.2(8)	F(5)-B(2)-F(8)	111.7(13)
N(9)-C(59)-H(59A)	118.4	F(6)-B(2)-F(7)	110.9(14)
C(58)-C(59)-H(59A)	118.4	F(5)-B(2)-F(7)	105.8(13)
C(65)-C(60)-C(61)	119.7(8)	F(8)-B(2)-F(7)	101.6(11)
C(65)-C(60)-C(52)	121.8(8)		

Symmetry transformations used to generate equivalent atoms:
#1 x+1,y,z+1 #2 x-1,y,z-1

Table 33. Anisotropic displacement parameters for **3**[d]

	U^{11}	U^{22}	U^{33}	U^{23}	U^{13}	U^{12}
Zn(1)	24(1)	55(1)	19(1)	-2(1)	3(1)	0(1)
Zn(2)	26(1)	47(1)	18(1)	-2(1)	9(1)	0(1)
F(1)	176(12)	189(12)	221(13)	12(10)	136(11)	90(10)
F(2)	208(14)	263(16)	110(9)	106(10)	5(9)	-46(12)
F(3)	107(8)	185(11)	117(8)	9(8)	43(7)	-3(8)

F(4)	147(10)	135(9)	185(11)	-58(8)	107(9)	-7(8)
F(5)	153(8)	126(7)	35(4)	-7(4)	32(5)	38(6)
F(6)	217(11)	88(6)	49(5)	-8(4)	48(6)	34(7)
F(7)	92(7)	123(8)	122(8)	38(6)	40(6)	-18(6)
F(8)	96(6)	172(9)	68(5)	12(5)	49(5)	-7(6)
O(1)	52(5)	137(9)	57(5)	55(6)	-15(4)	-13(6)
O(2)	23(3)	87(6)	38(4)	4(4)	5(3)	-5(4)
O(3)	28(4)	89(6)	68(5)	-33(5)	20(4)	-23(4)
O(5)	23(4)	175(10)	34(4)	-7(5)	5(3)	7(5)
O(6)	35(4)	112(7)	16(3)	10(4)	5(3)	-11(4)
N(1)	33(4)	63(6)	31(4)	-5(4)	20(4)	-1(4)
N(2)	21(3)	43(5)	17(3)	4(3)	9(3)	-3(4)
N(3)	20(4)	46(5)	23(4)	1(3)	-8(3)	9(4)
N(4)	35(4)	47(5)	30(4)	0(4)	22(4)	0(4)
N(5)	28(4)	47(5)	19(3)	2(3)	13(3)	10(4)
N(6)	26(4)	52(5)	23(4)	-6(3)	13(3)	-8(4)
N(7)	28(4)	50(5)	27(4)	-8(3)	15(4)	3(4)
N(8)	24(4)	46(5)	17(3)	-5(3)	12(3)	-5(4)
N(9)	19(4)	50(5)	16(3)	-3(3)	4(3)	1(3)
C(1)	43(6)	47(7)	36(6)	-12(5)	14(5)	0(5)
C(2)	39(6)	64(8)	70(8)	-19(6)	25(6)	-21(6)
C(3)	74(8)	51(7)	45(7)	-2(5)	34(7)	1(6)
C(4)	45(6)	54(7)	36(6)	4(5)	18(5)	16(5)
C(5)	16(4)	69(7)	24(4)	1(5)	8(4)	2(5)
C(6)	33(5)	44(6)	26(4)	0(4)	24(4)	0(4)
C(7)	18(4)	50(6)	22(4)	6(4)	12(4)	17(4)
C(8)	19(4)	45(6)	24(4)	6(4)	11(4)	8(4)
C(9)	19(4)	50(6)	24(4)	0(4)	7(4)	7(4)
C(10)	16(4)	56(6)	18(4)	2(4)	7(3)	0(4)
C(11)	15(4)	54(6)	33(5)	3(4)	17(4)	6(4)
C(12)	16(4)	49(6)	39(5)	2(5)	9(4)	-2(4)
C(13)	34(6)	45(6)	48(6)	14(5)	8(5)	2(5)
C(14)	32(5)	49(7)	48(6)	12(5)	14(5)	14(5)
C(15)	47(6)	82(9)	17(5)	23(5)	4(5)	18(6)
C(16)	19(4)	50(6)	21(4)	7(4)	9(4)	13(4)
C(17)	27(5)	61(7)	31(5)	3(5)	15(4)	-2(5)
C(18)	37(6)	81(8)	21(5)	7(5)	4(5)	-1(6)
C(19)	20(4)	63(7)	23(4)	8(5)	6(4)	3(5)
C(20)	25(5)	62(7)	21(4)	-8(4)	17(4)	-4(5)
C(21)	21(4)	62(7)	18(4)	7(4)	8(4)	5(5)
C(22)	29(5)	92(9)	30(5)	10(6)	5(5)	16(7)
C(23)	36(6)	66(7)	28(5)	4(5)	18(5)	0(5)
C(24)	42(6)	69(8)	51(7)	24(6)	34(6)	12(6)
C(25)	29(5)	60(7)	40(6)	-2(5)	11(5)	-16(5)
C(26)	24(5)	52(6)	35(5)	3(5)	11(4)	0(5)
C(27)	23(5)	54(6)	19(4)	-4(4)	12(4)	0(4)

C(28)	24(5)	43(6)	28(5)	3(4)	10(4)	7(4)
C(29)	26(5)	48(6)	25(4)	-5(4)	12(4)	-10(4)
C(30)	32(5)	49(6)	20(4)	-6(4)	11(4)	11(4)
C(31)	37(5)	43(5)	21(4)	0(4)	17(4)	2(5)
C(32)	23(4)	42(5)	28(4)	3(4)	18(4)	13(4)
C(33)	27(5)	47(6)	23(4)	1(4)	15(4)	7(4)
C(34)	32(5)	62(7)	29(5)	7(5)	17(4)	-4(5)
C(35)	41(6)	54(7)	36(5)	5(5)	25(5)	-6(5)
C(36)	37(6)	59(7)	50(6)	-15(5)	31(5)	-22(5)
C(37)	23(5)	55(7)	31(5)	-9(4)	9(4)	-8(5)
C(38)	29(5)	58(7)	20(4)	10(4)	17(4)	11(4)
C(39)	62(7)	64(7)	16(5)	-6(5)	14(5)	0(6)
C(40)	64(7)	66(7)	29(5)	-20(5)	32(5)	-21(6)
C(41)	22(4)	54(6)	16(4)	-5(4)	10(4)	-2(4)
C(42)	18(4)	56(6)	22(4)	0(4)	9(4)	0(4)
C(43)	22(4)	53(6)	26(5)	-8(4)	15(4)	-1(4)
C(44)	18(5)	57(7)	46(6)	-11(5)	8(5)	0(5)
C(45)	38(6)	55(6)	33(5)	-1(5)	24(5)	3(5)
C(46)	67(8)	49(6)	37(6)	1(5)	40(6)	6(6)
C(47)	65(8)	70(8)	69(8)	-2(6)	51(7)	19(6)
C(48)	38(6)	70(8)	42(6)	1(5)	27(5)	8(5)
C(49)	24(5)	42(6)	34(5)	6(4)	17(4)	4(4)
C(50)	22(4)	47(6)	17(4)	5(4)	11(4)	2(4)
C(51)	20(4)	51(6)	27(5)	4(4)	8(4)	5(4)
C(52)	18(4)	49(6)	25(4)	1(4)	5(4)	4(4)
C(53)	31(5)	52(6)	24(4)	0(4)	14(4)	6(5)
C(54)	23(4)	38(5)	22(4)	2(4)	13(4)	4(4)
C(55)	17(4)	51(6)	24(4)	-9(4)	11(4)	-4(4)
C(56)	29(5)	62(7)	21(4)	-10(4)	9(4)	-5(5)
C(57)	20(5)	57(7)	49(6)	-13(5)	17(5)	10(5)
C(58)	18(4)	46(6)	35(5)	1(4)	11(4)	10(4)
C(59)	18(4)	56(6)	25(5)	7(4)	5(4)	-3(4)
C(60)	23(4)	43(6)	30(5)	9(4)	10(4)	-1(4)
C(61)	26(5)	56(7)	30(5)	2(4)	6(4)	4(5)
C(62)	17(4)	61(7)	22(4)	-1(4)	1(4)	5(4)
C(63)	20(4)	42(5)	21(4)	12(4)	1(3)	2(4)
C(64)	24(5)	55(7)	29(5)	-4(4)	13(4)	-3(4)
C(65)	18(4)	50(6)	21(4)	6(4)	7(4)	8(4)
C(66)	25(5)	36(5)	25(5)	-4(4)	-4(4)	-3(4)
B(1)	92(16)	107(17)	79(14)	5(12)	26(13)	24(14)
B(2)	83(12)	73(11)	42(8)	-8(8)	27(9)	10(10)

Table 34. Crystal data and structure refinement for **4**

Identification code	$Zn_4(\mu\text{-}OH)(\mathbf{L})_4(HCOO)_2(BF_4)_2$
Empirical formula	$C_{360}H_{176}N_{48}O_{68}Zn_{16}$

Formula weight	7354.32	
Temperature	173(2) K	
Wavelength	0.71073 Å	
Crystal system	Tetragonal	
Space group	I-4	
Unit cell dimensions	a = 14.9993(15) Å	α= 90°.
	b = 14.9993(15) Å	β= 90°.
	c = 41.776(8) Å	γ = 90°.
Volume	9399(2) $Å^3$	
Z	1	
Density (calculated)	1.299 Mg/m^3	
Absorption coefficient	1.070 mm^{-1}	
F(000)	3631	
Theta range for data collection	1.44 to 28.38°.	
Index ranges	-20<=h<=20, -19<=k<=20, -55<=l<=55	
Reflections collected	49153	
Independent reflections	11746 [R(int) = 0.1949]	
Completeness to theta = 28.38°	99.8 %	
Refinement method	Full-matrix least-squares on F^2	
Data / restraints / parameters	11746 / 0 / 305	
Goodness-of-fit on F^2	1.342	
Final R indices [I>2sigma(I)]	R1 = 0.1386, wR2 = 0.2939	
R indices (all data)	R1 = 0.3066, wR2 = 0.3445	
Absolute structure parameter	0.00	
Largest diff. peak and hole	1.194 and -0.713 e.$Å^{-3}$	

Table 35. Atomic coordinates[a] and equivalent isotropic displacement parameters[b] for **4**

	x	y	z	U(eq)[c]
Zn(1)	-6174(1)	92(1)	-399(1)	77(1)
Zn(2)	-7201(1)	-3393(1)	-3178(1)	80(1)
O(1)	-6691(6)	-1446(6)	-3044(2)	73(3)
O(2)	-7579(7)	-2488(7)	-2868(2)	77(3)
O(3)	-7570(16)	829(15)	-228(6)	221(9)
O(4)	-6611(16)	218(16)	168(6)	228(9)
O(5)	-7288(11)	-5362(10)	-3380(4)	147(5)
O(6)	-7932(8)	-4375(9)	-3036(3)	117(4)
O(7)	-5000	0	-229(2)	72(4)
O(8)	-8588(14)	-4317(14)	-2462(5)	218(8)
O(9)	-9581(12)	-2422(12)	-2883(4)	171(6)
N(1)	-5890(8)	1297(8)	-669(2)	69(3)
N(2)	-6357(7)	-295(8)	-880(2)	63(3)
N(3)	-6560(9)	-1328(8)	-377(2)	85(4)

N(4)	-7819(8)	-3090(9)	-3603(2)	78(4)
N(5)	-6130(9)	-3475(8)	-3507(3)	85(4)
N(6)	-6111(12)	-3656(7)	-2915(3)	110(6)
C(1)	-5675(11)	2049(12)	-549(4)	91(5)
C(2)	-5391(12)	2782(13)	-720(4)	105(6)
C(3)	-5451(12)	2773(13)	-1101(5)	108(6)
C(4)	-5835(11)	1950(11)	-1214(4)	88(5)
C(5)	-5964(8)	1222(9)	-997(3)	60(3)
C(6)	-6231(8)	305(8)	-1098(3)	55(3)
C(7)	-6381(7)	125(8)	-1426(3)	51(3)
C(8)	-6601(8)	-742(8)	-1511(3)	53(3)
C(9)	-6731(10)	-1414(10)	-1276(4)	78(4)
C(10)	-6573(9)	-1104(11)	-943(3)	69(4)
C(11)	-6701(11)	-1693(11)	-668(4)	85(5)
C(12)	-6976(12)	-2568(13)	-716(5)	109(6)
C(13)	-7160(14)	-3170(13)	-427(5)	125(6)
C(14)	-6910(15)	-2581(17)	-109(6)	146(8)
C(15)	-6548(14)	-1772(15)	-130(5)	120(6)
C(16)	-6732(8)	-1009(9)	-1826(3)	63(3)
C(17)	-6442(9)	-467(9)	-2087(3)	66(4)
C(18)	-6560(10)	-739(10)	-2408(4)	78(4)
C(19)	-7000(9)	-1538(9)	-2484(3)	67(4)
C(20)	-7352(9)	-2039(9)	-2230(3)	67(4)
C(21)	-7178(9)	-1810(9)	-1917(3)	71(4)
C(22)	-7079(10)	-1831(10)	-2829(3)	63(4)
C(23)	-8695(14)	-2763(13)	-3655(5)	114(6)
C(24)	-9065(13)	-2587(12)	-3947(4)	104(6)
C(25)	-8549(13)	-2714(13)	-4237(5)	113(6)
C(26)	-7684(13)	-2969(12)	-4171(4)	106(6)
C(27)	-7246(11)	-3146(10)	-3868(4)	82(4)
C(28)	-6418(9)	-3346(8)	-3811(3)	57(3)
C(29)	-5742(9)	-3522(9)	-4022(4)	74(4)
C(30)	-4901(10)	-3809(10)	-3937(4)	78(4)
C(31)	-4704(11)	-3862(10)	-3635(4)	84(5)
C(32)	-5341(11)	-3731(9)	-3410(3)	68(4)
C(33)	-5255(10)	-3809(9)	-3087(3)	72(4)
C(34)	-4528(11)	-3964(10)	-2947(4)	79(4)
C(35)	-4413(15)	-4004(14)	-2559(5)	130(7)
C(36)	-5180(13)	-3880(11)	-2420(4)	98(5)
C(37)	-5971(14)	-3766(12)	-2595(5)	110(6)
C(38)	-4157(12)	-3998(11)	-4201(4)	93(5)
C(39)	-4310(18)	-3860(17)	-4534(6)	159(8)
C(40)	-3732(18)	-3936(16)	-4772(6)	146(8)
C(41)	-3070(20)	-4240(19)	-4691(7)	160(10)
C(42)	-2750(20)	-4570(20)	-4467(8)	177(11)
C(43)	-3444(15)	-4374(14)	-4096(5)	131(7)

C(44)	-7065(14)	513(14)	-57(5)	107(6)
C(45)	-7814(13)	-5205(15)	-3156(5)	114(6)

[a] x 10^4
[b] Å^2 x 10^3
[c] U(eq) is defined as one third of the trace of the orthogonalized U^{ij} tensor.

Table 36. Bond lengths (Å) and angles (°) for **4**

Zn(1)-O(7)	1.903(4)	C(4)-H(4A)	0.9300
Zn(1)-C(44)	2.06(2)	C(5)-C(6)	1.494(17)
Zn(1)-N(2)	2.110(10)	C(6)-C(7)	1.416(15)
Zn(1)-N(1)	2.173(12)	C(7)-C(8)	1.388(16)
Zn(1)-N(3)	2.210(12)	C(7)-H(7A)	0.9300
Zn(1)-O(4)	2.46(2)	C(8)-C(16)	1.389(17)
Zn(1)-O(3)	2.47(2)	C(8)-C(9)	1.421(18)
Zn(2)-O(6)	1.930(12)	C(9)-C(10)	1.487(19)
Zn(2)-O(2)	1.960(9)	C(10)-C(11)	1.46(2)
Zn(2)-N(6)	2.009(19)	C(11)-C(12)	1.39(2)
Zn(2)-N(4)	2.053(12)	C(12)-C(13)	1.53(3)
Zn(2)-N(5)	2.120(12)	C(12)-H(12A)	0.9300
O(1)-C(22)	1.217(15)	C(13)-C(14)	1.64(3)
O(2)-C(22)	1.249(16)	C(14)-C(15)	1.33(3)
O(3)-C(44)	1.14(2)	C(14)-H(14A)	0.9300
O(4)-C(44)	1.24(3)	C(15)-H(15A)	0.9300
O(5)-C(45)	1.25(2)	C(16)-C(17)	1.426(18)
O(6)-C(45)	1.35(2)	C(16)-C(21)	1.427(17)
O(7)-Zn(1)#1	1.903(4)	C(17)-C(18)	1.415(18)
N(1)-C(1)	1.277(18)	C(17)-H(17A)	0.9300
N(1)-C(5)	1.378(16)	C(18)-C(19)	1.405(18)
N(2)-C(10)	1.284(16)	C(18)-H(18A)	0.9300
N(2)-C(6)	1.292(14)	C(19)-C(20)	1.404(18)
N(3)-C(15)	1.23(2)	C(19)-C(22)	1.509(19)
N(3)-C(11)	1.352(19)	C(20)-C(21)	1.376(17)
N(4)-C(27)	1.407(18)	C(20)-H(20A)	0.9300
N(4)-C(23)	1.42(2)	C(21)-H(21A)	0.9300
N(5)-C(32)	1.308(18)	C(23)-C(24)	1.36(2)
N(5)-C(28)	1.354(16)	C(23)-H(23A)	0.9300
N(6)-C(37)	1.36(2)	C(24)-C(25)	1.45(2)
N(6)-C(33)	1.49(2)	C(24)-H(24A)	0.9300
C(1)-C(2)	1.38(2)	C(25)-C(26)	1.38(2)
C(1)-H(1A)	0.9300	C(26)-C(27)	1.45(2)
C(2)-C(3)	1.60(2)	C(26)-H(26A)	0.9300
C(2)-H(2A)	0.9300	C(27)-C(28)	1.300(19)
C(3)-C(4)	1.44(2)	C(28)-C(29)	1.370(17)
C(4)-C(5)	1.431(19)	C(29)-C(30)	1.379(19)

C(29)-H(29A)	0.9300
C(30)-C(31)	1.298(19)
C(30)-C(38)	1.59(2)
C(31)-C(32)	1.36(2)
C(31)-H(31A)	0.9300
C(32)-C(33)	1.358(19)
C(33)-C(34)	1.260(19)
C(34)-C(35)	1.63(2)
C(34)-H(34A)	0.9300
C(35)-C(36)	1.30(2)
C(36)-C(37)	1.40(2)
C(36)-H(36A)	0.9300
C(37)-H(37A)	0.9300
C(38)-C(43)	1.29(2)
C(38)-C(39)	1.43(3)
C(39)-C(40)	1.32(3)
C(39)-H(39A)	0.9300
C(40)-C(41)	1.14(3)
C(40)-H(40A)	0.9300
C(41)-C(42)	1.16(3)
C(45)-H(45A)	0.9300

O(7)-Zn(1)-C(44)	111.4(7)
O(7)-Zn(1)-N(2)	117.0(4)
C(44)-Zn(1)-N(2)	131.5(7)
O(7)-Zn(1)-N(1)	94.1(3)
C(44)-Zn(1)-N(1)	103.5(7)
N(2)-Zn(1)-N(1)	76.0(4)
O(7)-Zn(1)-N(3)	99.0(3)
C(44)-Zn(1)-N(3)	95.5(7)
N(2)-Zn(1)-N(3)	75.0(4)
N(1)-Zn(1)-N(3)	151.0(4)
O(7)-Zn(1)-O(4)	83.9(7)
C(44)-Zn(1)-O(4)	30.2(7)
N(2)-Zn(1)-O(4)	154.4(6)
N(1)-Zn(1)-O(4)	119.2(6)
N(3)-Zn(1)-O(4)	88.0(6)
O(7)-Zn(1)-O(3)	135.1(6)
C(44)-Zn(1)-O(3)	27.4(7)
N(2)-Zn(1)-O(3)	106.8(6)
N(1)-Zn(1)-O(3)	86.8(6)
N(3)-Zn(1)-O(3)	101.4(6)
O(4)-Zn(1)-O(3)	57.5(7)
O(6)-Zn(2)-O(2)	99.3(5)
O(6)-Zn(2)-N(6)	98.3(5)
O(2)-Zn(2)-N(6)	90.6(4)
O(6)-Zn(2)-N(4)	100.2(5)
O(2)-Zn(2)-N(4)	106.7(5)
N(6)-Zn(2)-N(4)	152.1(5)
O(6)-Zn(2)-N(5)	125.8(5)
O(2)-Zn(2)-N(5)	133.6(4)
N(6)-Zn(2)-N(5)	74.1(5)
N(4)-Zn(2)-N(5)	78.1(5)
C(22)-O(2)-Zn(2)	117.3(9)
C(44)-O(3)-Zn(1)	55.6(15)
C(44)-O(4)-Zn(1)	56.3(14)
C(45)-O(6)-Zn(2)	121.0(12)
Zn(1)-O(7)-Zn(1)#1	136.4(6)
C(1)-N(1)-C(5)	118.9(13)
C(1)-N(1)-Zn(1)	125.5(10)
C(5)-N(1)-Zn(1)	115.7(9)
C(10)-N(2)-C(6)	123.4(11)
C(10)-N(2)-Zn(1)	119.2(9)
C(6)-N(2)-Zn(1)	117.4(9)
C(15)-N(3)-C(11)	122.7(16)
C(15)-N(3)-Zn(1)	123.6(14)
C(11)-N(3)-Zn(1)	113.2(9)
C(27)-N(4)-C(23)	117.6(14)
C(27)-N(4)-Zn(2)	113.1(10)
C(23)-N(4)-Zn(2)	128.9(11)
C(32)-N(5)-C(28)	128.5(13)
C(32)-N(5)-Zn(2)	120.0(11)
C(28)-N(5)-Zn(2)	111.0(10)
C(37)-N(6)-C(33)	108.8(17)
C(37)-N(6)-Zn(2)	133.3(13)
C(33)-N(6)-Zn(2)	117.9(9)
N(1)-C(1)-C(2)	125.4(17)
N(1)-C(1)-H(1A)	117.3
C(2)-C(1)-H(1A)	117.3
C(1)-C(2)-C(3)	119.5(17)
C(1)-C(2)-H(2A)	120.2
C(3)-C(2)-H(2A)	120.2
C(4)-C(3)-C(2)	110.8(16)
C(5)-C(4)-C(3)	120.1(15)
C(5)-C(4)-H(4A)	119.9
C(3)-C(4)-H(4A)	119.9
N(1)-C(5)-C(4)	123.7(13)
N(1)-C(5)-C(6)	112.1(11)
C(4)-C(5)-C(6)	124.1(12)
N(2)-C(6)-C(7)	121.7(11)
N(2)-C(6)-C(5)	118.8(11)
C(7)-C(6)-C(5)	119.4(11)

C(8)-C(7)-C(6)	117.7(11)	N(4)-C(23)-H(23A)	117.2
C(8)-C(7)-H(7A)	121.1	C(23)-C(24)-C(25)	120.2(19)
C(6)-C(7)-H(7A)	121.1	C(23)-C(24)-H(24A)	119.9
C(7)-C(8)-C(16)	123.1(11)	C(25)-C(24)-H(24A)	119.9
C(7)-C(8)-C(9)	121.3(11)	C(26)-C(25)-C(24)	111.8(18)
C(16)-C(8)-C(9)	115.6(12)	C(25)-C(26)-C(27)	130.6(19)
C(8)-C(9)-C(10)	113.8(12)	C(25)-C(26)-H(26A)	114.7
N(2)-C(10)-C(11)	116.4(13)	C(27)-C(26)-H(26A)	114.7
N(2)-C(10)-C(9)	121.8(13)	C(28)-C(27)-N(4)	116.9(14)
C(11)-C(10)-C(9)	121.7(14)	C(28)-C(27)-C(26)	129.5(16)
N(3)-C(11)-C(12)	123.8(16)	N(4)-C(27)-C(26)	113.6(15)
N(3)-C(11)-C(10)	116.3(14)	C(27)-C(28)-N(5)	120.7(14)
C(12)-C(11)-C(10)	119.9(16)	C(27)-C(28)-C(29)	129.3(14)
C(11)-C(12)-C(13)	119.8(18)	N(5)-C(28)-C(29)	109.8(12)
C(11)-C(12)-H(12A)	120.1	C(28)-C(29)-C(30)	124.9(14)
C(13)-C(12)-H(12A)	120.1	C(28)-C(29)-H(29A)	117.5
C(12)-C(13)-C(14)	106.2(17)	C(30)-C(29)-H(29A)	117.5
C(15)-C(14)-C(13)	122(2)	C(31)-C(30)-C(29)	118.5(15)
C(15)-C(14)-H(14A)	118.9	C(31)-C(30)-C(38)	120.1(15)
C(13)-C(14)-H(14A)	118.9	C(29)-C(30)-C(38)	121.2(14)
N(3)-C(15)-C(14)	123(2)	C(30)-C(31)-C(32)	120.4(16)
N(3)-C(15)-H(15A)	118.6	C(30)-C(31)-H(31A)	119.8
C(14)-C(15)-H(15A)	118.6	C(32)-C(31)-H(31A)	119.8
C(8)-C(16)-C(17)	121.1(12)	N(5)-C(32)-C(31)	117.6(14)
C(8)-C(16)-C(21)	124.1(12)	N(5)-C(32)-C(33)	114.9(15)
C(17)-C(16)-C(21)	114.7(13)	C(31)-C(32)-C(33)	127.5(16)
C(18)-C(17)-C(16)	121.5(13)	C(34)-C(33)-C(32)	124.1(16)
C(18)-C(17)-H(17A)	119.2	C(34)-C(33)-N(6)	123.3(15)
C(16)-C(17)-H(17A)	119.2	C(32)-C(33)-N(6)	112.5(14)
C(19)-C(18)-C(17)	121.2(14)	C(33)-C(34)-C(35)	124.1(16)
C(19)-C(18)-H(18A)	119.4	C(33)-C(34)-H(34A)	118.0
C(17)-C(18)-H(18A)	119.4	C(35)-C(34)-H(34A)	118.0
C(20)-C(19)-C(18)	117.6(13)	C(36)-C(35)-C(34)	110.2(18)
C(20)-C(19)-C(22)	122.4(13)	C(35)-C(36)-C(37)	122.2(19)
C(18)-C(19)-C(22)	120.0(13)	C(35)-C(36)-H(36A)	118.9
C(21)-C(20)-C(19)	120.9(13)	C(37)-C(36)-H(36A)	118.9
C(21)-C(20)-H(20A)	119.6	N(6)-C(37)-C(36)	131.0(19)
C(19)-C(20)-H(20A)	119.6	N(6)-C(37)-H(37A)	114.5
C(20)-C(21)-C(16)	123.5(13)	C(36)-C(37)-H(37A)	114.5
C(20)-C(21)-H(21A)	118.2	C(43)-C(38)-C(39)	122(2)
C(16)-C(21)-H(21A)	118.2	C(43)-C(38)-C(30)	115.0(17)
O(1)-C(22)-O(2)	124.5(13)	C(39)-C(38)-C(30)	122.4(18)
O(1)-C(22)-C(19)	121.9(14)	C(40)-C(39)-C(38)	128(3)
O(2)-C(22)-C(19)	113.6(13)	C(40)-C(39)-H(39A)	116.1
C(24)-C(23)-N(4)	125.6(19)	C(38)-C(39)-H(39A)	116.1
C(24)-C(23)-H(23A)	117.2	C(41)-C(40)-C(39)	112(3)

C(41)-C(40)-H(40A)	123.8	O(4)-C(44)-Zn(1)	93.5(17)
C(39)-C(40)-H(40A)	123.8	O(5)-C(45)-O(6)	122(2)
C(40)-C(41)-C(42)	140(4)	O(5)-C(45)-H(45A)	118.9
O(3)-C(44)-O(4)	169(3)	O(6)-C(45)-H(45A)	118.9
O(3)-C(44)-Zn(1)	97.1(18)		

Symmetry transformations used to generate equivalent atoms:
#1 -x-1,-y,z

Table 37. Anisotropic displacement parameters for **4**[d]

	U^{11}	U^{22}	U^{33}	U^{23}	U^{13}	U^{12}
Zn(1)	69(1)	123(2)	39(1)	-2(1)	2(1)	11(1)
Zn(2)	101(1)	82(1)	58(1)	-12(1)	32(1)	-14(1)
O(1)	78(7)	92(7)	49(5)	-1(5)	11(5)	-21(5)
O(2)	80(7)	87(7)	62(6)	-11(5)	23(5)	-1(6)
O(6)	120(10)	142(11)	88(8)	-1(7)	48(7)	-34(8)
O(7)	53(8)	131(11)	30(6)	0	0	30(8)
N(1)	76(8)	72(8)	59(7)	-13(6)	-16(6)	-1(6)
N(2)	59(7)	86(9)	43(6)	16(6)	-1(5)	2(6)
N(3)	127(10)	96(9)	32(6)	26(6)	-4(7)	-13(8)
N(4)	70(8)	111(10)	52(6)	-12(7)	32(6)	-14(7)
N(5)	94(10)	59(8)	102(10)	-19(7)	27(8)	-36(7)
N(6)	213(17)	38(7)	78(9)	-18(6)	68(10)	-30(9)

[a] in $Å^2$ x 10.[3] The anisotropic displacement factor exponent takes the form: $-2\pi^2[h^2 a^{*2}U^{11} + ... + 2 h k a^* b^* U^{12}]$

Table 38. Crystal data and structure refinement for **5**

Identification code	$Zn_2(\mu\text{-}OH)(\mathbf{L})_2(BF_4)$	
Empirical formula	$C_{352}H_{192}N_{48}O_{152}Zn_{16}$	
Formula weight	8571.78	
Temperature	173(2) K	
Wavelength	0.71073 Å	
Crystal system	Tetragonal	
Space group	I-42d	
Unit cell dimensions	a = 14.549(4) Å	α= 90°.
	b = 14.549(4) Å	β= 90°.
	c = 47.06(2) Å	γ = 90°.
Volume	9961(6) $Å^3$	
Z	1	
Density (calculated)	1.429 Mg/m^3	
Absorption coefficient	1.042 mm^{-1}	
F(000)	4335	
Theta range for data collection	1.46 to 29.18°.	
Index ranges	-19<=h<=19, -19<=k<=19, -63<=l<=62	
Reflections collected	48931	
Independent reflections	6632 [R(int) = 0.4019]	
Completeness to theta = 29.18°	99.0 %	
Refinement method	Full-matrix least-squares on F^2	
Data / restraints / parameters	6632 / 0 / 286	
Goodness-of-fit on F^2	0.974	
Final R indices [I>2sigma(I)]	R1 = 0.1183, wR2 = 0.2735	
R indices (all data)	R1 = 0.2944, wR2 = 0.3443	
Absolute structure parameter	0.00	
Largest diff. peak and hole	0.929 and -0.546 e.$Å^{-3}$	

Table 39. Atomic coordinates[a] and equivalent isotropic displacement parameters[b] for **5**

	x	y	z	U(eq)[c]
Zn(1)	-1288(1)	-4924(1)	-5673(1)	70(1)
O(1)	-2846(8)	-3926(12)	-5464(2)	137(5)
O(2)	-1575(9)	-4542(8)	-5290(2)	112(4)
O(3)	0	-5000	-5589(2)	103(5)
O(4)	0	0	-4238(7)	240(11)
O(5)	-8783(12)	-937(12)	-4644(3)	187(6)
O(6)	-890(18)	-1308(17)	-3525(5)	264(11)
O(7)	-300(30)	-6490(30)	-4610(7)	398(19)
O(8)	-510(20)	-2760(20)	-5045(6)	310(14)

O(9)	-1873(15)	-7038(16)	-4565(5)	229(9)
O(10)	-40(80)	-6770(50)	-3643(16)	760(60)
O(11)	0	-5000	-4965(6)	216(10)
N(1)	-6254(8)	-3751(9)	-3439(2)	79(3)
N(2)	-4508(8)	-3640(7)	-3582(2)	68(3)
N(3)	-3614(8)	-3468(6)	-3118(2)	67(3)
C(1)	-7116(9)	-3820(11)	-3354(3)	85(4)
C(2)	-7849(11)	-3791(15)	-3516(4)	116(6)
C(3)	-7594(19)	-3684(14)	-3839(4)	136(8)
C(4)	-6784(11)	-3715(11)	-3922(3)	75(4)
C(5)	-6098(9)	-3764(9)	-3724(2)	69(3)
C(6)	-5110(10)	-3742(6)	-3799(2)	56(3)
C(7)	-4752(7)	-3877(6)	-4066(2)	45(3)
C(8)	-3808(11)	-3862(6)	-4122(2)	62(3)
C(9)	-3261(9)	-3764(8)	-3887(3)	66(3)
C(10)	-3604(8)	-3607(8)	-3611(2)	48(3)
C(11)	-3140(9)	-3500(8)	-3347(2)	56(3)
C(12)	-2212(15)	-3420(9)	-3340(3)	95(6)
C(13)	-1678(13)	-3293(10)	-3080(3)	97(5)
C(14)	-2272(12)	-3218(10)	-2842(3)	83(4)
C(15)	-3172(13)	-3296(10)	-2860(3)	87(5)
C(16)	-3405(10)	-3988(7)	-4409(2)	59(3)
C(17)	-3990(10)	-3827(10)	-4639(2)	82(4)
C(18)	-3605(11)	-3894(11)	-4922(2)	88(4)
C(19)	-2746(9)	-4137(9)	-4952(3)	64(3)
C(20)	-2227(11)	-4268(13)	-4729(3)	108(6)
C(21)	-2546(10)	-4155(10)	-4459(2)	77(4)
C(22)	-2395(14)	-4217(10)	-5260(3)	83(4)

[a] x 10^4
[b] $Å^2$ x 10^3
[c] U(eq) is defined as one third of the trace of the orthogonalized U^{ij} tensor.

Table 40. Bond lengths (Å) and angles (°) for **5**

Zn(1)-O(3)	1.918(3)	N(1)-C(5)	1.360(13)
Zn(1)-O(2)	1.933(10)	N(1)-Zn(1)#5	2.124(10)
Zn(1)-N(2)#1	2.095(8)	N(2)-C(10)	1.324(14)
Zn(1)-N(1)#1	2.124(10)	N(2)-C(6)	1.353(15)
Zn(1)-N(3)#1	2.171(12)	N(2)-Zn(1)#5	2.095(8)
O(1)-C(22)	1.239(18)	N(3)-C(11)	1.280(14)
O(2)-C(22)	1.292(19)	N(3)-C(15)	1.394(15)
O(3)-Zn(1)#2	1.918(3)	N(3)-Zn(1)#5	2.171(11)
O(6)-O(10)#3	2.17(10)	C(1)-C(2)	1.31(2)
O(10)-O(6)#4	2.17(10)	C(1)-H(1B)	0.9300
N(1)-C(1)	1.320(16)	C(2)-C(3)	1.57(2)

C(3)-C(4)	1.24(3)	C(5)-N(1)-Zn(1)#5	116.5(9)
C(3)-H(3C)	0.9300	C(10)-N(2)-C(6)	124.6(9)
C(4)-C(5)	1.367(17)	C(10)-N(2)-Zn(1)#5	119.3(7)
C(4)-H(4A)	0.9300	C(6)-N(2)-Zn(1)#5	115.6(9)
C(5)-C(6)	1.480(19)	C(11)-N(3)-C(15)	119.3(12)
C(6)-C(7)	1.377(13)	C(11)-N(3)-Zn(1)#5	114.9(8)
C(7)-C(8)	1.399(17)	C(15)-N(3)-Zn(1)#5	125.9(10)
C(7)-H(7A)	0.9300	N(1)-C(1)-C(2)	126.3(15)
C(8)-C(9)	1.371(16)	N(1)-C(1)-H(1B)	116.9
C(8)-C(16)	1.483(14)	C(2)-C(1)-H(1B)	116.9
C(9)-C(10)	1.408(15)	C(1)-C(2)-C(3)	112.0(16)
C(9)-H(9A)	0.9300	C(4)-C(3)-C(2)	121.6(19)
C(10)-C(11)	1.425(14)	C(4)-C(3)-H(3C)	119.2
C(11)-C(12)	1.36(2)	C(2)-C(3)-H(3C)	119.2
C(12)-C(13)	1.46(2)	C(3)-C(4)-C(5)	118.6(15)
C(12)-H(12A)	0.9300	C(3)-C(4)-H(4A)	120.7
C(13)-C(14)	1.42(2)	C(5)-C(4)-H(4A)	120.7
C(14)-C(15)	1.318(19)	N(1)-C(5)-C(4)	123.3(12)
C(14)-H(14A)	0.9300	N(1)-C(5)-C(6)	113.3(11)
C(15)-H(15A)	0.9300	C(4)-C(5)-C(6)	123.1(11)
C(16)-C(21)	1.294(17)	N(2)-C(6)-C(7)	117.5(12)
C(16)-C(17)	1.396(16)	N(2)-C(6)-C(5)	116.8(9)
C(17)-C(18)	1.447(16)	C(7)-C(6)-C(5)	125.5(10)
C(17)-H(17A)	0.9300	C(6)-C(7)-C(8)	122.7(10)
C(18)-C(19)	1.308(18)	C(6)-C(7)-H(7A)	118.6
C(18)-H(18A)	0.9300	C(8)-C(7)-H(7A)	118.6
C(19)-C(20)	1.306(18)	C(9)-C(8)-C(7)	114.9(10)
C(19)-C(22)	1.539(17)	C(9)-C(8)-C(16)	121.2(13)
C(20)-C(21)	1.363(17)	C(7)-C(8)-C(16)	123.9(11)
C(20)-H(20A)	0.9300	C(8)-C(9)-C(10)	123.7(12)
C(21)-H(21A)	0.9300	C(8)-C(9)-H(9A)	118.1
		C(10)-C(9)-H(9A)	118.1
O(3)-Zn(1)-O(2)	92.0(5)	N(2)-C(10)-C(11)	112.6(9)
O(3)-Zn(1)-N(2)#1	102.5(4)	N(2)-C(10)-C(9)	116.3(9)
O(2)-Zn(1)-N(2)#1	163.5(5)	C(11)-C(10)-C(9)	130.9(11)
O(3)-Zn(1)-N(1)#1	98.2(4)	N(3)-C(11)-C(12)	120.9(12)
O(2)-Zn(1)-N(1)#1	108.9(4)	N(3)-C(11)-C(10)	118.9(11)
N(2)#1-Zn(1)-N(1)#1	77.2(4)	C(12)-C(11)-C(10)	120.1(11)
O(3)-Zn(1)-N(3)#1	94.5(2)	C(11)-C(12)-C(13)	124.1(13)
O(2)-Zn(1)-N(3)#1	97.7(4)	C(11)-C(12)-H(12A)	117.9
N(2)#1-Zn(1)-N(3)#1	73.5(4)	C(13)-C(12)-H(12A)	117.9
N(1)#1-Zn(1)-N(3)#1	150.0(3)	C(14)-C(13)-C(12)	110.3(16)
C(22)-O(2)-Zn(1)	114.0(9)	C(15)-C(14)-C(13)	123.1(13)
Zn(1)-O(3)-Zn(1)#2	156.2(6)	C(15)-C(14)-H(14A)	118.5
C(1)-N(1)-C(5)	117.3(11)	C(13)-C(14)-H(14A)	118.5
C(1)-N(1)-Zn(1)#5	126.1(9)	C(14)-C(15)-N(3)	122.1(13)

C(14)-C(15)-H(15A)	118.9	C(20)-C(19)-C(22)	123.6(13)
N(3)-C(15)-H(15A)	118.9	C(18)-C(19)-C(22)	116.1(13)
C(21)-C(16)-C(17)	118.6(10)	C(19)-C(20)-C(21)	122.3(14)
C(21)-C(16)-C(8)	124.8(12)	C(19)-C(20)-H(20A)	118.8
C(17)-C(16)-C(8)	116.3(12)	C(21)-C(20)-H(20A)	118.8
C(16)-C(17)-C(18)	117.7(13)	C(16)-C(21)-C(20)	121.4(12)
C(16)-C(17)-H(17A)	121.1	C(16)-C(21)-H(21A)	119.3
C(18)-C(17)-H(17A)	121.1	C(20)-C(21)-H(21A)	119.3
C(19)-C(18)-C(17)	119.3(12)	O(1)-C(22)-O(2)	121.9(12)
C(19)-C(18)-H(18A)	120.4	O(1)-C(22)-C(19)	122.0(16)
C(17)-C(18)-H(18A)	120.4	O(2)-C(22)-C(19)	115.9(13)
C(20)-C(19)-C(18)	120.3(12)		

Symmetry transformations used to generate equivalent atoms:
#1 -y-1/2,-x-1,z-1/4 #2 -x,-y-1,z #3 -x,y+1/2,-z-3/4
#4 -x,y-1/2,-z-3/4 #5 -y-1,-x-1/2,z+1/4

Table 41. Anisotropic displacement parameters for **5**[d]

	U^{11}	U^{22}	U^{33}	U^{23}	U^{13}	U^{12}
Zn(1)	72(1)	106(1)	32(1)	-12(1)	15(1)	-17(1)
O(1)	121(9)	270(15)	20(4)	-9(7)	4(5)	-6(9)
O(2)	134(10)	142(10)	59(6)	-2(5)	42(6)	11(7)
O(3)	81(9)	173(13)	55(6)	0	0	-56(11)
N(1)	68(7)	139(10)	31(4)	-7(6)	0(5)	-28(7)
N(2)	121(10)	68(7)	13(4)	-15(4)	-2(4)	-9(6)
N(3)	115(9)	55(6)	31(4)	-10(4)	-1(5)	-6(6)
C(1)	49(9)	126(13)	80(10)	-6(9)	8(8)	-36(8)
C(2)	75(11)	167(17)	106(13)	-49(12)	16(10)	-52(11)
C(3)	190(20)	135(17)	83(13)	-31(12)	-34(14)	23(17)
C(4)	80(10)	101(11)	45(7)	-7(8)	-16(7)	0(9)
C(5)	66(8)	93(10)	47(6)	-34(7)	15(6)	-18(7)
C(6)	84(9)	36(5)	47(5)	-5(4)	5(6)	3(7)
C(7)	55(8)	39(6)	43(5)	-13(4)	0(4)	-24(5)
C(8)	132(12)	20(5)	33(5)	-9(4)	-7(6)	13(7)
C(9)	94(10)	40(7)	63(7)	-12(6)	19(7)	-15(7)
C(10)	42(7)	68(8)	35(5)	-14(5)	6(5)	3(6)
C(11)	46(7)	63(8)	58(7)	-23(6)	0(6)	18(6)
C(12)	190(20)	58(9)	36(7)	4(6)	16(9)	17(10)
C(13)	172(16)	65(9)	54(8)	11(7)	-14(9)	10(9)
C(14)	85(11)	108(12)	55(8)	-10(7)	-29(8)	21(9)
C(15)	135(15)	82(10)	43(7)	-9(6)	-11(8)	13(9)
C(16)	110(11)	32(6)	35(5)	-2(4)	4(6)	-10(6)
C(17)	92(10)	97(11)	58(7)	-14(7)	10(7)	21(8)
C(18)	95(11)	125(12)	46(7)	16(7)	-6(7)	13(10)

C(19)	51(8)	84(9)	58(7)	-15(6)	-3(6)	22(6)
C(20)	82(11)	189(18)	53(8)	-28(9)	18(8)	4(11)
C(21)	60(9)	129(12)	41(6)	2(7)	-1(6)	1(8)
C(22)	131(14)	81(10)	38(7)	-9(6)	17(8)	-29(10)

Table 42. Crystal data and structure refinement for **6**

Identification code	Pb(**L**)(NO_3)·1.3(H_2O)1.3(DMF)	
Empirical formula	C_{352} H_{272} N_{64} O_{104} Pb_{16}	
Formula weight	10377.38	
Temperature	446(2) K	
Wavelength	0.71073 Å	
Crystal system	Tetragonal	
Space group	P4/ncc	
Unit cell dimensions	a = 25.7511(18) Å	α= 90°.
	b = 25.7511(18) Å	β= 90°.
	c = 17.0110(17) Å	γ = 90°.
Volume	11280.3(16) $Å^3$	
Z	1	
Density (calculated)	1.528 Mg/m^3	
Absorption coefficient	6.022 mm^{-1}	
F(000)	4976	
Theta range for data collection	1.58 to 28.35°.	
Index ranges	-34<=h<=34, -33<=k<=34, -22<=l<=22	
Reflections collected	110860	
Independent reflections	7066 [R(int) = 0.2348]	
Completeness to theta = 28.35°	100.0 %	
Refinement method	Full-matrix least-squares on F^2	
Data / restraints / parameters	7066 / 4 / 314	
Goodness-of-fit on F^2	1.031	
Final R indices [I>2sigma(I)]	R1 = 0.0653, wR2 = 0.1769	
R indices (all data)	R1 = 0.1466, wR2 = 0.2172	
Largest diff. peak and hole	1.816 and -0.702 e.$Å^{-3}$	

Table 43. Atomic coordinates[a] and equivalent isotropic displacement parameters[b] for **6**

	x	y	z	U(eq)[c]
Pb(1)	3699(1)	2883(1)	5289(1)	41(1)
O(1W)	3068(8)	2315(8)	4510(11)	59(5)
O(2W)	2706(15)	2380(20)	4502(11)	92(9)
O(3W)	3847(12)	6153(12)	7500	261(17)
O(1)	4268(3)	2276(3)	4700(5)	50(2)
O(2)	3845(3)	1832(3)	5607(5)	48(2)

O(4)	5820(20)	2193(18)	5610(30)	117(19)
O(5)	5667(16)	2618(17)	4660(20)	76(12)
O(6)	5336(16)	5057(15)	7940(20)	123(13)
O(7)	5631(10)	4369(10)	7500	68(10)
O(8)	4872(6)	5128(6)	7500	61(6)
O(9)	5672(7)	4886(7)	7672(11)	77(5)
O(10)	2909(8)	2644(9)	1392(14)	86(8)
O(11)	2500	2500	2474(14)	75(6)
N(1)	3806(4)	3304(4)	3942(7)	49(3)
N(2)	4491(4)	3462(3)	5124(6)	41(2)
N(3)	4390(4)	2834(4)	6365(7)	53(3)
N(4)	5920(15)	2586(16)	5250(20)	47(10)
N(5)	5252(5)	4748(5)	7500	59(4)
N(6)	2500	2500	1705(16)	55(6)
C(1)	3467(5)	3209(5)	3342(10)	60(4)
C(2)	3453(5)	3473(5)	2657(9)	56(4)
C(3)	3814(5)	3875(6)	2561(8)	52(3)
C(4)	4166(5)	3978(5)	3157(8)	47(3)
C(5)	4160(5)	3687(4)	3845(7)	39(3)
C(6)	4533(4)	3769(4)	4480(7)	35(3)
C(7)	4908(4)	4150(5)	4427(7)	41(3)
C(8)	5277(4)	4225(4)	5022(7)	35(3)
C(9)	5231(5)	3882(4)	5663(7)	45(3)
C(10)	4842(5)	3511(5)	5702(7)	42(3)
C(11)	4813(5)	3155(5)	6370(8)	52(3)
C(12)	5165(6)	3136(6)	6959(8)	65(4)
C(13)	5123(7)	2794(6)	7581(9)	78(5)
C(14)	4682(8)	2446(6)	7578(11)	85(5)
C(15)	4334(6)	2496(6)	6959(9)	65(4)
C(16)	4211(5)	1884(5)	5139(7)	41(3)
C(17)	4601(5)	1451(5)	5075(8)	44(3)
C(18)	4901(5)	1384(5)	4395(8)	48(3)
C(19)	5271(5)	1005(5)	4357(8)	49(3)
C(20)	5370(5)	680(5)	5014(8)	44(3)
C(21)	5061(5)	747(5)	5671(8)	49(3)
C(22)	4693(5)	1127(5)	5707(9)	52(3)
O(3)	6220(20)	2910(20)	5510(40)	140(20)

[a] x 10^4

[b] $Å^2$ x 10^3

[c] U(eq) is defined as one third of the trace of the orthogonalized U^{ij} tensor.

Table 44. Bond lengths (Å) and angles (°) for **6**

Pb(1)-O(1)	2.364(8)	Pb(1)-N(1)	2.551(11)
Pb(1)-N(2)	2.542(10)	Pb(1)-N(3)	2.556(12)

Pb(1)-O(1W)	2.56(2)	C(4)-H(4A)	0.9300
O(1W)-O(2W)	0.95(3)	C(5)-C(6)	1.460(16)
O(1W)-O(2W)#1	1.53(7)	C(6)-C(7)	1.380(16)
O(1W)-O(2W)#2	1.77(5)	C(7)-C(8)	1.403(17)
O(2W)-O(2W)#1	0.87(3)	C(7)-H(7A)	0.9300
O(2W)-O(2W)#2	0.87(3)	C(8)-C(9)	1.408(16)
O(2W)-O(2W)#3	1.23(4)	C(8)-C(20)#5	1.471(16)
O(2W)-O(1W)#2	1.53(7)	C(9)-C(10)	1.384(17)
O(2W)-O(1W)#1	1.77(5)	C(9)-H(9A)	0.9300
O(3W)-H(1W)	1.02(2)	C(10)-C(11)	1.463(17)
O(1)-C(16)	1.264(14)	C(11)-C(12)	1.352(18)
O(2)-C(16)	1.241(15)	C(12)-C(13)	1.382(19)
O(4)-N(4)	1.213(19)	C(12)-H(12A)	0.9300
O(5)-N(4)	1.205(19)	C(13)-C(14)	1.45(2)
O(6)-O(9)	1.07(4)	C(13)-H(13A)	0.9300
O(6)-N(5)	1.12(4)	C(14)-C(15)	1.39(2)
O(6)-O(8)	1.42(4)	C(14)-H(14A)	0.9300
O(7)-O(9)#4	1.37(3)	C(15)-H(15A)	0.9300
O(7)-O(9)	1.37(3)	C(16)-C(17)	1.505(16)
O(7)-N(5)	1.38(4)	C(17)-C(22)	1.380(19)
O(8)-N(5)	1.38(3)	C(17)-C(18)	1.401(17)
O(8)-O(6)#4	1.42(4)	C(18)-C(19)	1.366(17)
O(9)-N(5)	1.176(19)	C(18)-H(18A)	0.9300
O(10)-N(6)	1.24(2)	C(19)-C(20)	1.420(18)
O(10)-O(10)#1	1.58(3)	C(19)-H(19A)	0.9300
O(10)-O(10)#2	1.58(3)	C(20)-C(21)	1.382(17)
O(11)-N(6)	1.31(3)	C(20)-C(8)#6	1.471(16)
N(1)-C(5)	1.352(15)	C(21)-C(22)	1.364(17)
N(1)-C(1)	1.364(17)	C(21)-H(21A)	0.9300
N(2)-C(10)	1.341(16)	C(22)-H(22A)	0.9300
N(2)-C(6)	1.356(14)		
N(3)-C(15)	1.340(16)	O(1)-Pb(1)-N(2)	81.1(3)
N(3)-C(11)	1.369(17)	O(1)-Pb(1)-N(1)	80.5(3)
N(4)-O(3)	1.22(2)	N(2)-Pb(1)-N(1)	64.2(3)
N(5)-O(6)#4	1.11(4)	O(1)-Pb(1)-N(3)	80.8(3)
N(5)-O(9)#4	1.176(19)	N(2)-Pb(1)-N(3)	63.2(3)
N(6)-O(10)#3	1.24(2)	N(1)-Pb(1)-N(3)	126.2(3)
N(6)-O(10)#2	1.24(2)	O(1)-Pb(1)-O(1W)	78.3(5)
N(6)-O(10)#1	1.24(2)	N(2)-Pb(1)-O(1W)	142.1(5)
C(1)-C(2)	1.349(19)	N(1)-Pb(1)-O(1W)	81.1(5)
C(1)-H(1A)	0.9300	N(3)-Pb(1)-O(1W)	141.8(5)
C(2)-C(3)	1.400(19)	O(2W)-O(1W)-O(2W)#1	31(4)
C(2)-H(2A)	0.9300	O(2W)-O(1W)-O(2W)#2	12(5)
C(3)-C(4)	1.385(17)	O(2W)#1-O(1W)-O(2W)#2	42.9(14)
C(3)-H(3A)	0.9300	O(2W)-O(1W)-Pb(1)	122(4)
C(4)-C(5)	1.390(16)	O(2W)#1-O(1W)-Pb(1)	96.2(11)

O(2W)#2-O(1W)-Pb(1) 131.1(12)
O(2W)#1-O(2W)-O(2W)#2 90.002(6)
O(2W)#1-O(2W)-O(1W) 115(10)
O(2W)#2-O(2W)-O(1W) 155(10)
O(2W)#1-O(2W)-O(2W)#3 45.007(9)
O(2W)#2-O(2W)-O(2W)#3 44.995(9)
O(1W)-O(2W)-O(2W)#3 160(10)
O(2W)#1-O(2W)-O(1W)#2 124(6)
O(2W)#2-O(2W)-O(1W)#2 34(6)
O(1W)-O(2W)-O(1W)#2 121(4)
O(2W)#3-O(2W)-O(1W)#2 79(6)
O(2W)#1-O(2W)-O(1W)#1 13(5)
O(2W)#2-O(2W)-O(1W)#1 103(5)
O(1W)-O(2W)-O(1W)#1 102(5)
O(2W)#3-O(2W)-O(1W)#1 58(5)
O(1W)#2-O(2W)-O(1W)#1 137.0(14)
C(16)-O(1)-Pb(1) 101.9(7)
O(9)-O(6)-N(5) 65(3)
O(9)-O(6)-O(8) 120(4)
N(5)-O(6)-O(8) 65(3)
O(9)#4-O(7)-O(9) 101(3)
O(9)#4-O(7)-N(5) 50.7(14)
O(9)-O(7)-N(5) 50.7(14)
N(5)-O(8)-O(6) 46.9(18)
N(5)-O(8)-O(6)#4 46.9(17)
O(6)-O(8)-O(6)#4 94(3)
O(6)-O(9)-N(5) 59(2)
O(6)-O(9)-O(7) 115(3)
N(5)-O(9)-O(7) 65.3(18)
N(6)-O(10)-O(10)#1 50.3(6)
N(6)-O(10)-O(10)#2 50.3(6)
O(10)#1-O(10)-O(10)#2 90.002(2)
C(5)-N(1)-C(1) 118.2(12)
C(5)-N(1)-Pb(1) 119.4(8)
C(1)-N(1)-Pb(1) 121.7(9)
C(10)-N(2)-C(6) 118.9(10)
C(10)-N(2)-Pb(1) 121.1(8)
C(6)-N(2)-Pb(1) 119.6(8)
C(15)-N(3)-C(11) 118.3(13)
C(15)-N(3)-Pb(1) 119.8(10)
C(11)-N(3)-Pb(1) 121.9(8)
O(5)-N(4)-O(4) 112(5)
O(5)-N(4)-O(3) 127(5)
O(4)-N(4)-O(3) 121(5)
O(6)#4-N(5)-O(6) 137(5)
O(6)#4-N(5)-O(9) 152(2)
O(6)-N(5)-O(9) 56(2)
O(6)#4-N(5)-O(9)#4 56(2)
O(6)-N(5)-O(9)#4 152(2)
O(9)-N(5)-O(9)#4 128(3)
O(6)#4-N(5)-O(7) 112(2)
O(6)-N(5)-O(7) 112(2)
O(9)-N(5)-O(7) 64.0(13)
O(9)#4-N(5)-O(7) 64.0(13)
O(6)#4-N(5)-O(8) 68(2)
O(6)-N(5)-O(8) 68(2)
O(9)-N(5)-O(8) 115.9(13)
O(9)#4-N(5)-O(8) 116.0(13)
O(7)-N(5)-O(8) 179.998(6)
O(10)#3-N(6)-O(10) 129(3)
O(10)#3-N(6)-O(10)#2 79.3(13)
O(10)-N(6)-O(10)#2 79.3(13)
O(10)#3-N(6)-O(10)#1 79.3(13)
O(10)-N(6)-O(10)#1 79.3(13)
O(10)#2-N(6)-O(10)#1 129(3)
O(10)#3-N(6)-O(11) 115.5(16)
O(10)-N(6)-O(11) 115.5(16)
O(10)#2-N(6)-O(11) 115.5(16)
O(10)#1-N(6)-O(11) 115.5(16)
C(2)-C(1)-N(1) 124.8(13)
C(2)-C(1)-H(1A) 117.6
N(1)-C(1)-H(1A) 117.6
C(1)-C(2)-C(3) 117.2(13)
C(1)-C(2)-H(2A) 121.4
C(3)-C(2)-H(2A) 121.4
C(4)-C(3)-C(2) 119.3(13)
C(4)-C(3)-H(3A) 120.4
C(2)-C(3)-H(3A) 120.4
C(3)-C(4)-C(5) 120.4(12)
C(3)-C(4)-H(4A) 119.8
C(5)-C(4)-H(4A) 119.8
N(1)-C(5)-C(4) 120.1(12)
N(1)-C(5)-C(6) 117.4(11)
C(4)-C(5)-C(6) 122.5(11)
N(2)-C(6)-C(7) 121.5(11)
N(2)-C(6)-C(5) 117.4(10)
C(7)-C(6)-C(5) 121.0(11)
C(6)-C(7)-C(8) 121.7(11)
C(6)-C(7)-H(7A) 119.1
C(8)-C(7)-H(7A) 119.1
C(7)-C(8)-C(9) 114.5(11)
C(7)-C(8)-C(20)#5 123.0(11)

C(9)-C(8)-C(20)#5	122.5(11)	O(2)-C(16)-O(1)	123.5(11)
C(10)-C(9)-C(8)	122.1(12)	O(2)-C(16)-C(17)	118.4(12)
C(10)-C(9)-H(9A)	118.9	O(1)-C(16)-C(17)	118.1(12)
C(8)-C(9)-H(9A)	118.9	C(22)-C(17)-C(18)	118.4(11)
N(2)-C(10)-C(9)	121.2(11)	C(22)-C(17)-C(16)	120.3(12)
N(2)-C(10)-C(11)	118.4(11)	C(18)-C(17)-C(16)	121.2(12)
C(9)-C(10)-C(11)	120.5(12)	C(19)-C(18)-C(17)	120.7(13)
C(12)-C(11)-N(3)	121.0(12)	C(19)-C(18)-H(18A)	119.7
C(12)-C(11)-C(10)	124.4(13)	C(17)-C(18)-H(18A)	119.7
N(3)-C(11)-C(10)	114.6(12)	C(18)-C(19)-C(20)	120.6(12)
C(11)-C(12)-C(13)	122.6(14)	C(18)-C(19)-H(19A)	119.7
C(11)-C(12)-H(12A)	118.7	C(20)-C(19)-H(19A)	119.7
C(13)-C(12)-H(12A)	118.7	C(21)-C(20)-C(19)	117.3(11)
C(12)-C(13)-C(14)	117.0(15)	C(21)-C(20)-C(8)#6	122.0(12)
C(12)-C(13)-H(13A)	121.5	C(19)-C(20)-C(8)#6	120.6(11)
C(14)-C(13)-H(13A)	121.5	C(22)-C(21)-C(20)	121.8(13)
C(15)-C(14)-C(13)	116.9(14)	C(22)-C(21)-H(21A)	119.1
C(15)-C(14)-H(14A)	121.6	C(20)-C(21)-H(21A)	119.1
C(13)-C(14)-H(14A)	121.6	C(21)-C(22)-C(17)	121.1(13)
N(3)-C(15)-C(14)	124.2(14)	C(21)-C(22)-H(22A)	119.4
N(3)-C(15)-H(15A)	117.9	C(17)-C(22)-H(22A)	119.4
C(14)-C(15)-H(15A)	117.9		

Symmetry transformations used to generate equivalent atoms:
#1 -y+1/2,x,z #2 y,-x+1/2,z #3 -x+1/2,-y+1/2,z
#4 -y+1,-x+1,-z+3/2 #5 y+1/2,-x+1,-z+1 #6 -y+1,x-1/2,-z+1

Table 45. Anisotropic displacement parameters for **6**[d]

	U^{11}	U^{22}	U^{33}	U^{23}	U^{13}	U^{12}
Pb(1)	38(1)	28(1)	56(1)	1(1)	9(1)	0(1)
O(1)	55(5)	35(4)	60(6)	1(4)	11(5)	6(4)
O(2)	40(5)	45(5)	58(6)	-1(4)	8(4)	11(4)
O(10)	93(18)	76(14)	88(16)	-11(13)	38(13)	-40(14)
O(11)	81(10)	81(10)	63(14)	0	0	0
N(1)	44(6)	49(6)	55(7)	3(5)	-1(5)	-4(5)
N(2)	46(6)	27(5)	50(7)	-4(4)	11(5)	5(4)
N(3)	73(8)	34(5)	51(7)	2(5)	11(6)	-12(5)
N(6)	51(8)	51(8)	65(18)	0	0	0
C(1)	44(8)	55(8)	79(11)	6(8)	-5(8)	-4(7)
C(2)	51(8)	56(9)	62(10)	-11(8)	-5(7)	4(7)
C(3)	54(8)	65(9)	38(7)	-5(7)	5(6)	10(7)
C(4)	47(7)	43(7)	50(8)	1(6)	4(6)	2(6)
C(5)	45(7)	35(6)	37(7)	-8(5)	10(5)	11(5)
C(6)	36(6)	29(6)	39(7)	3(5)	3(5)	1(5)

C(7)	36(6)	41(7)	47(7)	10(6)	8(5)	3(5)
C(8)	33(6)	32(6)	41(7)	6(5)	6(5)	6(5)
C(9)	54(8)	36(6)	46(8)	8(6)	2(6)	-5(6)
C(10)	48(7)	42(7)	37(7)	0(6)	9(6)	2(6)
C(11)	67(9)	41(7)	46(8)	15(6)	9(7)	7(7)
C(12)	67(9)	72(10)	57(10)	21(8)	-2(8)	-22(8)
C(13)	100(14)	81(12)	53(10)	11(9)	-9(9)	-12(10)
C(14)	133(17)	48(9)	72(11)	17(8)	5(12)	-20(10)
C(15)	76(10)	54(8)	66(10)	15(8)	10(8)	-15(8)
C(16)	40(7)	38(7)	47(8)	-11(6)	-9(6)	6(5)
C(17)	36(6)	35(6)	61(9)	-24(6)	-3(6)	4(5)
C(18)	46(7)	40(7)	58(8)	-3(6)	9(6)	7(6)
C(19)	44(7)	44(7)	61(9)	-1(7)	15(7)	7(6)
C(20)	40(7)	41(7)	51(7)	-7(6)	-1(6)	1(5)
C(21)	59(8)	44(7)	44(8)	-1(6)	9(7)	8(6)
C(22)	52(8)	43(7)	61(9)	7(7)	9(7)	7(6)

Table 46. Hydrogen coordinates[a] and isotropic displacement parameters[b] for **6**

	x	y	z	U(eq)[c]
H(1W)	3710(30)	5801(15)	7670(50)	10(20)
H(1A)	3227	2943	3411	72
H(2A)	3215	3392	2266	68
H(3A)	3818	4071	2101	63
H(4A)	4408	4243	3096	56
H(7A)	4916	4363	3985	49
H(9A)	5468	3905	6073	54
H(12A)	5447	3361	6944	78
H(13A)	5367	2787	7984	94
H(14A)	4634	2200	7972	102
H(15A)	4044	2282	6957	78
H(18A)	4847	1600	3964	58
H(19A)	5460	960	3896	59
H(21A)	5106	527	6099	59
H(22A)	4500	1169	6165	62

Calculated X-ray Powder Diffraction Pattern and d-spacing, I/I_0, and *hkl* values for the prominent peaks of **6**

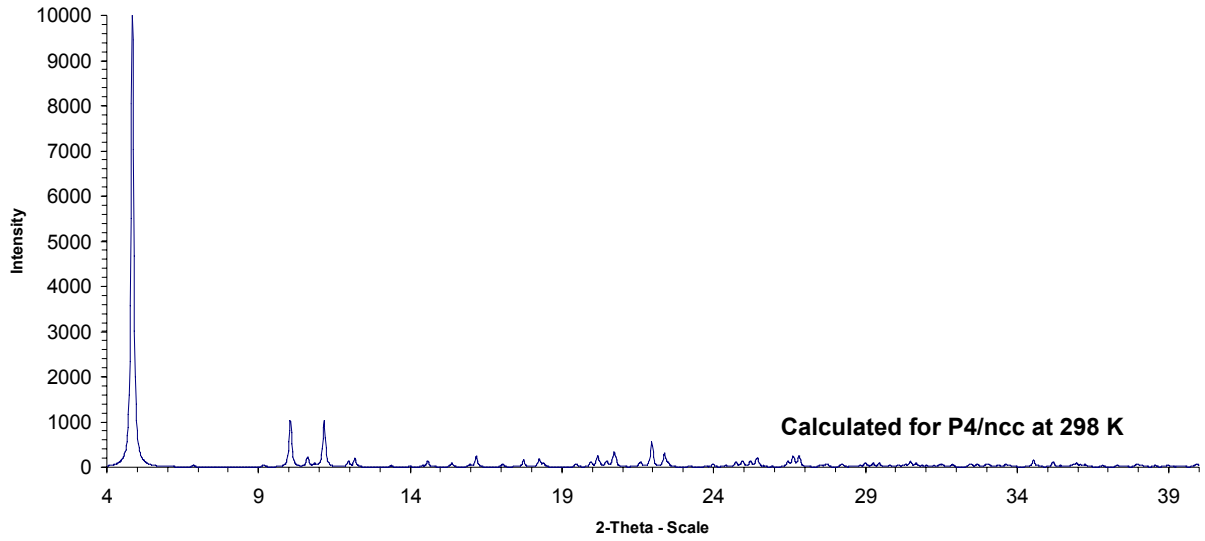

Figure 59. Calculated PXRD pattern for **6**

Single crystal X-ray data was measured at 173 K with tetragonal cell, a=25.7511, c=17.0110. The unit cell measured at room temperature is tetragonal, with a=25.7662, c=17.5922. The following chart contains the angles and intensities calculated for the structure obtained at 173 K. The following page contains a comparison chart for the angles and d spacing of the reflections calculated for the unit cell measured at room temperature and the unit cell measured at 173 K.

Table 47. Calculated PXRD peaks for **6**

Angle (2θ)°	d Spacing (Å)	Intensity(%)	hkl	2θ from original cell (°)	intensity from original cell (%)
4.846	18.21945	100	110	4.849	100.00
6.856	12.8831	0.39	200	6.860	0.16
10.048	8.7961	10.52	2	10.392	8.55
10.619	8.3244	2.17	102	10.946	1.88
11.161	7.92126	10.11	112	11.473	8.72
11.961	7.39348	1.29	311	12.040	1.16
12.174	7.26438	1.82	202	12.462	1.56
14.574	6.07315	1.36	330	14.582	1.30
16.175	5.47534	2.48	421	16.238	2.30
17.733	4.99767	1.59	332	17.939	1.47
18.252	4.85678	1.82	511	18.310	1.79
20.174	4.39805	2.28	4	20.871	1.97
20.709	4.28573	2.32	531	20.763	2.26
21.957	4.04474	5.42	442	22.130	5.36
22.382	3.96896	2.92	621	22.435	2.88

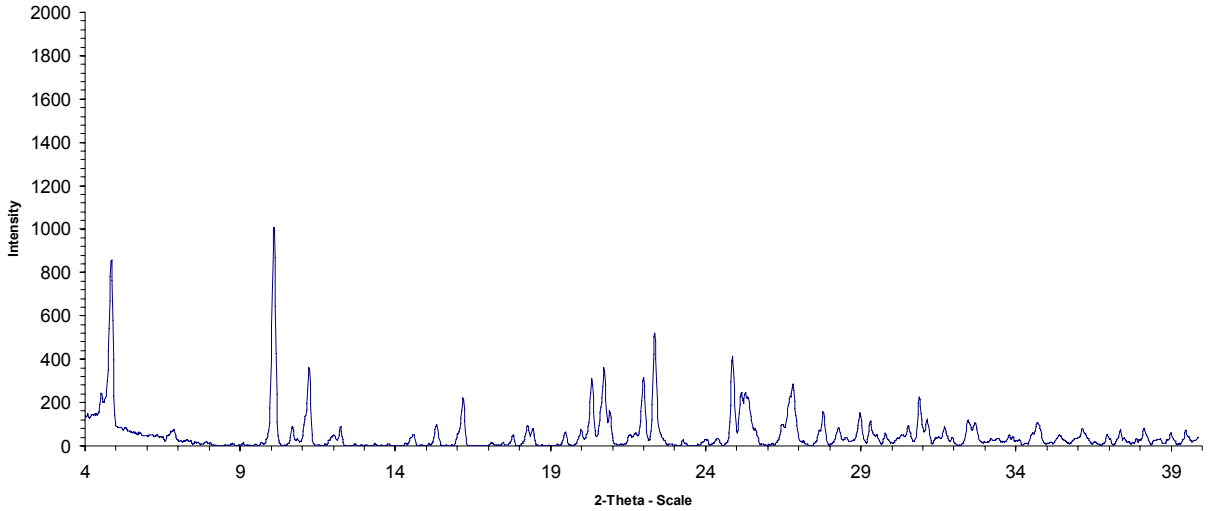

Figure 60. Experimental PXRD pattern of **6**

Single crystal X-ray data was measured at 173 K with tetragonal cell, a=25.7511, c=17.0110. The unit cell measured at room temperature is tetragonal, with a=25.7662, c=17.5922. The following chart contains the angles and intensities calculated for the structure obtained at 173 K with the unit cell parameters obtained at room temperature substituted for the original unit cell.

Table 48. Experimental PXRD peaks for **6**

Angle (2θ)°	d Spacing (Å)	Intensity (%)	*hkl*	calculated (2θ)°	difference (°)
4.86	18.094	85.09	110	4.846	0.034
6.86	12.875	7.74	200	6.856	0.004
10.08	8.768	10.52	002	10.048	0.032
10.68	8.277	100.00	102	10.619	0.061
11.22	7.880	35.94	112	11.161	0.059
12.02	7.357	4.92	311	11.961	0.059
12.24	7.225	8.77	202	12.174	0.066
14.58	6.071	5.13	330	14.574	0.006
16.18	5.474	22.06	421	16.175	0.005
17.80	4.979	4.99	332	17.733	0.067
18.26	4.855	9.26	511	18.252	0.008
20.34	4.363	30.81	004	20.174	0.166
20.72	4.283	36.07	531	20.709	0.011
22.00	4.037	31.11	442	21.957	0.043
22.36	3.973	51.63	621	22.382	-0.022

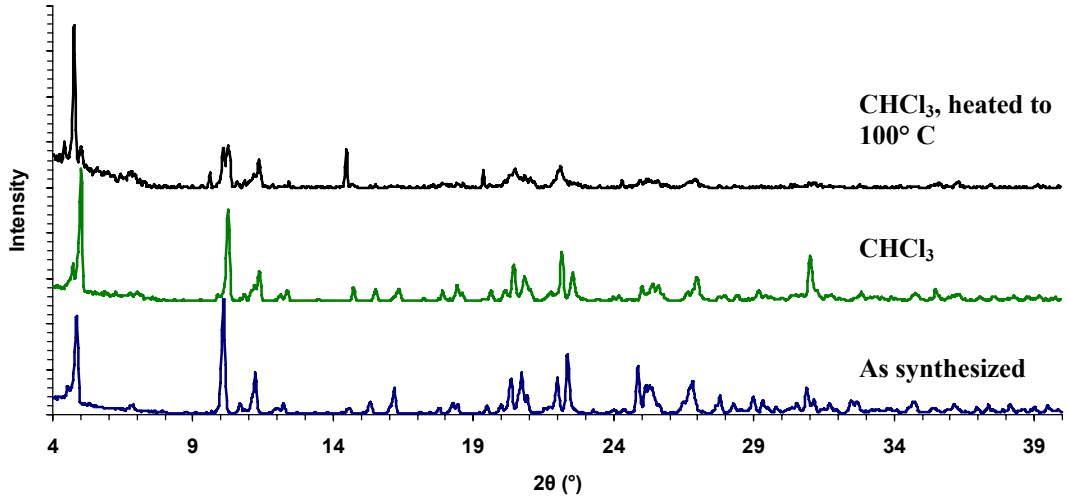

Figure 61. PXRD patterns of **6** after $CHCl_3$ exchange and heating to 100° C

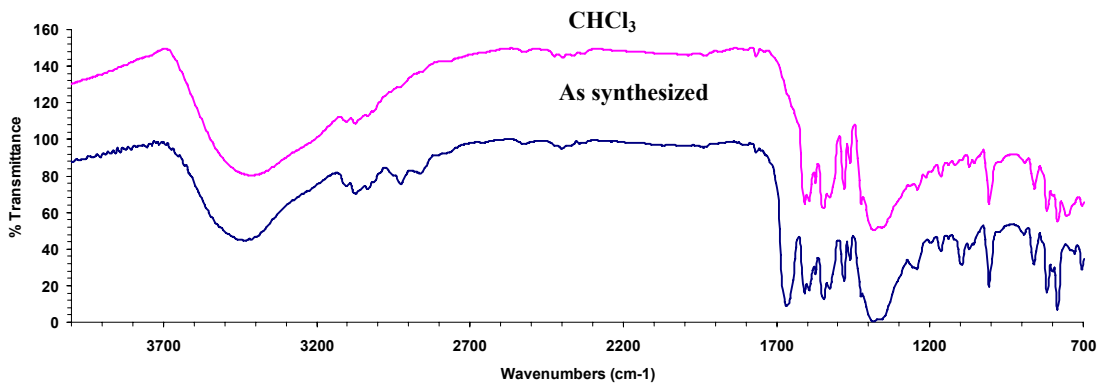

Figure 62. FT-IR spectra for as synthesized and chloroform exchanged samples of **6**
For as synthesized sample: FT-IR (KBr): 3434 (w), 3074 (w), 2925 (w, DMF), 1667 (s, DMF), 1609 (m), 1594 (m), 1547 (m), 1481 (m), 1385 (s), 1243 (m), 1096 (m), 1007 (m), 818 (m), 783 (s).

Table 49. Crystal data and structure refinement for **7**

Identification code	$Pb(L)(BF_4)$	
Empirical formula	$C_{17.60}H_{10.40}N_{2.40}O_{7.20}Pb_{0.80}$	
Formula weight	536.44	
Temperature	446(2) K	
Wavelength	0.71073 Å	
Crystal system	Tetragonal	
Space group	P4/n	
Unit cell dimensions	a = 25.7765(18) Å	α= 90°.
	b = 25.7765(18) Å	β= 90°.
	c = 8.3638(8) Å	γ = 90°.
Volume	5557.1(8) $Å^3$	
Z	10	
Density (calculated)	1.603 Mg/m^3	
Absorption coefficient	6.120 mm^{-1}	
F(000)	2560	
Theta range for data collection	1.58 to 28.36°.	
Index ranges	-34<=h<=34, -34<=k<=34, -11<=l<=11	
Reflections collected	43166	
Independent reflections	6347 [R(int) = 0.1563]	
Completeness to theta = 28.36°	91.3 %	
Refinement method	Full-matrix least-squares on F^2	
Data / restraints / parameters	6347 / 0 / 282	
Goodness-of-fit on F^2	0.922	
Final R indices [I>2sigma(I)]	R1 = 0.0574, wR2 = 0.1406	
R indices (all data)	R1 = 0.1186, wR2 = 0.1624	
Largest diff. peak and hole	1.719 and -1.038 $e.Å^{-3}$	

Table 50. Atomic coordinates[a] and equivalent isotropic displacement parameters[b] for **7**

	x	y	z	U(eq)[c]
Pb(1)	1267(1)	2088(1)	-8612(1)	44(1)
O(1)	663(3)	2651(3)	-9813(9)	52(2)
O(2)	1046(3)	3137(3)	-7991(10)	57(2)
O(2W)	4969(6)	5438(6)	-5270(20)	158(5)
O(3W)	2126(6)	2619(8)	-10000(19)	170(7)
O(4W)	5000	5000	-5000	185(10)
O(5W)	2500	2500	-5760(30)	112(7)
O(6W)	2500	2500	-4260(20)	52(4)
N(1)	1227(3)	1722(3)	-11417(10)	44(2)
N(2)	515(3)	1475(3)	-9090(11)	41(2)
N(3)	560(4)	2037(3)	-6434(11)	50(2)

C(1)	1580(4)	1839(4)	-12552(15)	54(3)
C(2)	1645(4)	1568(4)	-13940(14)	50(3)
C(3)	1330(4)	1152(4)	-14221(15)	52(3)
C(4)	955(4)	1023(4)	-13090(13)	50(3)
C(5)	908(4)	1322(4)	-11727(12)	40(2)
C(6)	482(4)	1228(3)	-10495(13)	44(2)
C(7)	72(4)	892(4)	-10854(13)	45(2)
C(8)	-303(4)	786(4)	-9725(13)	46(2)
C(9)	-246(5)	1043(4)	-8281(13)	51(3)
C(10)	153(4)	1394(4)	-7996(13)	46(2)
C(11)	201(4)	1684(4)	-6524(13)	46(2)
C(12)	-170(5)	1621(5)	-5261(14)	67(3)
C(13)	-86(6)	1917(5)	-3906(15)	75(4)
C(14)	311(6)	2269(5)	-3860(16)	72(4)
C(15)	618(6)	2317(5)	-5105(15)	68(3)
C(16)	-721(4)	402(4)	-10087(13)	47(3)
C(17)	-1151(5)	374(6)	-9080(16)	79(4)
C(18)	-1534(5)	6(5)	-9382(16)	79(4)
C(19)	-1509(4)	-331(3)	-10610(12)	40(2)
C(20)	-1080(5)	-309(5)	-11600(13)	55(3)
C(21)	-692(4)	70(5)	-11302(13)	56(3)
C(22)	699(4)	3075(4)	-9009(13)	45(3)
O(8W)	2013(9)	2614(11)	-6490(20)	217(9)
O(7W)	5456(10)	4931(10)	-5610(30)	237(10)
O(9W)	-874(18)	2707(17)	-7830(50)	420(20)
O(10W)	-1313(14)	3583(14)	-7470(50)	334(15)

[a] x 10^4
[b] $Å^2$ x 10^3
[c] U(eq) is defined as one third of the trace of the orthogonalized U^{ij} tensor.

Table 51. Bond lengths (Å) and angles (°) for **7**

Pb(1)-O(1)	2.353(7)	O(5W)-O(8W)#2	1.43(2)
Pb(1)-O(3W)	2.849(18)	O(5W)-O(8W)	1.43(2)
Pb(1)-N(2)	2.534(8)	O(5W)-O(8W)#3	1.43(2)
Pb(1)-N(1)	2.532(8)	O(5W)-O(8W)#4	1.43(2)
Pb(1)-N(3)	2.581(10)	N(1)-C(5)	1.342(12)
O(1)-C(22)	1.286(12)	N(1)-C(1)	1.349(14)
O(2)-C(22)	1.244(12)	N(2)-C(10)	1.323(14)
O(2W)-O(4W)	1.155(17)	N(2)-C(6)	1.339(12)
O(2W)-O(7W)#1	1.63(3)	N(3)-C(11)	1.298(13)
O(4W)-O(2W)#1	1.155(17)	N(3)-C(15)	1.335(13)
O(4W)-O(7W)#1	1.29(3)	C(1)-C(2)	1.364(15)
O(4W)-O(7W)	1.29(3)	C(2)-C(3)	1.365(14)
O(5W)-O(6W)	1.25(3)	C(3)-C(4)	1.392(16)

C(4)-C(5)	1.381(13)
C(5)-C(6)	1.527(15)
C(6)-C(7)	1.400(13)
C(7)-C(8)	1.378(14)
C(8)-C(9)	1.385(13)
C(8)-C(16)	1.494(13)
C(9)-C(10)	1.391(15)
C(10)-C(11)	1.446(14)
C(11)-C(12)	1.435(18)
C(12)-C(13)	1.382(16)
C(13)-C(14)	1.37(2)
C(14)-C(15)	1.313(19)
C(16)-C(21)	1.332(14)
C(16)-C(17)	1.394(15)
C(17)-C(18)	1.391(16)
C(18)-C(19)	1.348(15)
C(19)-C(20)	1.382(15)
C(19)-C(22)#5	1.468(13)
C(20)-C(21)	1.420(16)
C(22)-C(19)#6	1.468(13)
O(8W)-O(8W)#2	1.82(3)
O(8W)-O(8W)#3	1.82(3)
O(7W)-O(2W)#1	1.63(3)

O(1)-Pb(1)-O(3W)	92.5(4)
O(1)-Pb(1)-N(2)	79.1(3)
O(3W)-Pb(1)-N(2)	146.1(4)
O(1)-Pb(1)-N(1)	78.9(3)
O(3W)-Pb(1)-N(1)	80.4(4)
N(2)-Pb(1)-N(1)	65.8(3)
O(1)-Pb(1)-N(3)	82.3(3)
O(3W)-Pb(1)-N(3)	149.5(4)
N(2)-Pb(1)-N(3)	62.5(3)
N(1)-Pb(1)-N(3)	127.3(3)
C(22)-O(1)-Pb(1)	104.6(6)
O(4W)-O(2W)-O(7W)#1	52.1(11)
O(2W)#1-O(4W)-O(2W)	179.996(2)
O(2W)#1-O(4W)-O(7W)#	196.8(12)
O(2W)-O(4W)-O(7W)#1	83.2(12)
O(2W)#1-O(4W)-O(7W)	83.2(12)
O(2W)-O(4W)-O(7W)	96.8(12)
O(7W)#1-O(4W)-O(7W)	180(2)
O(6W)-O(5W)-O(8W)#2	115.4(14)
O(6W)-O(5W)-O(8W)	115.4(14)
O(8W)#2-O(5W)-O(8W)	79.4(11)
O(6W)-O(5W)-O(8W)#3	115.4(14)
O(8W)#2-O(5W)-O(8W)#	3129(3)
O(8W)-O(5W)-O(8W)#3	79.4(11)
O(6W)-O(5W)-O(8W)#4	115.4(14)
O(8W)#2-O(5W)-O(8W)#	479.4(11)
O(8W)-O(5W)-O(8W)#4	129(3)
O(8W)#3-O(5W)-O(8W)#	479.4(11)
C(5)-N(1)-C(1)	116.7(9)
C(5)-N(1)-Pb(1)	119.4(7)
C(1)-N(1)-Pb(1)	122.7(7)
C(10)-N(2)-C(6)	119.1(9)
C(10)-N(2)-Pb(1)	121.9(7)
C(6)-N(2)-Pb(1)	119.0(7)
C(11)-N(3)-C(15)	120.5(11)
C(11)-N(3)-Pb(1)	119.9(7)
C(15)-N(3)-Pb(1)	118.7(8)
N(1)-C(1)-C(2)	124.5(10)
C(1)-C(2)-C(3)	118.4(11)
C(2)-C(3)-C(4)	118.9(10)
C(5)-C(4)-C(3)	119.2(10)
N(1)-C(5)-C(4)	122.2(10)
N(1)-C(5)-C(6)	115.6(8)
C(4)-C(5)-C(6)	122.1(9)
N(2)-C(6)-C(7)	122.1(10)
N(2)-C(6)-C(5)	118.1(8)
C(7)-C(6)-C(5)	119.8(9)
C(8)-C(7)-C(6)	120.3(10)
C(7)-C(8)-C(9)	115.5(9)
C(7)-C(8)-C(16)	119.8(9)
C(9)-C(8)-C(16)	124.7(10)
C(10)-C(9)-C(8)	122.6(11)
N(2)-C(10)-C(9)	120.4(9)
N(2)-C(10)-C(11)	116.5(10)
C(9)-C(10)-C(11)	123.1(11)
N(3)-C(11)-C(12)	120.7(10)
N(3)-C(11)-C(10)	118.2(10)
C(12)-C(11)-C(10)	120.8(10)
C(13)-C(12)-C(11)	115.9(13)
C(12)-C(13)-C(14)	120.4(14)
C(15)-C(14)-C(13)	119.4(11)
C(14)-C(15)-N(3)	122.7(13)
C(21)-C(16)-C(17)	118.2(10)
C(21)-C(16)-C(8)	122.7(9)
C(17)-C(16)-C(8)	119.1(9)
C(18)-C(17)-C(16)	119.4(11)
C(19)-C(18)-C(17)	122.9(11)
C(18)-C(19)-C(20)	117.9(10)

C(18)-C(19)-C(22)#5	123.2(10)	O(1)-C(22)-C(19)#6	117.4(9)
C(20)-C(19)-C(22)#5	118.8(10)	O(5W)-O(8W)-O(8W)#2	50.3(6)
C(21)-C(20)-C(19)	119.1(10)	O(5W)-O(8W)-O(8W)#3	50.3(6)
C(16)-C(21)-C(20)	122.5(10)	O(8W)#2-O(8W)-O(8W)#3	89.997(4)
O(2)-C(22)-O(1)	121.3(9)	O(4W)-O(7W)-O(2W)#1	44.7(10)
O(2)-C(22)-C(19)#6	121.2(9)		

Symmetry transformations used to generate equivalent atoms:
#1 -x+1,-y+1,-z-1 #2 y,-x+1/2,z #3 -y+1/2,x,z
#4 -x+1/2,-y+1/2,z #5 y-1/2,-x,-z-2 #6 -y,x+1/2,-z-2

Table 52. Anisotropic displacement parameters for **7**[d]

	U^{11}	U^{22}	U^{33}	U^{23}	U^{13}	U^{12}
Pb(1)	39(1)	36(1)	56(1)	-20(1)	-14(1)	5(1)
O(1)	63(5)	48(4)	44(4)	-11(3)	-13(4)	11(3)
O(2)	49(4)	64(5)	57(5)	-20(4)	-22(4)	19(4)
N(1)	43(5)	40(5)	49(5)	-13(4)	-5(4)	-8(4)
N(2)	41(4)	37(4)	47(5)	-8(4)	-3(4)	-4(4)
N(3)	60(6)	44(5)	47(6)	-13(4)	-10(4)	-2(4)
C(1)	48(6)	44(6)	71(8)	-14(6)	-6(6)	-5(5)
C(2)	37(5)	47(6)	65(8)	-16(5)	2(5)	4(5)
C(3)	48(6)	52(6)	56(7)	-23(5)	7(5)	1(5)
C(4)	46(6)	52(6)	50(7)	-19(5)	-7(5)	-8(5)
C(5)	34(5)	36(5)	49(7)	-11(4)	-9(4)	2(4)
C(6)	58(6)	28(5)	47(7)	-7(4)	-15(5)	-1(4)
C(7)	55(6)	42(6)	38(6)	-11(5)	-2(5)	-9(5)
C(8)	53(6)	37(5)	47(7)	-16(5)	3(5)	-5(4)
C(9)	57(7)	56(7)	41(7)	-18(5)	2(5)	-10(5)
C(10)	55(6)	38(5)	46(6)	-13(5)	-7(5)	7(5)
C(11)	53(6)	47(6)	38(6)	-4(4)	-17(5)	-2(5)
C(12)	96(10)	72(8)	33(7)	-16(6)	-13(7)	20(7)
C(13)	118(12)	61(8)	46(8)	-18(6)	2(7)	16(8)
C(14)	110(11)	51(7)	54(9)	-28(6)	-41(8)	24(7)
C(15)	98(10)	61(8)	43(8)	-27(6)	-11(7)	-5(7)
C(16)	57(7)	47(6)	37(6)	-9(5)	6(5)	-13(5)
C(17)	75(9)	102(11)	58(8)	-47(8)	28(7)	-41(8)
C(18)	99(10)	82(9)	54(8)	-40(7)	37(7)	-47(8)
C(19)	43(5)	32(5)	43(6)	6(4)	10(4)	-8(4)
C(20)	65(7)	54(7)	47(7)	-10(5)	-1(5)	4(6)
C(21)	39(6)	76(8)	51(7)	-21(6)	4(5)	-21(5)
C(22)	54(6)	44(6)	38(6)	-12(5)	-6(5)	16(5)

Table 53. Hydrogen coordinates[a] and isotropic displacement parameters[b] for **7**

	x	y	z	U(eq)[c]
H(1A)	1794	2124	-12377	65
H(2A)	1897	1665	-14676	60
H(3A)	1365	959	-15152	62
H(4A)	739	739	-13250	59
H(7A)	52	738	-11859	54
H(9A)	-485	978	-7471	62
H(13A)	-301	1876	-3021	90
H(14A)	364	2472	-2956	86
H(15A)	887	2557	-5058	81
H(17A)	-1182	599	-8216	94
H(18A)	-1820	-7	-8706	94
H(20A)	-1046	-539	-12450	66
H(21A)	-407	87	-11982	67

Table 54. Crystal data and structure refinement for **8**

Identification code	$Pb_2(\mathbf{L})_2(NO_3)Cl$	
Empirical formula	$C_{14.67}\,C_{l0.33}\,N_{2.33}\,O_{5.33}\,Pb_{0.67}$	
Formula weight	444.11	
Temperature	173(2) K	
Wavelength	0.71073 Å	
Crystal system	Tetragonal	
Space group	P-4	
Unit cell dimensions	a = 17.9555(5) Å	α= 90°.
	b = 17.9555(5) Å	β= 90°.
	c = 9.0390(5) Å	γ = 90°.
Volume	2914.2(2) $Å^3$	
Z	6	
Density (calculated)	1.518 Mg/m^3	
Absorption coefficient	5.878 mm^{-1}	
F(000)	1244	
Theta range for data collection	1.60 to 28.32°.	
Index ranges	-23<=h<=23, -23<=k<=23, -11<=l<=12	
Reflections collected	30167	
Independent reflections	7206 [R(int) = 0.0509]	
Completeness to theta = 28.32°	99.9 %	
Refinement method	Full-matrix least-squares on F^2	
Data / restraints / parameters	7206 / 4 / 93	
Goodness-of-fit on F^2	2.778	
Final R indices [I>2sigma(I)]	R1 = 0.1217, wR2 = 0.3605	
R indices (all data)	R1 = 0.1293, wR2 = 0.3653	
Absolute structure parameter	0.00	
Largest diff. peak and hole	10.274 and -8.340 $e.Å^{-3}$	

Table 55. Atomic coordinates[a] and equivalent isotropic displacement parameters[b] for **8**

	x	y	z	U(eq)[c]
Pb(1)	4179(1)	6458(1)	19976(1)	24(1)
N(2)	3919(8)	7838(6)	19699(15)	44(5)
C(6)	4167(9)	8197(7)	18429(13)	34(5)
C(7)	4188(9)	8970(7)	18377(12)	27(4)
C(8)	3961(9)	9385(6)	19595(15)	39(6)
C(9)	3713(9)	9026(7)	20865(13)	26(4)
C(10)	3692(8)	8252(7)	20917(12)	24(4)
N(3)	3573(9)	7086(8)	22196(16)	40(5)
C(15)	3305(12)	6655(7)	23360(20)	100(15)
C(14)	2974(13)	6995(10)	24573(18)	56(8)
C(13)	2912(11)	7766(11)	24627(16)	63(9)

C(12)	3180(11)	8197(7)	23466(19)	42(6)
C(11)	3511(9)	7857(8)	22251(16)	28(4)
C(3)	4862(11)	7604(9)	14807(14)	64(8)
C(2)	4877(10)	6840(8)	15053(16)	42(5)
C(1)	4686(9)	6557(6)	16433(18)	47(7)
N(1)	4480(8)	7038(8)	17567(13)	29(4)
C(5)	4465(9)	7802(7)	17320(15)	38(5)
C(4)	4656(11)	8085(6)	15940(18)	47(6)
C(16)	3958(10)	10218(6)	19608(16)	37(6)
C(21)	3756(9)	10614(7)	18349(13)	26(4)
C(20)	3761(10)	11388(7)	18367(12)	32(5)
C(19)	3969(12)	11766(6)	19644(14)	62(9)
C(18)	4172(13)	11371(8)	20902(13)	65(9)
C(17)	4167(12)	10596(8)	20884(14)	46(7)
Cl(1)	5000	5000	18640(15)	77(3)
O(3)	5140(10)	5875(10)	19615(18)	42(4)
C(22)	4034(12)	12592(7)	19639(18)	26(4)
O(2)	3569(11)	12923(11)	18850(20)	46(4)
O(1)	4431(10)	12938(10)	20449(19)	41(4)
N(4)	5000	10000	14390(30)	42(7)
O(4)	5000	10000	16210(180)	340(60)
O(5)	5000	5000	17530(100)	200(30)
O(6)	1827(18)	8382(18)	10000(60)	115(9)
O(7)	2304(16)	9616(17)	9630(40)	88(9)
O(8)	3130(30)	7240(30)	18280(60)	167(19)
O(9)	4630(20)	9430(30)	14060(50)	138(14)

[a] x 10^4
[b] $Å^2$ x 10^3
[c] U(eq) is defined as one third of the trace of the orthogonalized U^{ij} tensor.

Table 56. Bond lengths (Å) and angles (°) for **8**

Pb(1)-O(3)	2.044(18)	C(8)-C(9)	1.3900
Pb(1)-O(3)#1	2.397(19)	C(8)-C(16)	1.497(14)
Pb(1)-N(1)	2.474(11)	C(9)-C(10)	1.3900
Pb(1)-O(2)#2	2.50(2)	C(10)-C(11)	1.436(15)
Pb(1)-N(2)	2.534(10)	N(3)-C(15)	1.3900
Pb(1)-N(3)	2.547(13)	N(3)-C(11)	1.3900
Pb(1)-O(8)	2.80(5)	C(15)-C(14)	1.3900
Pb(1)-O(1)#3	2.755(18)	C(14)-C(13)	1.3900
N(2)-C(6)	1.3900	C(13)-C(12)	1.3900
N(2)-C(10)	1.3900	C(12)-C(11)	1.3900
C(6)-C(5)	1.340(15)	C(3)-C(2)	1.3900
C(6)-C(7)	1.3900	C(3)-C(4)	1.3900
C(7)-C(8)	1.3900	C(2)-C(1)	1.3900

C(1)-N(1)	1.3900
N(1)-C(5)	1.3900
C(5)-C(4)	1.3900
C(16)-C(21)	1.3900
C(16)-C(17)	1.3900
C(21)-C(20)	1.3900
C(20)-C(19)	1.3900
C(19)-C(18)	1.3900
C(19)-C(22)	1.487(7)
C(18)-C(17)	1.3900
Cl(1)-O(5)	1.01(9)
Cl(1)-O(3)	1.82(2)
Cl(1)-O(3)#4	1.82(2)
Cl(1)-Cl(1)#5	2.46(3)
O(3)-Pb(1)#5	2.397(19)
C(22)-O(1)	1.20(2)
C(22)-O(2)	1.25(3)
O(2)-Pb(1)#6	2.50(2)
O(1)-Pb(1)#3	2.754(18)
N(4)-O(9)#3	1.25(4)
N(4)-O(9)	1.25(4)
N(4)-O(4)	1.65(16)

O(3)-Pb(1)-O(3)#1	63.5(10)
O(3)-Pb(1)-N(1)	83.7(6)
O(3)#1-Pb(1)-N(1)	124.1(5)
O(3)-Pb(1)-O(2)#2	145.2(7)
O(3)#1-Pb(1)-O(2)#2	83.0(6)
N(1)-Pb(1)-O(2)#2	125.5(6)
O(3)-Pb(1)-N(2)	129.9(6)
O(3)#1-Pb(1)-N(2)	166.7(6)
N(1)-Pb(1)-N(2)	62.7(5)
O(2)#2-Pb(1)-N(2)	83.9(6)
O(3)-Pb(1)-N(3)	135.5(6)
O(3)#1-Pb(1)-N(3)	107.4(6)
N(1)-Pb(1)-N(3)	126.9(5)
O(2)#2-Pb(1)-N(3)	44.4(6)
N(2)-Pb(1)-N(3)	64.3(5)
O(3)-Pb(1)-O(8)	137.4(12)
O(3)#1-Pb(1)-O(8)	123.6(12)
N(1)-Pb(1)-O(8)	56.9(12)
O(2)#2-Pb(1)-O(8)	68.7(13)
N(2)-Pb(1)-O(8)	48.0(12)
N(3)-Pb(1)-O(8)	85.4(13)
O(3)-Pb(1)-O(1)#3	57.4(6)
O(3)#1-Pb(1)-O(1)#3	113.7(6)
N(1)-Pb(1)-O(1)#3	76.9(5)
O(2)#2-Pb(1)-O(1)#3	139.5(6)
N(2)-Pb(1)-O(1)#3	78.3(5)
N(3)-Pb(1)-O(1)#3	95.2(5)
O(8)-Pb(1)-O(1)#3	119.6(12)
C(6)-N(2)-C(10)	120.0
C(6)-N(2)-Pb(1)	118.4(6)
C(10)-N(2)-Pb(1)	119.9(6)
C(5)-C(6)-C(7)	119.5(11)
C(5)-C(6)-N(2)	120.0(11)
C(7)-C(6)-N(2)	120.0
C(8)-C(7)-C(6)	120.0
C(9)-C(8)-C(7)	120.0
C(9)-C(8)-C(16)	117.2(10)
C(7)-C(8)-C(16)	122.8(10)
C(8)-C(9)-C(10)	120.0
C(9)-C(10)-N(2)	120.0
C(9)-C(10)-C(11)	121.9(10)
N(2)-C(10)-C(11)	117.8(11)
C(15)-N(3)-C(11)	120.0
C(15)-N(3)-Pb(1)	119.8(8)
C(11)-N(3)-Pb(1)	120.2(8)
N(3)-C(15)-C(14)	120.0
C(15)-C(14)-C(13)	120.0
C(12)-C(13)-C(14)	120.0
C(11)-C(12)-C(13)	120.0
C(12)-C(11)-N(3)	120.0
C(12)-C(11)-C(10)	122.9(12)
N(3)-C(11)-C(10)	116.4(12)
C(2)-C(3)-C(4)	120.0
C(1)-C(2)-C(3)	120.0
C(2)-C(1)-N(1)	120.0
C(5)-N(1)-C(1)	120.0
C(5)-N(1)-Pb(1)	123.5(7)
C(1)-N(1)-Pb(1)	116.4(7)
C(6)-C(5)-N(1)	114.2(11)
C(6)-C(5)-C(4)	125.2(12)
N(1)-C(5)-C(4)	120.0
C(5)-C(4)-C(3)	120.0
C(21)-C(16)-C(17)	120.0
C(21)-C(16)-C(8)	120.4(10)
C(17)-C(16)-C(8)	119.6(10)
C(20)-C(21)-C(16)	120.0
C(19)-C(20)-C(21)	120.0
C(20)-C(19)-C(18)	120.0
C(20)-C(19)-C(22)	120.4(5)

C(18)-C(19)-C(22)	119.4(5)	Cl(1)-O(3)-Pb(1)#5	100.1(8)
C(19)-C(18)-C(17)	120.0	Pb(1)-O(3)-Pb(1)#5	146.0(9)
C(18)-C(17)-C(16)	120.0	O(1)-C(22)-O(2)	120.1(15)
O(5)-Cl(1)-O(3)	119.0(7)	O(1)-C(22)-C(19)	124.3(14)
O(5)-Cl(1)-O(3)#4	119.0(7)	O(2)-C(22)-C(19)	115.0(15)
O(3)-Cl(1)-O(3)#4	122.0(13)	C(22)-O(2)-Pb(1)#6	101.4(12)
O(5)-Cl(1)-Cl(1)#5	180.00(5)	C(22)-O(1)-Pb(1)#3	130.5(15)
O(3)-Cl(1)-Cl(1)#5	61.0(7)	O(9)#3-N(4)-O(9)	152(5)
O(3)#4-Cl(1)-Cl(1)#5	61.0(7)	O(9)#3-N(4)-O(4)	104(3)
Cl(1)-O(3)-Pb(1)	113.8(9)	O(9)-N(4)-O(4)	104(3)

Symmetry transformations used to generate equivalent atoms:
#1 -y+1,x,-z+4 #2 y-1,-x+1,-z+4 #3 -x+1,-y+2,z
#4 -x+1,-y+1,z #5 y,-x+1,-z+4 #6 -y+1,x+1,-z+4

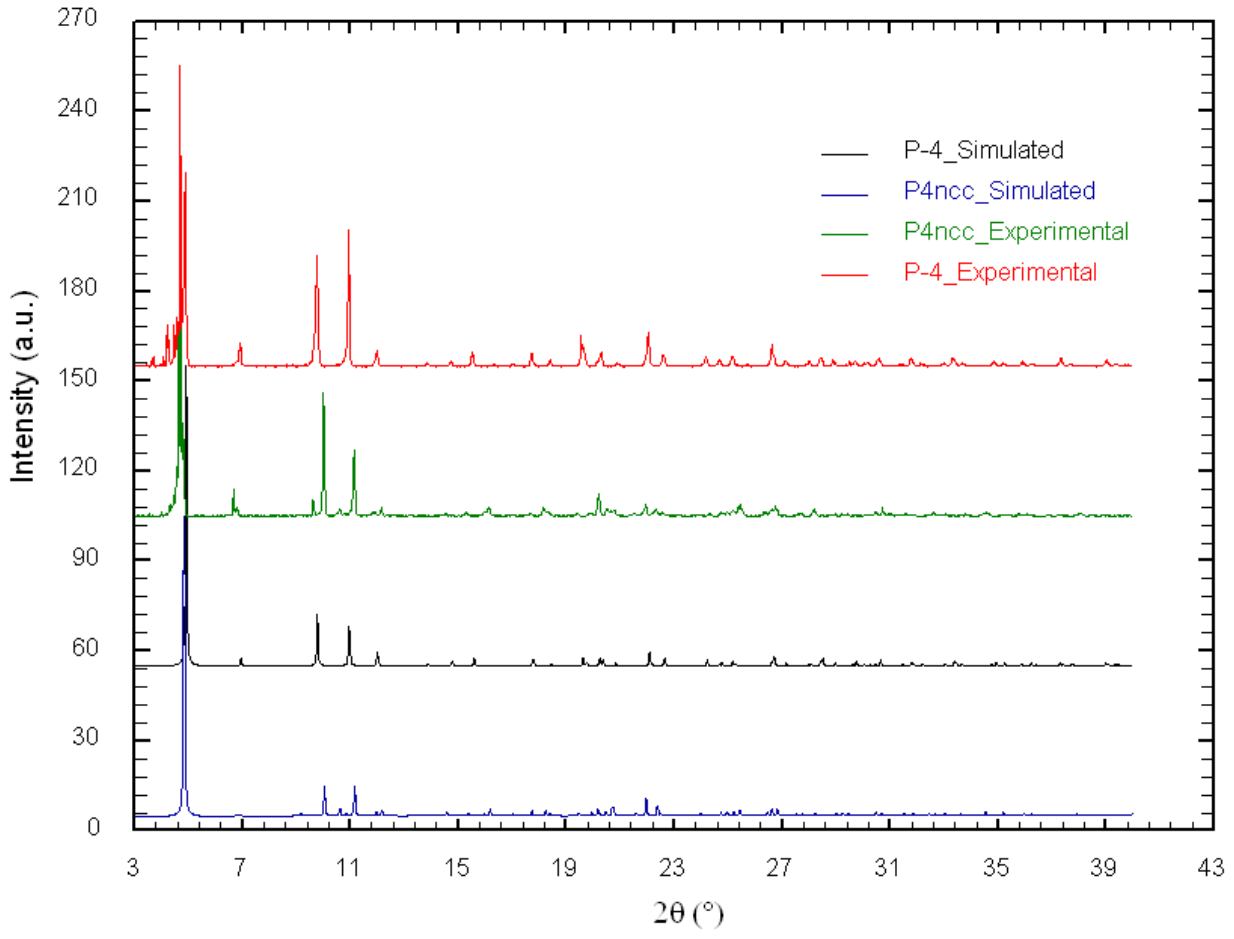

Figure 63. PXRD patterns for simulated and experimental **8** ("P-4") compared with simulated and experimental PXRD patterns for **6** ("P4ncc")

Table 57. Crystal data and structure refinement for **9**

Identification code	$Gd(\mathbf{L})_3$	
Empirical formula	$C_{264}\,H_{168}\,Gd_4\,N_{36}\,O_{24}$	
Formula weight	4857.34	
Temperature	446(2) K	
Wavelength	0.71073 Å	
Crystal system	Monoclinic	
Space group	C2/c	
Unit cell dimensions	a = 33.619(5) Å	α= 90°.
	b = 13.8463(17) Å	β= 108.827(5)°.
	c = 12.1501(15) Å	γ = 90°.
Volume	5353.3(12) $Å^3$	
Z	1	
Density (calculated)	1.507 Mg/m^3	
Absorption coefficient	1.304 mm^{-1}	
F(000)	2451	
Theta range for data collection	1.60 to 28.35°.	
Index ranges	-44<=h<=44, -18<=k<=18, -16<=l<=16	
Reflections collected	27277	
Independent reflections	6677 [R(int) = 0.1026]	
Completeness to theta = 28.35°	99.6 %	
Refinement method	Full-matrix least-squares on F^2	
Data / restraints / parameters	6677 / 0 / 373	
Goodness-of-fit on F^2	0.881	
Final R indices [I>2sigma(I)]	R1 = 0.0562, wR2 = 0.1338	
R indices (all data)	R1 = 0.0782, wR2 = 0.1498	
Largest diff. peak and hole	2.554 and -0.537 $e.Å^{-3}$	

Table 58. Atomic coordinates[a] and equivalent isotropic displacement parameters[b] for **9**

	x	y	z	U(eq)[c]
Gd(1)	0	2391(1)	-2500	21(1)
O(1)	263(1)	3929(2)	-2876(3)	28(1)
O(2)	-730(1)	1917(3)	-3476(3)	45(1)
O(3)	448(1)	2849(3)	-513(3)	34(1)
N(1)	0	10561(4)	-2500	30(1)
N(2)	339(1)	11601(3)	-3835(4)	29(1)
N(3)	2764(1)	998(3)	5630(4)	34(1)
N(4)	1925(2)	1488(4)	6788(4)	48(1)
N(5)	3373(2)	929(4)	3713(4)	48(1)
C(1)	541(2)	12162(4)	-4367(5)	33(1)
C(2)	833(2)	11821(4)	-4843(5)	39(1)
C(3)	921(2)	10867(4)	-4777(6)	53(2)

C(4)	714(2)	10262(4)	-4224(6)	52(2)
C(5)	431(2)	10650(3)	-3750(5)	32(1)
C(6)	210(2)	10069(3)	-3094(4)	27(1)
C(7)	215(2)	9057(3)	-3102(4)	30(1)
C(8)	0	8537(5)	-2500	30(2)
C(9)	0	7473(4)	-2500	29(1)
C(10)	-137(2)	6952(4)	-1707(5)	34(1)
C(11)	-139(2)	5955(4)	-1715(5)	34(1)
C(12)	0	5445(5)	-2500	28(2)
C(13)	0	4367(4)	-2500	26(1)
C(14)	1860(2)	1609(6)	7805(6)	64(2)
C(15)	2178(2)	1566(5)	8864(6)	59(2)
C(16)	2579(2)	1364(4)	8862(5)	48(2)
C(17)	2647(2)	1228(4)	7824(5)	37(1)
C(18)	2316(2)	1312(4)	6789(5)	35(1)
C(19)	2379(2)	1251(4)	5634(4)	31(1)
C(20)	2052(2)	1482(4)	4639(5)	34(1)
C(21)	2126(2)	1478(4)	3572(4)	30(1)
C(22)	2526(2)	1232(4)	3565(5)	33(1)
C(23)	2830(2)	998(4)	4603(4)	30(1)
C(24)	3263(2)	726(4)	4649(5)	39(1)
C(25)	3535(2)	286(5)	5622(6)	56(2)
C(26)	3932(2)	36(6)	5629(7)	75(3)
C(27)	4047(2)	259(6)	4703(7)	71(2)
C(28)	3767(2)	704(6)	3759(7)	61(2)
C(29)	1782(2)	1730(4)	2488(4)	30(1)
C(30)	1490(2)	2432(4)	2495(5)	35(1)
C(31)	1163(2)	2663(4)	1494(5)	32(1)
C(32)	1122(2)	2168(3)	470(4)	29(1)
C(33)	1419(2)	1481(3)	445(4)	29(1)
C(34)	1747(2)	1259(4)	1449(4)	29(1)
C(35)	748(2)	2333(3)	-587(4)	27(1)

[a] x 10^4
[b] $Å^2$ x 10^3
[c] U(eq) is defined as one third of the trace of the orthogonalized U^{ij} tensor.

Table 59. Bond lengths (Å) and angles (°) for **9**

Gd(1)-O(1)#1	2.405(3)	Gd(1)-N(2)#3	2.513(4)
Gd(1)-O(1)	2.405(3)	Gd(1)-N(1)#2	2.534(5)
Gd(1)-O(2)	2.446(3)	Gd(1)-C(13)	2.736(6)
Gd(1)-O(2)#1	2.446(3)	Gd(1)-C(35)	2.821(5)
Gd(1)-O(3)#1	2.480(4)	Gd(1)-C(35)#1	2.821(5)
Gd(1)-O(3)	2.480(4)	O(1)-C(13)	1.272(4)
Gd(1)-N(2)#2	2.513(4)	O(2)-C(35)#1	1.260(6)

O(3)-C(35)	1.263(6)	C(20)-C(21)	1.398(8)
N(1)-C(6)#1	1.347(5)	C(20)-H(20A)	0.9300
N(1)-C(6)	1.347(5)	C(21)-C(22)	1.388(7)
N(1)-Gd(1)#4	2.534(5)	C(21)-C(29)	1.488(7)
N(2)-C(1)	1.330(6)	C(22)-C(23)	1.382(7)
N(2)-C(5)	1.350(6)	C(22)-H(22A)	0.9300
N(2)-Gd(1)#4	2.513(4)	C(23)-C(24)	1.489(7)
N(3)-C(23)	1.336(7)	C(24)-C(25)	1.381(8)
N(3)-C(19)	1.343(7)	C(25)-C(26)	1.377(9)
N(4)-C(14)	1.334(8)	C(25)-H(25A)	0.9300
N(4)-C(18)	1.337(7)	C(26)-C(27)	1.338(12)
N(5)-C(24)	1.333(8)	C(26)-H(26A)	0.9300
N(5)-C(28)	1.343(8)	C(27)-C(28)	1.373(10)
C(1)-C(2)	1.374(8)	C(27)-H(27A)	0.9300
C(1)-H(1B)	0.9300	C(28)-H(28A)	0.9300
C(2)-C(3)	1.350(8)	C(29)-C(30)	1.382(7)
C(2)-H(2B)	0.9300	C(29)-C(34)	1.392(7)
C(3)-C(4)	1.392(8)	C(30)-C(31)	1.390(7)
C(3)-H(3B)	0.9300	C(30)-H(30A)	0.9300
C(4)-C(5)	1.370(7)	C(31)-C(32)	1.388(7)
C(4)-H(4B)	0.9300	C(31)-H(31A)	0.9300
C(5)-C(6)	1.489(7)	C(32)-C(33)	1.385(7)
C(6)-C(7)	1.401(6)	C(32)-C(35)	1.497(7)
C(7)-C(8)	1.384(6)	C(33)-C(34)	1.390(6)
C(7)-H(7A)	0.9300	C(33)-H(33A)	0.9300
C(8)-C(7)#1	1.384(6)	C(34)-H(34A)	0.9300
C(8)-C(9)	1.474(8)	C(35)-O(2)#1	1.261(6)
C(9)-C(10)	1.395(6)		
C(9)-C(10)#1	1.395(6)	O(1)#1-Gd(1)-O(1)	55.41(15)
C(10)-C(11)	1.381(7)	O(1)#1-Gd(1)-O(2)	87.54(14)
C(10)-H(10A)	0.9300	O(1)-Gd(1)-O(2)	121.22(12)
C(11)-C(12)	1.384(6)	O(1)#1-Gd(1)-O(2)#1	121.22(12)
C(11)-H(11A)	0.9300	O(1)-Gd(1)-O(2)#1	87.54(14)
C(12)-C(11)#1	1.384(6)	O(2)-Gd(1)-O(2)#1	148.9(2)
C(12)-C(13)	1.492(9)	O(1)#1-Gd(1)-O(3)#1	79.25(12)
C(13)-O(1)#1	1.272(4)	O(1)-Gd(1)-O(3)#1	74.53(11)
C(14)-C(15)	1.384(10)	O(2)-Gd(1)-O(3)#1	52.98(12)
C(14)-H(14A)	0.9300	O(2)#1-Gd(1)-O(3)#1	137.69(13)
C(15)-C(16)	1.377(9)	O(1)#1-Gd(1)-O(3)	74.53(11)
C(15)-H(15A)	0.9300	O(1)-Gd(1)-O(3)	79.25(12)
C(16)-C(17)	1.365(8)	O(2)-Gd(1)-O(3)	137.69(13)
C(16)-H(16A)	0.9300	O(2)#1-Gd(1)-O(3)	52.98(12)
C(17)-C(18)	1.389(7)	O(3)#1-Gd(1)-O(3)	150.34(17)
C(17)-H(17A)	0.9300	O(1)#1-Gd(1)-N(2)#2	141.13(12)
C(18)-C(19)	1.487(8)	O(1)-Gd(1)-N(2)#2	89.52(12)
C(19)-C(20)	1.383(7)	O(2)-Gd(1)-N(2)#2	99.38(14)

O(2)#1-Gd(1)-N(2)#2	66.64(13)	C(13)-Gd(1)-C(35)#1	91.62(9)
O(3)#1-Gd(1)-N(2)#2	75.05(13)	C(35)-Gd(1)-C(35)#1	176.75(19)
O(3)-Gd(1)-N(2)#2	118.73(13)	C(13)-O(1)-Gd(1)	90.8(3)
O(1)#1-Gd(1)-N(2)#3	89.52(12)	C(35)#1-O(2)-Gd(1)	93.6(3)
O(1)-Gd(1)-N(2)#3	141.13(12)	C(35)-O(3)-Gd(1)	92.0(3)
O(2)-Gd(1)-N(2)#3	66.64(13)	C(6)#1-N(1)-C(6)	119.2(6)
O(2)#1-Gd(1)-N(2)#3	99.38(14)	C(6)#1-N(1)-Gd(1)#4	120.4(3)
O(3)#1-Gd(1)-N(2)#3	118.73(13)	C(6)-N(1)-Gd(1)#4	120.4(3)
O(3)-Gd(1)-N(2)#3	75.05(13)	C(1)-N(2)-C(5)	117.8(5)
N(2)#2-Gd(1)-N(2)#3	128.44(18)	C(1)-N(2)-Gd(1)#4	118.0(3)
O(1)#1-Gd(1)-N(1)#2	152.29(8)	C(5)-N(2)-Gd(1)#4	121.1(3)
O(1)-Gd(1)-N(1)#2	152.29(8)	C(23)-N(3)-C(19)	117.1(4)
O(2)-Gd(1)-N(1)#2	74.43(10)	C(14)-N(4)-C(18)	118.5(6)
O(2)#1-Gd(1)-N(1)#2	74.43(10)	C(24)-N(5)-C(28)	117.1(6)
O(3)#1-Gd(1)-N(1)#2	104.83(9)	N(2)-C(1)-C(2)	123.4(5)
O(3)-Gd(1)-N(1)#2	104.83(9)	N(2)-C(1)-H(1B)	118.3
N(2)#2-Gd(1)-N(1)#2	64.22(9)	C(2)-C(1)-H(1B)	118.3
N(2)#3-Gd(1)-N(1)#2	64.22(9)	C(3)-C(2)-C(1)	118.9(5)
O(1)#1-Gd(1)-C(13)	27.71(8)	C(3)-C(2)-H(2B)	120.5
O(1)-Gd(1)-C(13)	27.71(8)	C(1)-C(2)-H(2B)	120.5
O(2)-Gd(1)-C(13)	105.57(10)	C(2)-C(3)-C(4)	119.0(5)
O(2)#1-Gd(1)-C(13)	105.57(10)	C(2)-C(3)-H(3B)	120.5
O(3)#1-Gd(1)-C(13)	75.17(9)	C(4)-C(3)-H(3B)	120.5
O(3)-Gd(1)-C(13)	75.17(9)	C(5)-C(4)-C(3)	119.2(5)
N(2)#2-Gd(1)-C(13)	115.78(9)	C(5)-C(4)-H(4B)	120.4
N(2)#3-Gd(1)-C(13)	115.78(9)	C(3)-C(4)-H(4B)	120.4
N(1)#2-Gd(1)-C(13)	180.0	N(2)-C(5)-C(4)	121.6(5)
O(1)#1-Gd(1)-C(35)	98.80(13)	N(2)-C(5)-C(6)	115.2(4)
O(1)-Gd(1)-C(35)	84.10(13)	C(4)-C(5)-C(6)	123.1(4)
O(2)-Gd(1)-C(35)	151.63(13)	N(1)-C(6)-C(7)	121.2(5)
O(2)#1-Gd(1)-C(35)	26.48(13)	N(1)-C(6)-C(5)	116.9(4)
O(3)#1-Gd(1)-C(35)	155.34(13)	C(7)-C(6)-C(5)	121.9(4)
O(3)-Gd(1)-C(35)	26.58(13)	C(8)-C(7)-C(6)	120.5(5)
N(2)#2-Gd(1)-C(35)	92.91(14)	C(8)-C(7)-H(7A)	119.8
N(2)#3-Gd(1)-C(35)	85.68(14)	C(6)-C(7)-H(7A)	119.8
N(1)#2-Gd(1)-C(35)	88.38(9)	C(7)#1-C(8)-C(7)	117.4(6)
C(13)-Gd(1)-C(35)	91.62(9)	C(7)#1-C(8)-C(9)	121.3(3)
O(1)#1-Gd(1)-C(35)#1	84.10(12)	C(7)-C(8)-C(9)	121.3(3)
O(1)-Gd(1)-C(35)#1	98.80(13)	C(10)-C(9)-C(10)#1	117.8(6)
O(2)-Gd(1)-C(35)#1	26.48(13)	C(10)-C(9)-C(8)	121.1(3)
O(2)#1-Gd(1)-C(35)#1	151.63(13)	C(10)#1-C(9)-C(8)	121.1(3)
O(3)#1-Gd(1)-C(35)#1	26.58(13)	C(11)-C(10)-C(9)	121.0(5)
O(3)-Gd(1)-C(35)#1	155.34(13)	C(11)-C(10)-H(10A)	119.5
N(2)#2-Gd(1)-C(35)#1	85.68(14)	C(9)-C(10)-H(10A)	119.5
N(2)#3-Gd(1)-C(35)#1	92.91(14)	C(10)-C(11)-C(12)	120.8(5)
N(1)#2-Gd(1)-C(35)#1	88.38(9)	C(10)-C(11)-H(11A)	119.6

C(12)-C(11)-H(11A)	119.6	N(5)-C(24)-C(25)	122.3(6)
C(11)#1-C(12)-C(11)	118.6(6)	N(5)-C(24)-C(23)	116.9(5)
C(11)#1-C(12)-C(13)	120.7(3)	C(25)-C(24)-C(23)	120.7(6)
C(11)-C(12)-C(13)	120.7(3)	C(26)-C(25)-C(24)	119.2(7)
O(1)#1-C(13)-O(1)	123.0(6)	C(26)-C(25)-H(25A)	120.4
O(1)#1-C(13)-C(12)	118.5(3)	C(24)-C(25)-H(25A)	120.4
O(1)-C(13)-C(12)	118.5(3)	C(27)-C(26)-C(25)	118.7(7)
O(1)#1-C(13)-Gd(1)	61.5(3)	C(27)-C(26)-H(26A)	120.6
O(1)-C(13)-Gd(1)	61.5(3)	C(25)-C(26)-H(26A)	120.6
C(12)-C(13)-Gd(1)	180.0	C(26)-C(27)-C(28)	119.9(6)
N(4)-C(14)-C(15)	123.1(7)	C(26)-C(27)-H(27A)	120.0
N(4)-C(14)-H(14A)	118.4	C(28)-C(27)-H(27A)	120.0
C(15)-C(14)-H(14A)	118.4	N(5)-C(28)-C(27)	122.7(7)
C(16)-C(15)-C(14)	118.2(6)	N(5)-C(28)-H(28A)	118.6
C(16)-C(15)-H(15A)	120.9	C(27)-C(28)-H(28A)	118.6
C(14)-C(15)-H(15A)	120.9	C(30)-C(29)-C(34)	118.9(5)
C(17)-C(16)-C(15)	118.9(6)	C(30)-C(29)-C(21)	120.7(5)
C(17)-C(16)-H(16A)	120.5	C(34)-C(29)-C(21)	120.4(4)
C(15)-C(16)-H(16A)	120.5	C(29)-C(30)-C(31)	121.3(5)
C(16)-C(17)-C(18)	120.1(5)	C(29)-C(30)-H(30A)	119.4
C(16)-C(17)-H(17A)	119.9	C(31)-C(30)-H(30A)	119.4
C(18)-C(17)-H(17A)	119.9	C(32)-C(31)-C(30)	119.5(5)
N(4)-C(18)-C(17)	121.1(5)	C(32)-C(31)-H(31A)	120.2
N(4)-C(18)-C(19)	116.6(5)	C(30)-C(31)-H(31A)	120.2
C(17)-C(18)-C(19)	122.3(5)	C(33)-C(32)-C(31)	119.7(5)
N(3)-C(19)-C(20)	123.5(5)	C(33)-C(32)-C(35)	119.9(5)
N(3)-C(19)-C(18)	116.7(4)	C(31)-C(32)-C(35)	120.4(5)
C(20)-C(19)-C(18)	119.8(5)	C(32)-C(33)-C(34)	120.4(5)
C(19)-C(20)-C(21)	118.7(5)	C(32)-C(33)-H(33A)	119.8
C(19)-C(20)-H(20A)	120.6	C(34)-C(33)-H(33A)	119.8
C(21)-C(20)-H(20A)	120.6	C(33)-C(34)-C(29)	120.2(5)
C(22)-C(21)-C(20)	118.0(5)	C(33)-C(34)-H(34A)	119.9
C(22)-C(21)-C(29)	122.1(5)	C(29)-C(34)-H(34A)	119.9
C(20)-C(21)-C(29)	119.9(5)	O(2)#1-C(35)-O(3)	121.1(4)
C(23)-C(22)-C(21)	119.0(5)	O(2)#1-C(35)-C(32)	119.1(4)
C(23)-C(22)-H(22A)	120.5	O(3)-C(35)-C(32)	119.7(4)
C(21)-C(22)-H(22A)	120.5	O(2)#1-C(35)-Gd(1)	59.9(2)
N(3)-C(23)-C(22)	123.7(5)	O(3)-C(35)-Gd(1)	61.5(3)
N(3)-C(23)-C(24)	115.0(4)	C(32)-C(35)-Gd(1)	171.9(3)
C(22)-C(23)-C(24)	121.3(5)		

Symmetry transformations used to generate equivalent atoms:
#1 -x,y,-z-1/2 #2 x,y-1,z #3 -x,y-1,-z-1/2
#4 x,y+1,z

Table 60. Anisotropic displacement parameters for **9**[d]

	U^{11}	U^{22}	U^{33}	U^{23}	U^{13}	U^{12}
Gd(1)	18(1)	18(1)	23(1)	0	2(1)	0
O(1)	27(2)	18(2)	41(2)	0(1)	13(2)	-1(1)
O(2)	30(2)	61(3)	32(2)	18(2)	-7(2)	-16(2)
O(3)	23(2)	41(2)	32(2)	0(2)	2(2)	6(2)
N(1)	33(3)	16(3)	46(4)	0	18(3)	0
N(2)	34(2)	24(2)	27(2)	1(2)	5(2)	-1(2)
N(3)	28(2)	34(2)	34(2)	1(2)	2(2)	4(2)
N(4)	35(3)	73(4)	38(3)	-1(2)	13(2)	3(2)
N(5)	29(3)	66(3)	49(3)	-18(3)	10(2)	2(2)
C(1)	42(3)	24(2)	32(3)	2(2)	10(2)	-3(2)
C(2)	41(3)	33(3)	50(3)	3(2)	24(3)	-6(2)
C(3)	57(4)	42(3)	81(5)	0(3)	50(4)	1(3)
C(4)	67(4)	21(3)	88(5)	2(3)	55(4)	6(3)
C(5)	33(3)	23(2)	40(3)	1(2)	14(2)	1(2)
C(6)	30(3)	23(2)	30(3)	0(2)	11(2)	1(2)
C(7)	35(3)	21(2)	38(3)	-5(2)	17(2)	-1(2)
C(8)	30(4)	25(3)	34(4)	0	8(3)	0
C(9)	30(4)	19(3)	37(4)	0	10(3)	0
C(10)	45(3)	24(2)	38(3)	-5(2)	20(2)	1(2)
C(11)	39(3)	26(2)	41(3)	2(2)	18(2)	0(2)
C(12)	22(3)	22(3)	37(4)	0	6(3)	0
C(13)	29(4)	16(3)	25(3)	0	-1(3)	0
C(14)	46(4)	97(6)	51(4)	-7(4)	18(3)	-6(4)
C(15)	76(5)	67(5)	41(4)	-1(3)	29(4)	-4(4)
C(16)	54(4)	50(4)	34(3)	4(3)	5(3)	2(3)
C(17)	33(3)	39(3)	36(3)	6(2)	7(2)	5(2)
C(18)	34(3)	29(3)	40(3)	3(2)	8(2)	-4(2)
C(19)	26(3)	29(2)	29(3)	-1(2)	-1(2)	2(2)
C(20)	23(3)	37(3)	36(3)	2(2)	1(2)	2(2)
C(21)	24(2)	31(3)	30(3)	4(2)	0(2)	5(2)
C(22)	24(3)	39(3)	34(3)	1(2)	8(2)	3(2)
C(23)	18(2)	34(3)	31(3)	-2(2)	-2(2)	6(2)
C(24)	29(3)	42(3)	42(3)	-12(2)	6(2)	6(2)
C(25)	34(3)	72(5)	51(4)	-1(3)	-3(3)	24(3)
C(26)	42(4)	94(6)	70(5)	-22(4)	-5(4)	32(4)
C(27)	24(3)	98(6)	79(6)	-36(5)	2(4)	21(3)
C(28)	38(4)	80(5)	67(5)	-30(4)	22(3)	-4(3)
C(29)	23(2)	31(2)	31(3)	4(2)	3(2)	3(2)
C(30)	27(3)	44(3)	28(3)	-4(2)	-2(2)	4(2)
C(31)	22(2)	36(3)	31(3)	-6(2)	-1(2)	6(2)
C(32)	25(2)	26(2)	32(3)	3(2)	3(2)	-5(2)
C(33)	24(2)	34(3)	25(2)	-2(2)	4(2)	-1(2)

C(34)	20(2)	33(3)	33(3)	5(2)	6(2)	4(2)
C(35)	22(2)	28(2)	26(2)	1(2)	2(2)	-2(2)

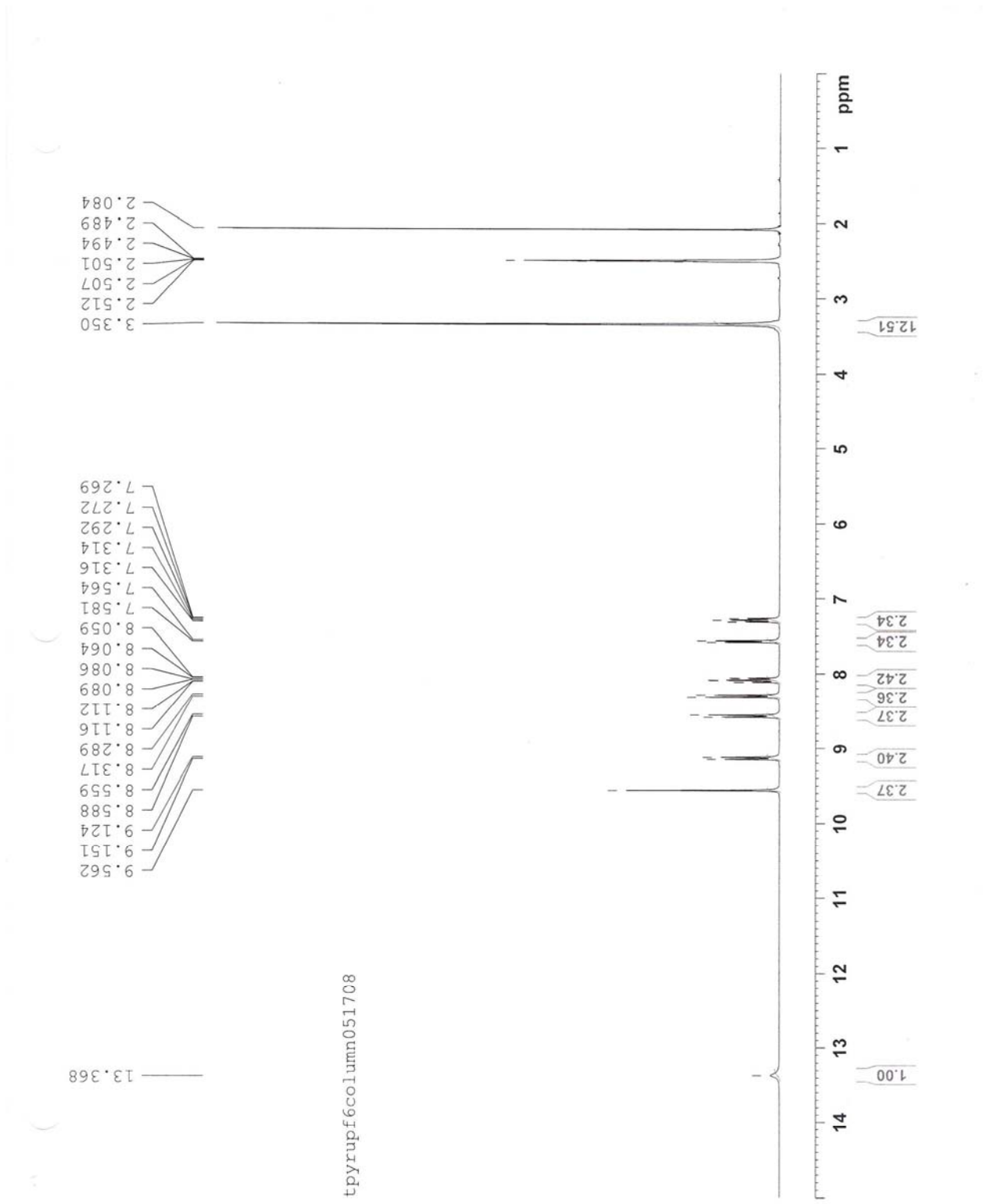

Figure 64. ^{1}H NMR for $[Ru(H\mathbf{L})_2][PF_6]_2$ (0 – 15 ppm)

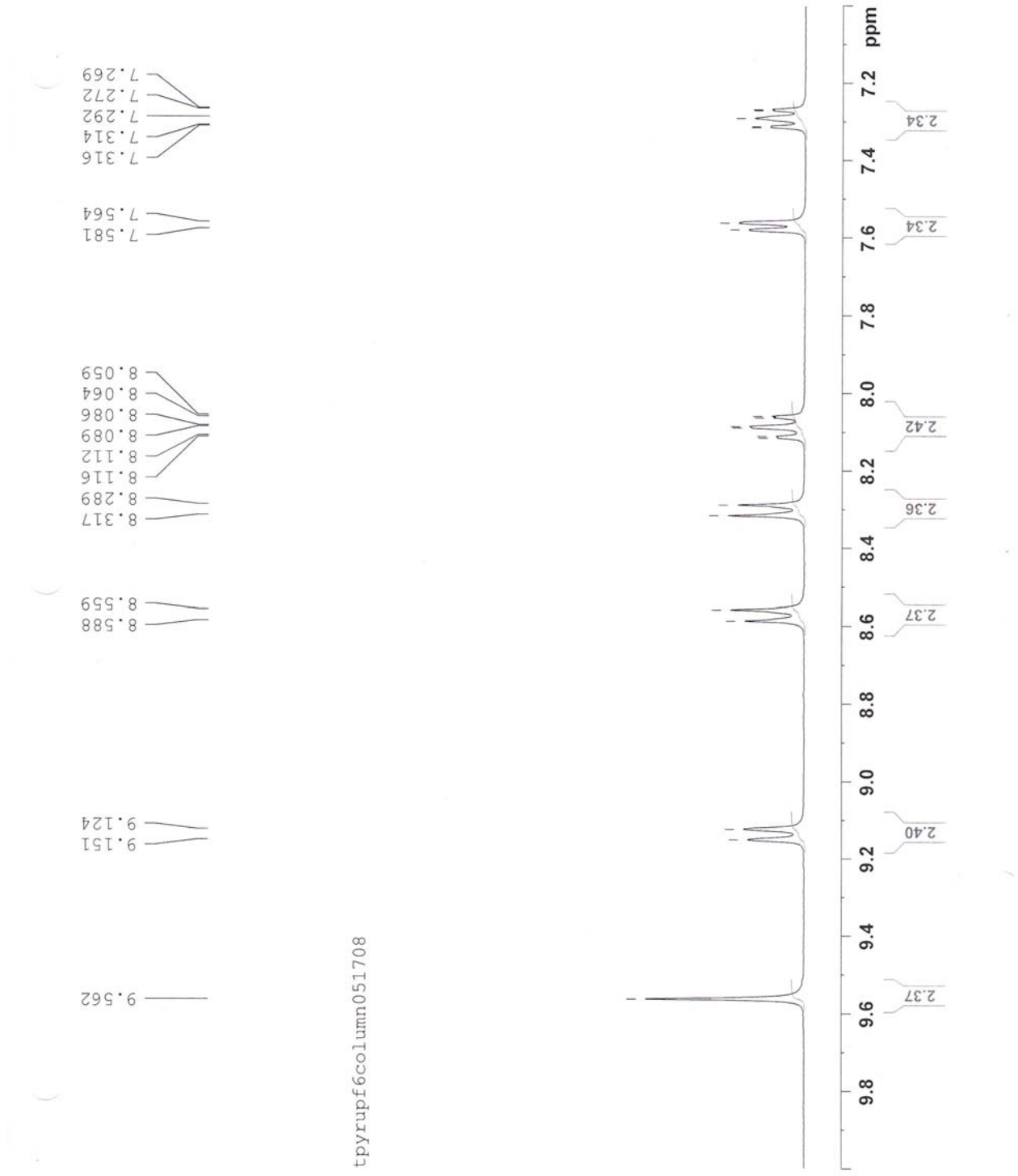

Figure 65. ^{1}H NMR for $[Ru(HL)_2][PF_6]_2$ (7.1 – 9.9 ppm)

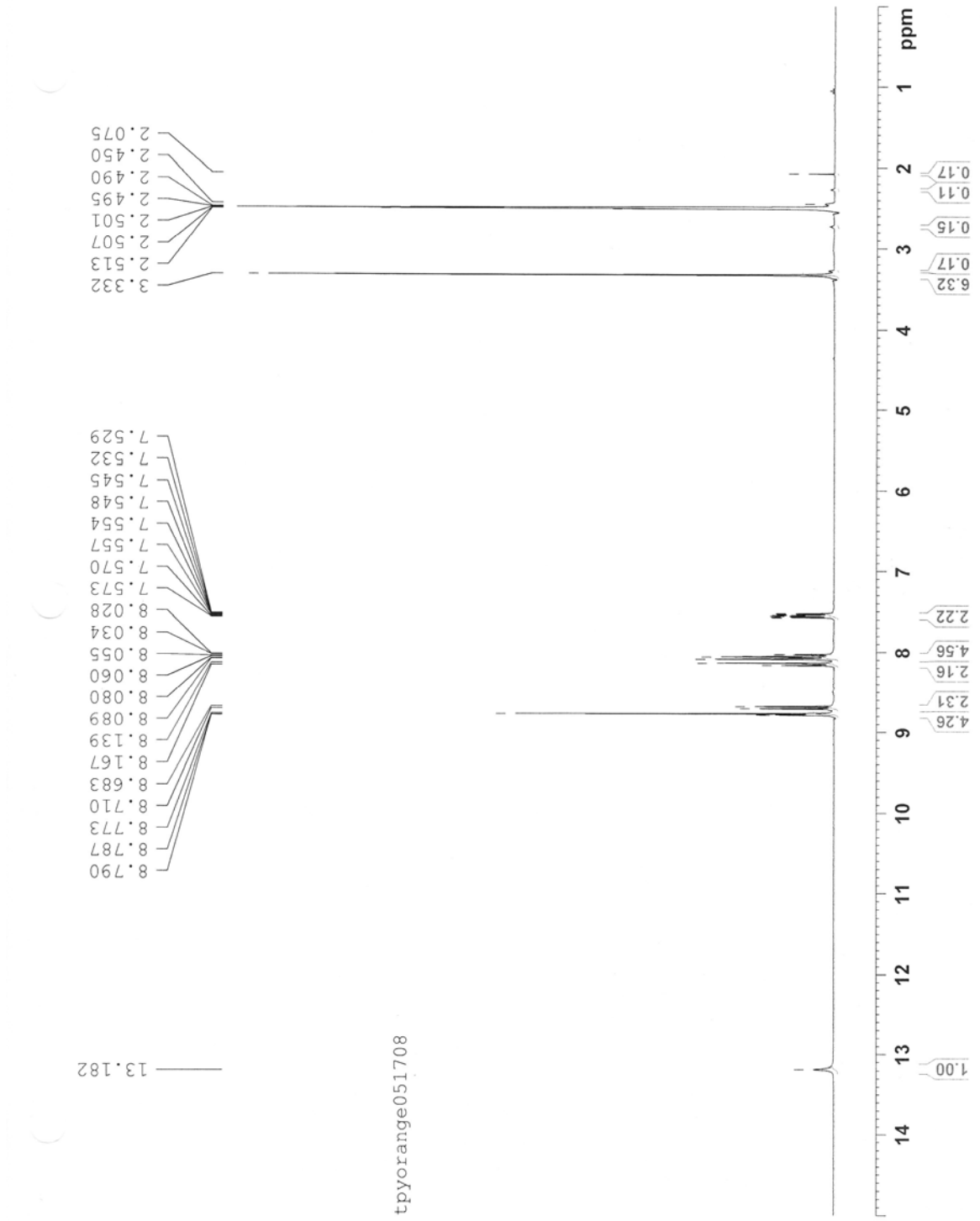

Figure 66. ^{1}H NMR for H**L**, after reflux in H_2O (0 – 15 ppm)

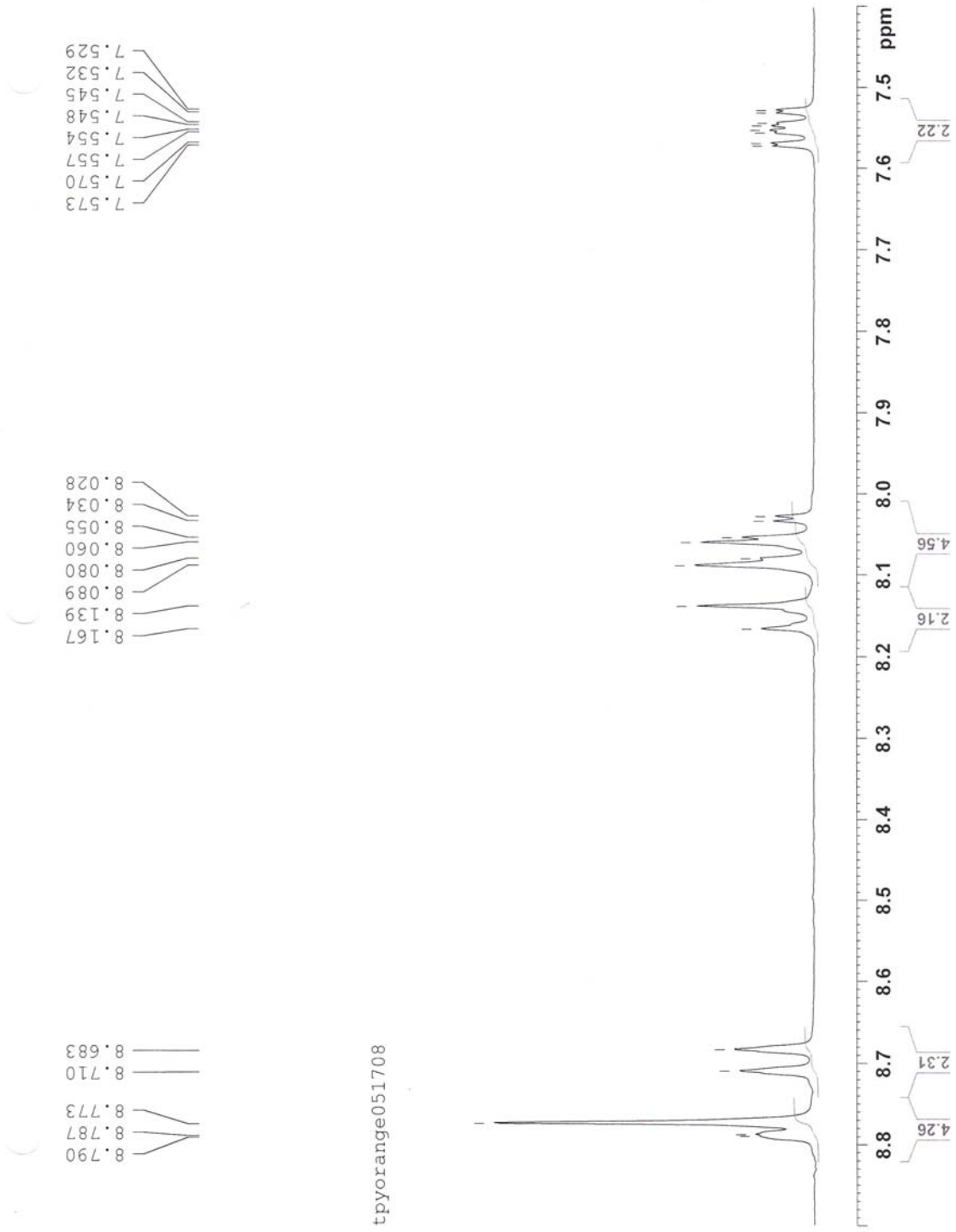

Figure 67. ^{1}H NMR for H**L**, after reflux in H_2O (7.4 – 8.9 ppm)

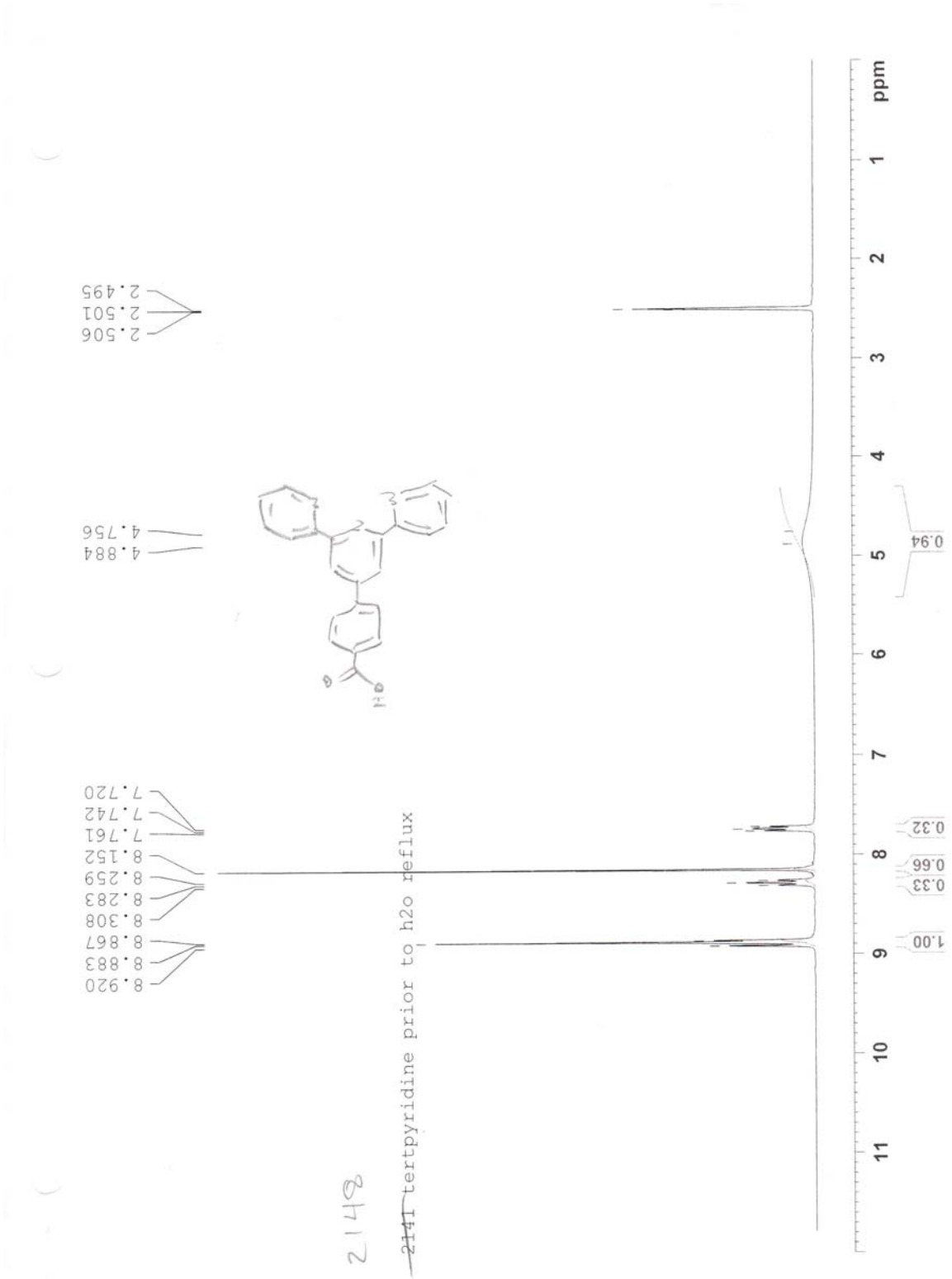

Figure 68. ^{1}H NMR for H**L**, prior to reflux in H_2O (0 – 12 ppm)

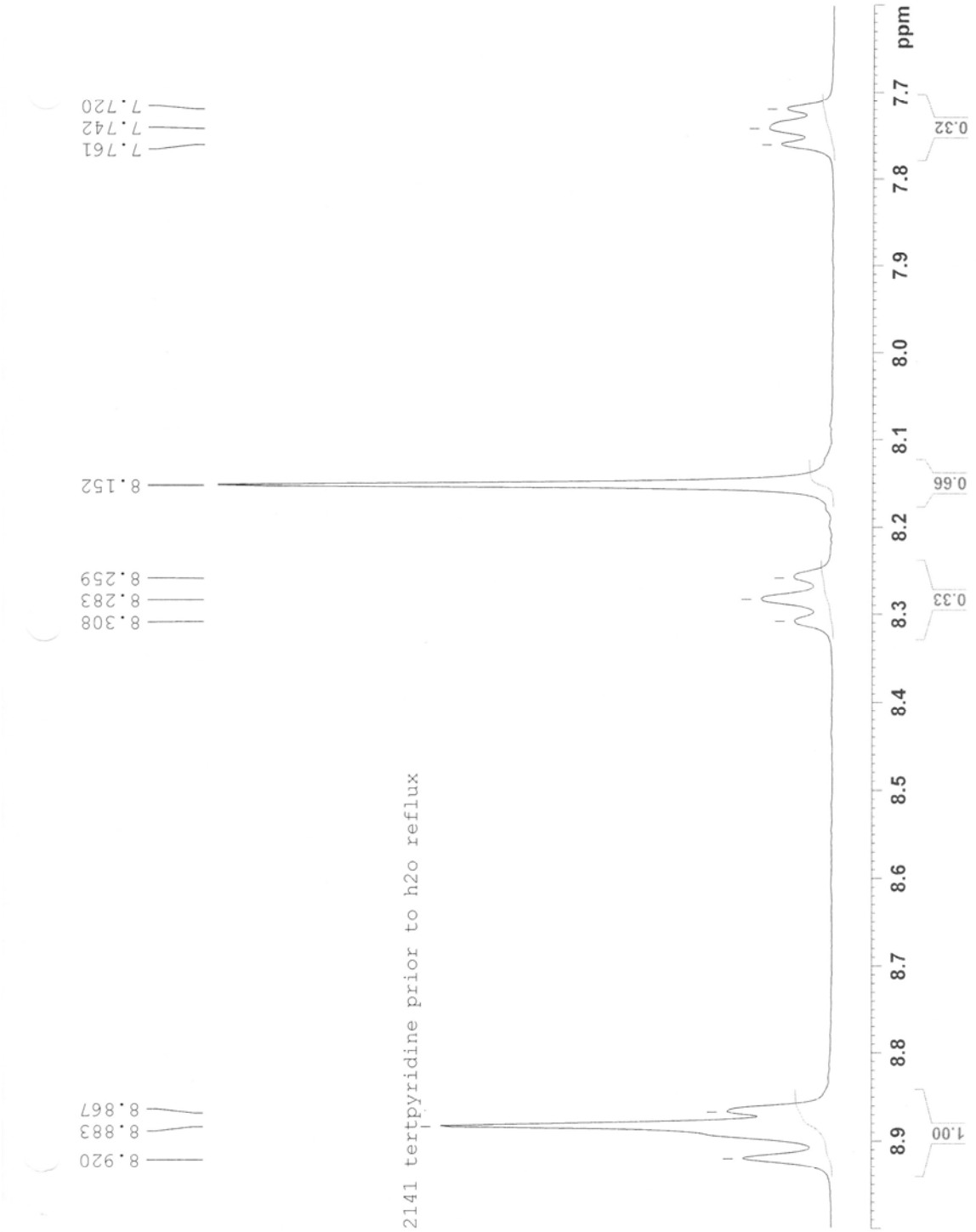

Figure 69. ^{1}H NMR for H**L**, prior to reflux in H_2O (7.6 – 9.0 ppm)

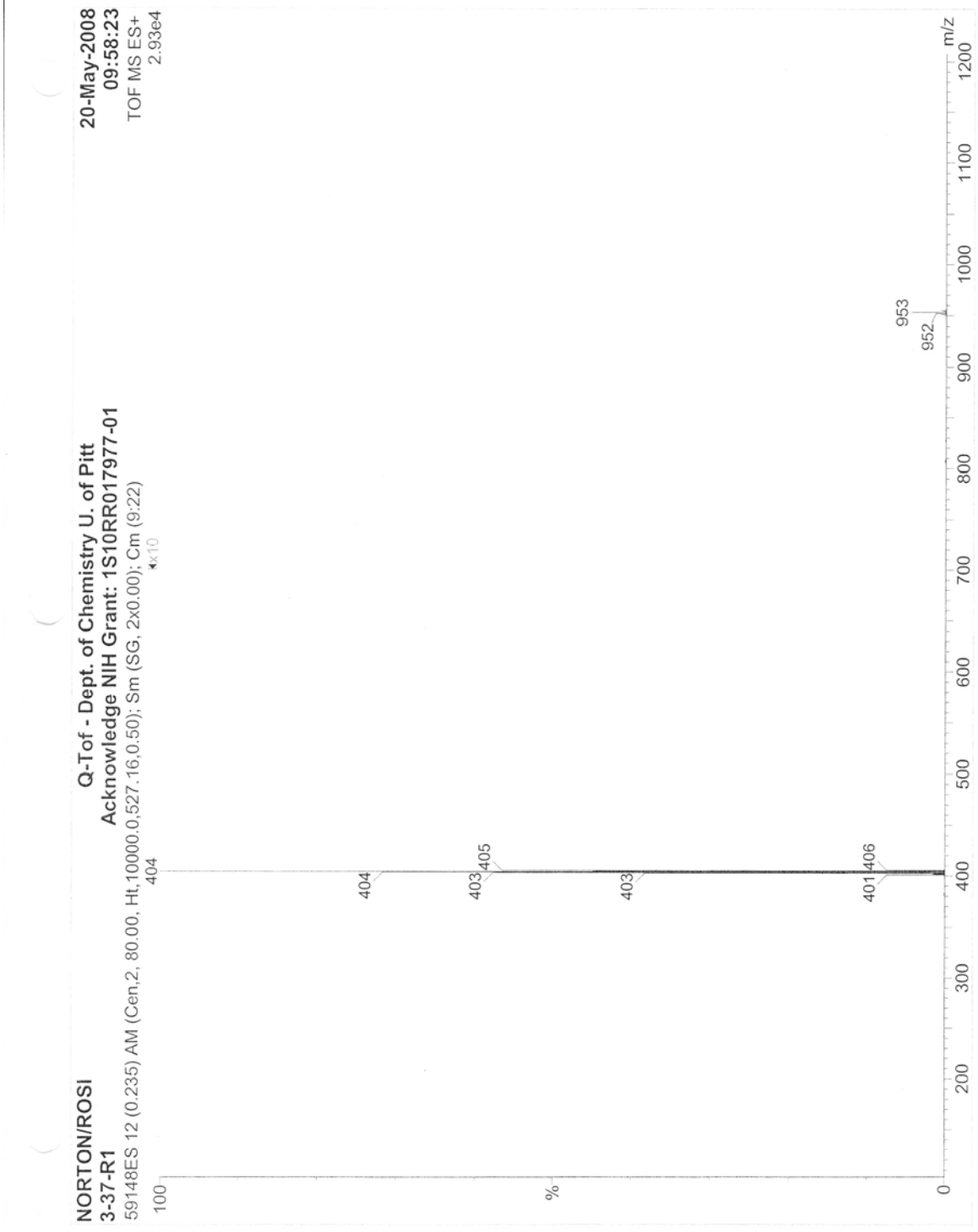

Figure 70. Mass Spec for $[Ru(HL)_2][PF_6]_2$ (100 – 1200 m/z)

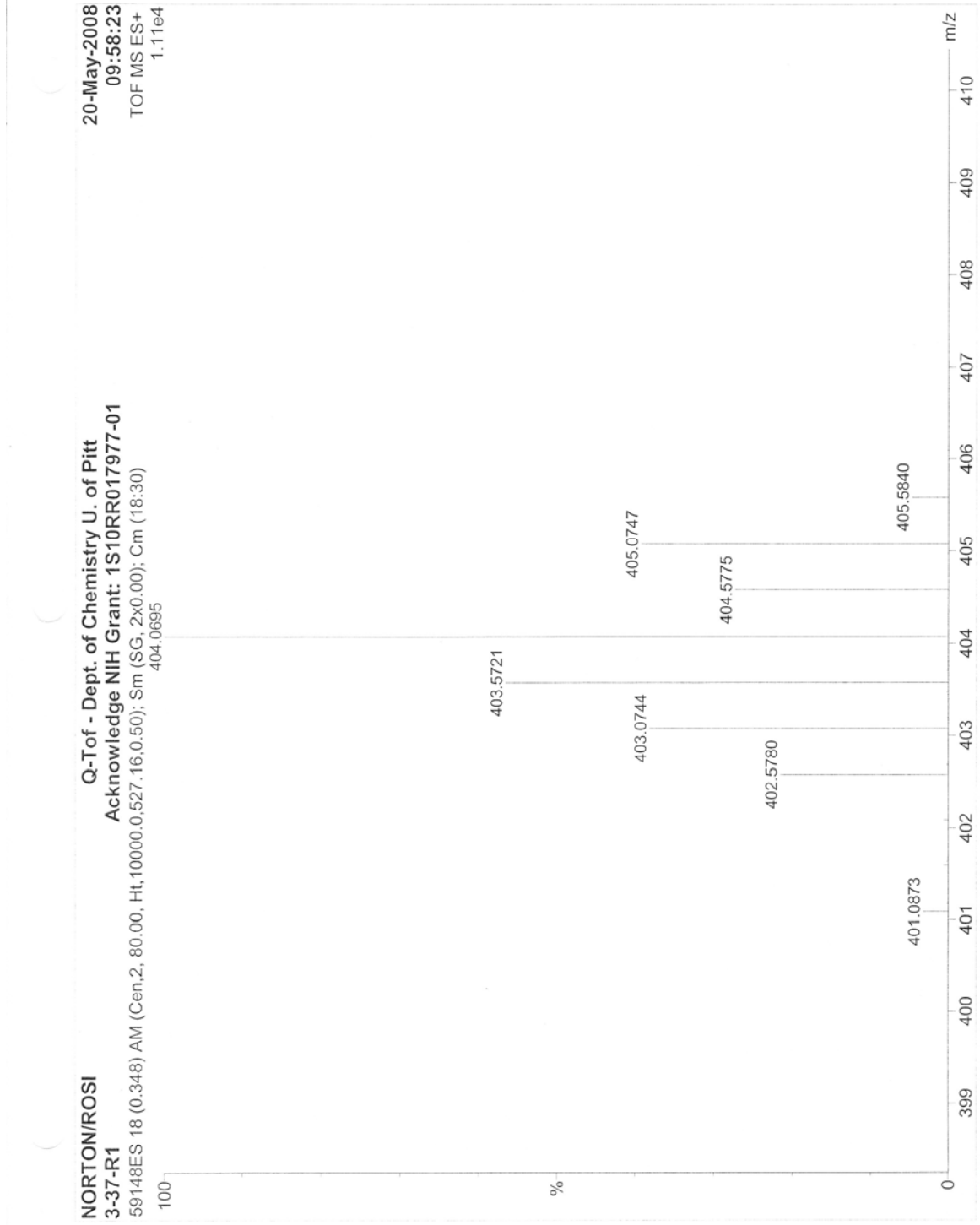

Figure 71. MS for $[Ru(HL)_2][PF_6]_2$ (398 – 411 m/z)

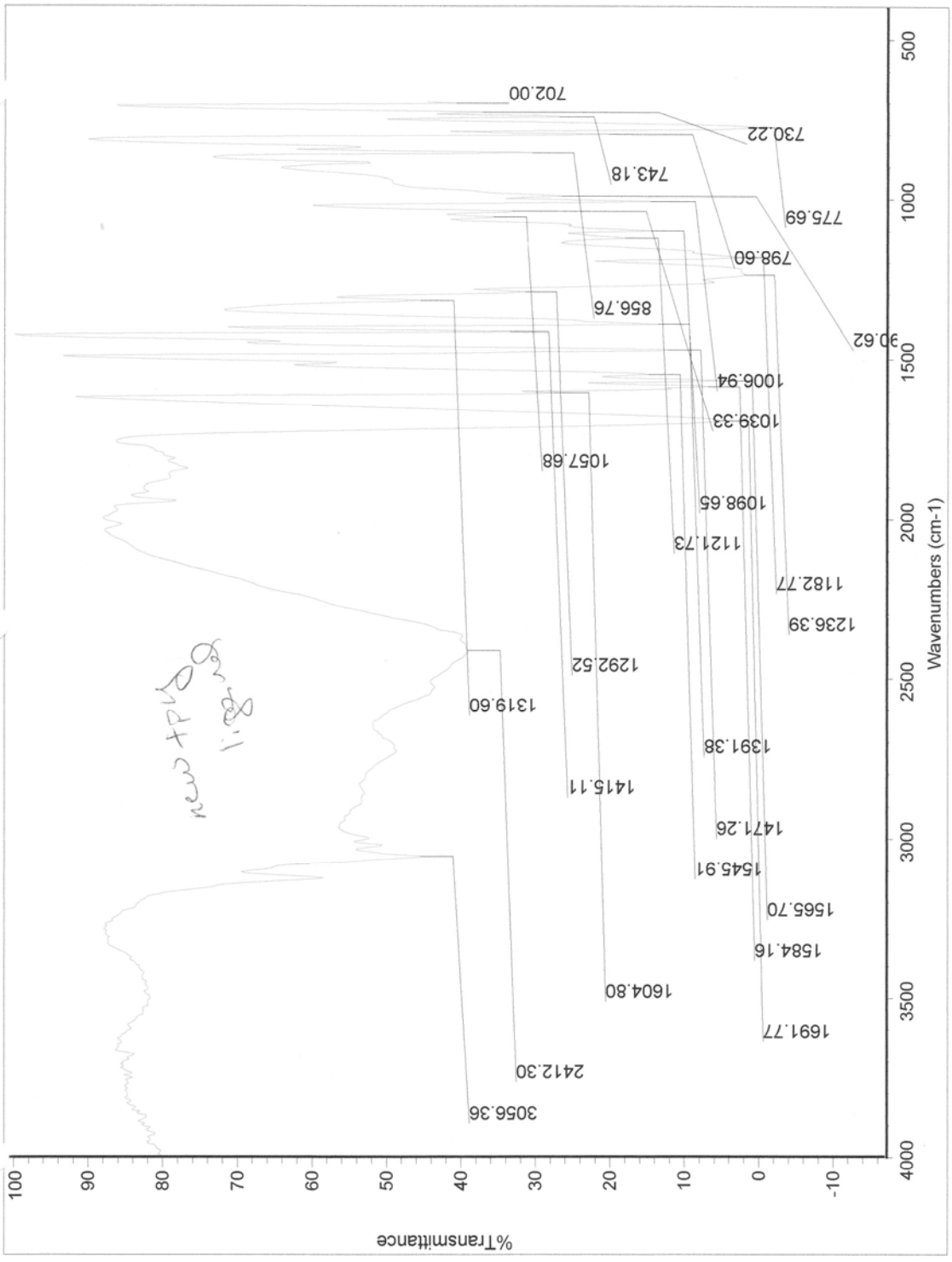

Figure 72. FT-IR for H**L**

Table 61. Atomic coordinates[a] and equivalent isotropic displacement parameters[b] for **10a**

	x	y	z	U(eq)[c]
Ru(1)	5000	7500	1250	39(1)
N(1)	5987(7)	6065(7)	1137(2)	48(2)
N(2)	5000	7500	698(3)	41(2)
O(1)	5815(17)	6851(11)	-1861(3)	178(7)
O(2)	10000	2500	1250	190(17)
O(3)	10000	2500	569(11)	232(15)
O(4)	7498(16)	4510(30)	-240(4)	288(16)
C(1)	6505(10)	5347(10)	1391(3)	65(3)
C(2)	7146(16)	4430(13)	1275(4)	102(5)
C(3)	7273(16)	4199(13)	909(4)	110(6)
C(4)	6846(12)	4953(12)	652(4)	90(4)
C(5)	6143(9)	5839(8)	763(2)	52(2)
C(6)	5590(9)	6653(8)	508(2)	48(2)
C(7)	5615(11)	6657(8)	126(3)	61(3)
C(8)	5000	7500	-498(4)	80(6)
C(9)	5000	7500	-83(4)	71(5)
C(10)	5691(14)	6774(10)	-702(3)	110(6)
C(11)	5000	7500	-1282(4)	135(14)
C(12)	5687(15)	6740(10)	-1088(3)	124(8)
C(13)	5000	7500	-1690(7)	660(100)

[a] x 10^4
[b] $Å^2$ x 10^3
[c] U(eq) is defined as one third of the trace of the orthogonalized U^{ij} tensor.

Table 62. Atomic coordinates[a] and equivalent isotropic displacement parameters[b] for **10b**

	x	y	z	U(eq)[c]
Ru(2)	5748(1)	2502(1)	2705(1)	18(1)
O(1)	6938(11)	4384(8)	-3981(5)	42(2)
O(2)	8842(12)	3236(8)	-4048(6)	47(3)
O(3)	2089(14)	1455(11)	9487(6)	66(4)
O(4)	346(14)	393(9)	9267(6)	56(3)
N(1)	4668(10)	1035(8)	2907(5)	22(2)
N(2)	5162(10)	2188(7)	3911(5)	20(2)
N(3)	6578(10)	3851(8)	2986(6)	23(2)
N(4)	3803(10)	3214(7)	2512(5)	20(2)
N(5)	6193(10)	2762(7)	1507(5)	21(2)
N(6)	7938(10)	1971(8)	2413(6)	23(2)
C(1)	4426(13)	510(9)	2342(6)	24(2)
C(2)	3505(14)	-407(10)	2536(8)	34(3)

C(3)	2866(14)	-782(9)	3351(8)	34(3)
C(4)	3146(13)	-254(9)	3918(7)	25(2)
C(5)	4019(12)	663(10)	3687(7)	25(2)
C(6)	4285(12)	1331(10)	4273(7)	25(2)
C(7)	3699(15)	1166(10)	5095(7)	30(3)
C(8)	3982(12)	1896(9)	5559(6)	20(2)
C(9)	4895(13)	2778(9)	5161(6)	25(2)
C(10)	5461(12)	2930(9)	4336(7)	23(2)
C(11)	6348(13)	3855(9)	3812(7)	25(2)
C(12)	6925(13)	4660(10)	4074(7)	27(2)
C(13)	7732(14)	5496(11)	3534(7)	31(3)
C(14)	7880(14)	5508(10)	2726(7)	29(2)
C(15)	7316(14)	4673(9)	2480(7)	28(2)
C(16)	3316(13)	1739(9)	6437(7)	27(2)
C(17)	3996(13)	2143(10)	6960(7)	28(2)
C(18)	3403(13)	1958(10)	7791(7)	29(3)
C(19)	2120(15)	1312(10)	8124(7)	31(3)
C(20)	1394(16)	937(10)	7602(7)	34(3)
C(21)	1970(14)	1107(11)	6780(7)	33(3)
C(22)	1540(20)	1036(11)	9022(8)	46(4)
C(23)	2633(12)	3452(9)	3051(7)	24(2)
C(24)	1327(14)	3951(10)	2862(8)	32(3)
C(25)	1304(14)	4225(12)	2045(8)	35(3)
C(26)	2536(12)	3946(10)	1467(6)	27(3)
C(27)	3732(12)	3454(9)	1703(6)	22(2)
C(28)	5088(12)	3153(9)	1138(7)	24(2)
C(29)	5284(13)	3270(11)	309(7)	28(3)
C(30)	6638(12)	2941(10)	-165(7)	25(2)
C(31)	7718(12)	2509(9)	258(7)	24(2)
C(32)	7462(11)	2452(8)	1076(6)	20(2)
C(33)	8547(12)	2048(9)	1601(7)	22(2)
C(34)	10014(12)	1794(9)	1289(7)	24(2)
C(35)	10908(13)	1469(10)	1845(7)	28(2)
C(36)	10313(13)	1399(10)	2667(7)	29(2)
C(37)	8837(13)	1654(10)	2929(7)	28(2)
C(38)	6867(12)	3112(10)	-1049(7)	25(2)
C(39)	5930(13)	3706(11)	-1471(7)	30(3)
C(40)	6186(14)	3884(11)	-2307(7)	33(3)
C(41)	7405(13)	3489(9)	-2755(7)	25(2)
C(42)	8392(14)	2883(11)	-2360(7)	32(3)
C(43)	8162(15)	2678(12)	-1537(7)	36(3)
C(44)	7721(15)	3758(11)	-3672(7)	33(3)
Cl(1)	9207(7)	5375(6)	334(4)	87(2)
O(6)	10094(13)	5692(9)	-547(6)	51(3)
O(8)	8110(70)	6187(13)	722(13)	430(40)
Q(9)	7580(20)	5299(16)	422(12)	63(5)

O(5)	1458(14)	3774(9)	4842(6)	57(3)
O(7)	9405(19)	2006(11)	4746(9)	95(6)

[a] x 10^4
[b] $Å^2$ x 10^3
[c] U(eq) is defined as one third of the trace of the orthogonalized U^{ij} tensor.

Table 63. Atomic coordinates[a] and equivalent isotropic displacement parameters[b] for **10c**

	x	y	z	U(eq)[c]
Ru(2)	9877(1)	2511(1)	2486(1)	30(1)
F(1)	6522(16)	3942(7)	4384(6)	172(6)
F(2)	6510(10)	2832(7)	5201(4)	102(3)
F(3)	6456(9)	2205(7)	4121(4)	101(3)
F(4)	4434(9)	2884(8)	4369(5)	116(3)
O(1)	13911(9)	3713(7)	8316(4)	69(2)
O(2)	11534(11)	3559(9)	8317(4)	93(3)
O(3)	5840(8)	1368(6)	-3386(3)	47(2)
O(4)	8180(8)	855(6)	-3319(3)	47(2)
O(5)	7607(8)	598(5)	5323(4)	47(2)
O(6)	3852(8)	1239(6)	-4701(4)	57(2)
O(7)	5676(11)	4349(8)	-396(5)	96(3)
O(8)	12670(20)	341(15)	-402(9)	186(7)
O(9)	6320(40)	-1140(30)	530(16)	371(17)
O(10)	11326(18)	4657(12)	406(8)	174(6)
N(1)	11006(8)	4014(6)	2641(4)	32(2)
N(2)	10382(8)	2732(6)	3521(4)	28(2)
N(3)	8947(8)	1099(5)	2748(4)	28(2)
N(4)	7741(8)	3112(6)	2245(4)	32(2)
N(5)	9381(8)	2273(5)	1454(4)	28(2)
N(6)	11769(8)	1810(5)	2310(4)	28(2)
C(1)	11310(11)	4640(8)	2157(5)	41(2)
C(2)	12216(12)	5589(8)	2332(6)	49(3)
C(3)	12800(11)	5910(8)	3034(6)	46(3)
C(4)	12478(10)	5272(7)	3535(5)	37(2)
C(5)	11579(10)	4351(7)	3337(4)	31(2)
C(6)	11162(10)	3650(7)	3843(5)	30(2)
C(7)	11510(10)	3828(7)	4557(5)	33(2)
C(8)	11037(10)	3089(7)	4971(4)	30(2)
C(9)	10223(10)	2125(7)	4623(5)	35(2)
C(10)	9916(10)	1965(7)	3901(4)	32(2)
C(11)	9079(9)	1045(7)	3458(5)	29(2)
C(12)	8488(10)	185(7)	3707(5)	36(2)
C(13)	7685(11)	-658(8)	3239(6)	41(2)
C(14)	7585(10)	-593(7)	2536(5)	32(2)

C(15)	8210(10)	280(7)	2316(5)	33(2)
C(16)	11409(11)	3235(7)	5761(5)	35(2)
C(17)	10334(11)	3020(8)	6132(5)	42(2)
C(18)	10721(12)	3155(8)	6867(5)	46(3)
C(19)	12125(12)	3486(7)	7215(5)	38(2)
C(20)	13191(12)	3699(8)	6837(5)	46(3)
C(21)	12826(11)	3592(8)	6099(5)	45(3)
C(22)	12607(15)	3613(8)	8018(5)	50(3)
C(23)	6894(11)	3468(7)	2704(5)	38(2)
C(24)	5504(11)	3785(7)	2475(5)	38(2)
C(25)	4834(12)	3725(8)	1772(6)	48(3)
C(26)	5662(10)	3374(8)	1281(5)	39(2)
C(27)	7085(10)	3045(7)	1534(5)	34(2)
C(28)	8023(10)	2580(7)	1071(5)	30(2)
C(29)	7662(10)	2447(7)	342(5)	33(2)
C(30)	8643(10)	1955(7)	-13(4)	29(2)
C(31)	9991(10)	1632(7)	392(5)	31(2)
C(32)	10353(9)	1811(7)	1113(4)	26(2)
C(33)	11730(9)	1549(7)	1615(5)	30(2)
C(34)	12919(10)	1103(7)	1407(5)	35(2)
C(35)	14208(11)	901(8)	1906(5)	41(2)
C(36)	14239(11)	1168(7)	2615(5)	38(2)
C(37)	13022(10)	1618(7)	2792(5)	36(2)
C(38)	8267(10)	1792(7)	-793(4)	31(2)
C(39)	6806(10)	1936(8)	-1184(5)	37(2)
C(40)	6457(10)	1761(8)	-1918(5)	36(2)
C(41)	7506(10)	1445(7)	-2263(4)	28(2)
C(42)	8928(11)	1301(8)	-1886(5)	41(2)
C(43)	9321(11)	1500(8)	-1161(5)	43(3)
C(44)	7101(11)	1218(7)	-3046(5)	35(2)
B(1)	6011(17)	3038(12)	4504(6)	55(4)

[a] x 10^4

[b] $Å^2$ x 10^3

[c] U(eq) is defined as one third of the trace of the orthogonalized U^{ij} tensor.

Table 64. Atomic coordinates[a] and equivalent isotropic displacement parameters[b] for **10d**

	x	y	z	U(eq)[c]
Zn(1)	-1940(1)	1513(1)	-5729(1)	26(1)
O(1)	-2272(5)	-1549(1)	-8693(4)	52(1)
O(2)	-39(5)	-1596(1)	-8022(4)	61(1)
O(3)	-6355(8)	4466(2)	-4333(5)	104(2)
O(4)	-4359(7)	4681(2)	-4957(7)	121(3)
N(1)	-1866(4)	935(1)	-6137(3)	25(1)
N(2)	215(4)	1325(1)	-5193(3)	27(1)

N(3)	-4064(4)	1405(1)	-6486(3)	29(1)
N(4)	-995(4)	1832(1)	-7011(3)	28(1)
N(5)	-2129(4)	2088(1)	-5311(3)	26(1)
N(6)	-2960(4)	1498(1)	-4235(3)	26(1)
C(1)	1196(6)	1542(2)	-4689(4)	33(1)
C(2)	2530(6)	1399(2)	-4356(4)	37(1)
C(3)	2856(6)	1013(2)	-4540(4)	36(1)
C(4)	1848(6)	788(2)	-5072(4)	33(1)
C(5)	544(5)	951(1)	-5387(4)	27(1)
C(6)	-620(5)	733(1)	-5956(4)	27(1)
C(7)	-481(6)	354(1)	-6303(4)	31(1)
C(8)	-1633(6)	179(1)	-6849(4)	30(1)
C(9)	-2930(6)	396(1)	-6995(4)	30(1)
C(10)	-3006(5)	772(1)	-6634(4)	26(1)
C(12)	-4281(5)	1030(1)	-6747(4)	29(1)
C(13)	-5668(6)	903(2)	-7095(4)	37(1)
C(14)	-6813(6)	1168(2)	-7192(5)	41(1)
C(15)	-6546(6)	1546(2)	-6924(4)	39(1)
C(16)	-5179(6)	1654(2)	-6573(4)	36(1)
C(17)	-1512(6)	-225(1)	-7232(4)	32(1)
C(18)	-252(7)	-442(2)	-7030(5)	46(2)
C(19)	-147(6)	-820(2)	-7373(5)	49(2)
C(20)	-1275(6)	-992(1)	-7928(4)	32(1)
C(21)	-2504(6)	-783(2)	-8129(5)	41(1)
C(22)	-2640(7)	-401(2)	-7787(5)	43(2)
C(23)	-1107(6)	-1412(2)	-8212(5)	38(1)
C(24)	-4074(6)	1877(2)	-2930(4)	34(1)
C(25)	-3339(5)	1845(1)	-3839(4)	27(1)
C(26)	-2934(5)	2181(1)	-4482(4)	28(1)
C(27)	-3312(6)	2566(2)	-4276(4)	34(1)
C(28)	-2868(6)	2855(1)	-4946(4)	32(1)
C(29)	-1992(6)	2756(1)	-5780(4)	32(1)
C(30)	-1654(5)	2368(1)	-5959(4)	28(1)
C(31)	-886(5)	2220(1)	-6856(4)	27(1)
C(32)	-101(6)	2456(2)	-7515(4)	36(1)
C(33)	555(6)	2294(2)	-8364(4)	40(1)
C(34)	419(6)	1899(2)	-8532(4)	37(1)
C(35)	-347(6)	1678(2)	-7831(4)	32(1)
C(36)	-3381(7)	3260(2)	-4819(4)	35(1)
C(37)	-2508(7)	3570(2)	-5064(5)	47(2)
C(38)	-3087(7)	3952(2)	-5005(5)	48(2)
C(39)	-4519(8)	4007(2)	-4721(5)	46(2)
C(40)	-5381(8)	3698(2)	-4487(5)	48(2)
C(41)	-4823(7)	3326(2)	-4518(4)	44(2)
C(42)	-5119(9)	4416(2)	-4666(5)	55(2)
C(43)	-3982(6)	1186(2)	-2781(4)	37(1)

C(44)	-3282(6)	1175(1)	-3703(4)	32(1)
C(45)	-4393(6)	1543(2)	-2385(4)	38(1)
O(5)	-7990(5)	2240(1)	-565(3)	51(1)
O(6)	-6670(5)	2713(1)	5(4)	62(1)
O(7)	-5967(5)	2394(1)	-1311(4)	63(1)
N(7)	-6874(5)	2456(1)	-648(4)	39(1)
C(47)	-870(20)	208(7)	-9907(18)	254(10)
F(1)	-3382(11)	138(3)	-2015(7)	195(4)
F(2)	-4976(17)	292(4)	-4877(12)	317(7)
F(3)	-2780(6)	163(2)	-4196(4)	96(2)
C(46)	-9290(13)	806(3)	-9037(9)	115(4)

[a] x 10^4

[b] $Å^2$ x 10^3

[c] U(eq) is defined as one third of the trace of the orthogonalized U^{ij} tensor.

Table 65. Atomic coordinates[a] and equivalent isotropic displacement parameters[b] for **10e**

	x	y	z	U(eq)[c]
Zn(1)	5075(1)	2528(1)	2553(1)	30(1)
F(1)	4817(8)	7604(6)	3757(5)	139(3)
F(2)	6753(12)	7696(8)	3160(7)	218(5)
F(3)	4670(20)	7442(9)	2373(6)	362(12)
F(4)	5332(10)	6287(5)	3005(5)	159(3)
O(1)	277(5)	6883(3)	-1973(3)	43(1)
O(2)	-226(5)	7775(4)	-793(3)	54(1)
O(3)	9368(4)	-2131(3)	7012(3)	41(1)
O(4)	11021(5)	-831(3)	7555(3)	45(1)
O(5)	12835(10)	797(7)	8085(6)	144(3)
O(6)	1561(8)	6715(6)	3395(5)	114(3)
O(7)	-1206(6)	7894(5)	832(4)	79(2)
O(8)	9303(7)	7234(5)	2409(4)	87(2)
O(9)	1046(6)	9902(5)	-568(4)	77(2)
N(1)	5577(5)	2157(4)	1247(3)	30(1)
N(2)	4050(5)	3382(4)	1836(3)	27(1)
N(3)	4056(5)	3360(3)	3507(3)	28(1)
N(4)	3745(5)	1102(4)	2405(3)	29(1)
N(5)	6128(5)	1774(3)	3366(3)	27(1)
N(6)	6988(5)	3546(4)	3086(3)	32(1)
C(1)	6260(6)	1445(5)	980(4)	38(2)
C(2)	6274(7)	1096(5)	117(4)	42(2)
C(3)	5543(7)	1472(6)	-499(4)	48(2)
C(4)	4854(7)	2221(5)	-243(4)	43(2)
C(5)	4872(5)	2542(4)	634(4)	30(1)
C(6)	4136(6)	3309(4)	982(4)	31(1)
C(7)	3549(6)	3921(4)	486(4)	31(1)

C(8)	2850(6)	4607(4)	880(4)	30(1)
C(9)	2783(6)	4657(4)	1782(3)	29(1)
C(10)	3407(5)	4041(4)	2239(4)	27(1)
C(11)	3443(6)	4049(4)	3199(4)	28(1)
C(12)	2920(6)	4718(5)	3740(4)	37(1)
C(13)	3004(6)	4671(5)	4619(4)	39(2)
C(14)	3636(6)	3970(5)	4941(4)	35(1)
C(15)	4139(6)	3333(5)	4372(4)	33(1)
C(16)	2209(6)	5257(4)	364(4)	31(1)
C(17)	1659(6)	4917(5)	-505(4)	33(1)
C(18)	1038(6)	5518(4)	-985(4)	32(1)
C(19)	941(6)	6461(4)	-613(4)	33(1)
C(20)	1467(6)	6786(4)	250(4)	38(2)
C(21)	2097(6)	6198(4)	736(4)	37(2)
C(22)	259(6)	7104(5)	-1141(4)	38(2)
C(23)	2598(6)	764(5)	1837(4)	35(1)
C(24)	1910(6)	-175(5)	1715(4)	34(1)
C(25)	2382(6)	-821(5)	2206(4)	39(2)
C(26)	3564(6)	-502(5)	2799(4)	35(1)
C(27)	4226(6)	465(4)	2886(4)	29(1)
C(28)	5542(5)	875(4)	3463(3)	27(1)
C(29)	6151(6)	373(4)	4054(4)	31(1)
C(30)	7425(6)	813(4)	4553(3)	28(1)
C(31)	8002(6)	1745(4)	4417(3)	29(1)
C(32)	7335(5)	2217(4)	3823(3)	25(1)
C(33)	7854(6)	3210(4)	3641(3)	29(1)
C(34)	9112(6)	3800(4)	4019(4)	34(1)
C(35)	8538(7)	5077(5)	3280(4)	39(2)
C(36)	7329(6)	4453(5)	2911(4)	37(2)
C(37)	9449(7)	4738(4)	3833(4)	36(1)
C(38)	8108(5)	288(4)	5181(3)	26(1)
C(39)	7738(6)	-717(5)	5121(4)	36(1)
C(40)	8332(6)	-1215(4)	5723(4)	35(1)
C(41)	9362(6)	-709(4)	6381(4)	28(1)
C(42)	9769(6)	292(5)	6422(4)	34(1)
C(43)	9147(6)	788(4)	5833(4)	31(1)
C(44)	9994(6)	-1249(5)	7045(4)	32(1)
B(1)	5442(18)	7246(10)	3015(10)	106(5)

[a] x 10^4

[b] $Å^2$ x 10^3

[c] U(eq) is defined as one third of the trace of the orthogonalized U^{ij} tensor.

Table 66. Atomic coordinates[a] and equivalent isotropic displacement parameters[b] for **10f**

	x	y	z	U(eq)[c]
Zn(1)	2525(1)	1319(1)	2523(1)	37(1)
O(1)	378(10)	1881(5)	-3206(4)	76(3)
O(2)	-1810(11)	1566(5)	-3186(5)	92(4)
O(3)	3944(9)	647(4)	8194(4)	70(3)
O(4)	6170(10)	383(4)	8193(4)	69(3)
O(5)	6075(8)	2253(3)	4998(4)	43(2)
O(6)	5736(7)	-130(3)	9878(3)	40(2)
O(7)	7974(15)	48(5)	5083(7)	40(3)
O(8)	9596(15)	713(6)	5018(7)	43(3)
O(9)	10190(18)	186(7)	5927(9)	59(4)
N(1)	3474(9)	2084(3)	2324(4)	38(2)
N(2)	1954(9)	1389(3)	1456(4)	36(2)
N(3)	1236(9)	599(3)	2172(4)	36(2)
N(4)	712(9)	1661(3)	2848(4)	40(2)
N(5)	3115(9)	1231(3)	3586(4)	37(2)
N(6)	4676(10)	943(4)	2730(4)	43(2)
N(7)	9324(9)	254(3)	5326(4)	41(2)
C(1)	4284(11)	2405(4)	2793(6)	43(2)
C(2)	4996(12)	2844(5)	2622(6)	48(3)
C(3)	4868(14)	2954(5)	1954(6)	54(3)
C(4)	4035(12)	2634(4)	1467(6)	46(3)
C(5)	3368(11)	2194(4)	1659(5)	37(2)
C(6)	2438(11)	1811(4)	1166(5)	39(2)
C(7)	2074(13)	1878(4)	451(5)	46(3)
C(8)	1151(12)	1490(4)	42(5)	41(2)
C(9)	685(12)	1058(4)	370(6)	45(3)
C(10)	1080(11)	1012(4)	1077(5)	39(2)
C(11)	639(11)	567(4)	1487(5)	37(2)
C(12)	-270(12)	164(4)	1214(6)	46(3)
C(13)	-635(13)	-224(5)	1640(6)	52(3)
C(14)	-66(12)	-194(4)	2330(6)	46(3)
C(15)	832(11)	219(4)	2572(6)	44(2)
C(16)	720(12)	1531(4)	-718(5)	44(2)
C(17)	1750(13)	1741(5)	-1067(5)	47(3)
C(18)	1305(12)	1774(5)	-1772(5)	48(3)
C(19)	-63(12)	1640(5)	-2132(5)	47(3)
C(20)	-1071(12)	1467(5)	-1783(6)	49(3)
C(21)	-668(12)	1396(4)	-1070(5)	44(2)
C(22)	-495(13)	1707(5)	-2900(5)	52(3)
C(23)	-497(12)	1882(5)	2426(6)	48(3)
C(24)	-1656(13)	2079(5)	2688(6)	54(3)
C(25)	-1461(15)	2086(5)	3377(6)	62(3)

C(26)	-293(14)	1857(5)	3813(6)	56(3)
C(27)	798(11)	1646(4)	3545(5)	41(2)
C(28)	2152(11)	1384(4)	3953(5)	39(2)
C(29)	2452(11)	1301(4)	4651(5)	39(2)
C(30)	3706(11)	1006(5)	4979(5)	44(2)
C(31)	4678(11)	867(4)	4578(5)	41(2)
C(32)	4340(11)	987(4)	3883(5)	38(2)
C(33)	5302(11)	865(4)	3416(5)	42(2)
C(34)	6734(12)	698(5)	3635(6)	50(3)
C(35)	7536(14)	604(6)	3121(8)	69(4)
C(36)	6972(16)	695(5)	2472(6)	62(3)
C(37)	5449(13)	853(5)	2269(6)	54(3)
C(38)	4049(11)	884(4)	5737(5)	40(2)
C(39)	2963(13)	942(6)	6094(6)	58(3)
C(40)	3272(11)	833(5)	6784(5)	50(3)
C(41)	4593(13)	653(4)	7131(6)	45(3)
C(42)	5684(12)	588(4)	6785(5)	45(3)
C(43)	5384(12)	697(5)	6084(6)	49(3)
C(44)	4947(13)	561(5)	7902(6)	49(3)
O(10)	6064(11)	2686(4)	4768(5)	78(3)
O(11)	4591(12)	2384(5)	4739(6)	90(3)

[a] x 10^4

[b] $Å^2$ x 10^3

[c] U(eq) is defined as one third of the trace of the orthogonalized U^{ij} tensor.

Table 67. Atomic coordinates[a] and equivalent isotropic displacement parameters[b] for **10h**

	x	y	z	U(eq)[c]
Ni(1)	8741(1)	2204(1)	2049(1)	48(1)
O(1)	4860(7)	-2621(7)	6585(6)	64(2)
O(2)	13948(7)	6325(6)	-2455(6)	56(2)
O(3)	15499(7)	6390(6)	-1541(6)	60(2)
O(8)	5181(9)	-1044(7)	7716(7)	89(3)
N(1)	7582(6)	2254(6)	983(6)	41(2)
N(2)	7752(7)	1423(5)	2773(6)	44(2)
N(3)	8292(8)	587(7)	1262(6)	53(2)
N(7)	9832(8)	2926(7)	1326(7)	46(2)
N(8)	10304(7)	2328(7)	2717(6)	45(2)
N(9)	8805(8)	3549(7)	3226(6)	51(2)
C(1)	5635(9)	-1030(9)	6189(8)	50(3)
C(2)	5185(9)	-1612(10)	6890(8)	51(3)
C(3)	7427(9)	494(13)	2627(8)	64(4)
C(4)	5384(12)	-1660(9)	5192(9)	66(3)
C(5)	12544(12)	2547(13)	3453(10)	83(5)
C(6)	7192(10)	1553(10)	4329(8)	56(3)

C(7)	7579(9)	-144(8)	1621(8)	46(2)
C(8)	6392(9)	-55(8)	4829(8)	49(3)
C(9)	7689(10)	2069(10)	3691(8)	57(3)
C(10)	10128(10)	3651(9)	49(8)	55(3)
C(11)	10937(8)	3123(9)	1517(7)	42(2)
C(12)	8037(9)	3984(8)	4630(7)	48(2)
C(13)	6614(12)	559(10)	5823(9)	65(3)
C(14)	11277(9)	2812(9)	2360(8)	46(3)
C(15)	11284(9)	3876(8)	263(8)	43(2)
C(16)	7424(10)	2644(9)	-506(8)	54(3)
C(17)	13626(9)	5524(8)	-1255(8)	46(3)
C(18)	10540(11)	2016(11)	3481(9)	68(4)
C(19)	14095(10)	5530(10)	-336(9)	62(3)
C(20)	5701(11)	1714(12)	-34(10)	68(4)
C(21)	9257(10)	4526(9)	3321(8)	54(3)
C(22)	14477(11)	6150(9)	-1764(9)	52(3)
C(23)	7149(10)	-1214(9)	1188(8)	53(3)
C(24)	6925(10)	-133(10)	3205(8)	56(3)
C(25)	8135(9)	3200(9)	3849(8)	46(2)
C(26)	11703(10)	3618(8)	1029(8)	49(3)
C(27)	12117(9)	4473(9)	-247(8)	47(3)
C(28)	13244(10)	4893(10)	80(9)	64(3)
C(29)	8517(11)	5029(11)	4724(9)	64(3)
C(30)	8128(10)	2729(9)	353(8)	49(3)
C(31)	9351(10)	3079(9)	522(8)	49(3)
C(32)	11611(10)	2099(10)	3837(9)	62(3)
C(33)	6852(9)	496(8)	4139(8)	49(3)
C(34)	8002(11)	-924(9)	-121(9)	67(3)
C(35)	6433(8)	1809(8)	815(8)	43(2)
C(36)	8450(11)	143(9)	352(8)	62(3)
C(37)	11708(10)	4528(11)	-1144(9)	60(3)
C(38)	12342(10)	2888(9)	2668(8)	52(3)
C(39)	7355(12)	-1632(9)	271(9)	64(3)
C(40)	6204(12)	23(11)	6458(10)	74(4)
C(41)	6271(10)	2205(11)	-648(9)	67(4)
C(42)	9197(10)	5370(10)	4106(9)	57(3)
C(43)	12480(10)	5103(10)	-1588(9)	58(3)
C(44)	5786(13)	-1138(11)	4545(10)	80(4)
F(34)	1096(7)	5838(7)	1925(6)	88(2)
F(60)	1617(9)	6770(6)	3500(6)	98(3)
F(78)	2203(9)	5470(6)	2931(6)	99(3)
F(102)	2924(8)	7017(7)	2563(7)	99(3)
B(142)	1945(15)	6235(10)	2695(9)	56(4)
O(7)	5792(10)	7131(8)	2254(8)	97(4)
N(13)	5637(13)	6159(10)	3267(10)	82(4)
C(89)	5191(14)	6451(10)	2563(11)	71(4)

C(90)	4915(18)	5463(12)	3704(12)	105(6)
C(91)	6860(20)	6585(17)	3524(17)	145(9)
O(200)	167(13)	1789(15)	5463(11)	153(6)
N(200)	13(11)	1376(10)	6815(9)	79(3)
C(200)	-430(20)	1433(19)	7682(13)	149(9)
C(201)	680(30)	780(20)	6640(20)	195(13)
C(202)	-169(17)	1851(18)	6200(15)	115(7)

[a] x 10^4

[b] $Å^2$ x 10^3

[c] U(eq) is defined as one third of the trace of the orthogonalized U^{ij} tensor.

Table 68. Atomic coordinates[a] and equivalent isotropic displacement parameters[b] for **10i**

	x	y	z	U(eq)[c]
Co(3)	8786(1)	2321(1)	2950(1)	29(1)
O(1)	13368(7)	2683(4)	7455(3)	45(2)
O(2)	14604(7)	1652(5)	7163(3)	47(2)
O(3)	4139(7)	2569(5)	-1502(3)	51(2)
O(4)	3034(8)	1473(5)	-1271(3)	62(2)
N(1)	7789(7)	3211(5)	3405(3)	34(2)
N(2)	9763(7)	2336(5)	3684(3)	29(2)
N(3)	10157(8)	1435(5)	2792(3)	31(2)
N(4)	9812(7)	3139(5)	2486(3)	30(2)
N(5)	7854(7)	2282(5)	2228(3)	27(2)
N(6)	7420(7)	1496(5)	3158(3)	30(2)
C(1)	6736(10)	3660(7)	3230(5)	45(3)
C(2)	6257(12)	4273(8)	3566(6)	57(3)
C(3)	6840(12)	4431(8)	4101(5)	58(4)
C(4)	7899(11)	3993(7)	4296(5)	48(3)
C(5)	8323(9)	3392(6)	3953(4)	30(2)
C(6)	9433(9)	2865(6)	4120(4)	30(2)
C(7)	10101(9)	2865(6)	4660(4)	31(2)
C(8)	11126(9)	2338(6)	4774(4)	32(2)
C(9)	11456(9)	1806(6)	4305(4)	31(2)
C(10)	10760(9)	1825(6)	3770(4)	29(2)
C(11)	10995(9)	1282(6)	3261(4)	28(2)
C(12)	11936(10)	716(6)	3236(4)	37(3)
C(13)	12011(11)	242(7)	2740(5)	43(3)
C(14)	11216(11)	355(7)	2280(4)	42(3)
C(15)	10263(9)	951(6)	2304(4)	29(2)
C(16)	11821(9)	2293(6)	5347(4)	32(2)
C(17)	12780(10)	1714(6)	5472(4)	38(3)
C(18)	13448(11)	1701(6)	6022(4)	42(3)
C(19)	13141(9)	2235(6)	6464(4)	33(2)
C(20)	12189(11)	2801(8)	6344(5)	56(4)

C(21)	11597(11)	2856(8)	5794(4)	58(4)
C(22)	13778(10)	2154(7)	7055(4)	34(3)
C(23)	10847(10)	3587(6)	2678(4)	36(3)
C(24)	11428(9)	4149(6)	2323(5)	36(2)
C(25)	10935(11)	4267(7)	1755(5)	47(3)
C(26)	9873(10)	3818(6)	1540(4)	38(3)
C(27)	9357(10)	3252(6)	1922(4)	32(2)
C(28)	8227(9)	2739(6)	1768(4)	31(2)
C(29)	7624(9)	2672(7)	1210(4)	38(2)
C(30)	6566(9)	2157(6)	1125(4)	36(3)
C(31)	6185(10)	1697(6)	1619(4)	38(3)
C(32)	6831(9)	1768(6)	2145(4)	30(2)
C(33)	6589(9)	1303(6)	2699(4)	33(2)
C(34)	5622(10)	702(6)	2727(4)	37(2)
C(35)	5498(10)	307(6)	3266(5)	40(3)
C(36)	6346(10)	503(6)	3743(4)	35(2)
C(37)	7264(11)	1080(7)	3664(4)	44(3)
C(38)	5916(9)	2090(6)	537(4)	34(2)
C(39)	6069(11)	2654(8)	97(5)	56(3)
C(40)	5407(11)	2636(8)	-439(5)	57(3)
C(41)	4543(9)	2020(7)	-556(4)	35(2)
C(42)	4384(12)	1455(8)	-144(5)	60(4)
C(43)	5058(12)	1485(8)	391(5)	56(3)
C(44)	3849(11)	2001(8)	-1163(5)	43(3)
O(5)	9011(13)	779(8)	823(6)	128(5)
O(6)	8631(17)	1001(10)	5113(8)	178(7)

[a] x 10^4

[b] $Å^2$ x 10^3

[c] U(eq) is defined as one third of the trace of the orthogonalized U^{ij} tensor.

Table 69. Atomic coordinates[a] and equivalent isotropic displacement parameters[b] for **10j**

	x	y	z	U(eq)[c]
Co(2)	4702(2)	5196(1)	2517(1)	61(1)
O(1)	5473(13)	9381(9)	-2077(4)	113(3)
O(2)	3407(16)	10869(9)	-1703(3)	145(5)
O(3)	3385(9)	-390(7)	6849(3)	91(3)
O(4)	5488(10)	251(8)	6889(3)	101(3)
N(1)	6193(10)	3868(7)	2029(3)	64(2)
N(2)	4789(10)	6097(8)	1778(3)	64(2)
N(3)	3259(9)	6784(7)	2815(3)	59(2)
N(4)	3109(9)	4298(7)	2453(3)	62(2)
N(5)	4647(7)	4277(6)	3249(2)	44(2)
N(6)	6281(9)	5826(7)	2793(3)	56(2)
C(1)	6866(13)	2697(10)	2206(4)	69(3)

C(2)	7975(14)	1810(11)	1812(4)	79(3)
C(3)	8404(17)	2216(11)	1234(5)	103(4)
C(4)	7592(18)	3428(11)	1048(5)	109(5)
C(5)	6490(15)	4218(9)	1431(4)	76(3)
C(6)	5617(14)	5516(10)	1281(4)	72(3)
C(7)	5676(19)	6148(10)	722(4)	112(5)
C(8)	4701(18)	7370(11)	693(4)	105(5)
C(9)	3873(15)	7957(10)	1214(4)	83(4)
C(10)	3884(15)	7273(11)	1753(4)	86(4)
C(11)	2911(13)	7720(11)	2359(4)	75(3)
C(12)	1927(15)	8862(11)	2471(5)	84(4)
C(13)	1119(13)	9080(11)	3051(5)	80(3)
C(14)	1428(13)	8130(12)	3493(5)	77(3)
C(15)	2509(11)	7020(10)	3359(4)	60(3)
C(16)	4770(20)	8046(11)	67(5)	127(7)
C(17)	5820(20)	7707(12)	-395(4)	132(7)
C(18)	5710(20)	8355(12)	-946(5)	145(8)
C(19)	4540(20)	9267(11)	-1039(5)	113(6)
C(20)	3380(30)	9609(13)	-558(5)	169(9)
C(21)	3470(20)	9016(11)	15(5)	133(7)
C(22)	4490(20)	9923(14)	-1660(6)	117(6)
C(23)	1099(15)	3855(12)	2042(5)	106(5)
C(24)	2319(14)	4434(11)	2016(4)	91(4)
C(25)	728(14)	3072(14)	2517(5)	108(5)
C(26)	1583(14)	2900(12)	2988(4)	95(4)
C(27)	2735(12)	3533(9)	2947(4)	64(3)
C(28)	3625(11)	3521(9)	3412(4)	58(2)
C(29)	3589(9)	2820(8)	3941(3)	50(2)
C(30)	4518(9)	2946(8)	4334(3)	43(2)
C(31)	5524(9)	3792(8)	4170(3)	46(2)
C(32)	5558(9)	4435(8)	3606(3)	43(2)
C(33)	6557(10)	5304(8)	3341(3)	46(2)
C(34)	7690(9)	5592(9)	3579(4)	53(2)
C(35)	8538(11)	6379(10)	3251(4)	68(3)
C(36)	8270(10)	6950(9)	2717(4)	57(2)
C(37)	7125(11)	6625(9)	2506(4)	63(3)
C(38)	4517(10)	2213(8)	4920(3)	50(2)
C(39)	3204(11)	1796(10)	5214(4)	68(3)
C(40)	3205(12)	1125(10)	5767(4)	72(3)
C(41)	4417(10)	890(8)	6027(3)	51(2)
C(42)	5640(12)	1278(10)	5750(4)	72(3)
C(43)	5726(11)	1901(11)	5183(4)	73(3)
C(44)	4380(14)	210(10)	6639(4)	73(3)
F(6)	9603(19)	5853(14)	1041(8)	262(7)
B(14)	1118(18)	6585(14)	1192(9)	102(5)
F(18)	260(20)	7075(12)	312(4)	304(10)

F(19)	1650(30)	5550(20)	562(7)	413(14)
O(5)	7799(9)	4309(8)	5178(4)	103(3)
O(6)	-1589(10)	1841(9)	3417(4)	111(3)
O(7)	9682(15)	-1039(13)	1449(6)	183(5)
O(8)	14(18)	1415(18)	4423(7)	241(7)

[a] x 10^4

[b] $Å^2$ x 10^3

[c] U(eq) is defined as one third of the trace of the orthogonalized U^{ij} tensor.

Table 70. Atomic coordinates[a] and equivalent isotropic displacement parameters[b] for **11**

	x	y	z	U(eq)[c]
O(1)	3121(1)	794(2)	1154(1)	32(1)
O(2)	3750(1)	355(2)	2109(1)	35(1)
N(1)	9300(1)	-1972(2)	-1401(1)	25(1)
N(2)	11168(1)	-3124(2)	-66(1)	23(1)
N(3)	12141(1)	-3788(2)	1470(1)	31(1)
C(1)	3983(2)	362(2)	1580(1)	26(1)
C(2)	5283(2)	-143(2)	1317(1)	24(1)
C(3)	5582(2)	370(2)	736(1)	25(1)
C(4)	6181(2)	-1208(2)	1646(1)	25(1)
C(5)	7342(2)	-1785(2)	1384(1)	26(1)
C(6)	6749(2)	-188(2)	478(1)	25(1)
C(7)	7639(2)	-1303(2)	794(1)	22(1)
C(8)	8862(2)	-1948(2)	499(1)	22(1)
C(9)	9965(2)	-2473(2)	828(1)	24(1)
C(10)	11457(2)	-3246(2)	-1296(1)	28(1)
C(11)	8944(2)	-2036(2)	-122(1)	24(1)
C(12)	10115(2)	-2589(2)	-388(1)	22(1)
C(13)	11085(2)	-3077(2)	532(1)	23(1)
C(14)	12258(2)	-3727(2)	874(1)	24(1)
C(15)	13410(2)	-4234(2)	589(1)	31(1)
C(16)	14463(2)	-4834(3)	933(1)	35(1)
C(17)	14350(2)	-4928(2)	1543(1)	34(1)
C(18)	13171(2)	-4386(3)	1791(1)	36(1)
C(19)	10286(2)	-2611(2)	-1050(1)	22(1)
C(20)	11624(2)	-3183(2)	-1906(1)	32(1)
C(21)	9480(2)	-1940(2)	-1993(1)	31(1)
C(22)	10624(2)	-2505(3)	-2266(1)	34(1)

[a] x 10^4

[b] $Å^2$ x 10^3

[c] U(eq) is defined as one third of the trace of the orthogonalized U^{ij} tensor.

Table 71. Atomic coordinates[a] and equivalent isotropic displacement parameters[b] for **12**

	x	y	z	U(eq)[c]
Cd(1)	5000	-1347(1)	7500	30(1)
O(4)	3329(4)	-1345(1)	7780(5)	46(1)
O(3)	6272(4)	-2170(2)	7922(5)	52(1)
N(1)	3765(3)	-985(2)	5041(4)	29(1)
N(3)	5000	-280(2)	7500	23(1)
C(1)	3187(5)	-1355(2)	3834(6)	35(1)
C(2)	2469(4)	-1139(2)	2404(5)	38(1)
C(3)	2326(4)	-495(2)	2172(5)	37(1)
C(4)	2927(4)	-105(2)	3406(5)	33(1)
C(5)	3643(3)	-362(2)	4828(4)	24(1)
C(6)	4342(4)	31(2)	6205(4)	24(1)
C(7)	4325(4)	679(2)	6168(4)	27(1)
C(8)	5000	1016(3)	7500	25(1)
C(9)	5000	1705(3)	7500	26(1)
C(10)	4180(6)	2044(2)	6211(5)	48(1)
C(11)	4196(6)	2678(2)	6229(5)	52(2)
C(12)	5000	3008(3)	7500	36(1)
O(5)	545(7)	179(3)	8697(9)	117(2)
N(5)	0	1113(3)	7500	36(1)
C(15)	0	511(3)	7500	37(1)
C(14)	566(5)	1465(2)	8877(6)	47(1)
N(4)	3090(3)	-1904(2)	7388(4)	34(1)
O(2)	2291(4)	-2183(2)	7335(5)	59(1)
O(1)	4257(4)	3985(2)	6299(5)	62(1)
C(13)	5000	3706(4)	7500	48(2)

[a] x 10^4
[b] $Å^2$ x 10^3
[c] U(eq) is defined as one third of the trace of the orthogonalized U^{ij} tensor.

Table 72. Atomic coordinates[a] and equivalent isotropic displacement parameters[b] for **13**

	x	y	z	U(eq)[c]
Zn(1)	5400(1)	4600(1)	4600(1)	146(2)
Ru(1)	5000	0	5000	845(8)
O(1)	4071(15)	4071(15)	4071(15)	740(40)
O(2)	5301(3)	4726(3)	3920(3)	153(3)
O(3)	5000	5000	5000	110(11)

C(1)	5000	5000	3088(5)	370(20)
C(2)	5000	5000	3791(7)	121(9)
C(3)	5000	5000	1565(6)	290(17)
C(4)	4451(6)	4451(6)	4451(6)	1300(110)

[a] x 10^4
[b] $Å^2$ x 10^3
[c] U(eq) is defined as one third of the trace of the orthogonalized U^{ij} tensor.

Table 73. Anisotropic displacement parameters for **13**[d]

	U^{11}	U^{22}	U^{33}	U^{23}	U^{13}	U^{12}
Zn(1)	146(2)	146(2)	146(2)	0(2)	0(2)	0(2)
Ru(1)	1174(16)	170(3)	1192(16)	0	0	0
O(1)	740(40)	740(40)	740(40)	10(50)	10(50)	10(50)
O(2)	95(7)	210(9)	155(8)	-33(8)	-8(7)	40(8)
O(3)	110(11)	110(11)	110(11)	0	0	0
C(1)	600(50)	520(40)	0(11)	0	0	-470(40)
C(2)	0(5)	260(20)	100(14)	0	0	157(10)
C(3)	410(40)	410(40)	47(15)	0	0	-170(30)
C(4)	1300(110)	1300(110)	1300(110)	-680(60)	-680(60)	-680(60)

REFERENCES

1. Ferey, G., Hybrid porous solids: past, present, future. *Chemical Society Reviews* **2008,** *37* (1), 191-214.
2. Kitagawa, S.; Kitaura, R.; Noro, S., Functional porous coordination polymers. *Angewandte Chemie-International Edition* **2004,** *43* (18), 2334-2375.
3. Rao, C. N. R.; Cheetham, A. K.; Thirumurugan, A., Hybrid inorganic-organic materials: a new family in condensed matter physics. *Journal of Physics-Condensed Matter* **2008,** *20* (8).
4. Constable, E. C.; Dunphy, E. L.; Housecroft, C. E.; Neuburger, M.; Schaffner, S.; Schaper, F.; Batten, S. R.; Zf, Expanded ligands: bis(2,2 ': 6 ',2 "-terpyridine carboxylic acid) ruthenium(II) complexes as metallosupramolecular analogues of dicarboxylic acids. *Dalton Transactions* **2007,** (38), 4323-4332.
5. Li, H.; Eddaoudi, M.; O'Keeffe, M.; Yaghi, O. M., Design and synthesis of an exceptionally stable and highly porous metal-organic framework. *Nature* **1999,** *402* (6759), 276-279.
6. Schlapbach, L.; Zuttel, A., Hydrogen-storage materials for mobile applications. *Nature* **2001,** *414* (6861), 353-358.
7. FreedomCAR/DOE hydrogen storage technical targets explanation, http://www.eere.energy.gov/hydrogenandfuelcells/pdfs/freedomcar_targets_explanations.pdf, November 2008.
8. van den Berg, A. W. C.; Arean, C. O., Materials for hydrogen storage: current research trends and perspectives. *Chemical Communications* **2008,** (6), 668-681.
9. Wang, P.; Kang, X. D., Hydrogen-rich boron-containing materials for hydrogen storage. *Dalton Transactions* **2008,** (40), 5400-5413.
10. Cumalioglu, I.; Ertas, A.; Ma, Y.; Maxwell, T., State of the art: Hydrogen storage. *Journal of Fuel Cell Science and Technology* **2008,** *5* (3).
11. Morris, R. E.; Wheatley, P. S., Gas storage in nanoporous materials. *Angewandte Chemie-International Edition* **2008,** *47* (27), 4966-4981.
12. Rosi, N. L.; Eckert, J.; Eddaoudi, M.; Vodak, D. T.; Kim, J.; O'Keeffe, M.; Yaghi, O. M., Hydrogen storage in microporous metal-organic frameworks. *Science* **2003,** *300* (5622), 1127-1129.
13. Rowsell, J. L. C.; Yaghi, O. M., Effects of functionalization, catenation, and variation of the metal oxide and organic linking units on the low-pressure hydrogen adsorption properties of metal-organic frameworks. *Journal of the American Chemical Society* **2006,** *128* (4), 1304-1315.
14. Dinca, M.; Long, J. R., Hydrogen storage in microporous metal-organic frameworks with exposed metal sites. *Angewandte Chemie-International Edition* **2008,** *47* (36), 6766-6779.

15. Lin, X.; Jia, J. H.; Hubberstey, P.; Schroder, M.; Champness, N. R., Hydrogen storage in metal-organic frameworks. *Crystengcomm* **2007,** *9* (6), 438-448.
16. Rowsell, J. L. C.; Yaghi, O. M.; Hx, Strategies for hydrogen storage in metal-organic frameworks. *Angewandte Chemie-International Edition* **2005,** *44* (30), 4670-4679.
17. Eddaoudi, M.; Moler, D. B.; Li, H. L.; Chen, B. L.; Reineke, T. M.; O'Keeffe, M.; Yaghi, O. M., Modular chemistry: Secondary building units as a basis for the design of highly porous and robust metal-organic carboxylate frameworks. *Accounts of Chemical Research* **2001,** *34* (4), 319-330.
18. O'Keeffe, M.; Eddaoudi, M.; Li, H. L.; Reineke, T.; Yaghi, O. M., Frameworks for extended solids: Geometrical design principles. *Journal of Solid State Chemistry* **2000,** *152* (1), 3-20.
19. Ockwig, N. W.; Delgado-Friedrichs, O.; O'Keeffe, M.; Yaghi, O. M., Reticular chemistry: Occurrence and taxonomy of nets and grammar for the design of frameworks. *Accounts of Chemical Research* **2005,** *38* (3), 176-182.
20. Rowsell, J. L. C.; Yaghi, O. M., Metal-organic frameworks: a new class of porous materials. *Microporous and Mesoporous Materials* **2004,** *73* (1-2), 3-14.
21. Yaghi, O. M.; O'Keeffe, M.; Ockwig, N. W.; Chae, H. K.; Eddaoudi, M.; Kim, J., Reticular synthesis and the design of new materials. *Nature* **2003,** *423* (6941), 705-714.
22. Furukawa, H.; Miller, M. A.; Yaghi, O. M., Independent verification of the saturation hydrogen uptake in MOF-177 and establishment of a benchmark for hydrogen adsorption in metal-organic frameworks. *Journal of Materials Chemistry* **2007,** *17* (30), 3197-3204.
23. Chae, H. K.; Siberio-Perez, D. Y.; Kim, J.; Go, Y.; Eddaoudi, M.; Matzger, A. J.; O'Keeffe, M.; Yaghi, O. M., A route to high surface area, porosity and inclusion of large molecules in crystals. *Nature* **2004,** *427* (6974), 523-527.
24. Dinca, M.; Dailly, A.; Liu, Y.; Brown, C. M.; Neumann, D. A.; Long, J. R., Hydrogen storage in a microporous metal-organic framework with exposed Mn2+ coordination sites. *Journal of the American Chemical Society* **2006,** *128* (51), 16876-16883.
25. Panella, B.; Hones, K.; Muller, U.; Trukhan, N.; Schubert, M.; Putter, H.; Hirscher, M., Desorption studies of hydrogen in metal-organic frameworks. *Angewandte Chemie-International Edition* **2008,** *47* (11), 2138-2142.
26. Rowsell, J. L. C.; Spencer, E. C.; Eckert, J.; Howard, J. A. K.; Yaghi, O. M., Gas adsorption sites in a large-pore metal-organic framework. *Science* **2005,** *309* (5739), 1350-1354.
27. Spencer, E. C.; Howard, J. A. K.; McIntyre, G. J.; Rowsell, J. L. C.; Yaghi, O. M., Determination of the hydrogen absorption sites in Zn4O(1,4-benzenedicarboxylate) by single crystal neutron diffraction. *Chemical Communications* **2006,** (3), 278-280.
28. Belof, J. L.; Stern, A. C.; Eddaoudi, M.; Space, B., On the mechanism of hydrogen storage in a metal-organic framework material. *Journal of the American Chemical Society* **2007,** *129* (49), 15202-15210.
29. Yildirim, T.; Hartman, M. R., Direct observation of hydrogen adsorption sites and nanocage formation in metal-organic frameworks. *Physical Review Letters* **2005,** *95* (21).
30. Blomqvist, A.; Araujo, C. M.; Srepusharawoot, P.; Ahuja, R., Li-decorated metal-organic framework 5: A route to achieving a suitable hydrogen storage medium. *Proceedings of the National Academy of Sciences of the United States of America* **2007,** *104* (51), 20173-20176.

31. Frost, H.; Duren, T.; Snurr, R. Q., Effects of surface area, free volume, and heat of adsorption on hydrogen uptake in metal-organic frameworks. *Journal of Physical Chemistry B* **2006,** *110* (19), 9565-9570.
32. Frost, H.; Snurr, R. Q., Design requirements for metal-organic frameworks as hydrogen storage materials. *Journal of Physical Chemistry C* **2007,** *111* (50), 18794-18803.
33. Lochan, R. C.; Khaliullin, R. Z.; Head-Gordon, M., Interaction of molecular hydrogen with open transition metal centers for enhanced binding in metal-organic frameworks: A computational study. *Inorganic Chemistry* **2008,** *47* (10), 4032-4044.
34. Mueller, T.; Ceder, G., A density functional theory study of hydrogen adsorption in MOF-5. *Journal of Physical Chemistry B* **2005,** *109* (38), 17974-17983.
35. Sagara, T.; Klassen, J.; Ganz, E., Computational study of hydrogen binding by metal-organic framework-5. *Journal of Chemical Physics* **2004,** *121* (24), 12543-12547.
36. Sagara, T.; Klassen, J.; Ortony, J.; Ganz, E., Binding energies of hydrogen molecules to isoreticular metal-organic framework materials. *Journal of Chemical Physics* **2005,** *123* (1).
37. Sagara, T.; Ortony, J.; Ganz, E., New isoreticular metal-organic framework materials for high hydrogen storage capacity. *Journal of Chemical Physics* **2005,** *123* (21).
38. Samanta, A.; Furuta, T.; Li, J., Theoretical assessment of the elastic constants and hydrogen storage capacity of some metal-organic framework materials. *Journal of Chemical Physics* **2006,** *125* (8).
39. Song, M. K.; No, K. T., Molecular simulation of hydrogen adsorption in organic zeolite. *Catalysis Today* **2007,** *120* (3-4), 374-382.
40. Trewin, A.; Darling, G. R.; Cooper, A. I., "Naked" fluoride binding sites for physisorptive hydrogen storage. *New Journal of Chemistry* **2008,** *32* (1), 17-20.
41. Yang, Q. Y.; Zhong, C. L., Understanding hydrogen adsorption in metal-organic frameworks with open metal sites: A computational study. *Journal of Physical Chemistry B* **2006,** *110* (2), 655-658.
42. Yang, Q. Y.; Zhong, C. L., Molecular simulation of adsorption and diffusion of hydrogen in metal-organic frameworks. *Journal of Physical Chemistry B* **2005,** *109* (24), 11862-11864.
43. Kuc, A.; Heine, T.; Seifert, G.; Duarte, H. A., H-2 adsorption in metal-organic frameworks: Dispersion or electrostatic interactions? *Chemistry-a European Journal* **2008,** *14* (22), 6597-6600.
44. Lochan, R. C.; Head-Gordon, M., Computational studies of molecular hydrogen binding affinities: The role of dispersion forces, electrostatics, and orbital interactions. *Physical Chemistry Chemical Physics* **2006,** *8* (12), 1357-1370.
45. Kesanli, B.; Cui, Y.; Smith, M. R.; Bittner, E. W.; Bockrath, B. C.; Lin, W. B., Highly interpenetrated metal-organic frameworks for hydrogen storage. *Angewandte Chemie-International Edition* **2005,** *44* (1), 72-75.
46. Luo, J. H.; Xu, H. W.; Liu, Y.; Zhao, Y. S.; Daemen, L. L.; Brown, C.; Timofeeva, T. V.; Ma, S. Q.; Zhou, H. C., Hydrogen adsorption in a highly stable porous rare-earth metal-organic framework: Sorption properties and neutron diffraction studies. *Journal of the American Chemical Society* **2008,** *130* (30), 9626-+.
47. Rowsell, J. L. C.; Millward, A. R.; Park, K. S.; Yaghi, O. M., Hydrogen sorption in functionalized metal-organic frameworks. *Journal of the American Chemical Society* **2004,** *126* (18), 5666-5667.

48. Chen, B. L.; Ockwig, N. W.; Millward, A. R.; Contreras, D. S.; Yaghi, O. M., High H-2 adsorption in a microporous metal-organic framework with open metal sites. *Angewandte Chemie-International Edition* **2005,** *44* (30), 4745-4749.
49. Kitaura, R.; Onoyama, G.; Sakamoto, H.; Matsuda, R.; Noro, S.; Kitagawa, S., Immobilization of a metallo Schiff base into a microporous coordination polymer. *Angewandte Chemie-International Edition* **2004,** *43* (20), 2684-2687.
50. Smithenry, D. W.; Wilson, S. R.; Suslick, K. S., A robust microporous zinc porphyrin framework solid. *Inorganic Chemistry* **2003,** *42* (24), 7719-7721.
51. Kosal, M. E.; Chou, J. H.; Wilson, S. R.; Suslick, K. S., A functional zeolite analogue assembled from metalloporphyrins. *Nature Materials* **2002,** *1* (2), 118-121.
52. Constable, E. C., Expanded ligands - An assembly principle for supramolecular chemistry. *Coordination Chemistry Reviews* **2008,** *252* (8-9), 842-855.
53. Beves, J. E.; Constable, E. C.; Housecroft, C. E.; Kepert, C. J.; Price, D. J., The first example of a coordination polymer from the expanded 4,4 '-bipyridine ligand [Ru(pytpy)(2)](2+) (pytpy=4 '-(4-pyridyl)2,2 ': 6 ',2 "-terpyridine). *Crystengcomm* **2007,** *9* (6), 456-459.
54. Beves, J. E.; Constable, E. C.; Housecroft, C. E.; Neuburger, M.; Schaffner, S., A one-dimensional copper(II) coordination polymer containing [Fe(pytpy)(2)](2+) (pytpy=4 '-(4-pyridyl)-2,2 ': 6 ',2 "-terpyridine) as an expanded 4,4 '-bipyridine ligand: a hydrogen-bonded network penetrated by rod-like polymers. *Crystengcomm* **2008,** *10* (3), 344-348.
55. Feng, H.; Zhou, X. P.; Wu, T.; Li, D.; Yin, Y. G.; Ng, S. W., Hydrothermal synthesis of copper complexes of 4 '-pyridyl terpyridine: From discrete monomer to zigzag chain polymer. *Inorganica Chimica Acta* **2006,** *359* (12), 4027-4035.
56. Gou, L.; Wu, Q. R.; Hu, H. M.; Qin, T.; Xue, G. L.; Yang, M. L.; Tang, Z. X., An investigation of the positional isomeric effect of terpyridine derivatives: Self-assembly of novel cadmium coordination architectures driven by N-donor covalence and pi...pi non-covalent interactions. *Polyhedron* **2008,** *27* (5), 1517-1526.
57. Hou, L.; Li, D.; Shi, W. J.; Yin, Y. G.; Ng, S. W., Ligand-controlled mixed-valence copper rectangular grid-type coordination polymers based on pyridylterpyridine. *Inorganic Chemistry* **2005,** *44* (22), 7825-7832.
58. Kawahara, M.; Kabir, K.; Yamada, K.; Adachi, K.; Kumagai, H.; Narumi, Y.; Kindo, K.; Kitagawa, S.; Kawata, S., Module-based assembly of copper(II) chloranilate compounds: Syntheses, crystal structures, and magnetic properties of {[Cu-2(CA)(terpy)(2)][Cu(CA)(2)]}(n) and (Cu-2(CA)(terpy)(2)(dmso)(2)][Cu(CA)(2)(dmso)(2)](EtOH)}(n) (H(2)CA = chloranilic acid, terpy = 2,2 ': 6 ',2 "-terpyridine, dmso = dimethyl sulfoxide). *Inorganic Chemistry* **2004,** *43* (1), 92-100.
59. Luan, X. J.; Cai, X. H.; Wang, Y. Y.; Li, D. S.; Wang, C. J.; Liu, P.; Hu, H. M.; Shi, Q. Z.; Peng, S. M., An investigation of the self-assembly of neutral, interlaced, triple-stranded molecular braids. *Chemistry-a European Journal* **2006,** *12* (24), 6281-6289.
60. Zhang, S. S.; Zhan, S. Z.; Li, M.; Peng, R.; Li, D., A rare chiral self-catenated network formed by two cationic and one anionic frameworks. *Inorganic Chemistry* **2007,** *46* (11), 4365-4367.
61. Gregg, B. A., Excitonic solar cells. *Journal of Physical Chemistry B* **2003,** *107* (20), 4688-4698.

62. Hagfeldt, A.; Gratzel, M., Molecular photovoltaics. *Accounts of Chemical Research* **2000,** *33* (5), 269-277.
63. Gratzel, M., Dye-sensitized solar cells. *Journal of Photochemistry and Photobiology C-Photochemistry Reviews* **2003,** *4* (2), 145-153.
64. Coakley, K. M.; McGehee, M. D., Conjugated polymer photovoltaic cells. *Chemistry of Materials* **2004,** *16* (23), 4533-4542.
65. Gunes, S.; Neugebauer, H.; Sariciftci, N. S., Conjugated polymer-based organic solar cells. *Chemical Reviews* **2007,** *107* (4), 1324-1338.
66. Wang, P.; Zakeeruddin, S. M.; Moser, J. E.; Nazeeruddin, M. K.; Sekiguchi, T.; Gratzel, M., A stable quasi-solid-state dye-sensitized solar cell with an amphiphilic ruthenium sensitizer and polymer gel electrolyte. *Nature Materials* **2003,** *2* (6), 402-407.
67. Nazeeruddin, M. K.; Pechy, P.; Renouard, T.; Zakeeruddin, S. M.; Humphry-Baker, R.; Comte, P.; Liska, P.; Cevey, L.; Costa, E.; Shklover, V.; Spiccia, L.; Deacon, G. B.; Bignozzi, C. A.; Gratzel, M.; Lx, Engineering of efficient panchromatic sensitizers for nanocrystalline TiO2-based solar cells. *Journal of the American Chemical Society* **2001,** *123* (8), 1613-1624.
68. Ito, S.; Miura, H.; Uchida, S.; Takata, M.; Sumioka, K.; Liska, P.; Comte, P.; Pechy, P.; Graetzel, M., High-conversion-efficiency organic dye-sensitized solar cells with a novel indoline dye. *Chemical Communications* **2008,** (41), 5194-5196.
69. Qin, H.; Wenger, S.; Xu, M.; Gao, F.; Jing, X.; Wang, P.; Zakeeruddin, S. M.; Gratzel, M., An organic sensitizer with a fused dithienothiophene unit for efficient and stable dye-sensitized solar cells. *Journal of the American Chemical Society* **2008,** *130* (29), 9202-+.
70. Zhu, K.; Neale, N. R.; Miedaner, A.; Frank, A. J., Enhanced charge-collection efficiencies and light scattering in dye-sensitized solar cells using oriented TiO2 nanotubes arrays. *Nano Letters* **2007,** *7* (1), 69-74.
71. Mor, G. K.; Shankar, K.; Paulose, M.; Varghese, O. K.; Grimes, C. A., Use of highly-ordered TiO2 nanotube arrays in dye-sensitized solar cells. *Nano Letters* **2006,** *6* (2), 215-218.
72. Law, M.; Greene, L. E.; Johnson, J. C.; Saykally, R.; Yang, P. D., Nanowire dye-sensitized solar cells. *Nature Materials* **2005,** *4* (6), 455-459.
73. Alvaro, M.; Carbonell, E.; Ferrer, B.; Xamena, F.; Garcia, H., Semiconductor behavior of a metal-organic framework (MOF). *Chemistry-a European Journal* **2007,** *13* (18), 5106-5112.
74. Xamena, F.; Corma, A.; Garcia, H., Applications for metal-organic frameworks (MOFs) as quantum dot semiconductors. *Journal of Physical Chemistry C* **2007,** *111* (1), 80-85.
75. Tachikawa, T.; Choi, J. R.; Fujitsuka, M.; Majima, T., Photoinduced charge-transfer processes on MOF-5 nanoparticles: Elucidating differences between metal-organic frameworks and semiconductor metal oxides. *Journal of Physical Chemistry C* **2008,** *112* (36), 14090-14101.
76. Constable, E. C., 2,2 ': 6 ',2 "-terpyridines: From chemical obscurity to common supramolecular motifs. *Chemical Society Reviews* **2007,** *36* (2), 246-253.
77. Baranoff, E.; Collin, J. P.; Flamigni, L.; Sauvage, J. P., From ruthenium(II) to iridium(III): 15 years of triads based on bis-terpyridine complexes. *Chemical Society Reviews* **2004,** *33* (3), 147-155.
78. Hofmeier, H.; Schubert, U. S., Recent developments in the supramolecular chemistry of terpyridine-metal complexes. *Chemical Society Reviews* **2004,** *33* (6), 373-399.

79. Sauvage, J. P.; Collin, J. P.; Chambron, J. C.; Guillerez, S.; Coudret, C.; Balzani, V.; Barigelletti, F.; Decola, L.; Flamigni, L., Ruthenium(II) and osmium(II) bis(terpyridine) complexes in covalently-linked multicomponent systems - synthesis, electrochemical-behavior, absorbtion-spectra, and photochemical and photophysical properties. *Chemical Reviews* **1994,** *94* (4), 993-1019.
80. Li, Y. Q.; Bricks, J. L.; Resch-Genger, U.; Spieles, M.; Rettig, W., Bifunctional charge transfer operated fluorescent probes with acceptor and donor receptors. 2. Bifunctional cation coordination behavior of biphenyl-type sensor molecules incorporating 2,2 ': 6 ', 2 "-terpyridine acceptors. *Journal of Physical Chemistry A* **2006,** *110* (38), 10972-10984.
81. Dumitru, F.; Petit, E.; van der Lee, A.; Barboiu, M., Homo- and heteroduplex complexes containing terpyridine-type ligands and Zn2+. *European Journal of Inorganic Chemistry* **2005,** (21), 4255-4262.
82. Righetto, S.; Rondena, S.; Locatelli, D.; Roberto, D.; Tessore, F.; Ugo, R.; Quici, S.; Roma, S.; Korystov, D.; Srdanov, V. I., An investigation on the two-photon absorption activity of various terpyridines and related homoleptic andheteroleptic cationic Zn(II) complexes. *Journal of Materials Chemistry* **2006,** *16* (15), 1439-1444.
83. Chen, X. G.; Zhou, Q. G.; Cheng, Y. X.; Geng, Y. H.; Ma, D. G.; Xie, Z. Y.; Wang, L. X., Synthesis, structure and luminescence properties of zinc (II) complexes with terpyridine derivatives as ligands. *Journal of Luminescence* **2007,** *126* (1), 81-90.
84. Eddaoudi, M.; Kim, J.; O'Keeffe, M.; Yaghi, O. M., Cu-2[o-Br-C6H3(CO2)(2)](2)(H2O)(2)center dot(DMF)(8)(H2O)(2): A framework deliberately designed to have the NbO structure type. *Journal of the American Chemical Society* **2002,** *124* (3), 376-377.
85. Sun, J. Y.; Weng, L. H.; Zhou, Y. M.; Chen, J. X.; Chen, Z. X.; Liu, Z. C.; Zhao, D. Y., QMOF-1 and QMOF-2: Three-dimensional metal-organic open frameworks with a quartzlike topology. *Angewandte Chemie-International Edition* **2002,** *41* (23), 4471-+.
86. Ferey, G.; Mellot-Draznieks, C.; Serre, C.; Millange, F.; Dutour, J.; Surble, S.; Margiolaki, I., A chromium terephthalate-based solid with unusually large pore volumes and surface area. *Science* **2005,** *309* (5743), 2040-2042.
87. Moulton, B.; Zaworotko, M. J., From molecules to crystal engineering: Supramolecular isomerism and polymorphism in network solids. *Chemical Reviews* **2001,** *101* (6), 1629-1658.
88. Speck, A. L. *"PLATON, a multipurpose crystallographic tool." Utrecht University, Utrecht, The Netherlands, 2001,* http://www.cryst.chem.uu.nl/platon/.
89. Bazzicalupi, C.; Bencini, A.; Berni, E.; Bianchi, A.; Danesi, A.; Giorgi, C.; Valtancoli, B.; Lodeiro, C.; Lima, J. C.; Pina, F.; Bernardo, M. A., New terpyridine-containing macrocycle for the assembly of dimeric Zn(II) and Cu(II) complexes coupled by bridging hydroxide anions and pi-stacking interactions. *Inorganic Chemistry* **2004,** *43* (16), 5134-5146.
90. Yaghi, O.; Eddaoudi, M.; Li, H.; Kim, J.; Rosi, N. Isoreticular metal-organic frameworks, process for forming the same, and systematic design of pore size and functionality therein, with application for gas storage. 2005.
91. Eddaoudi, M.; Kim, J.; Rosi, N.; Vodak, D.; Wachter, J.; O'Keefe, M.; Yaghi, O. M., Systematic design of pore size and functionality in isoreticular MOFs and their application in methane storage. *Science* **2002,** *295* (5554), 469-472.

92. Chen, B. L.; Liang, C. D.; Yang, J.; Contreras, D. S.; Clancy, Y. L.; Lobkovsky, E. B.; Yaghi, O. M.; Dai, S., A microporous metal-organic framework for gas-chromatographic separation of alkanes. *Angewandte Chemie-International Edition* **2006,** *45* (9), 1390-1393.
93. Zhang, L.; Wang, Q.; Wu, T.; Liu, Y. C., Understanding adsorption and interactions of alkane isomer mixtures in isoreticular metal-organic frameworks. *Chemistry-a European Journal* **2007,** *13* (22), 6387-6396.
94. Hartmann, M.; Kunz, S.; Himsl, D.; Tangermann, O.; Ernst, S.; Wagener, A., Adsorptive separation of isobutene and isobutane on Cu-3(BTC)(2). *Langmuir* **2008,** *24* (16), 8634-8642.
95. Dubbeldam, D.; Galvin, C. J.; Walton, K. S.; Ellis, D. E.; Snurr, R. Q., Separation and molecular-level segregation of complex alkane mixtures in metal-organic frameworks. *Journal of the American Chemical Society* **2008,** *130* (33), 10884-+.
96. Finsy, V.; Verelst, H.; Alaerts, L.; De Vos, D.; Jacobs, P. A.; Baron, G. V.; Denayer, J. F. M., Pore-filling-dependent selectivity effects in the vapor-phase separation of xylene isomers on the metal-organic framework MIL-47. *Journal of the American Chemical Society* **2008,** *130* (22), 7110-7118.
97. Zhang, J. P.; Chen, X. M., Exceptional framework flexibility and sorption behavior of a multifunctional porous cuprous triazolate framework. *Journal of the American Chemical Society* **2008,** *130* (18), 6010-6017.
98. Reynolds, J. G.; Coronado, P. R.; Hrubesh, L. W., Hydrophobic aerogels for oil-spill cleanup - Intrinsic absorbing properties. *Energy Sources* **2001,** *23* (9), 831-843.
99. Adebajo, M. O.; Frost, R. L.; Kloprogge, J. T.; Carmody, O.; Kokot, S., Porous materials for oil spill cleanup: A review of synthesis and absorbing properties. *Journal of Porous Materials* **2003,** *10* (3), 159-170.
100. Dewal, M. B.; Lufaso, M. W.; Hughes, A. D.; Samuel, S. A.; Pellechia, P.; Shimizu, L. S., Absorption properties of a porous organic crystalline apohost formed by a self-assembled bis-urea macrocycle. *Chemistry of Materials* **2006,** *18* (20), 4855-4864.
101. Yaghi, O. M.; Davis, C. E.; Li, G. M.; Li, H. L., Selective guest binding by tailored channels in a 3-D porous zinc(II)-benzenetricarboxylate network. *Journal of the American Chemical Society* **1997,** *119* (12), 2861-2868.
102. Li, H. L.; Davis, C. E.; Groy, T. L.; Kelley, D. G.; Yaghi, O. M., Coordinatively unsaturated metal centers in the extended porous framework of Zn-3(BDC)(3).6CH(3)OH (BDC=1,4-benzenedicarboxylate). *Journal of the American Chemical Society* **1998,** *120* (9), 2186-2187.
103. Li, H.; Eddaoudi, M.; Groy, T. L.; Yaghi, O. M., Establishing microporosity in open metal-organic frameworks: Gas sorption isotherms for Zn(BDC) (BDC = 1,4-benzenedicarboxylate). *Journal of the American Chemical Society* **1998,** *120* (33), 8571-8572.
104. Qiu, Y. C.; Liu, Z. H.; Li, Y. H.; Deng, H.; Zeng, R. H.; Zeller, M., Reversible anion exchange and sensing in large porous materials built from 4,4 '-bipyridine via pi center dot center dot center dot pi and H-bonding interactions. *Inorganic Chemistry* **2008,** *47* (12), 5122-5128.
105. Wang, Y.; Cheng, P.; Song, Y.; Liao, D. Z.; Yanl, S. P., Self-assembly and anion-exchange properties of a discrete cage and 3D coordination networks based on cage structures. *Chemistry-a European Journal* **2007,** *13* (29), 8131-8138.

106. Xu, G. C.; Ding, Y. J.; Huang, Y. Q.; Liu, G. X.; Sun, W. Y., Structure diversity and anion exchange property of zinc(II) coordination polymers with flexible tripodal ligand 1,3,5-tris(imidazol-1-ylmethyl) benzene. *Microporous and Mesoporous Materials* **2008,** *113* (1-3), 511-522.
107. Kesanli, B.; Lin, W. B., Chiral porous coordination networks: rational design and applications in enantioselective processes. *Coordination Chemistry Reviews* **2003,** *246* (1-2), 305-326.
108. Lin, W. B., Metal-organic frameworks for asymmetric catalysis and chiral separations. *Mrs Bulletin* **2007,** *32* (7), 544-548.
109. Bradshaw, D.; Prior, T. J.; Cussen, E. J.; Claridge, J. B.; Rosseinsky, M. J., Permanent microporosity and enantioselective sorption in a chiral open framework. *Journal of the American Chemical Society* **2004,** *126* (19), 6106-6114.
110. Lacour, J.; Frantz, R., New chiral anion mediated asymmetric chemistry. *Organic & Biomolecular Chemistry* **2005,** *3* (1), 15-19.
111. Lacour, J.; Hebbe-Viton, V., Recent developments in chiral anion mediated asymmetric chemistry. *Chemical Society Reviews* **2003,** *32* (6), 373-382.
112. Schroeder, F.; Esken, D.; Cokoja, M.; van den Berg, M. W. E.; Lebedev, O. I.; van Tendeloo, G.; Walaszek, B.; Buntkowsky, G.; Limbach, H. H.; Chaudret, B.; Fischer, R. A., Ruthenium nanoparticles inside porous [Zn4O(bdC)(3)] by hydrogenolysis of adsorbed [Ru(cod)(cot)]: A solid-state reference system for surfactant-stabilized ruthenium colloids. *Journal of the American Chemical Society* **2008,** *130* (19), 6119-6130.
113. Cheon, Y. E.; Suh, M. P., Multifunctional fourfold interpenetrating diamondoid network: Gas separation and fabrication of palladium nanoparticles. *Chemistry-a European Journal* **2008,** *14* (13), 3961-3967.
114. Muller, M.; Hermes, S.; Kaehler, K.; van den Berg, M. W. E.; Muhler, M.; Fischer, R. A., Loading of MOF-5 with Cu and ZnO nanoparticles by gas-phase infiltration with organometallic precursors: properties of Cu/ZnO@MOF-5 as catalyst for methanol synthesis. *Chemistry of Materials* **2008,** *20* (14), 4576-4587.
115. Yoo, Y.; Jeong, H. K., Rapid fabrication of metal organic framework thin films using microwave-induced thermal deposition. *Chemical Communications* **2008,** (21), 2441-2443.
116. Sheldrick, G. M., A short history of SHELX. *Acta Crystallographica Section A* **2008,** *64*, 112-122.